Report No: P WMA
19/G10/00/2413/3

Department of Water Affairs
Directorate: Options Analysis

PRE-FEASIBILITY AND FEASIBILITY STUDIES FOR AUGMENTATION OF THE WESTERN CAPE WATER SUPPLY SYSTEM BY MEANS OF FURTHER SURFACE WATER DEVELOPMENTS

REPORT No.1 – VOLUME 3
Berg Estuary Environmental Water Requirements

APPENDIX No.D

Specialist Report - Modelling

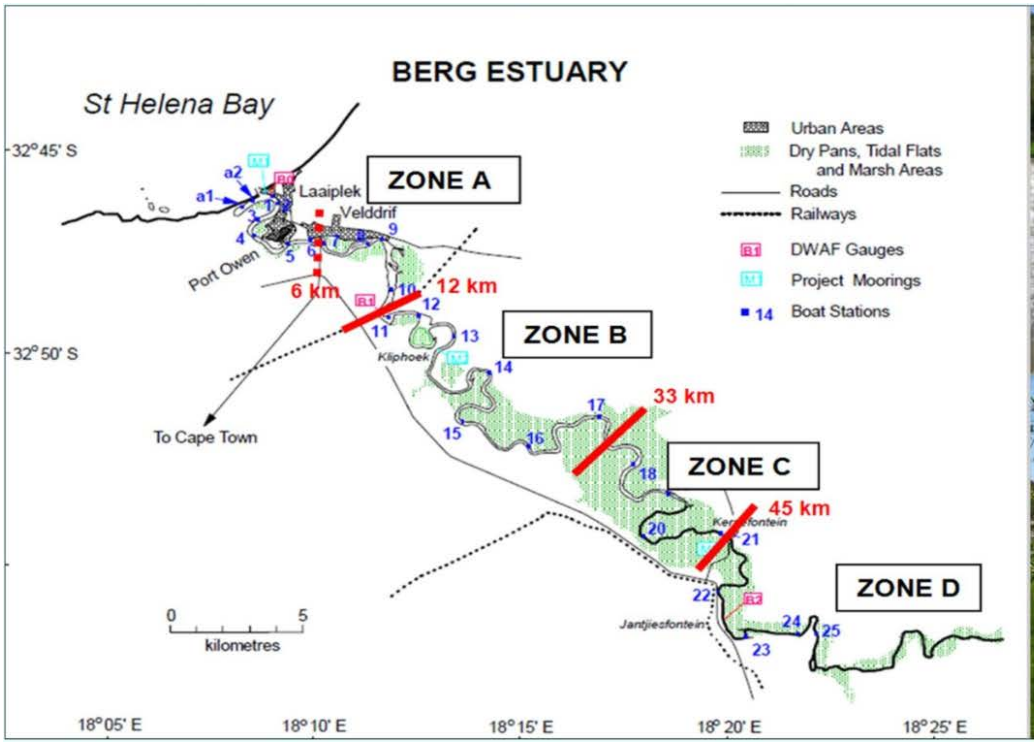

June 2012

STUDY REPORT LIST

REPORT No	REPORT TITLE	VOLUME No.	DWA REPORT No.	VOLUME TITLE
1	ECOLOGICAL WATER REQUIREMENT ASSESSMENTS	Vol 1	PWMA19 G10/00/2413/1	**Riverine Environmental Water Requirements**
				Appendix 1: EWR data for the Breede River
				Appendix 2: EWR data for the Palmiet River
				Appendix 3: EWR data for the Berg River
				Appendix 4: Task 3.1: Rapid Reserve assessments (quantity) for the Steenbras, Pombers and Kromme Rivers
				Appendix 5: Habitat Integrity Report – Breede River
		Vol 2	PWMA19 G10/00/2413/2	**Rapid Determination of the Environmental Water Requirements of the Palmiet River Estuary**
				Appendix A: Summary of data available for the RDM investigations undertaken during 2007 and 2008
				Appendix B: Summary of baseline data requirements and the long-term monitoring programme
				Appendix C: Abiotic Specialist Report
		Vol 3	PWMA19 G10/00/2413/3	**Berg Estuary Environmental Water Requirements**
				Appendix A: Available information and data
				Appendix B: Measurement of streamflows in the Lower Berg downstream of Misverstand Dam
				Appendix C: Specialist Report – Physical dynamics and water quality
				Appendix D: Specialist Report – Modelling
				Appendix E: Specialist Report – Microalgae
				Appendix F: Specialist Report – Invertebrates
				Appendix G: Specialist Report – Fish
				Appendix H: Specialist Report – Birds
				Appendix I: Specialist Report – The economic value of the Berg River Estuary
2	PRELIMINARY ASSESSMENT OF OPTIONS		PWMA19 G10/00/2413/4	Appendix 1: Scheme Yield Assessments and Diversion Functions
				Appendix 2: Unit Reference Value Calculation Sheets
				Appendix 3: Yield Analysis and Dam Size Optimization
				Appendix 4: Dam Design Inputs
				Appendix 5: Diversion Weir Layout Drawings
				Appendix 6: Voëlvlei Dam Water Quality Assessment
				Appendix 7: Botanical Considerations
				Appendix 8: Heritage Considerations
				Appendix 9: Agricultural Economic Considerations

STUDY REPORT LIST (cntd)

REPORT No	REPORT TITLE	VOLUME No.	DWA REPORT No.	VOLUME TITLE
3	FEASIBILITY STUDIES	Vol 1	PWMA19 G10/00/2413/5	**Berg River-Voëlvlei Augmentation Scheme**
				Appendix 1: Updating of the Western Cape Water Supply System Analysis for the Berg River-Voëlvlei Augmentation Scheme
				Appendix 2: Configuration, Calibration and Application of the CE-QUAL-W2 model to Voëlvlei Dam for the Berg River-Voëlvlei Augmentation Scheme
				Appendix 3: Monitoring Water Quality During Flood Events in the Middle Berg River (Winter 2011), for the Berg River-Voëlvlei Augmentation Scheme
				Appendix 4: Dispersion Modelling in Voëlvlei Dam from Berg River Water Transfers for the Berg River-Voëlvlei Augmentation Scheme
				Appendix 7 - 12: See list under Volume 2 below
		Vol 2	PWMA19 G10/00/2413/6	**Breede-Berg (Michell's Pass) Water Transfer Scheme**
				Appendix 5: Scheme Operation and Yield Analyses with Ecological Flow Requirements for the Breede-Berg (Michell's Pass) Water Transfer Scheme
				Appendix 6: Preliminary Design of Papenkuils Pump Station Upgrade and Pre-Feasibility Design of the Boontjies Dam, for the Breede-Berg (Michell's Pass) Water Transfer Scheme
				Appendix 7: Ecological Water Requirements Assessment Summary for the Berg River-Voëlvlei Augmentation Scheme , and the Breede Berg (Michell's Pass) Water Transfer Scheme
				Appendix 8: Geotechnical Investigations for the Berg River-Voëlvlei Augmentation Scheme, and the Breede-Berg (Michell's Pass) Water Transfer Scheme
				Appendix 9: LiDAR Aerial Survey, for the Berg River-Voëlvlei Augmentation Scheme, and the Breede-Berg (Michell's Pass) Water Transfer Scheme
				Appendix 10: Conveyance Infrastructure Design Report, for the Berg River-Voëlvlei Augmentation Scheme, and the Breede-Berg (Michell's Pass) Water Transfer Scheme
				Appendix 11: Diversion Weirs Design for the Berg River-Voëlvlei Augmentation Scheme, and the Breede-Berg (Michell's Pass) Water Transfer Scheme
				Appendix 12: Cost Estimates for the Berg River-Voëlvlei Augmentation Scheme, and the Breede-Berg (Michell's Pass) Water Transfer Scheme
4	RECORD OF IMPLEMENTATION DECISIONS		PWMA19 G10/00/2413/7	

STUDY REPORT MATRIX DIAGRAM

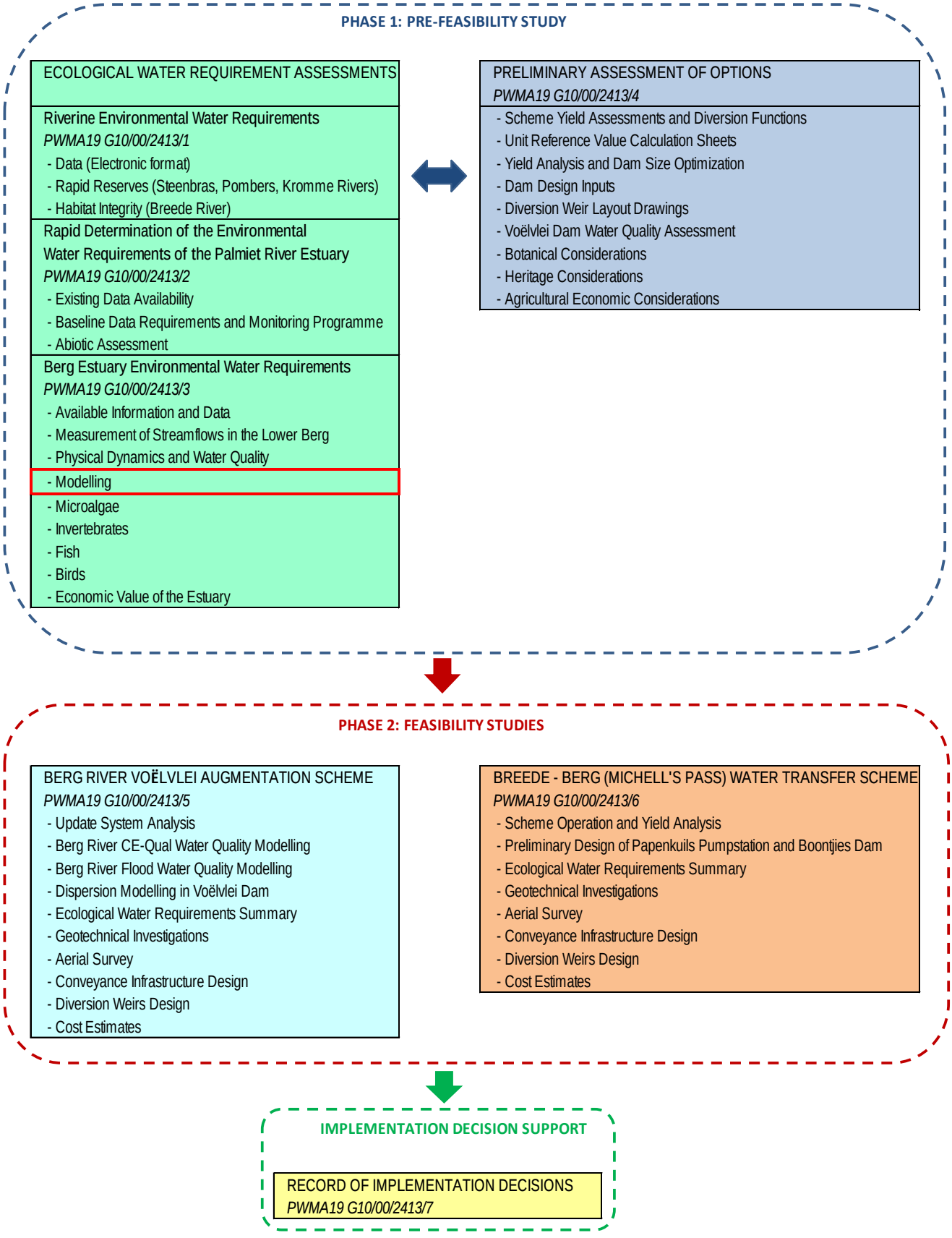

ACKNOWLEDGEMENTS

PREPARED FOR THE WCWC JV BY:
CSIR, Environmentek
P O Box 320
7599
STELLENBOSCH

AUTHOR:
R. van Ballegooyen

REVIEWER:
C.A. Brown

LEAD CONSULTANT:
Anchor Environmental

EDITOR:
B. Clark

TABLE OF CONTENTS

1. INTRODUCTION 1

1.1. Purpose of the hydrodynamic modelling study 1

1.2. Structure of the Hydrodynamic Modelling Report 2

1.3. Assumptions and Limitations of the Modelling Study 3

2. DESCRIPTION OF THE ESTUARY AND SURROUNDS 4

2.1. Physiography of the Estuary 4

2.2. Climate, rainfall and run-off 8

2.3. Hydrodynamic functioning of the Berg River Estuary 12
2.3.1. Flushing Mechanisms 12
2.3.2. Water level *variability* 14
2.3.3. Water Quality and associated hydrographic regimes 33

2.4. Review of Previous Modelling Studies 37

3. MODEL SET-UP, CALIBRATION AND VERIFICATION 40

3.1. Description of the Hydrodynamic Model 40

3.2. AVAILABLE DATA FOR BERG RIVER ESTUARY MODEL IMPLEMENTATION 43

3.3. Model Set-up 46
3.3.1. Computational grid and bathymetry 46
3.3.2. Open Ocean Boundary Conditions 53
3.3.3. Upstream Boundary Condition 54
3.3.4. Surface fluxes 54
3.3.5. Initial conditions 55
3.3.6. Model Parameters 56
3.3.7. Monitoring Stations and defined zone in the Berg River Estuary. 60

3.4. Model calibration and verification 67
3.4.1. Water level calibration 67
3.4.2. Salinity calibration 68
3.4.3. Flood level calibration 71

4. WATER QUALITY MODEL RESULTS 73

4.1. Scenarios Modelled 73

4.2. Model Results 75

5. FLOOD MODEL RESULTS 81

5.1. Scenarios Modelled 81
5.1.1. Background 81
5.1.2. Scenarios used to assess RDM flooding requirements 85

6. CONCLUSIONS AND RECOMMENDATIONS 94

7. REFERENCES 95

ANNEX A: SALINITY DISTRIBUTIONS IN THE BERG ESTUARY 98

ANNEX B: RESULTS OF THE WATER QUALITY MODELLING STUDY 122

ANNEX C: RESULTS OF THE FLOOD MODELLING STUDY 129

1. INTRODUCTION

1.1. Purpose of the hydrodynamic modelling study

The CSIR was approached by Anchor Environmental Consultants cc to conduct hydrodynamic modelling exercise on the Berg River Estuary as input to the Reserve Determination Study that was undertaken for the system.

The hydrodynamic modelling is intended to provide information for decisions on the quantity of freshwater and the nature of the flow patterns required to achieve certain desired ecological outcomes. Of concern was both the water quality (particularly the salinity distribution) in the Berg River Estuary under various water use scenarios as well as ecological impacts associated with changes in the flooding and inundation regime.

The modelling approach required to address these two issues is very different and require two distinct modelling approaches, each requiring its own modelling exercise. To address water quality issues, both long and short duration simulations were required to assess likely changes in salinity distribution in the estuary over annual, seasonal as well as flushing time scales, while the issue of flooding and potential changes in the inundation regime only needed to be resolved at the event scale level (*i.e*. short-term simulations).

Previous hydrodynamic studies of the region have been undertaken using both the MIKE-11 model (CSIR 1993, Slinger and Taljaard 1994) and, more recently, the MIKE 21 model (Beck and Basson 2007). In addition the MIKE 11 Model was used to undertake preliminary simulations of water quality in the Berg River Estuary (Slinger *et al*. 1998); The MIKE 11 modelling was undertaken in one-dimension (integrated across the estuary and also vertically) while the MIKE 21 modelling was undertaken in two-dimensions (vertically integrated).

The MIKE-11 modelling was undertaken primarily to investigate the potential water quality (salinity) changes due to various water usage scenarios. The Mike-11 one-dimensional model is eminently well-suited to such a study as stratification effects are limited within the Berg Estuary. Note that while stratification does occur (especially after freshettes and floods), it is not anticipated that stratification dynamics will substantively affect the longer-term salinity flushing characteristics within the estuary. (Stratification effects on mixing characteristics in such one-dimensional models are typically included by increasing the diffusion coefficients). Furthermore, the fact that the estuary is long and responds relatively slowly to freshwater inflows, requires longer simulations than would normally be the case for most South African estuaries. The one-dimensional nature of the MIKE-11 model means that it is computationally efficient and consequently well-suited to running such long simulations.

Conversely, the MIKE-21 modelling suite, being two-dimensional, is able to better resolve and describe flooding and inundation dynamics due to its spatial resolution in the horizontal plane. In the study by Beck and Basson (2007), two separate models were set-up, one to investigate tidal action and the other to investigate flooding effects. The tidal modelling was

undertaken for a typical summer and winter period and was intended to describe typical tidal dynamics (flow velocities and tidal inundation) under these conditions. Salinity was not included in these simulations so no information was produced on potential changes in water quality due to various water use scenarios. In the flood simulations, flood hydrographs were simulated (hydrodynamics and sediment transport) for both the present as well as post-dam flood release scenarios in order to determine the effect that the Berg River Dam may have on estuarine dynamics (see Beck and Basson (2004, 2007) for details on the two scenarios). Based on these simulations, inundation dynamics (*i.e*. extent of areas flooded) were described. The model also addressed issues around the likely scour and deposition of sediments in the estuary during flooding. In their study, scour seemed to be focussed on the outer banks of the channel with deposition occurring towards the middle of the channel. They predicted that the scour would increase from a maximum of 0.2 m for small floods (~90 m^3/s) to over 0.5 m for large floods (> 600 m^3/s).

In the present modelling study, two distinct modelling studies have been undertaken. The first is focussed on water quality issues, particularly the salinity distribution within the estuary. The second is focussed on flooding and inundations effects.

The water quality modelling constitutes an investigation of more detailed flow scenarios that were not available to the original MIKE-11 study undertaken in 1993 (CSIR, 1993). The focus in these studies was on the potential changes in longitudinal salinity distributions in the estuary, an issue also not addressed in the more recent MIKE-21 studies (Beck and Basson, 2007), undertaken to investigate potential pre- and post- Berg River Dam scenarios.

The flooding scenarios investigated in this study essentially are those investigated in the 2007 MIKE-21 flooding studies, however, here a greater focus is placed on the duration of inundation (*i.e*. the inclusion of rainfall and evaporation effects on particularly pans) during such events. (Although salinity distributions were not modelled in these flood simulations, salinity distribution during and after flood events can be estimated from both existing measured data and the water quality modelling simulations). Unlike the 2007 studies, sediment dynamics were not simulated. It has been assumed that the exclusion of sediment dynamics will not substantively affect the inundation dynamics associated with flooding.

1.2. Structure of the Hydrodynamic Modelling Report

This report describes the hydrodynamic modelling study undertaken in support of the Reserve Determination Studies for the Berg estuary. Section A2 provides a description of the environment and the functioning of the Berg estuary to the extent that it is relevant to the modelling study. Section A3 describes the model set-up, calibration and verification, while Section A4 and A5 summarise the scenarios modelled and contains the model results describing the hydrodynamic and water quality (salinity) functioning of the Berg estuary and the flooding dynamics within the estuary, respectively. The major findings of these model simulations (in terms of defining hydrodynamic states of relevance) are reported in the main body of this report. Section A6 contains the conclusions and recommendations of the modelling study.

1.3. Assumptions and Limitations of the Modelling Study

The following assumptions and limitations pertain to this study:

- No new data has been collected as part of this study. It is based on the historical measurements by the CSIR and information collated and collected during the intensive monitoring programme conducted on the Great Berg system in 2002-2005 (DWAF, 2007a-f). The latter were as provided to the CSIR by Anchor Environmental Consultants;

- It is assumed that the simulated run-off scenarios (50 – 70 years) of river inflow at the head of the Great Berg Estuary provided to the CSIR are an accurate representation of flows entering the estuary. These scenarios include the reference condition, the present state and a range of additional potential future scenarios as agreed between the CSIR, Anchor Environmental Consultants and DWAF;

- Numerical modelling was based on available information, *e.g*. bathymetry and sediment data provided by. Anchor Environmental Consultants, supplemented by CSIR measured data prior to the Berg River Baseline Monitoring Programme;

- Hydrodynamic modelling only comprises modelling of the water column and inundation of the floodplain under various scenarios provided by Anchor Environmental Consultants (through DWAF);

- No sediment modelling was undertaken as part of this study.

Particular limitations of the modelling study are:

- the uncertainty introduced into both modelling studies by limitations in the in-channel bathymetry data. Considerable supplementation and correction needed to be made to the Digital Terrain Model (DTM) supplied to the CSIR;

- the uncertainty introduced into the water quality (salinity) modelling study resulting from the uncertainty in the estimates of freshwater inflows to the estuary, particularly during low flow periods;

- the uncertainty introduced into the flood modelling study due to the lack of quantitative data to verify the flood modelling (areas of inundation under various floods), as well as the lack of water level measurements in the estuary between an upstream site at Jantjiesfontein and a downstream site just seawards of the Railway Bridge.

2. DESCRIPTION OF THE ESTUARY AND SURROUNDS

The estuary and floodplain are of national conservation importance for estuarine birds, fish, invertebrates and vegetation. Anthropogenic influences such as water abstraction and dams (that change the hydrodynamics and water quality of the estuary and reduce the frequency and intensity of the flooding of the floodplain) threaten the ecological functioning of the estuary. Agricultural and urban encroachment have reduced the extent of natural vegetation on the floodplain, thus also posing a threat to the ecosystem.

The description of the Berg estuary that follows is limited to those features that are of relevance to the hydrodynamic functioning of the estuary. A more complete description of the estuary and its surrounds is given in the main body of the report.

2.1. Physiography of the Estuary

The form of an estuary develops as a consequence of the interaction between the dominant riverine and marine processes (Dyer, 1997). In addition, there will be anthropogenic impacts from developments such as the building of canals, breakwaters and harbours, while agriculture, particularly in the upper reaches, can severely influence the functioning of an estuary. All these influences play a role in the functioning of the Berg estuary and in the end determine the resulting hydrodynamics, water quality and ecological processes in the estuary.

The Berg River has its source in the Drakenstein and Franschhoek Mountains south of Franschhoek and flows into the sea at St Helena Bay (32°46' S; 18°08' E) some 285 km downstream. St Helena Bay, being on the West coast of South Africa, lies within the lies within the Benguela upwelling system (Shillington, 1998)[1]. The Berg River is reported to have a catchment of approximately 9 000 km^2 (Ractliffe, 2007). The river flows through mountainous terrain from its source at an altitude of 1 522 m in the Groot Drakenstein Mountains, to the town of Paarl and then through undulating agricultural lands from Paarl towards the sea (Figure 2.1).

The Berg estuary extends approximately 70 km upstream from the Berg River mouth through very flat terrain that rises only 1 m in the first 50 km upstream of the mouth (Day, 1981). Consequently the Berg River Estuary is long and sinuous and meanders upstream through extensive dry pans, tidal flats and marsh areas (Slinger & Taljaard 1994). The estuary and its floodplain are estimated to cover an area of 61 km2 (Turpie & Clarke 2007a)[2]. The estuary's shallow gradient and extensive floodplain make it atypical in relation to most South African estuaries (Schuman 2007).

---

1 *The southern Benguela upwelling system is dominated by wind-driven upwelling, specifically in summer when southeasterly winds drive surface waters offshore, allowing colder, nutrient-rich bottom waters to reach the surface at the coast. Nelson & Hutchings (1983) identified Cape Columbine as an upwelling centre, though waters in St Helena Bay remain warmer. In winter north-westerly winds cause downwelling, resulting in an increase in surface water temperatures.*

2 *From the flood modelling study, a flood peak of 1 000 m^3/s suggests that the estuary and its floodplain covers an area of approximately 69 km^2*

The mouth of the Berg estuary is permanently open mouth, having been canalised in the late 1966's through the coastal dunes. The purpose of this was to allow the estuary to function as a fishing harbour. The channel in the lower 4 km of the estuary has been dredged to a depth of at least -4m MSL. Consequently fishing vessels are now able to enter the fishing harbour at Laaiplek without hindrance. The original mouth has silted up and the former channel currently forms a blind arm or lagoon extending running parallel to the coast westward of the present mouth. This canalised entrance channel ensures a relatively unconstructed exchange of water between the estuary and the adjacent ocean. Recent bathymetric surveys of the mouth (January 2003) indicate channel depths that in places exceed -5 m MSL (Triton Surveys, 2003).

The main channel at Veldrif is about 100-200 m wide, becoming progressively narrower and shallower upstream. The depth of the estuary is about 3 to 5 m on average but can be up to 9 m in places, particularly where there are constrictions in the estuary.

The total volume of the estuary is estimated to be about 12 Mm^3 (Beck & Basson 2007). Based on the digital elevation model for the estuary at a 25 m resolution, and that the measured mean sea level in St Helena Bay and the Berg River Estuary is ~0.2 m above MSL[3], the total volume of the estuary is estimated to be 17.8 Mm^3. However, this estimate does not take into account the fact that much of the lower estuary floodplain has been reclaimed for salt production, suggesting that reality lies between these two estimates.

The sensitivity of estimates of both i) the spatial extent of inundated areas for various water levels and ii) the volume of the estuary, to small changes in water level, is a consequence of the estuary being surrounded by terrain that is very flat (marshes, flood plain, *etc*).

The estuary, being river-dominated, disperses sediment seaward of the river mouth resulting in an offshore depo-centre of muds. Only two other South African estuaries are characterised by having offshore mud deposit centres, namely the Orange or Gariep and the Thukela (Cooper 2001).

The lower 4 km of the estuary is dredged to a depth of at least 4 m to allow for boat navigation. The main channel at Veldrif is about 100-200 m wide, becoming progressively narrower and shallower upon moving upstream. The average width and depth of the channel is about 150 m and 3 m respectively. In the uppermost 15 km, steep banks covered in riparian woodland bound the estuary. Downstream, the estuary is flanked by a floodplain that varies in width from 1.5 to 4 km in the middle reaches, to <1.5 km in the lower reaches (Figure 2.2). More detailed descriptions of the estuarine morphology and modifications of the lower estuary are given in Morant *et al* (2001).

[3] Note that the MSL datum referred to as a vertical datum for most data sets (water levels, bathymetry, *etc*) is actually land levelling datum (LLD). This datum does not necessarily represent actual measured mean water levels of the ocean at any particular location. The actual water level is referred to as mean level in the South African Hydrographer's Tide Tables. The mean water level in Saldanha Bay, and by assumption St Helena Bay and the lower reaches of the Berg River Estuary is approximately 0.2 m MSL (actually LLD).

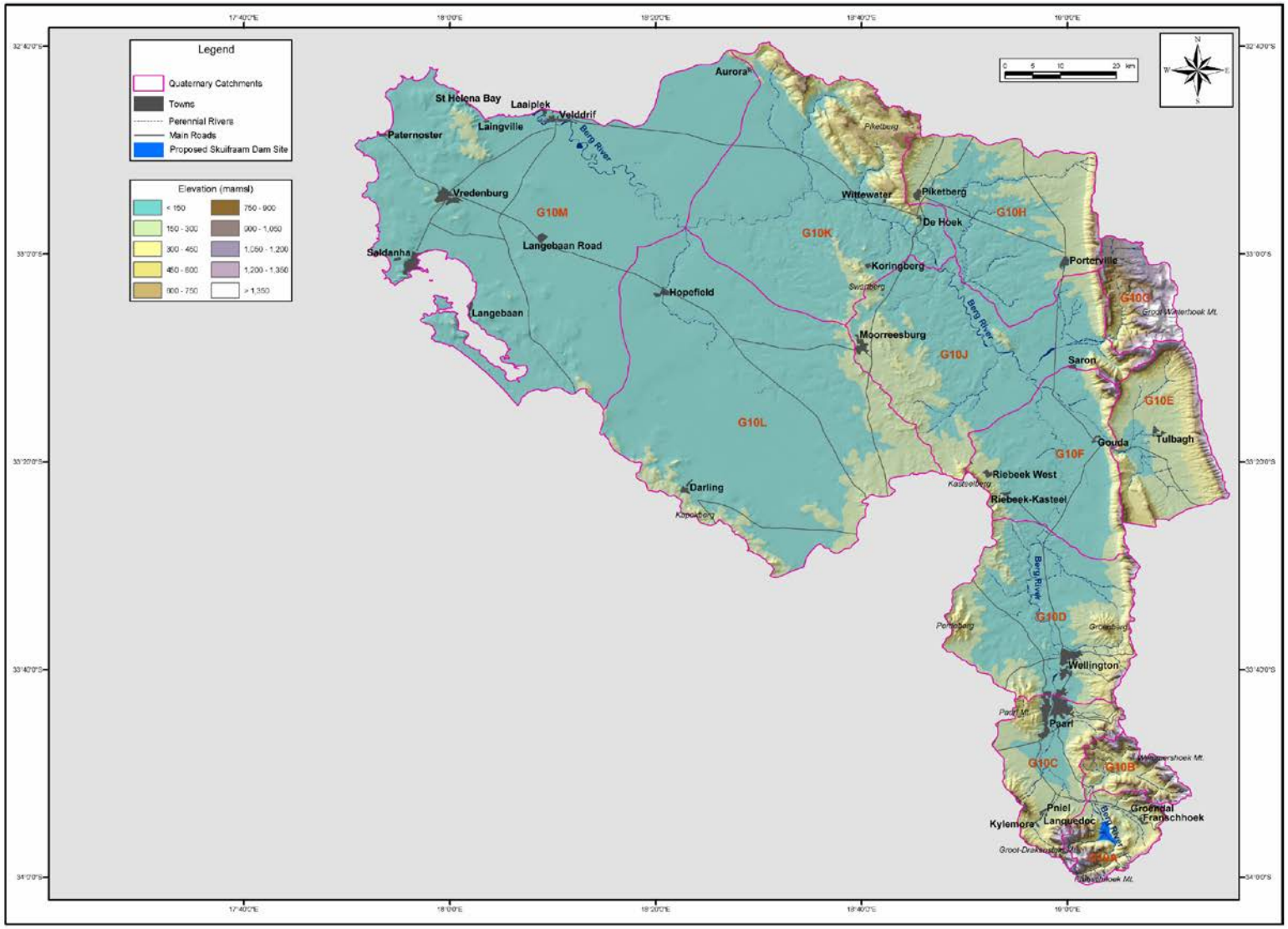

Figure 2.1 Orientation and topographical map of the Berg River catchment (after Ractliffe, 2007)

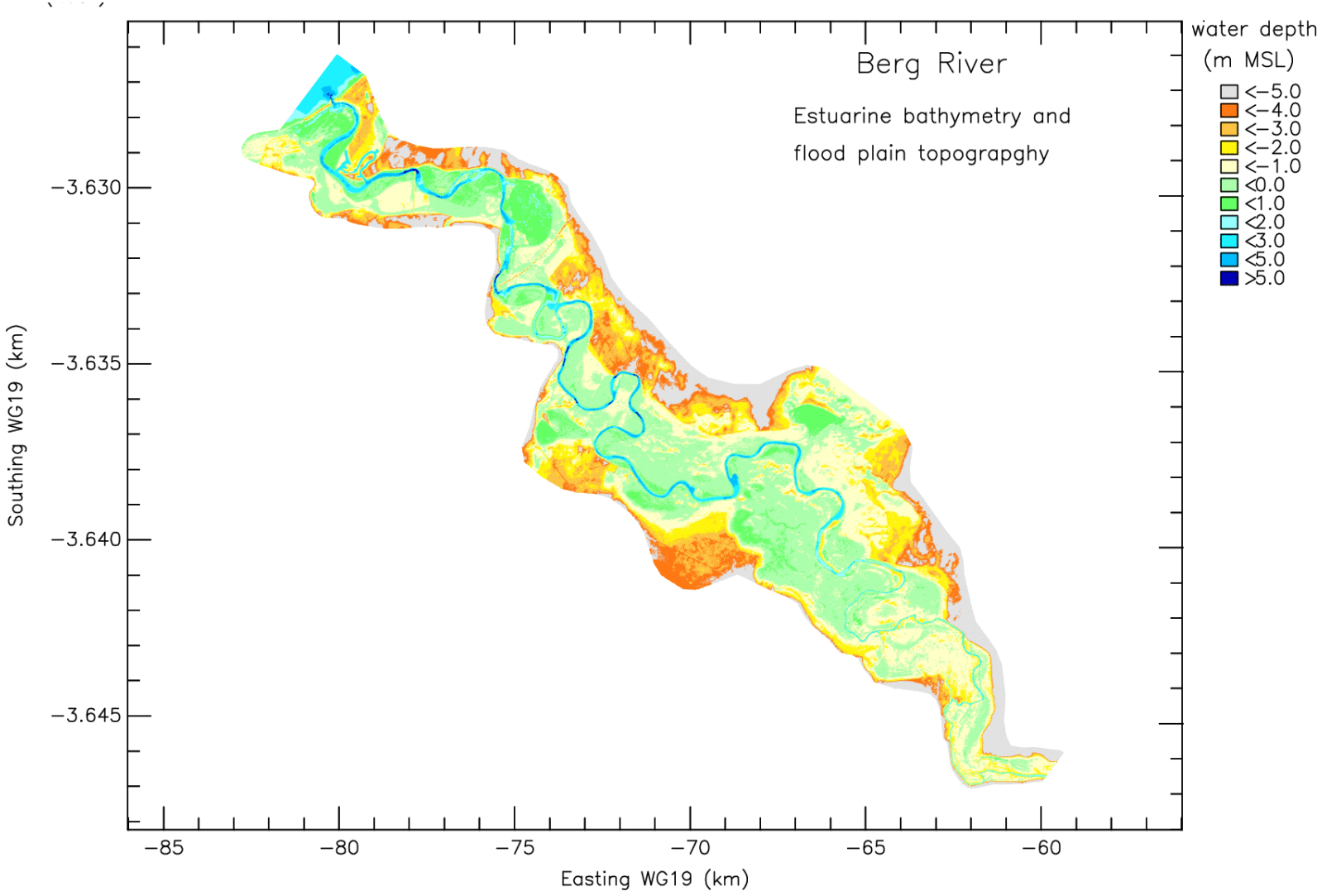

Figure 2.2 Bathymetry of the Berg Estuary and topography of the Berg Estuary flood plain

2.2. Climate, rainfall and run-off

The Berg River Catchment has a Mediterranean climate with warm dry summers and cool wet winters. Rainfall is an episodic event comprising fontal rain associated with the passing of mid-latitude cyclones and their associated coastal lows. Rainfall normally extends over a couple of days interspersed with significant periods of clear weather. More than 80% of the rain in this region falls in winter (Tyson, 1986) with very little rainfall in summer. The rainy season extends from April through to October.

There is a large spatial variation in the mean annual precipitation (MAP) over the catchment (Figure 2.3). The mountainous areas in the southern parts of the catchment experience MAP in excess of 2 600 mm/a. Jonkershoek near Stellenbosch has an average rainfall of over 3200 mm/a (Schulze, 1984). (It is in these mountainous areas that the Berg River catchment derives most of its runoff, particularly that which causes the winter spates of fresh water which play such an important role in the dynamics of the estuary). North of Wellington, MAP drops to 500 mm/a thereafter gradually decreasing westwards to about 300 mm/a along the West Coast. The average rainfall for the estuary area is around 300 mm/a. The potential evaporation over the catchment is somewhat less variable. In general, the mean annual potential evaporation (MAPE) in the Berg River Catchment exceeds 2000 mm/a (Figure 2.4). Only in the southern parts of the catchment is the MAPE lower (approximately 1500 mm/a). Like rainfall, MAPE exhibits marked seasonal differences. During the summer, monthly evaporation losses are approximately 250 mm/a, reducing to the order of 50 mm/a in winter (Ractliffe, 2007). The data displayed in Figures 2.3 and 2.4 were interpolated from the 1 x 1 inch grid data of the Computing Centre for Water Research (Schultze 1997).

The estimated present-day annual runoff from the Berg River catchment is 682 million m^3/a (DWAF, 1993), approximately 30% less than the total natural runoff of 931 million m^3/a (Beck and Basson, 2007), nearly half of which (45%) is generated in the top three quarternary catchments which cover 7% of the area (Ractliffe, 2007). This modified flow is attributed to direct abstraction from the river for irrigation, storage and abstraction for urban water supply (i.e. the 66 Mm^3 Wemmershoek Dam and the 170 Mm^3 Voelvlei Dam), development of forestry within the basin, irrigation return flow, and releases from large storage dams (*i.e*. the Voëlvlei, Wemmershoek and Theewaterskloof Dams, the latter via the Berg River Syphon). The recent completion of the Berg River Dam is expected to reduce the present day annual run-off by a further 5%. The development scenarios to be assessed in this study constitute a further reduction in the post-Berg River Dam freshwater flows described above.

As a consequence of the high degree of seasonality in rainfall, the Berg estuary itself is highly seasonal. Of particular consequence, are the spates of fresh water resulting from winter rainfall in the mountainous catchment to the southeast (Schumann, 2009). These spates flush out seawater, which penetrates into the lower reaches of the estuary due to tidal influences. During the summer, when little rain falls, the saline waters have been observed

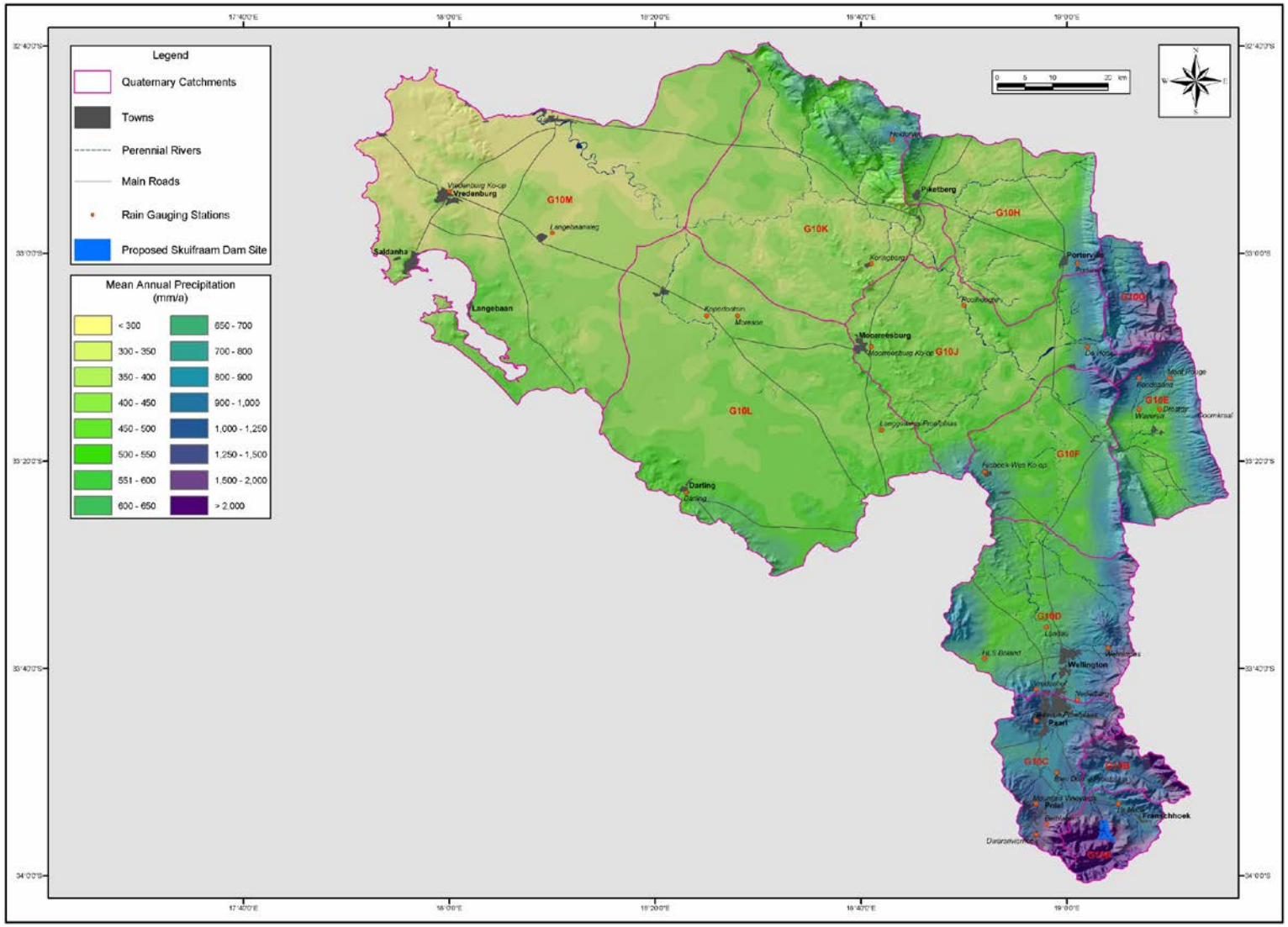

Figure 2.3 Mean annual precipitation in the Berg River Catchment (Ractliffe, 2007).

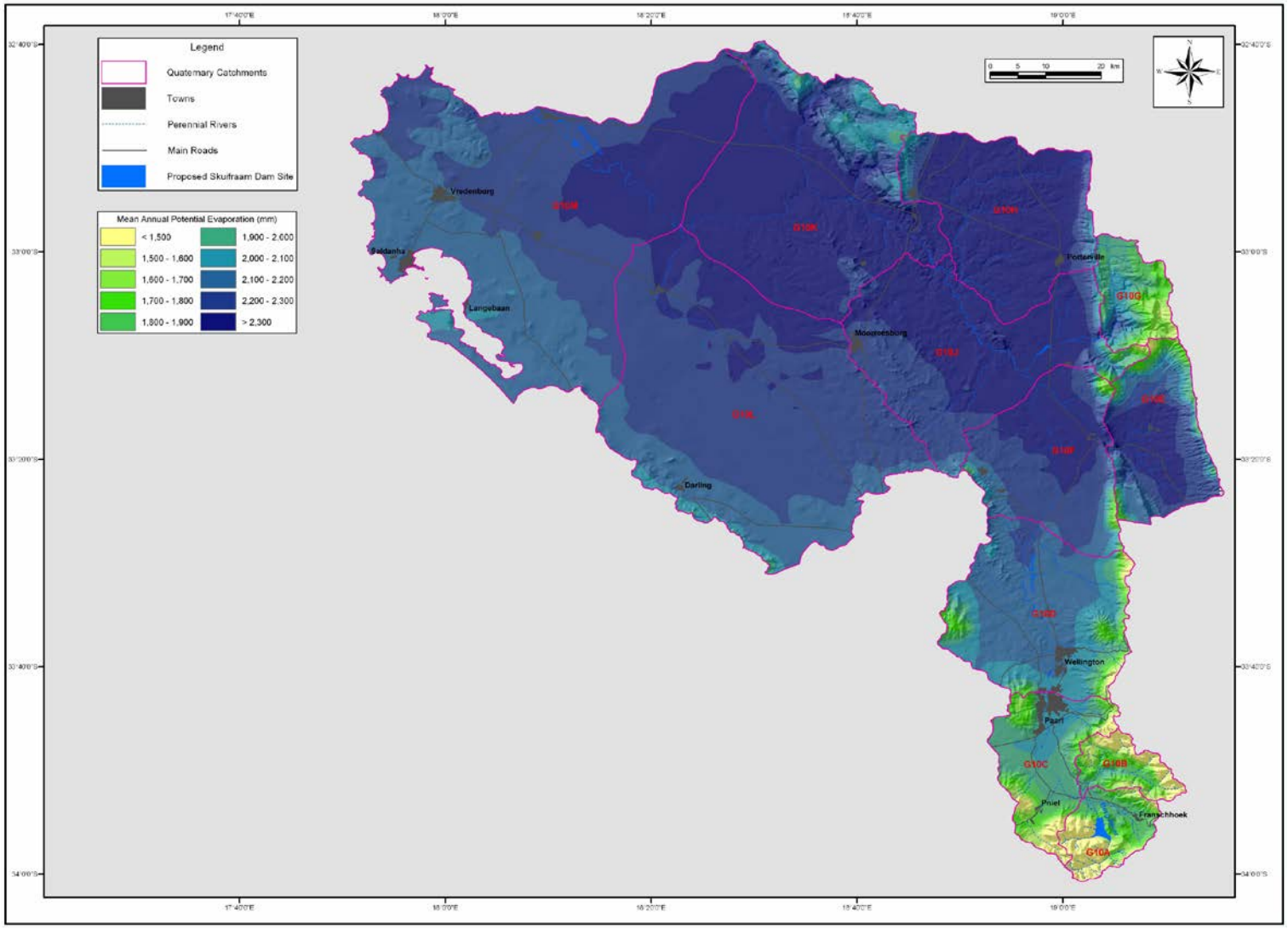

Figure 2.4 Mean annual potential evaporation in the Berg River Catchment (Ractliffe, 2007)

to penetrate far upstream (> 40 km)[4], however these saline waters are readily flushed from the estuary by the freshwater spates if they are of sufficient magnitude. Freshwater spates exceeding 140 m^3/s seemingly are sufficient to fully flush the estuary of saline waters (Schumann, 2009).

In addition to the flushing of saline waters, these freshwater spates are important in that they cause large changes in water level, particularly in the upper reaches of the estuary. This results in the inundation of the estuarine flood plain that is important in terms of supporting the vegetation in the flood plains and also the large numbers of wading birds.

During floods, flows reach 150 to 600 m^3/s along the river. A typical annual flood peak into the estuary is about 90 m^3/s, with a 1:10 year flood measuring about 622 m^3/s (Beck & Basson 2007).

There is also considerable inter-annual variability (Figure 2.5). The smallest flow on record over the last 20 years actually occurred during the 3-year baseline monitoring period. Consequently, the results of the Berg River baseline monitoring study need to be interpreted within this context.

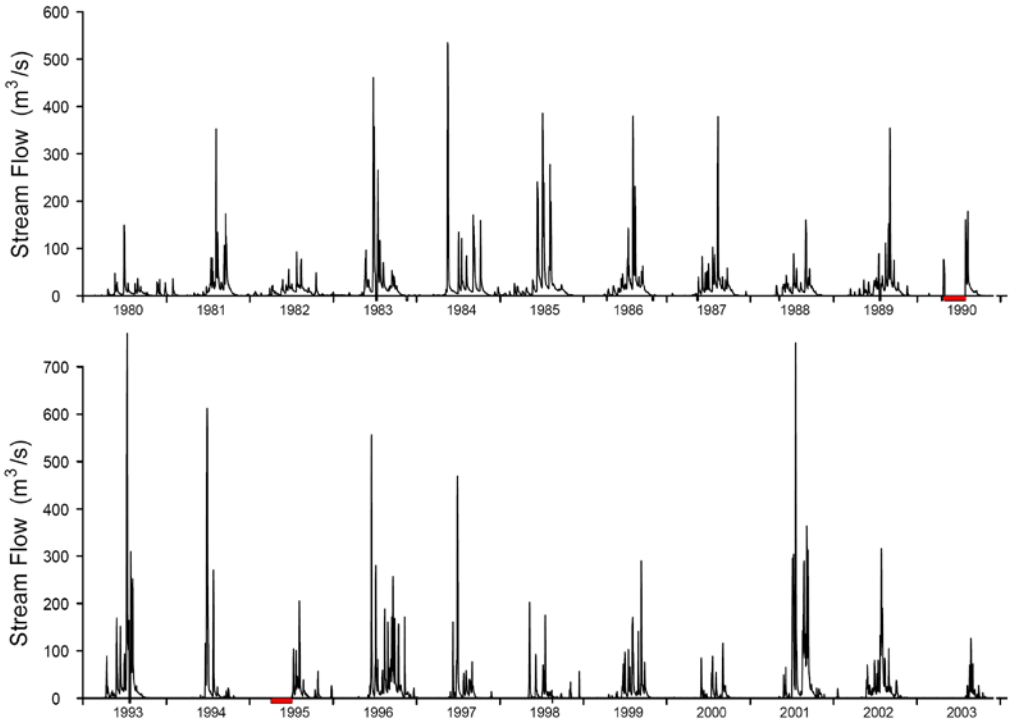

Figure 2.5 **Streamflow measured at the weir at Misverstand over the years 1980 to 2005. Where no readings were taken a negative flow of -10 m^3/s is shown; in particular the three periods missing data in 1990, 1992 and 1995 are indicated in red (after Schumann, 2007).**

[4] *Day (1981) has reported that a salinity of 9 was recorded at Kersefontein in February, 1979, some 45 km from the mouth, that he considered to be partially due to inflows from the Sout River. It should, however, be noted that under present conditions no other observations have been made of saline waters penetrating upstream of Kersefontein.*

2.3. Hydrodynamic functioning of the Berg River Estuary

The Berg estuary is permanently open to the sea and reflects strong seasonal patterns in hydrology, which drive ecological functioning in the estuary. Furthermore, the estuarine floodplain is extensive and an integral part of the river system. It is seasonally inundated and supports large numbers of wading birds. The estuary and floodplain are of national conservation importance for estuarine birds, fish, invertebrates and vegetation. Anthropogenic influences such as water abstraction and dams have reduced the frequency and intensity of the flooding of the floodplain, while agricultural and urban encroachment has reduced the extent of natural vegetation on the floodplain.

The hydrographic character and hydrodynamic functioning of the estuary has been the subject of a number of studies over the years. The most significant of these in terms of the present study are the initial bathymetric surveys and modelling studies by the CSIR (CSIR 1993, Taljaard & Slinger 1992; Taljaard *et al*. 1992a; Slinger & Taljaard, 1994, 1996; Slinger *et al*. 1996, and Slinger *et al*. 1998) and those undertaken as part of the Berg River Baseline Monitoring Programme (Schumann & Brink 2009, Schumann 2009, and Beck & Basson 2007).

The hydrodynamics of the Berg River estuary are complex, owing to the extreme variation in inflow conditions from winter to summer, the gentle gradient (one meter in the last 50 km, Day 1981) and the length of the estuary. The physical characteristics of the estuary are influenced by a range of different processes and driving forces, and their interaction with the morphology of the estuary and its flood plain.

Oceanic influences include sea level variations from tides and weather effects as well as inherent water characteristics such as temperature, salinity, dissolved oxygen, and nutrients. Similarly, at the head of the estuary changes in the volume and characteristics of ***freshwater inflows from the catchment*** strongly influence the physical and biogeochemical characteristics of the estuary. In addition ***groundwater inflow*** within the estuary itself, weather effects such as wind, rain, air temperature, insolation and evaporation, as well as the channel morphology, sediment structure and vegetation on the estuary banks, influence the manner in which the water circulates and mixes under both normal flows and floods.

The renewal of water (flushing) in the estuary, and consequently the water quality within the estuary, is primarily due to tides and freshwater inflows at the head of the estuary. Other potential mechanisms influencing water circulation and water quality include the effects of sub-tidal water level variations in the adjacent ocean, intrusions of cold upwelled oceanic waters and local wind stress (and air-sea interactions).

2.3.1. Flushing Mechanisms

The primary modes of water renewal (flushing) in the estuary are ***tidal diffusion*** and ***through-flow***, while the effects of classical ***estuarine circulation*** are expected to be limited.

The exchange with the adjacent ocean (*i.e*. water of St Helena Bay), is driven mostly by changes in water level (barotropic processes) with only a limited influence of processes

associated with density differences (baroclinic processes) between the estuarine waters and those of the adjacent ocean.

Tidal diffusion

Tidal diffusion results from the cycle of in- and outflows due to the tides. The magnitude of tidal diffusion is proportional to the product of the tidal excursion and tidal velocity, which in turn are determined by the tidal range and variations in channel cross-sectional area. Tidal diffusion is strongest where there are significant changes in estuary width and depth. .

Towards the mouth of the estuary, the tidal water level variations and flows are strong, particularly at the mouth of the estuary. The canalised entrance channel ensures a relatively unconstricted exchange of water between the estuary and the adjacent ocean. Consequently, there is little evidence of the tidal asymmetry observed in estuarine systems with restricted mouths (that typically result in 'tidal pumping" where the fast narrow jet of the incoming tide is followed by a broader more diffuse return flow of the outgoing tide). An element of "tidal pumping" may occur at certain locations in the estuary where the fast narrow jet of the incoming tides is in constrained channels that open out onto tidal flats, and are then followed by a broader more diffuse return flow of the outgoing tide from tidal flats that converge towards the narrow channel areas. This would increase tidal diffusion in the vicinity of these locations.

In addition to tidal forcing, a more slowly varying forcing occurs due to changes in water level at the mouth associated with sub-tidal coastal-trapped wave in the so-called "weather band". This is not only expected to influence the tidal dynamics and mixing but also to have a significant influence on floodplain inundation due to freshwater spates and floods.

Through-flow

Through flow is associated with the freshwater spates and floods that occur during the rainy season when the river flow is strong enough to push the existing waters out of the estuary and replace these with new river water. Due to the tendency for a freshwater layer to develop over the denser saline water in estuaries, fully-developed through-flow only occurs when the freshwater inflows are strong enough to overcome these stratification effects. Whilst such stratification is observed in the early stages of such freshwater inflows into the Berg estuary, the stratification does not persist and consequently the saline waters are relatively easily flushed from the estuary, especially in the upper and middle reaches of the system. Such through-flow effects in the Berg River are thus significant, particularly in the upper reaches which are relatively easily flushed by even moderate freshwater inflows. Schumann (2009) estimated that freshwater spates exceeding 140 m^3/s would completely flush saline waters out of the estuary on the outgoing tide.

Estuarine circulation

Classical estuarine circulation in the Berg estuary is limited, as most of the time the Berg estuary remains largely unstratified. Tidal flows and other mixing mechanisms generally ensure a well-mixed water column in the estuary. Stratification is only observed for short periods in the middle reaches of the estuary during freshettes and floods and, to a much

lesser extent, near the mouth of the estuary during periods of strong upwelling, particularly during spring tides. However, in the middle reaches of the estuary, stratification is observed during neap tides (see Figures A,6c and d and A8c and d) rather than spring tides (see Figures A 6a and b and A 8a and b) when the water column is well-mixed. The implication is that the strong flows and significant flooding of intertidal areas associated with spring tides in the middle to upper reaches, results in the well-mixed water column observed during spring tides. During neap tides the tidal turbulence and flooding of adjacent intertidal areas is significantly reduced (compared to spring tides), allowing a degree of stratification to develop in the water column. The limited estuarine circulation means that the estuary is more easily flushed by a specific magnitude of freshwater flow than would an estuary where estuarine circulation is significant (*e.g*. van Ballegooyen *et al*. 2004).

Largier *et al*. (2000) succinctly summarise the efficacy of these flushing mechanisms as follows: The extent of tidal diffusion depends on the tidal range and variations in channel cross-sectional area. The efficacy of through-flow depends on the flow rate of the river. The efficacy of estuarine circulation depend on the magnitude and extent of the longitudinal density gradient and magnitude of vertical mixing that, in turn, are related to river flow, strength of tidal flows, water depth, the nature of the bottom and the strength of local winds and local air-sea interactions. As noted above estuarine-type circulation is insignificant in the Berg estuary.

2.3.2. Water **level** *variability*

The largest contribution to water level variability in the estuary is that of the tides, however at the upstream extremity of the estuary the water level variability associated with freshwater inflows dominates.

High frequency variability

Shillington (1984) has described the existence of edge waves with periods of 20 to 60 minutes, which reached an amplitude of 1.5 m near the Orange River some 500 km to the north of the mouth of the Berg River in St Helena Bay. These are ignored for the purposes of this study as the high frequency nature of these oscillations is unlikely to substantive influence the estuarine dynamics of relevance in this study.

Tidal variability

The tides along the South African coastline are semi-diurnal and dominated by the M2 lunar tide with a period of 12.42 hours (Open University, 1989). Interaction of the M2 lunar tide with the K1 solar diurnal tide (with a period of 23.93 hours) results in spring and neap tides, characterised by a spring tide range seldom reaching above 2 m and a neap tide range as small as 0.5 m. The measured water levels at Saldanha Bay are considered a good proxy for those occurring in St Helena Bay (see Table 2.1). It is not expected that analyses of measured water levels at Laaiplek will indicate significantly different tidal characteristics to those tabulated below.

Table 2.1 Tidal characteristics for Saldanha Bay.

Tidal Characteristic	Tidal level relative to Chart Datum (m)
Highest Astronomical Tide	*2.03*
Mean High Water Springs	*1.75*
Mean High Water Neaps	*1.27*
Mean Level	*0.99*
Mean Low Water Neaps	*0.70*
Mean Low WaterSprings	*0.24*
Lowest Astronomical Tide	*0*

The only data available to characterise temporal and spatial scales of the water level variations within the Berg estuary are those measured by the CSIR in 1996 as input into one-dimensional modelling studies (*e.g.* CSIR 1992) and ongoing measurements at the Department of Water Affairs (DWAF) water level gauges (see Table 2.2) at Kliphoek and Jantjiesfontein (since 1980) and at Laaiplek (since October 2003).

Table 2.2 Continuous water level recorders in the Berg Estuary

Site	ID	Start date of measurements
Kliphoek	G1H024	1980.10.01
Jantjiesfontein	G1H023	1980.10.01
Laaiplek	G1H074	2003.10.21

Changes in water level due to tides are not the only water level variations of importance in the Berg estuary. de Cuevas *et al.* (1986) described subtidal coastal-trapped waves with typical amplitudes around 15 cm (*i.e*. sub-tidal water level variability range ~ 30 cm). Brundrit (1984) investigated variability on monthly and seasonal scales of these waves. On even longer time scales, Hughes *et al.* (1991) demonstrated that there has been a sea level rise of about 1.2 mm/yr, consistent with other tectonically stable world trends.

During March 1990, six water level recorders were installed by the CSIR in the Berg estuary for a few weeks (see Figure 2.6). To illustrate the complexity of tidal variation, data collected on 11-12 March 1990 (spring tides) are used. Fortuitously, the tidal ranges during this period correspond very well with the mean spring and neap tide conditions reported by the South African Hydrographic Office (Table 2.2).

The recorded water level variation immediately inside the mouth was roughly the same as the predicted tidal variation at Saldanha Bay, which implies that the present mouth is not sufficiently restrictive to reduce tidal variation. Between the mouth and the farm Kliphoek[5],

[5] *Although the Kliphoek water levels were measured in an occluded meander of the Berg River Estuary and could thus suffer a reduction in amplitude in this meander due to potential restrictions in bathymetry, the data show no strong evidence in the amplitude or form of the tidal variations of this having occurred. It is for this reason that it is recommended that a water level gauge be installed in the estuary somewhere between 20*

approximately 15 km upstream, a reduction in tidal amplitude of between 65% (spring tides) and 56% (neap tides) occurs (see Table 2.3 and Figure 2.7). A slight amplification in tidal variation takes place between Kliphoek and Kersefontein, 46 km upstream of the mouth. It is not clear how the tidal amplitudes vary between these stations as no water levels have been measured between Kliphoek and Kersefontein. Such amplifications in tidal variation are known to occur in estuaries and are usually caused by funnelling as the estuary becomes shallower and narrower with distance upstream. Just upstream of Kersefontein, the estuary narrows as does the adjacent floodplain. The tidal amplitude decreases rapidly between Kersefontein and Rasgat, where the tidal amplitude ranges between 11% (spring tide) and 17% (neap tide) of that measured at the mouth of the estuary. At Steenbokfontein the tidal amplitude reduces to between 4% and 10% of that measured at the mouth of the estuary. The measured data reported by Schumann and Brink (2009) show similar trends (Table 2.3 and Figure 2.8).

Table 2.3 Tidal range and normalised tidal range (normalised by tidal range at the mouth of the estuary) at various location on the Berg River Estuary

Site	Distance upstream (m)	Spring tide		Neap tide	
		Tidal range (m)	Normalised tidal range (m)	Tidal range (m)	Normalised tidal range (m)
Mouth (CSIR 1990)	0	1.51	1.00	0.60	1.00
Laaiplek (G1H074)	545	-	0.93*	-	-
Kliphoek (G1H024)	11300	-	0.35*	-	-
Kliphoek (CSIR 1990)	15000	0.53	0.35	0.26	0.44
Kersefontein (CSIR 1990)	46990	0.62	0.41	0.36	0.60
Jantjiesfontein (G1H023)	51000	-	0.14*	-	-
Rasgat (CSIR 1990)	57528	0.17	0.11	0.1	0.17
SoutKloof (CSIR 1990)	65070	0.09	0.06	0.06	0.11
Steenbokfontein (CSIR 1990)	70987	0.06	0.04	0.06	0.10

** values estimated from water level data reported in Schumann and Brink (2009).*

and 40 km upstream to clarify how tidal water level variability changes between Kliphoek and Kersefontein. This knowledge is important to both the water quality and flooding studies.

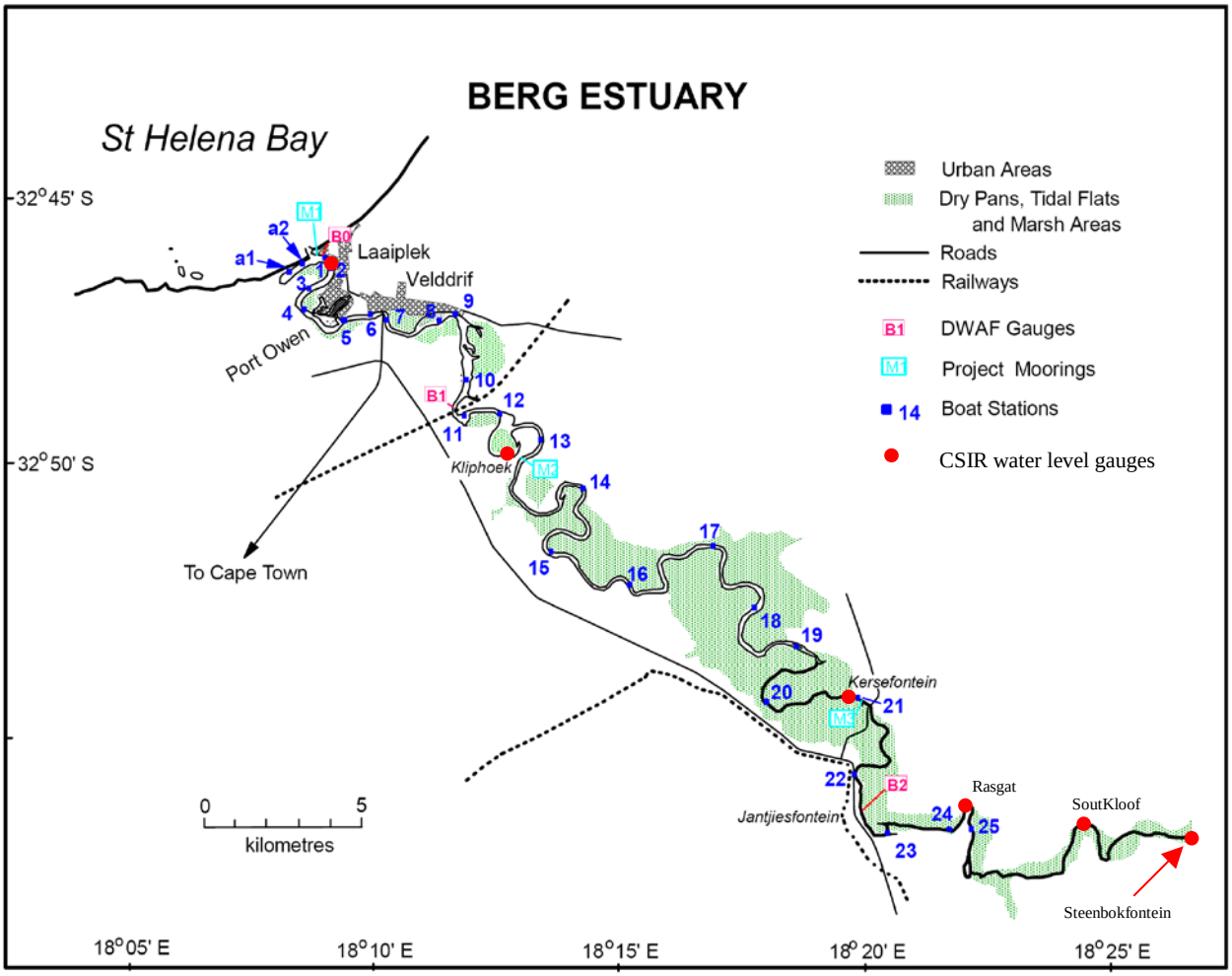

Figure 2.6 **Map showing the location of water level measurements in the Berg estuary as well as the boat (water quality) stations occupied during the Berg River Baseline Monitoring Programme (map adapted from Schumann 2007)**

The water depth varies considerably along the length of the estuary, and there are wide tidal flats with very shallow areas. Water depth in the estuary varies with the tide, affecting the speed of the tidal wave. However, the lags in tidal variations along the estuary are predominantly a frictional effect. Slinger & Taljaard (1994) report that high tide lagged the mouth by 4 hours at Kliphoek and 2.3 hours at low tide. At a position 56 km from the mouth, the lags were 7 hours and 6.7 hours at low and high tides respectively. Note that these readings did not consider the effects of the longer-period water level variations. A more detailed analysis of tidal lags from both the CSIR March 1990 water levels recordings and measured water levels from DWAF water level recorders is given in Table 2.4.

Flow direction in the upper estuary can be opposite to those at the mouth due to these tidal delays (Huizinga *et al*. 1994; Slinger & Taljaard, 1994).

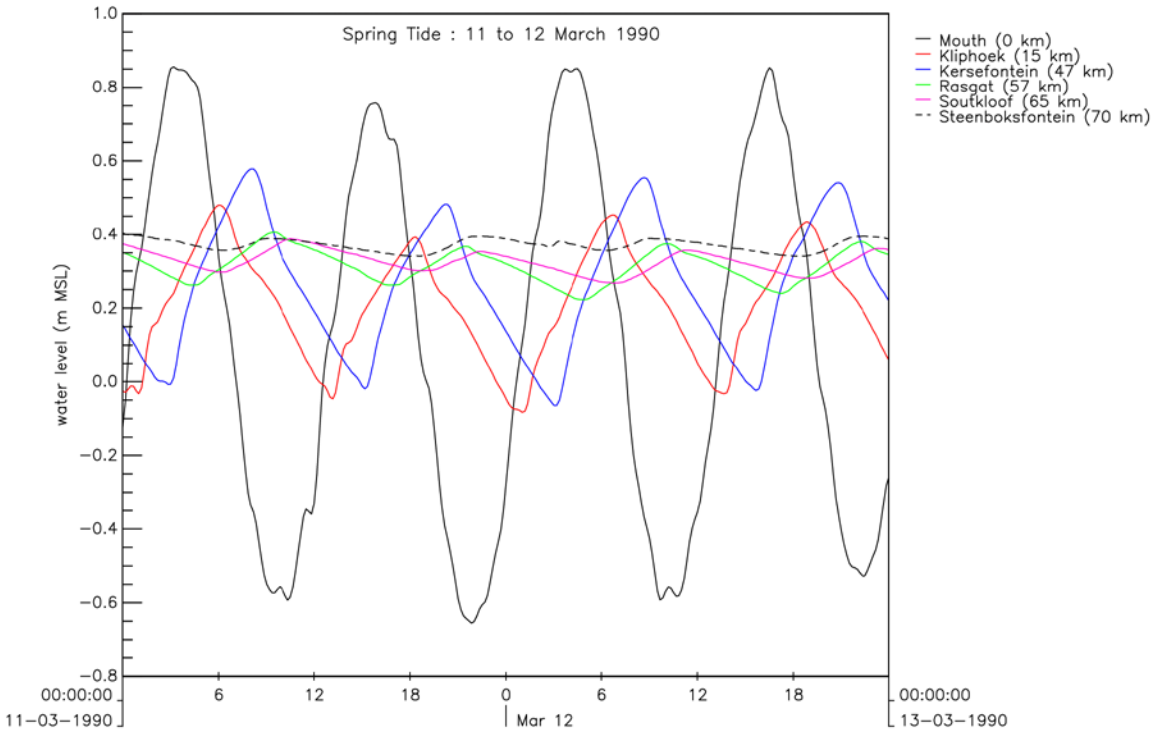

Figure 2.7a Spring tide water levels as measured by the CSIR in March 1990.

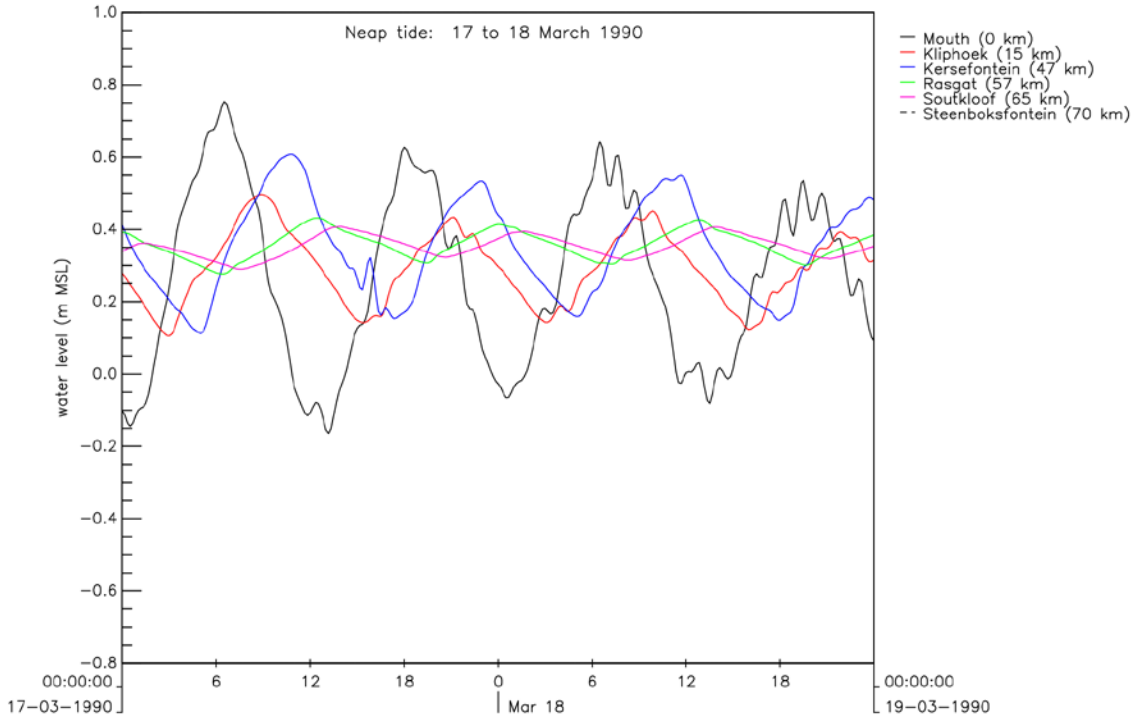

Figure 2.7b Neap tide water levels as measured by the CSIR in March 1990.

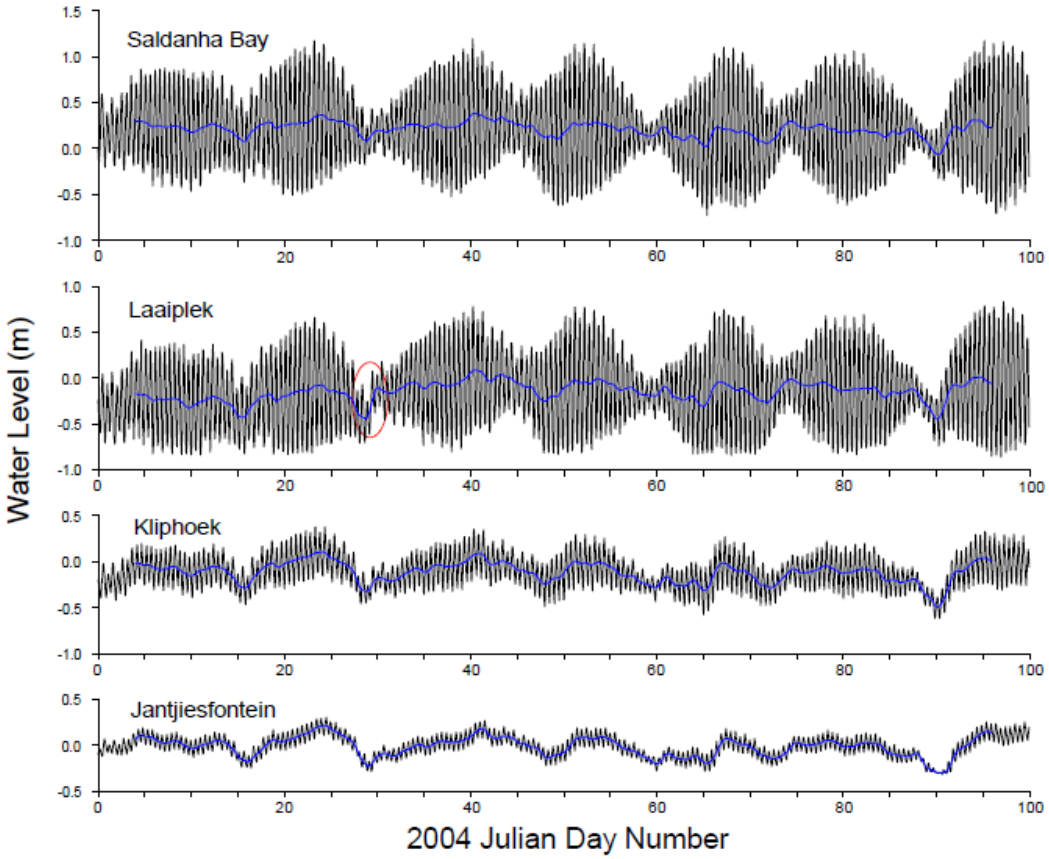

Figure 2.8 **Measured water level[6] at Saldanha Bay, Laaiplek, Kliphoek and Jantjiesfontein. The blue lines show the longer-period fluctuations (Source: Schumann 2007).**

Table 2.4 **Tidal range and normalised tidal range (normalised by tidal range at the mouth of the estuary) at various location on the Berg River Estuary.**

Site	Distance upstream (m)	Spring tide		Neap tide	
		Tidal lag (trough)	Tidal lag (peak)	Tidal lag (trough)	Tidal lag (peak)
Mouth (CSIR 1990)	0	0 m	0 m	0.60	1.00
Laaiplek (G1H074)	545	35 m*	35 m*	-	-
Kliphoek (G1H024)	11300	3h 24m*	3h 07m*	-	-
Kliphoek (CSIR 1990)	15000	3h 14m	2h 42m	2h 50m	2h 50m
Kersefontein (CSIR 1990)	46990	5h 16m	4h 42m	4h 37	3h 35m
Jantjiesfontein (G1H023)	51000	6h 40 m*	6h 22m*	-	-
Rasgat (CSIR 1990)	57528	6h 57m	6h 05m	6h 24m	5h 27m
SoutKloof (CSIR 1990)	65070	7h 00m	7h 12m	6h 55m	6h 43m
Steenbokfontein (CSIR 1990)	70987	8h 50m	8h 28m	-	-

**Tidal lags (compared to Saldanha Bay water level measurements) as reported by Schumann and Brink (2009) for a period between spring and neap tides.*

[6] *These data are reportedly referenced to MSL, however this is incorrect as the water levels as reported would imply that the water level at Saldanha Bay is some 0.5 m higher than at Laaiplek, a situation that is unlikely to be correct.*

Longer period variability

Subtidal water level fluctuations are observed along the entire length of the estuary. These subtidal water level fluctuations have typical amplitudes of 15 to 20 cm, ranging up to 30 cm or more on occasion. These subtidal water level fluctuations, so called event scale variability, are associated with subtidal changes in water level in the adjacent ocean (coastally trapped waves and more local weather effects) that propagate upstream in the Berg estuary. Negative fluctuations in subtidal water levels in St Helena Bay (*i.e.* at the mouth of the estuary) are associated with S to SE wind conditions offshore, and associated upwelling of cold waters, while positive fluctuations are associated with NW offshore winds and downwelling (and to a lesser degree wave set-up). Figure 2.8 shows the water level variability both at tidal periods and at periods longer than the diurnal tidal period (Schumann 2007).

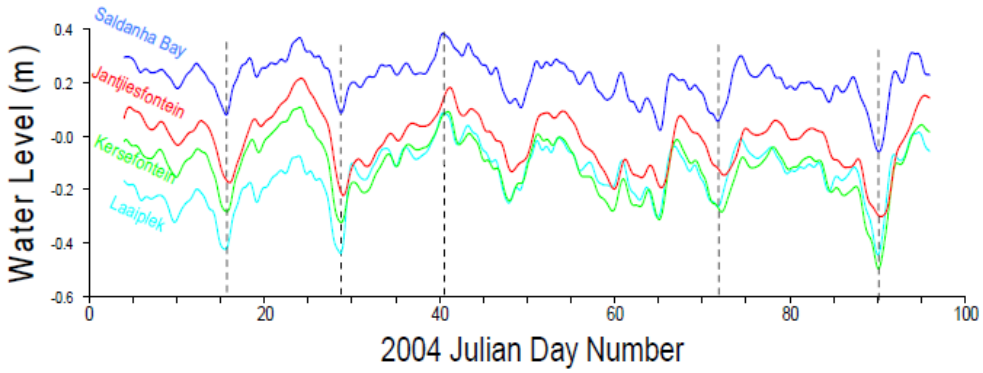

Figure 2.9 Longer-period water level variability at Saldanha Bay, Laaiplek, Kliphoek and Jantjiesfontein (Source: Schumann, 2007).

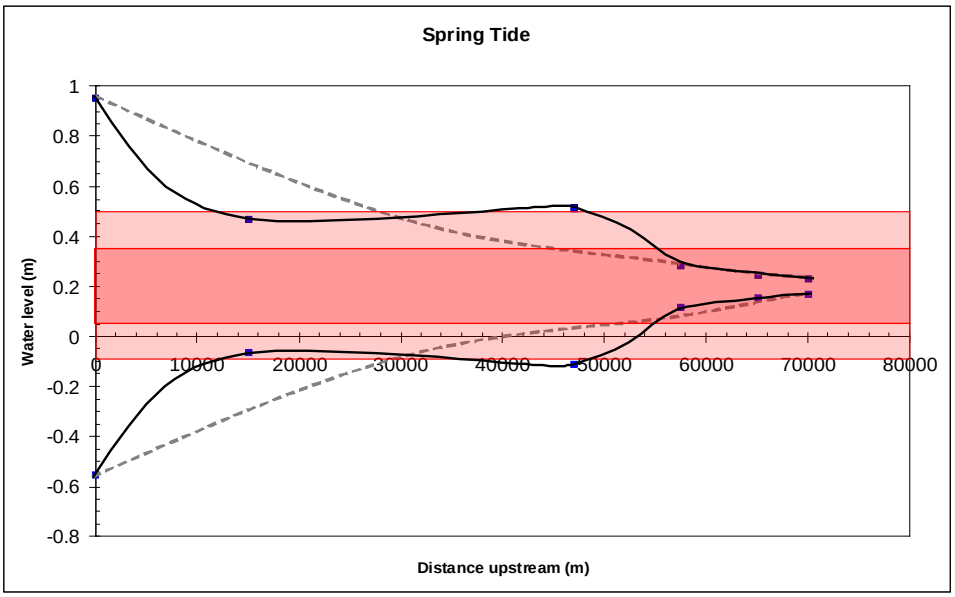

Figure 2.10 Water level variability plotted as a function of upstream distance. [7]

[7] The black solid line is the measured spring tide tidal range, the dotted black line is the theoretical upstream decay in spring tide tidal range and the light red area denotes the likely range of extreme amplitudes of subtidal fluctuations and the darker region the most likely range of typical subtidal fluctuations in water level.

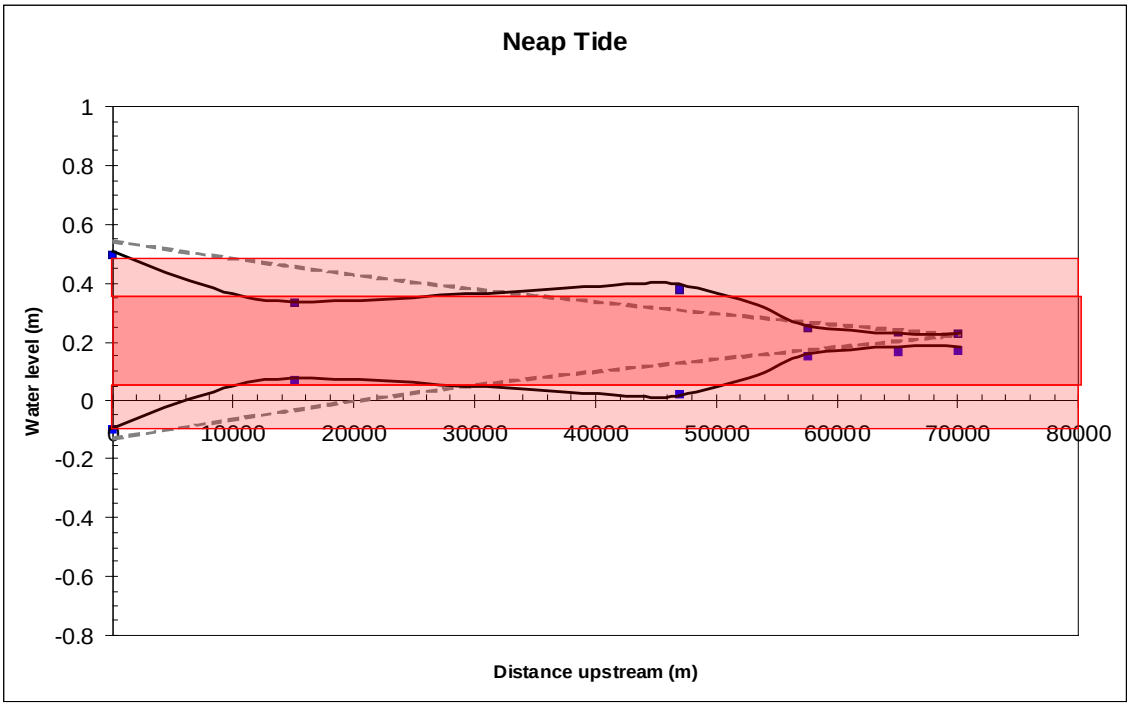

Figure 2.10b Water level variability plotted as a function of upstream distance. [8]

These low frequency water level fluctuations propagate largely unattenuated upstream to at least Jantiesfontein and probably much further (see Figure 2.9). There is a small amplification of the subtidal signal in water levels measured immediately within the estuary at Laaiplek compared to those measured in the adjacent ocean[9] at Saldanha Bay (Figure 2.9).

Spectral analyses of the water level data at Laaiplek, Kliphoek and Jantjiesfontein show a phase lag of 4 hours at Kliphoek and 11 hours at Jantjiesfontein over the whole subtidal frequency band (Schumann and Brink, 2009). This compares well with visual estimates of a 10 hour phase lag in subtidal water level fluctuation for Jantjiesfontein.

These longer-period oceanic water level variations are more noticeable in the upper reaches of the Berg Estuary than tidal variations. Schumann & Brink (2009), using only the three DWAF water level gauges on the Berg River Estuary, report that the sub-tidal water level fluctuations start to dominate upstream of Kliphoek. However this is not strictly true as there is an amplification of tidal levels upstream of Kliphoek, such that the observed tidal fluctuations at Kersefontein exceed those measured at Kliphoek.

8 The lack solid line is the measured neap tide tidal range, the dotted black line is the theoretical upstream decay in neap tide tidal range while the light red area denotes the likely range of extreme amplitude of subtidal fluctuations and the darker region the most likely range of typical subtidal fluctuations in water level.

9 Water level measurements at Saldanha Bay are considered to adequately represent water level variability occurring in St Helena Bay, particularly those associated with subtidal water level variability. This amplification of the subtidal signal at Laaiplek may be an artifact of this assumption should the amplitude of subtidal water level variability be greater in St Helena Bay than in Saldanha Bay.

The relative magnitude of tidal (derived from the more detailed CSIR 1990 water level measurements) and sub-tidal fluctuations on moving upstream in the estuary are plotted in Figures 2.10a and b. These data indicate that the subtidal fluctuations under spring tide conditions only really dominate normal tidal water level variability upstream of Jantjiesfontein (> 50 km upstream). Under neap tide conditions, tidal water level variations are either on a par with or slightly exceed typical subtidal water level variations between Kliphoek and Kersefontein, depending on the magnitude of the subtidal water level variations. Only upstream of Jantjiesfontein does the magnitude of subtidal water level variability clearly exceed that of normal tidal water level variations.

The total intertidal area of the various reaches was estimated from the DTM and tidal water level (that have been adjusted for the upstream attenuation of the tidal signal). These estimates of inundation (and intertidal) areas and volumes are listed in Tables 2.5a and 2.5b, respectively.

Table 2.5a Inundation areas for various water levels and spring and neap tide intertidal areas (with water levels adjusted for attenuation of tidal signal upon moving upstream)

	Water Level (m MSL)	Reach 1	Reach 2	Reach 3	Reach4	Total for all Reaches
		Total Area Inundated (km²)				
MHWS	0.97	5.96	8.20	1.93	9.65	25.73
MHWN	0.49	4.76	6.90	1.74	8.42	21.82
ML	0.21	1.78	5.10	1.40	7.24	15.51
MLWN	-0.08	1.36	3.71	1.12	5.54	11.73
MLWS	-0.54	1.11	3.26	1.07	5.36	10.80
	Tidal Range (m)	Total Intertidal area (km²)				
Spring tides	1.51	4.85	4.93	0.86	4.29	14.93
Neap tides	0.57	3.40	3.19	0.62	2.88	10.09

Table 2.5b: Inundation volumes for various water levels and spring and neap tide intertidal areas (water levels adjusted for attenuation of tidal signal upon moving upstream)

	Water Level (m MSL)	Reach 1	Reach 2	Reach 3	Reach4	Total for all Reaches
		Total Area Inundated (km²)				
MHWS	0.97	3.14	7.37	2.58	11.85	24.93
MHWN	0.49	2.61	6.53	2.42	9.83	21.39
ML	0.21	2.63	5.40	2.09	7.70	17.81
MLWN	-0.08	1.21	4.57	1.82	5.97	13.57
MLWS	-0.54	0.88	4.22	1.74	5.83	12.68
	Tidal Range (m)	Total Intertidal area (km²)				
Spring tides	1.51	2.25	3.14	0.84	6.02	12.25
Neap tides	0.57	1.39	1.96	0.60	3.86	7.82

Changes in upstream water levels due to freshwater inflows

The remaining driver of significant water level variability in the Berg River estuary is that due to freshwater inflows into the upper estuary. The magnitudes of these increases in water level associated with freshwater inflows are significant in the uppermost reaches of the estuary only.

Measured data indicate that water levels in the upper reaches of the estuary increase with both increasing base flows (Figure 2.11) as well as for freshettes and floods (Figure 2.13). The measured water levels at Jantjiesfontein and freshwater inflows to the estuary as reported by Beck & Basson (2007) show a clear relationship between water level and magnitude of winter baseflow. The water level at Jantjiesfontein increases more or less linearly with increasing freshwater inflows up to approximately 40 m^3/s. For freshwater inflows above 40 m^3/s the rate of increase in water level (measured at Jantjiesfontein) with increasing freshwater inflows begins to slow until, at freshwater inflows exceeding between 80 and 100 m^3/s, there is little or no increase in water level with increasing freshwater inflow. The reason for this is that the water level rises to such an extent for these higher flows that the estuary breaks its banks and flows onto the adjacent flood plain.

This relationship between the rise in upstream water level and the magnitude of seasonal base flows was utilised to develop appropriate model scenarios for determining the effects changes in winter base flow on the flooding regime in the estuary.

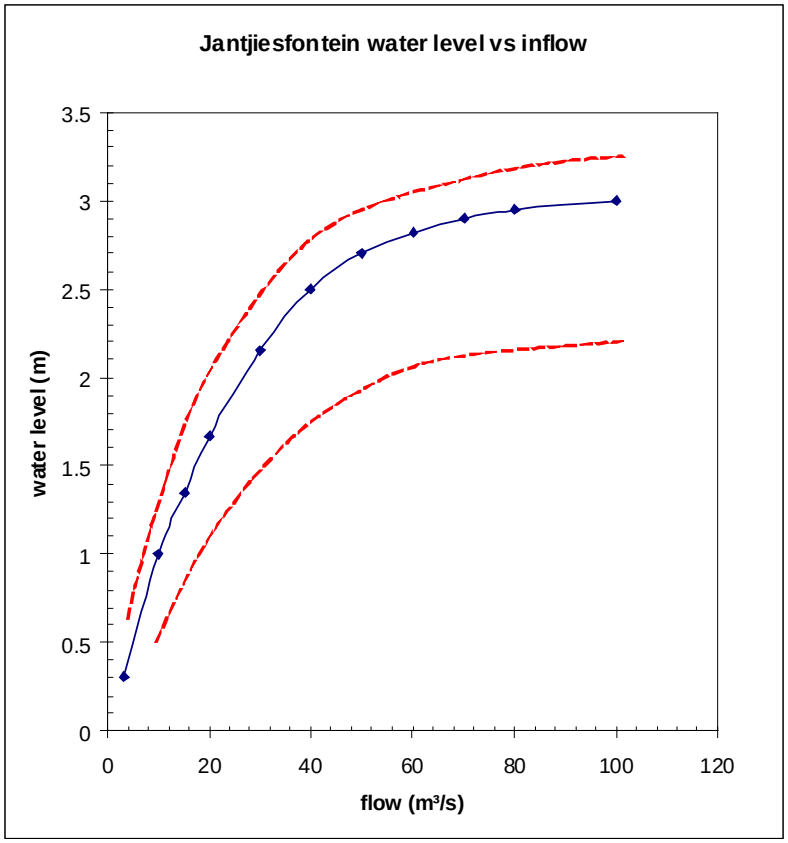

Figure 2.11 Schematic of the relationship between the measured water level at Jantjiesfontein and the estimated freshwater inflows to the estuary for the period January 1995 to November 2003.

What is not clear is how the water levels vary with changing base flow at other locations further downstream in the estuary. This change in water level (for changing winter base flows) upon moving downstream is important in characterising potential flooding[10] associated with combinations base flows and flood sizes associated with past (natural), present (with Berg River dam) and potential future scenarios.

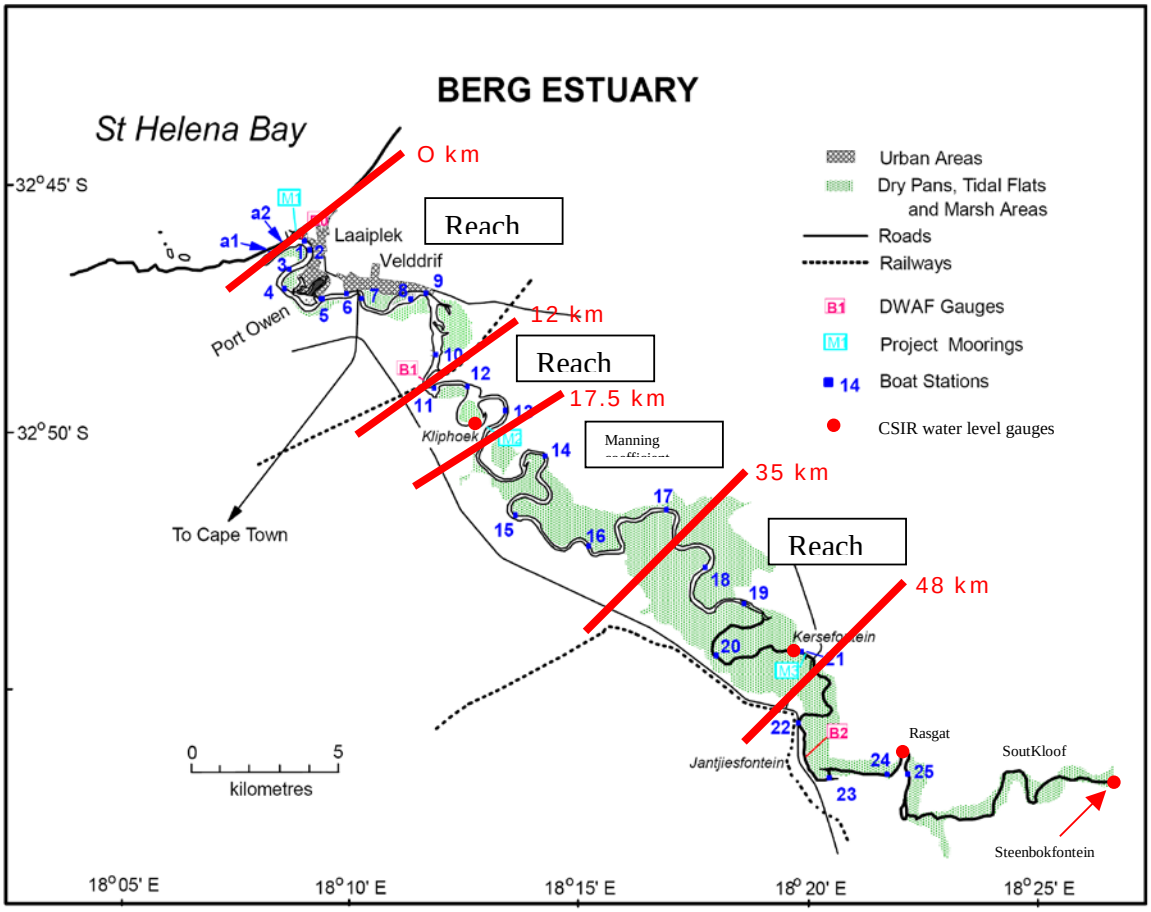

Figure 2.12 Flood zones defined for the Berg River Baseline Modelling Studies (Beck and Basson (2007).

The morphology of the estuary and its adjacent flood plains (and associated vegetation types and ecology) was used to define a number of flood reaches in the estuary (see Figure 2.12) for the Berg River Baseline Monitoring Programme. Beck & Basson (2007) used these in

[10] *Past studies suggested a very strong relationship between the extent of flooding and the magnitude of winter base flows (Beck & Basson 2007; Ractliffe, 2009). However, these finding were based on the flood modelling studies of Beck & Basson (2007,) that seemingly failed to fully take into account this variation in water level upon moving downstream for specified winter base flows. In their flood modelling studies, Beck and Basson (2007) used a linear interpolation of the water level measured at Jantiesfontein and that measured at the mouth of the estuary as an initial water level condition in their modelling domain, rather than specifying in more detail the changes in water level profile along the length of the estuary under the various winter base flow scenarios considered. This led to the overemphasis of the importance of the magnitude of winter base flows and the underestimation of the importance of flood sizes in their studies as well as those of Ractliffe (2009).*

their flood modelling studies. In this study we have adopted these definitions so as to ensure continuity between their results and those presented here.

Due to the existence of only three (DWAF) water level gauges along the length of the estuary (see Figure 2.6) it is not possible to use measured water levels to characterise the changes in water level that occur along the length of the estuary for various steady winter base flows. The existence of extensive flood plains downstream of Jantjiesfontein, suggests that the strong relationship between measured water level and rate of freshwater inflows will break down as the waters flood the adjacent floodplains upon moving downstream. This is confirmed by the flood modelling results of this study. These results make it possible to characterise the changes in water levels that occur for various characteristic base flows and flood sizes and consequently to estimate the likely effect of changes in winter base flow conditions on the flooding regime in the estuary.

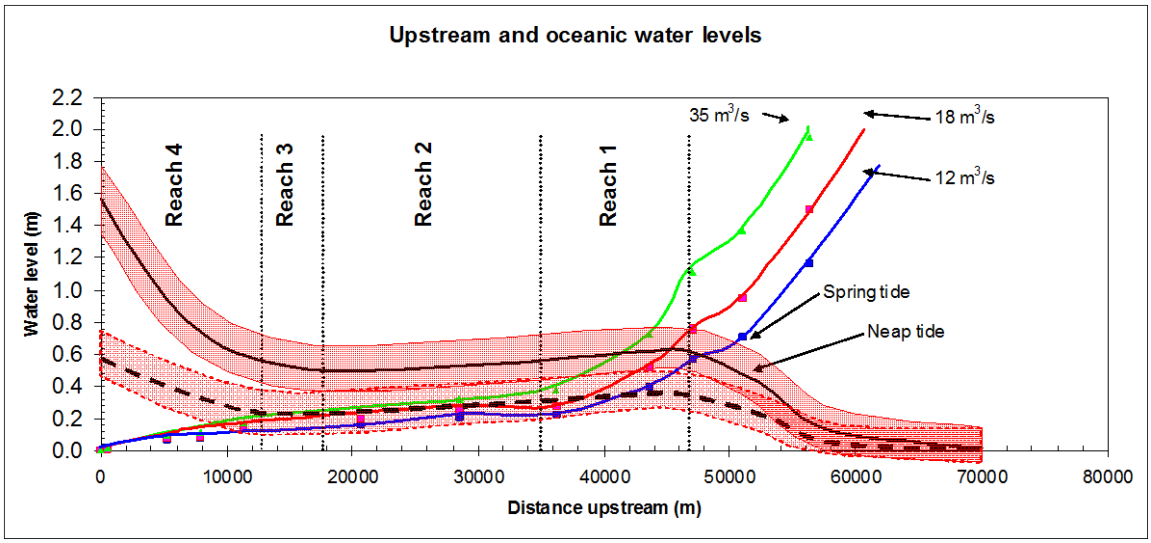

Figure 2.13a Schematic of the along estuary water level profile (relative to the mean water level of 0.2m MSL) associated with various winter base flows. For reference, the magnitude of the spring (solid black line) and neap (dotted black line) tidal ranges have also been plotted. The red bands around the tidal ranges in the plot represent the magnitude of possible change in tidal water levels associated with sub-tidal water level variability.

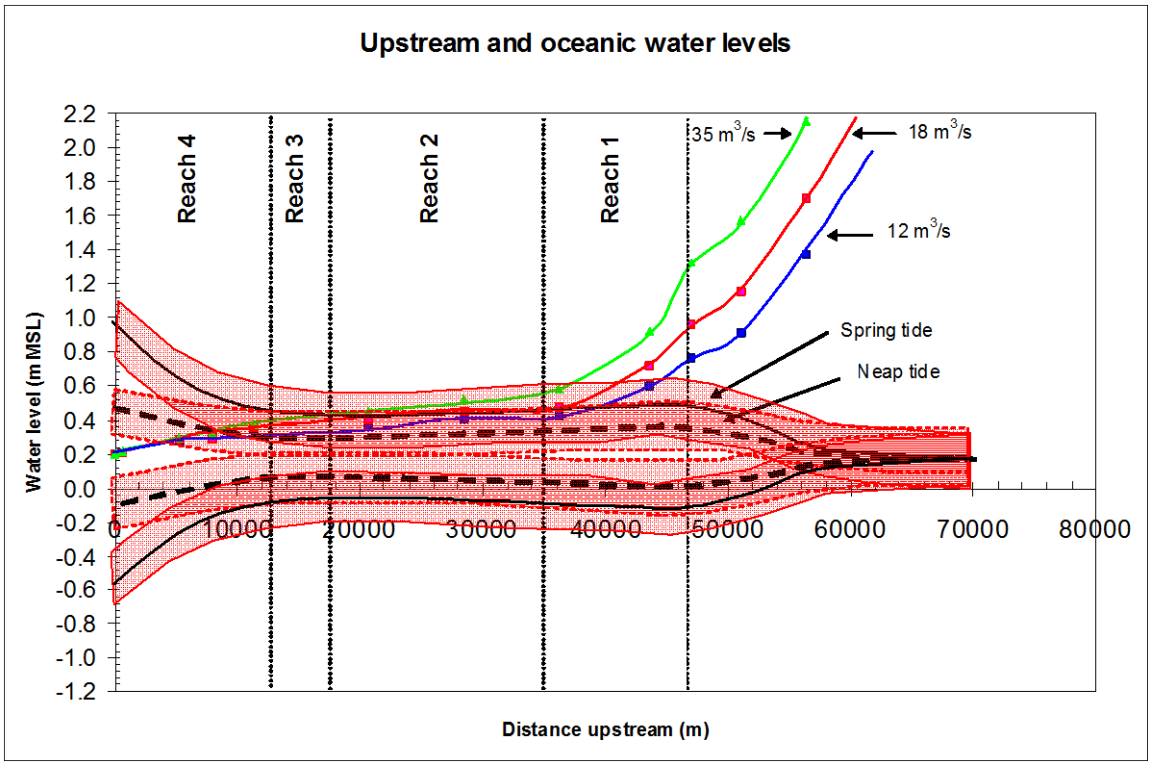

Figure 2.13b Schematic of the along estuary water level profile (relative to MSL) associated with various winter base flows. For reference, the high and low tide water levels during spring (solid black line) and neap (dotted black line) tide have also been plotted. The red bands around the tidal water levels represent the magnitude of possible change in tidal water levels associated with sub-tidal water level variability.

The model results in Figure 2.13a indicate a rapid decrease in water levels downstream of Rasgat (~51 km upstream) and a "flattening of these water levels between Jantjiesfontein (~51 km upstream) and Kersefontein (~45 km upstream), followed by a continued rapid downstream decline in measured water levels until the boundary between flood reach 1 and flood reach 2 is reached (*i.e*. approximately 33 km upstream of the mouth). Downstream of this location there is very little difference between the water level for winter baseline flows of between 35 m^3/s (natural base flow conditions) and 12 m^3/s (base flow conditions under the more extreme development scenarios considered in this study). The implication is that variations in winter base flow are unlikely to influence significantly the flooding behaviour in the estuary downstream of flood Reach 1. Comparison of Figures 2.10 and 2.13a suggest that tidal influences on water level will predominate downstream of Kliphoek (~15 km upstream), i.e. in Reach 4. The influence on water level variability due to tides (and to a lesser extent subtidal fluctuations originating in the adjacent ocean) will predominate between Kliphoek and the boundary between Reach 1 and 2 (*i.e*. will predominate in flood Reaches 2 and 3). Within Reach 2, the effect of winter base flow (compared to that of the dry season) on the water levels in the estuary is comparable to that of sub-tidal changes in sea level in the adjacent ocean. The results in Figure 2.13a also suggest that upstream of Reach 2 the effect of changes in winter base flow on water levels is likely to exceed those due to both tides and sub-tidal variability. In flood Reach 1 and further upstream, the predominant influence on the water levels measured is that of freshwater inflows (i.e. winter

base flows, freshettes and floods). The sub-tidal variations in oceanic water levels propagate upstream more or less unattenuated and thus also play a role (albeit small) in the variability in water levels in these upstream reaches.

Maximum modelled water levels along the axis of the estuary for a range of flood sizes (Figure 2.14a and b) suggest that water level variability in Reaches 1 and 2 (and to a lesser extent Reach 3, depending on flood size) is predominantly driven by freshettes and floods. These results also suggest that only floods exceeding 500 m^3/s will be clearly identified in the measured water levels downstream of the Kliphoek water level gauge (*i.e*. downstream of the railway bridge).

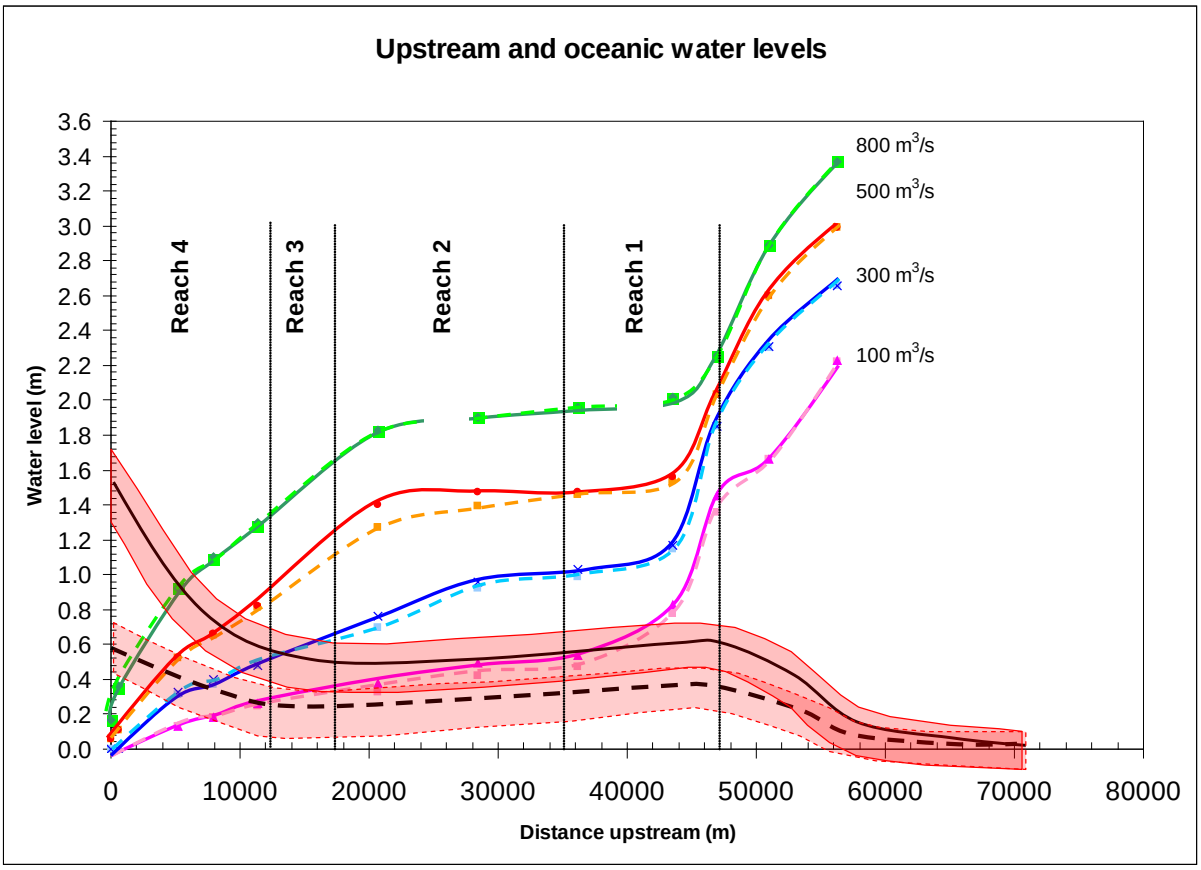

Figure 2.14a Schematic of the along estuary water level profile (relative to the mean water level of 0.2m MSL) associated with a range of flood sizes. For reference, the magnitude of the spring (solid black line) and neap (dotted black line) tidal ranges have also been plotted. The red bands around the tidal ranges in the plot represent the magnitude of possible change in tidal water levels associated with sub-tidal water level variability.

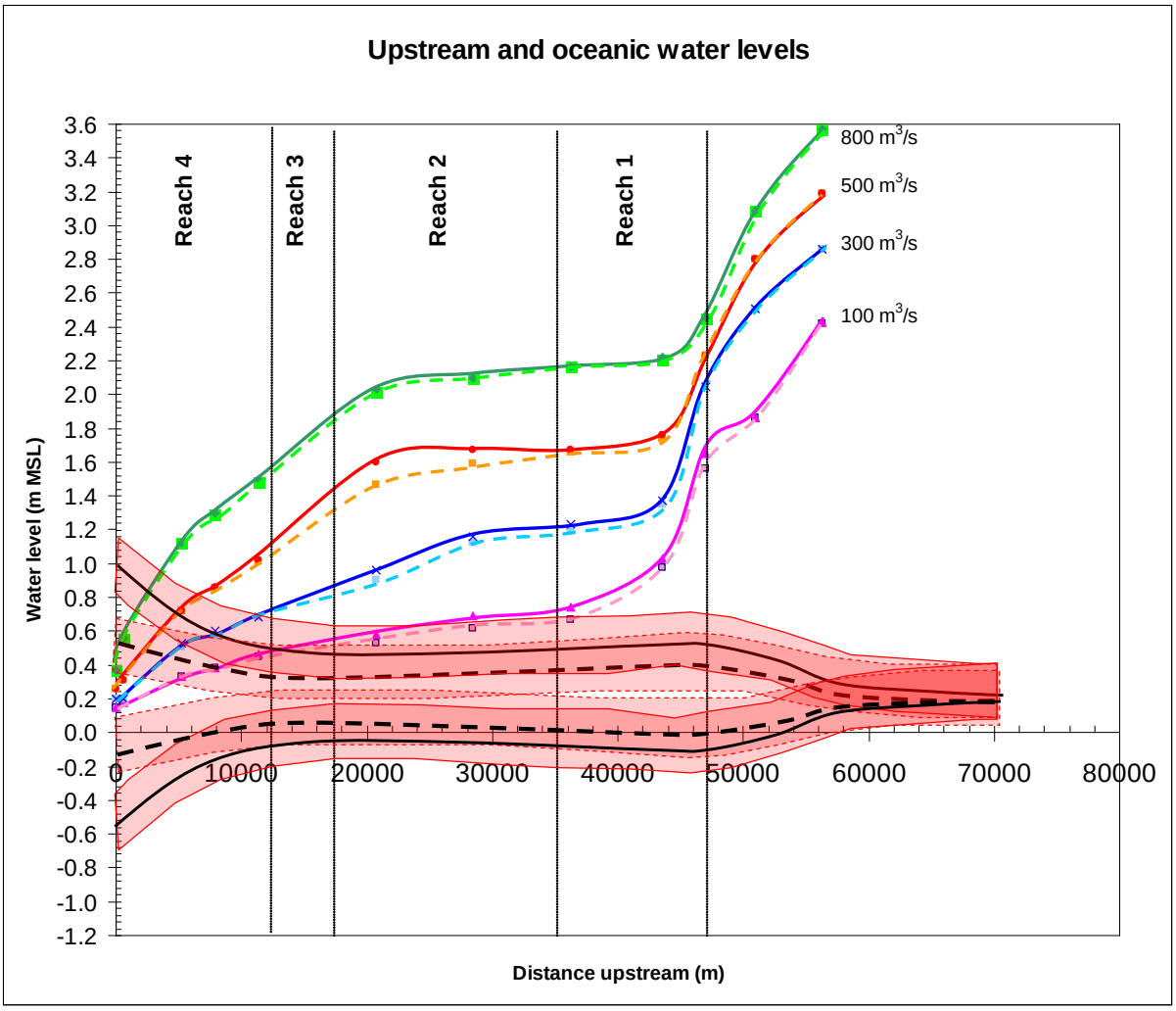

Figure 2.14b Schematic of the along estuary water level profile (relative to MSL) associated with of flood sizes. For reference the high and low tide water levels during spring (solid black line) and neap (dotted black line) tide have also been plotted. The red bands around the tidal water levels represent the magnitude of possible change in tidal water levels associated with sub-tidal water level variability.

Analysis of the measured water level (with tidal effects removed by low pass filtering[11]) at the Kliphoek water level gauging site (just downstream of the Railway Bridge) indicate that there is a slow linear rise in water level with increasing freshwater inflows, ranging from 0.1 m at approximate inflows of 3m^3/s to 0.2 m at approximate inflows of 40 m^3/s. Water levels at Kliphoek only start to rise significantly for flows exceeding 500 m^3/s to 600 m^3/s (although longer duration and persistent flows exceeding 300 m^3/s can have the same effect). The maximum recorded water level (excluding tidal effects) measured at the Kliphoek site between 1980 and 2003 was just more than 1.4 m. (above MSL). The maximum recorded water level during the period 1995 to 2003 (for which there exists the accurate inflow data of Beck & Basson (2007)), was approximately 1.2 m (MSL), corresponding to an short duration

[11] The water level reported here have been low pass filtered using a cosine-lanczos filter with 97 unique weights and a quarter power point of 0.031 cycles per hour (representing an approximate 32 hour periodicity)

flood with an estimated peak flow of approximately 900 m^3/s (July 2001). The water level (excluding tidal effects) measured at Jantjiesfontein at this time was approximately 3.4 m (MSL). Unfortunately, measured water levels do not exist for Reach 1 (Jantjiesfontein lies just upstream of flood Reach 1), flood Reach 2 or flood Reach 3. (The Kliphoek water level gauge lies just downstream of Reach 3).

The absence of water level data, in particularly the lower end of flood Reach 1 (where there is a fairly rapid changes in water levels with downstream distance) and in flood Reach 2 (where the importance of flooding and the associated inundation extents are the greatest), remains problematic. Not only does this mean that there is no water level data to calibrate the flood modelling in these regions, it also means that one has to rely on the flood modelling alone to describe the evolution of water levels (and associated flooding) in these stretches of the estuary. Of perhaps the greatest concern to this study is that the persistence of flooding (*i.e*. the persistence of high water levels) in these reaches cannot be confidently determined, particularly as computational limitations meant that the duration of flood runs were limited to durations of less than one week.

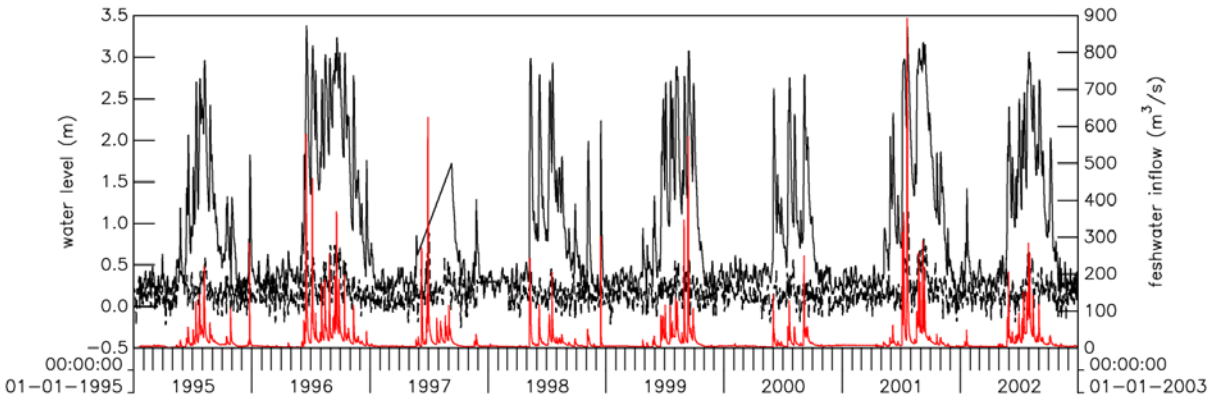

Figure 2.15 Plot of the freshwater inflow rates (red line) to the Berg River Estuary and associated water level variability (with tides removed by low-pass filtering) at Jantjiesfontein (solid black line) and Kliphoek (dotted black line)

The relationship between freshwater inflow rates is plotted in Figures 2.15 and 2.16 for the period 1995 to 2003. From these data it is clear that the upstream water levels measured at Jantjiesfontein readily respond to all but the smallest of floods, while those at Kliphoek do not respond significantly to all but the largest of floods. Due to the lack of measured data between these two locations it is not possible to estimate the downstream evolution and persistence of higher water levels associated with floods in the estuary between these two locations. It is therefore strongly recommended that a water level recorder be placed in this stretch of the river to provide the information necessary to estimate flooding and inundation as well as validate future flood modelling studies.

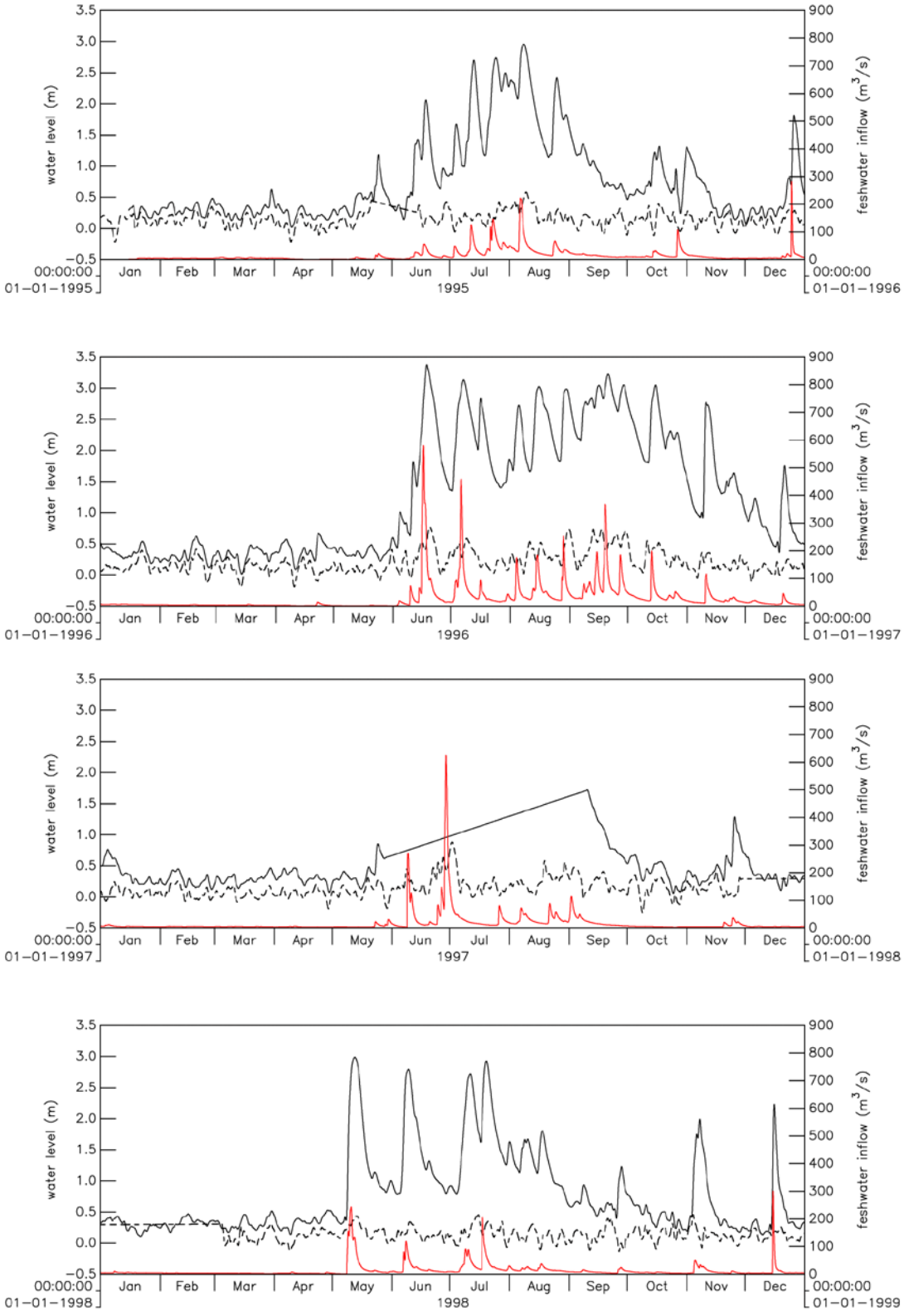

Figure 2.16 Freshwater inflow rates (red line) to the Berg River Estuary and associated water level variability (with tides removed by low-pass filtering) at Jantjiesfontein (solid black line) and Kliphoek (dotted black line)

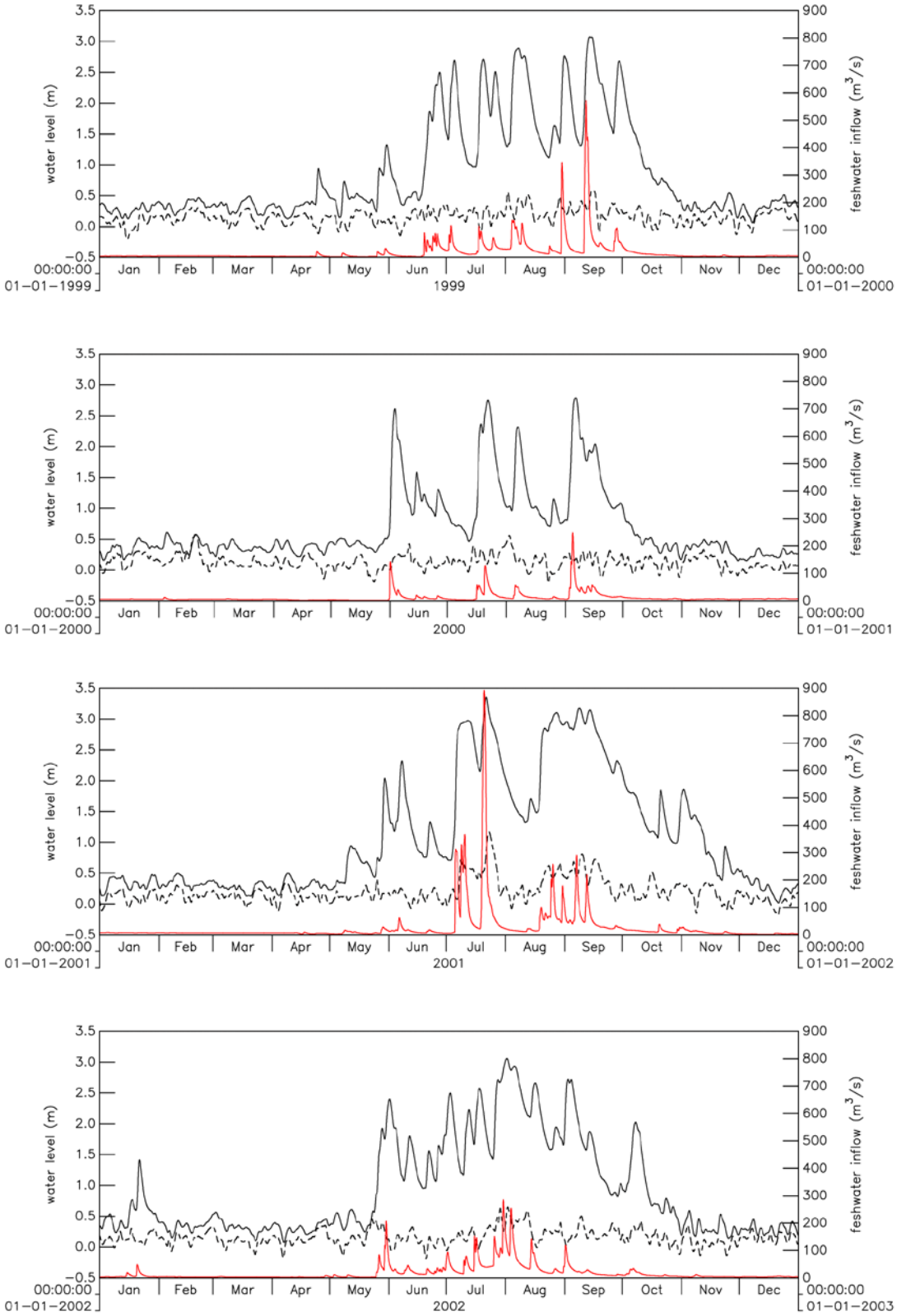

Figure 2.16 (continued)

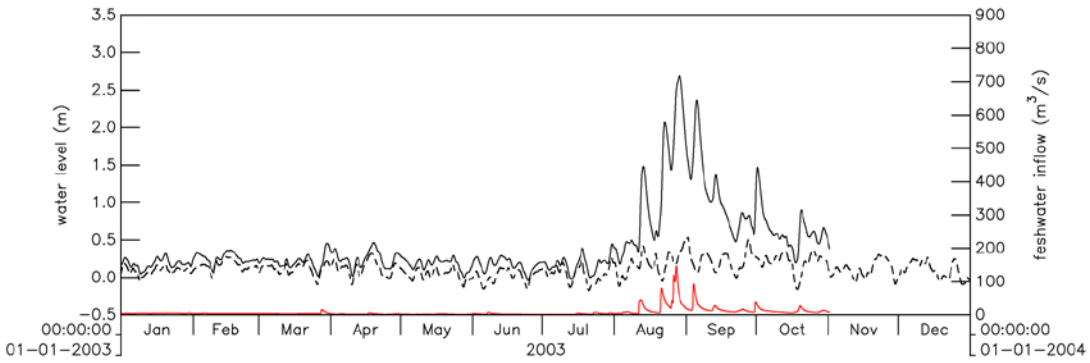

Figure 2.16 (continued)

In summary

Under normal winter base flow (non-flood flow conditions) tidal water level variability dominates in the region between the mouth and 12 km upstream under neap tide conditions and up to between 45 and 50 km upstream under spring tide conditions. Upstream of this water levels are dominated by freshwater inflows should they be of any significance (*i.e.* winter base flows). Sub-tidal water level fluctuation are comparable to neap tide water level variations between 12 km and approximately 50 km upstream, but only exceed spring tide water level variability upstream of 50 km from the mouth of the estuary.

Tidal water level variability exceeds that associated with small floods (< 100 m^3/s) from the mouth to approximately 33 km to 45 km upstream. For larger floods (> 500 m^3/s) tidal water level fluctuations only dominate downstream of the railway bridge (~ 12 km upstream of the mouth). During neap tides the influence on water levels of these larger floods can exceed that associated with the tide. The above observations are confirmed by the water level data measured at the DWAF water level gauge at Kliphoek.

The significance of the above observations is that past studies suggested a very strong relationship between the extent of flooding and the magnitude of winter base flows (Beck & Basson 2009) as well as sub-tidal water level fluctuations at the mouth of the estuary. The present study that took more explicit cognisance of the rapid downstream decrease in water level increases associated with winter base flows), has shown that there is only a weak relationship between base flow and the extent of flooding in all but most upstream reaches of the estuary.

The influence of sub-tidal water level variability remains significant throughout the estuary. Under small flood conditions (100 to 200 m^3/s) sub-tidal variability is expected to influence flood extents from the mouth to approximately 30 to 33 km upstream (depending on the magnitude of the sub-tidal water level fluctuations). Under large flood conditions it is expected that the influence of sub-tidal fluctuation will be limited to the region downstream of the railway bridge. Under non-flood conditions, sub-tidal water level variability is expected to significantly influence that area of the estuary where normal tidal water level variability dominates that associated with freshwater inflows, *i.e.* typically downstream of Kersefontein

during winter base flow conditions but as far upstream as Steenbokfontein (approximately 70 km upstream) during the low flow conditions of summer.

2.3.3. Water Quality and associated hydrographic regimes

The water quality and hydrographic regimes on the Berg River Estuary are descried in greater detail in the main body of the report; however a brief description of the salinity distributions and how they vary seasonally is given here in support of the modelling study.

Slinger & Taljaard (1994) undertook a preliminary investigation of this seasonal character of the Berg Estuary. Their results showed that during the rainy season (September), the penetration of seawater extended about 10 km upstream at flood tide, whereas in the following summer (February/March) this had reached farther than 40 km upstream. While tidal oscillations (albeit small) are observed as far as 69 km upstream (approximately 30 km as the crow flies), historically seawater has been observed to penetrate only as far as approximately 45 km upstream by the end of the dry summer season, even under extreme low flow conditions. In all the sections measured by Slinger & Taljaard (1994), little vertical stratification of the water column was observed. Water temperatures in the estuary were consistently warmer than in the sea, with the lowest temperatures in the sea observed in February (13.7°C). Due to limited historical data (both salinity and sufficiently robust estimates of freshwater inflows to the estuary), it was not possible to assess how typical the measurement period (1989/1990) was of long-term conditions in the estuary. Further more limited observational studiws were undertaken in support of specific scientific investigations (*e.g*. Slinger & Taljaard 1996; Slinger *et al*. 1996).

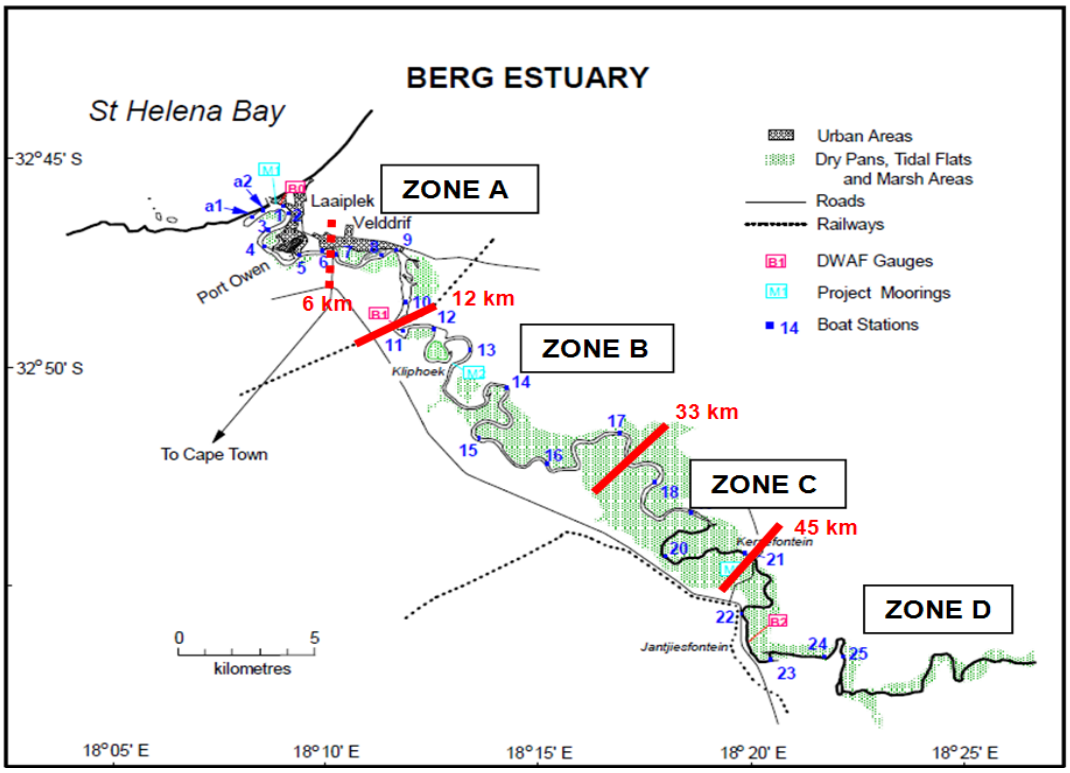

Figure 2.17 Different abiotic zones identified for the Great Berg Estuary (map adapted from Schumann, 2007)

Schumann (2007) reported typical seasonal distributions of salinity in the Great Berg Estuary primarily based on quarterly measurements collected during the period 2002 to 2005, supplemented by a sub-set of the data measured by the CSIR during the period 1989 to 1996 (when the CSIR measured 22 longitudinal sections on 18 different days, comprising temperature and salinity profiles at each station dissolved oxygen and pH observations only at the surface and near the bottom (in many cases only at the surface).

Schumann (2007) reported that the distributions were similar to those observed in earlier studies (*e.g*. Taljaard *et al*. 1992; Slinger & Taljaard, 1996; Slinger *et al*. 1996). Both the data of the CSIR and Schumann are described in greater detail in the main body of the report where the data has been used to demarcate abiotic zones and define hydrodynamic and water quality "states" typical of the Berg River estuary. These abiotic zones (Figure 2.17) correspond reasonably well with the flood reaches described earlier. This is not surprising as the hydrographic, water quality and flooding regimes are all determined by the same factors, *i.e*. mainly tidal and subtidal water level variability, freshwater inflows to the estuary and the morphology of the estuary mouth, channels and adjacent flood plains.

Schumann (2007) concluded that for the most part, the Great Berg Estuary was well-mixed. Stratification seldom occurred, and did not seem to last very long, probably because of strong mixing from tidal exchange and fresh water inflow. Stratified conditions in the estuary are observed only for short periods in the middle reaches of the estuary during freshettes and floods and, to a much lesser extent, near the mouth of the estuary during periods of strong upwelling, particularly during spring tides. The absence of such estuarine circulation means that the estuary is more easily flushed by a specific magnitude of freshwater flow that would an estuary where estuarine circulation associated with more highly stratified conditions is significant (*e.g*. the Kromme and Palmiet estuaries as reported in van Ballegooyen *et al.* 2004). This general lack of observed stratification in the Berg River Estuary led Schumann (2007) to consider it appropriate to integrate salinity and other water quality data over water depth at each station, using a mean value for each station.

While the influence of groundwater is largely unknown, vegetation (particularly in the vicinity of De Plaat) suggests that there must be the presence of groundwater inflows along some if not much of the estuary. Furthermore the groundwater atlas from the Berg River Baseline Monitoring Programme (DWAF, 2007f) provides strong evidence for groundwater inflows into the estuary (Figure 2.18 and 2.19).

Both the early CSIR (1993) one-dimensional and the present two-dimensional modelling study suggest that salinities in the middle reaches of the estuary could rise above that of seawater. Neither of the two models took account of potential groundwater inflows. While these predictions of elevated salinity could be a consequence of uncertainties in river inflow, rainfall and evaporation or the model studies themselves, these predictions could equally well be the consequence of the fact that groundwater inflows were ignored.

The occurrence and extent of possible groundwater inflows into the Berg River is discussed in greater detail in the sections of this report dealing with the calibration of the water quality modelling and the reporting of the model results.

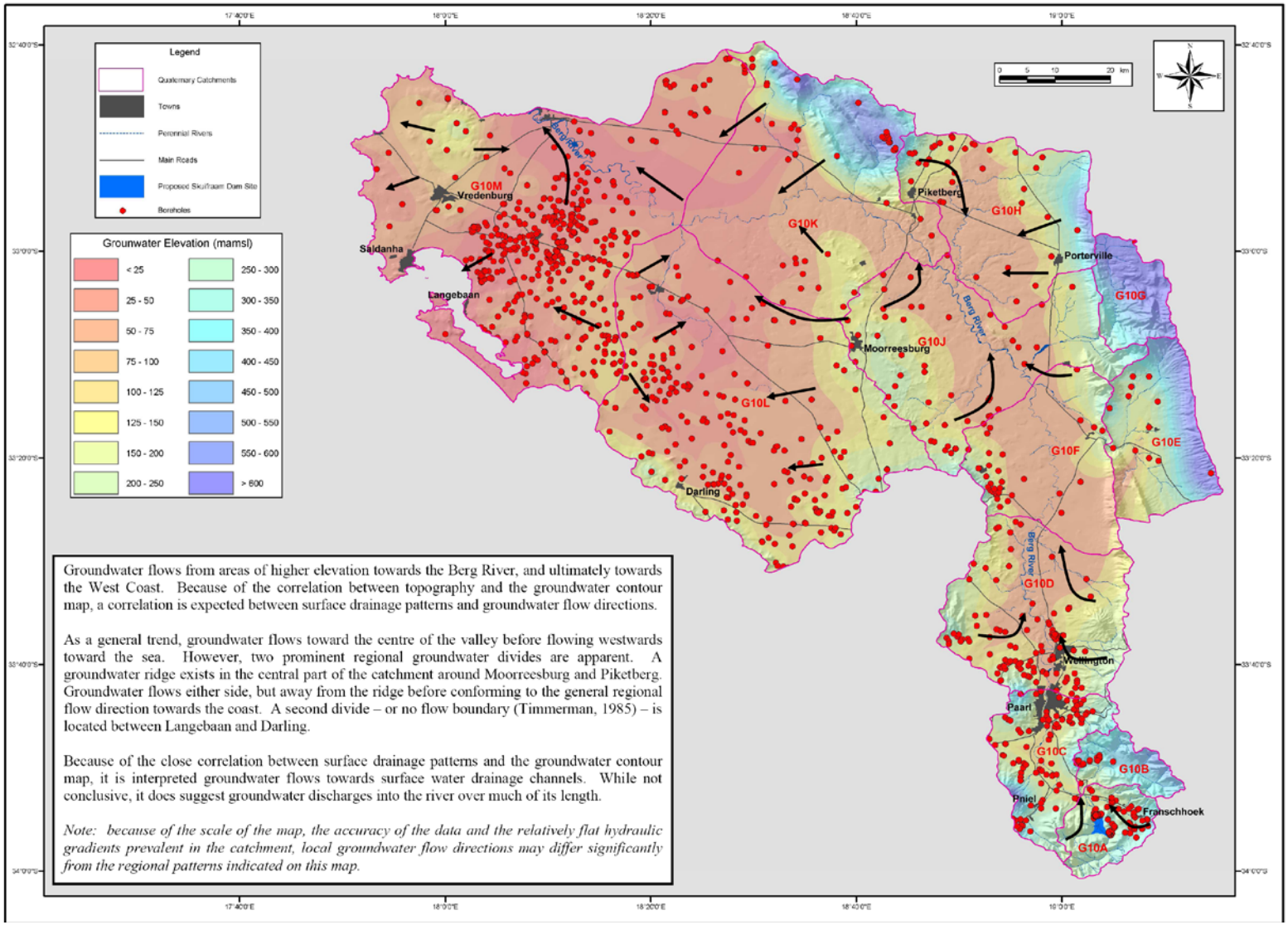

Figure 2.18 Inferred groundwater flow directions (DWAF 2007f)

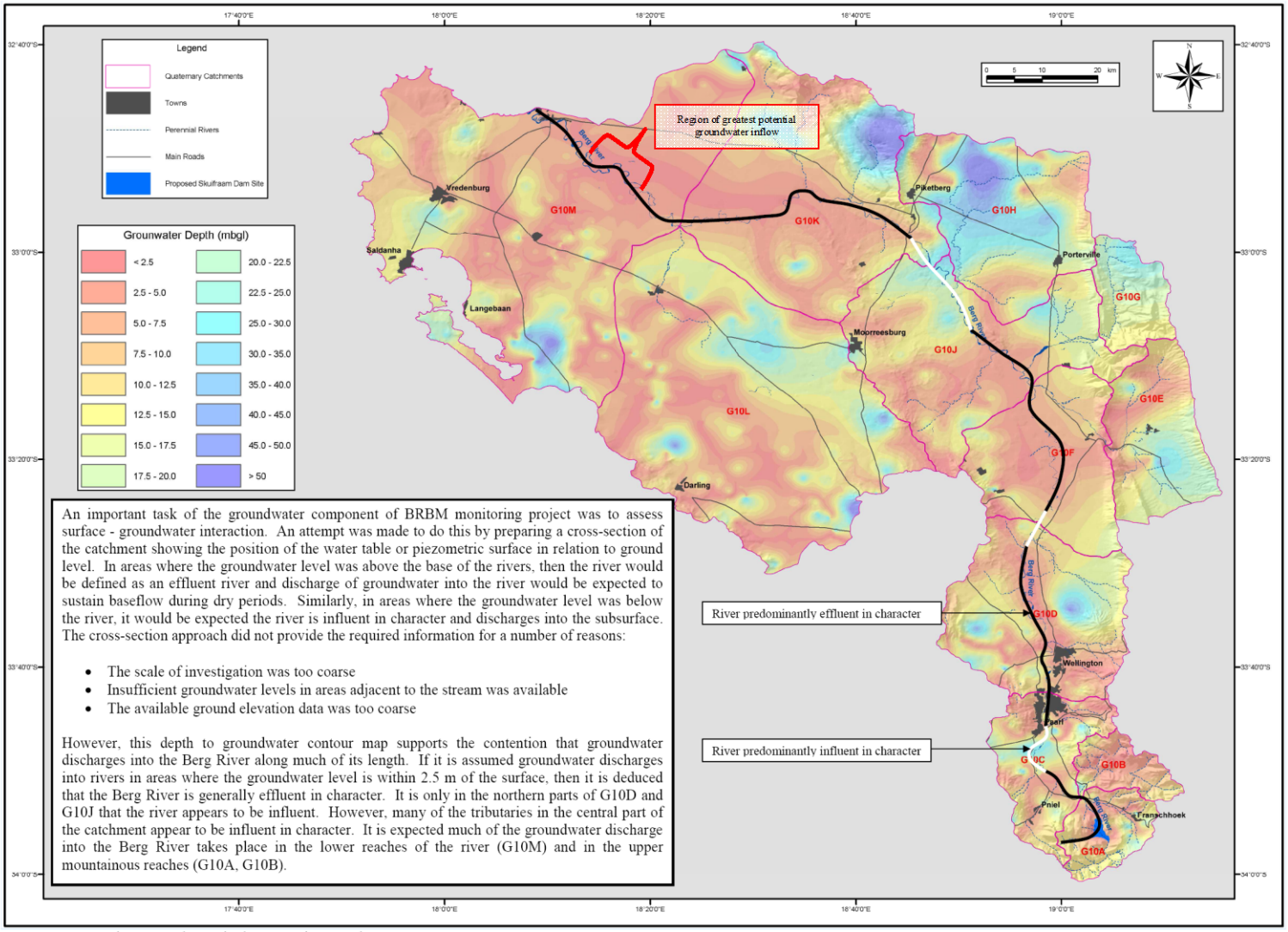

Figure 2.19 Ground water depth (mbgl) (DWAF 2007f)

2.4. Review of Previous Modelling Studies

A number of modelling studies of the Estuary have been undertaken in the last 15 years. In 1993, the salinity distribution and aspects of flooding in the Berg River Estuary were investigated using the one-dimensional MIKE-11 model (CSIR, 1993). The hydrodynamic model covers 68.4 km along the length of the estuary from the mouth to the farm at Steenboksfontein (see Figure 6). Sixty three cross-sections were included in the model, 48 of these located between the estuary mouth and Kersefontein (approximately 45 km upstream of the mouth.

Water levels were recorded in March 1990 at six locations along the estuary, these being:

- The Mouth (chainage 0 km)
- Kliphoek (chainage 16.3 km)
- Kersefontein (Chainage 45,1 km)
- Rasgat (chainage 55,5 km)
- Southrivier (62,9 km)
- Steenboksfontein (68,4 km)

The hydrodynamic model was calibrated by adjusting bottom shear stress co-efficients until a satisfactory comparison between recorded and computed water levels was reached. The calibration simulations were conducted using water levels recorded at the mouth for the mouth boundary conditions and unpstream a constant discharge of 0.2 m^3/s (representative summer flow) was applied at the upstream river flow boundary at Steenboksfontein.

An important feature of the measured water levels is a strong reduction in water level variation between the mouth and Kliphoek and an increase between Kliphoek and Kersefontein. The model simulation reproduced these features.

Model simulations were undertaken for period of up to one year to simulate the effects of run-off, evaporation and tidal forces. Average spring-neap-spring tidal conditions representative of Saldanha Bay were applied at the offshore boundary. This approach was justified based on the reasoning that there is a close agreement between the predicted tidal variations for Saldanha Bay and those at the mouth of the Great Berg River (Huizinga *et al*. 1993). It should be noted that these model results predicted that elevated salinities would be observed in the estuary between 10 km and 30 km upstream of the mouth under the assumption of no river inflow. These salinities were predicted to rise to 38 PSU by the end of March. However the inclusion of river inflows of 0.6 m^3/s removed any suggestion of elevated salinities (i.e. above 35 PSU) in the estuary.

Subsequently Slinger *et al.* (1998) used the Mike 11 one-dimensional model to simulate hydrodynamic and water quality conditions in the Berg estuary. Reasonable salinity structures were obtained, but it is difficult to assess the success of the temperature simulations because of the lack of real data as a comparison. Dissolved oxygen (DO) simulations were also performed, but with less successful results compared to measurements, especially in the mouth region.

More recently the tidal dynamics (currents and sediment transports) and flood dynamics of the Berg River estuary have been modelled as part of the Berg River Baseline Monitoring Programme. These studies are important as they provided a great deal of insight and data for the present modelling study reported upon here.

Both of their modelling studies were based on a digital terrain model that was developed specifically for the study. The model bathymetry was based on the 2003 aerial survey (Digital Terrain Model) of the estuary and floodplain (Beck & Basson 2007). As the DTM did not include points in the main river channel (these were under water), this (the river channel) was added on later. This was done by extracting the outline of the main river channel from the DTM and creating the bathymetry by interpolation from a series of cross section across the estuary channel taken in 2004 as well as a longitudinal profile along the length of the main channel. It is not clear whether the cross-section data measured during January 2003 were also used in this manner. The along estuary survey line used to "tie in" the cross-sections was not ideal as it did not always follow the deepest part of the channel. As a consequence the depths along the longitudinal survey line undulate as the line moves upstream over the shallower inner bank across the deepest part of the channel and over the next shallow inner bank. This led to unrealistically shallow waters and restricted cross-sections on the bend of the river where no cross-sectional data existed. These inaccuracies in the assumed bathymetry would have led to difficulties in calibrating the upstream water levels in the tidal model. A corrected version of this digital terrain model has been used in the present modelling studies.

The parameters used for the two modelling studies are summarised in Table 2.5.

Table 2.5 Parameters used in the Beck and Basson (2007) modelling studies

Tidal Modelling	
Hydrodynamic time step	15 s
Flooding depth	0.2 m
Drying depth	0.1 m
Manning n	45 $m^{0.33}/s$
Eddy viscosity	0.1 m^2/s
Flood Modelling	
Hydrodynamic time step	5 or 6 s
Morphological time step	21 or 24 s
Flooding depth	0.2 m
Drying depth	0.1 m
Manning n	45 $m^{0.33}/s$
Median grain diameter	0.22 mm
Sediment transport formula	Engelund and Fredsøe
Eddy viscosity	0.1 m^2/s
Mass density of sediment	2650 kg/m^3
Porosity	0.35

Beck and Baason (2007) report that the tidal model was calibrated using the downstream water level gauge at the Railway Bridge (G1H024) for the period February 1999 and subsequently validated using water levels measured during the March 2003 field survey (not reported) and upstream water level data at Jantjiesfontein (G1H023). The simulated upstream tidal variations at Jantjiesfontein were found to be of the same magnitude at those measures at this site. It is not clear that consideration was given to time lags in the tides and water levels between these two measurement locations.

Calibration of the flood model was more difficult as very little appropriate water level data exist for such a calibration exercise. A detailed description of the calibration exercise for the flood modelling is contained in Beck & Basson (2007). The calibration parameters were adjusted until modelled and measured water levels at Jantjiesfointein (G1H023) matched to within 0.5 m. Of relevance to the present modelling study is that the simulated water levels were somewhat higher than those measured at Jantjiesfontein and also seemed to display a greater degree of “peakiness”.

The legacy of these studies contributed significantly to the success of the present modelling study in that they provided:

- a digital elevation model that formed the basis of the “corrected” digital elevation model used in this study;
- routed estuarine inflows for the period 1996 to 2003 that contributed greatly to the water level and flow analysis undertaken prior to the modelling study, as well as the characterisation of the flood events used in the flood modelling study reported here;
- long-term simulations time series of water level in pans, marshes and other low-lying areas that were used in the analyses of the extent and duration of the inundation of pans in the Berg estuary.

3. Model set-up, calibration and verification

3.1. Description of the Hydrodynamic Model

The model used in this study is the DELFT3D-FLOW 3D hydrodynamic model. The DELFT3D-FLOW hydrodynamic model includes formulations and equations that take into account:

- Tidal forcing;
- Wind shear stress on the water surface;
- Wave-driven flows;
- Bed shear stress at the seabed (including wave effects);
- Drying and flooding on tidal flats;
- Secondary currents (helical or spiral flow) in two-dimensional simulations
- The effect of the earth's rotation (Coriolis force);
- Free surface gradients (barotropic effects);
- Horizontal gradients in pressure due to changes in water density (baroclinic effects);
- Water with variable density due to temperature or salinity differences (equation of state);
- Turbulence-induced mass and momentum fluxes (k-ε turbulence closure model);
- Insolation and air-sea interactions at the sea surface;
- Transport of conservative constituents (advection-diffusion equation).

The system of equations in DELFT3D-FLOW comprise the horizontal momentum equations, the continuity equation, the equation of state, the advection-diffusion equation for heat, salt and other conservative tracers, as well as formulations which take into account the role of insolation and air-sea fluxes in determining the stratification of the water column. The equations and their numerical implementation are described in detail in WL|Delft Hydraulics (2009). Simplified versions of these equations follow.

Conservation of momentum in x-direction:

$$\frac{\partial u}{\partial t} + u\frac{\partial u}{\partial x} + v\frac{\partial u}{\partial y} + g\frac{\partial \eta}{\partial x} - f.v + \frac{g.u\,|U|}{C^2(d+\eta)} - \frac{F_x}{\rho(d+\eta)} - \upsilon\left(\frac{\partial^2 u}{\partial^2 x} + \frac{\partial^2 u}{\partial^2 y}\right) = 0$$

Conservation of momentum in y-direction:

$$\frac{\partial v}{\partial t} + u\frac{\partial v}{\partial x} + v\frac{\partial v}{\partial y} + g\frac{\partial \eta}{\partial y} + f.u + \frac{g.v\,|U|}{C^2(d+\eta)} - \frac{F_y}{\rho(d+\eta)} - \upsilon\left(\frac{\partial^2 v}{\partial^2 x} + \frac{\partial^2 v}{\partial^2 y}\right) = 0$$

Conservation of mass, continuity equation:

$$\frac{\partial \eta}{\partial t} + \frac{\partial[(d+\eta)u]}{\partial x} + \frac{\partial[(d+\eta)v]}{\partial y} = Q$$

The global source or sink of water per unit area, *Q*, (expressed in m/s) is calculated as:

$$Q = (d+\eta)\int_{-H}^{\eta}(q_{in} - q_{out})\,\partial z + P - E$$

where

η = water level elevation (m)
d = water depth (m)

u,v	=	velocity in the x-, y-directions, respectively (m.s^{-1})
U	=	magnitude of total current velocity (m.s^{-1})
$F_{x,y}$	=	x- and y- components of external forces (Pa)
f	=	Coriolis parameter $2\Omega \sin\theta$, where Ω is the earth's angular velocity and θ is the geographic latitude (rad.s^{-1})
g	=	acceleration due to gravity (m.s^{-2})
ρ	=	water density (kg.m^{-3})
ν	=	eddy viscosity (m2.s^{-1})
C	=	Chézy coefficient (m$^{1/2}$.s^{-1})
q_{in}	=	local source per unit volume from inflows/discharges (1/s)
qout	=	local sink per unit volume due to outflows/intakesintakes (1/s)
P	=	precipitation (m/s)
E	=	evaporation (m/s)

The model incorporates a sophisticated ***k-ε*** turbulence closure scheme (WL|Delft Hydraulics, 2009).

The constituents of the water in the estuary are simulated using an advection-duffusion equation as indicated below.

Advection-diffusion equation:

$$\frac{\partial c}{\partial t} - \frac{\partial}{\partial x}\left(D_x \frac{\partial c}{\partial x} - u\,.\,c \right) - \frac{\partial}{\partial y}\left(D_y \frac{\partial c}{\partial y} - v\,.\,c \right) = Source - Sink$$

where:

c	=	constituent, e.g. salinity, temperature
u,v	=	current velocity in the x-, y-directions, respectively (m.s^{-1})
$D_{x,y}$	=	dispersion coefficients in the x-, y-directions (m^2.s^{-1})
Source	=	source term, *e.g.* heat influx when the constituent modeled is temperature
Sink	=	sink term, *e.g.* atmospheric heat loss when the constituent modelled is temperature

The horizontal turbulent dispersive transport of momentum and other constituents, such as temperature, are computed using prescribed eddy viscosity coefficients and eddy diffusivity coefficients, respectively. The vertical eddy viscosity and eddy diffusivity coefficients are computed by a *k-ε* turbulence closure model. The shear stress (τ_{seabed}) at the seabed induced by turbulent flow is assumed to be given by a quadratic friction law:

$$\tau_{seabed} = \rho \,.\, \frac{g}{C_{3D}^2} \,|u_b|^2$$

where u_b is the near-bottom current speed and C_{3D} is a function of the two-dimensional friction co-efficient given by the Chézy formulation (m^{½}/s), the White Colebrook formulation (WL|Delft Hydraulics, 2009):

$$C_{2D} = 18 \log_{10}\left(\frac{12H}{k_s} \right)$$

where H is the total water depth (m) and k_s is the Nikuradse roughness length (m), or given by the Manning formulation (WL|Delft Hydraulics, 2008):

$$C_{2D} = \left(\frac{\sqrt[6]{H}}{n} \right)$$

where H is the total water depth (m) and n is the Manning co-efficient (s/m$^{1/3}$).

The relationship between the three-dimensional Chézy co-efficient, C_{3D} , and the two-dimensional Chézy co-efficient, C_{2D}, is as follows (WL|Delft Hydraulics, 2005):

$$C_{3D} = C_{2D} + \frac{\sqrt{g}}{\kappa} \ln \left(\frac{\Delta z_b}{2H} \right)$$

provided that the vertical velocity in the three-dimensional simulation remains a logarithmic profile.

Enhanced bed stresses due to wave effects can be incorporated in the model using the friction formulation of Fredsøe (1984), however here we are not simulating wave effects..

The magnitude of the wind shear stress on the water surface may be modelled by the following quadratic expression

$$\tau_{wind} = \rho_a \cdot C_D \ (U_{10}) \cdot U_{10}^2$$

where:

ρ_a	=	density of air (kg.m^{-3})
C_D	=	wind drag coefficient which is typically a function of wind speed
U_{10}	=	wind speed 10 m above the water surface (m.s^{-1})

However, no atmospheric weather forcing (wind mixing) or atmospheric heat fluxes are applied in this model.

Precipitation and evaporation have been included in the simulations and these are merely added globally as a specified precipitation and evaporation rate.

While formulations are available to simulate morphological changes and resultant feedbacks on the flows, this model capability was not invoked as the computational overhead was not warranted for the present study (see Section A1.3 for assumptions and limitations relevant to this study).

In the horizontal direction an irregularly spaced, orthogonal, curvilinear grid has been used is used in the water quality (salinity distribution) simulations while a regular grid with a 15 m resolution. Typically In the vertical direction use is made of a sigma-coordinate grid that results in a constant number of layers over the horizontal computational area. The thickness of the layer is thus proportional to the water depth at each horizontal position. An “anti-creep” procedure is available that is designed to limit numerical diffusion associated with the use of sigma-coordinates. However, here all model simulations have been undertaken in two-dimensions (*i.e*. vertically integrated) and consequently only one vertical layer has been used. The mixing effects of vertically sheared flows have been incorporated in the model by

an appropriate increase if the diffusivity co-efficient from those values normally used for three-dimensional simulations.

The time integration method used to solve the equations in DELFT3D-FLOW is the Alternating Direct Implicit type where the water levels and velocities are solved implicitly along grid lines. The accuracy of wave propagation in the grid is related to the Courant number. An appropriate time step is typically determined by comparison of the relevant model results for successively decreasing time steps (*i.e*. the time step is halved in successive simulations until further changes in the model outputs are negligible). In the water quality simulations a time step of 30 seconds was used while in the flood simulations the time step had to be reduced to 15 seconds to ensure accurate model simulations.

3.2. Available data for Berg River Estuary Model Implementation

Data available for the implementation and the calibration of the Delft 3D-FLOW hydrodynamic model of the Berg River Estuary are listed in Table 3.1.

Table 3.1: Data available for the implementation of the Delft 3D-FLOW in the Berg River Estuary.

DATA TYPE	*COMMENT*
Model Set-up:	
Bathymetry	*A comprehensive Digital Terrain model (referenced to WG19 and Mean Sea Level here considered to be the Land Levelling Datum) exists for the Berg estuary floodplain. This was supplemented by surveys of the main channel in January 2003, June 2004 and March 2006. Surveys of 63 cross-sections were undertaken by the CSIR in the period 1990 to 1994, however these data were not fully geo-referenced and this had to be re-done for this study.* *The lagoon area at the mouth was surveyed by the CSIR in 1986, 1987, 1988, twice in 1990, in 1997 and in 1999. These data were fully geo-referenced (Clarke 1880) and referenced to MSL. The co-ordinates were converted to WG19.* *The mouth of the Berg estuary was surveyed in January 2003 by Triton Surveys (WGS1984 and referenced to MSL)* *Offshore bathymetry data have been obtained from SAN Charts 1009 and 118.*
Mouth Dynamics	*While the mouth depths are likely to have changed over time, it is not expected that these changes would have been substantial after the "training walls" were built at the mouth. Despite the uncertainty introduced, the January 2003 Triton surveys were used in both modeling studies.*
Water levels at mouth of the estuary	*Water level measurements that can be used as boundary conditions at the estuary mouth are:* *i) Water levels measured by the South African Hydrographic office (1996, 1997 and for the period 2000 to 2008. Measured data are not available for the period 1997-1998);*

DATA TYPE	*COMMENT*
	ii) Water levels measured by DWAF (Department of Water Affairs) at a location just inside the mouth of the estuary (Laaiplek - G1H074); *The analyses by Schumann and Brink (2009) provide clear evidence that the Laaiplek water level measurements are not surveyed relative to MSL as there exists an >0.5m difference between the water levels at Saldanha Bay and Laaiplek reported in Schumann and Brink (2009).*
River inflow	*There is considerable uncertainty as to a representative flow entering the estuary. Schumann (2009) used the flows measured at the Misverstand Dam (G1H031), however Howard & Ratcliffe (2007) report that the data from this gauge (G1H031) measuring spillage from the Misverstand Dam are considered highly unreliable particularly for low flows.* *In this study the inflow estimates used are the routed inflows to the estuary for the period 1996 to early 2003 as estimated by Beck & Basson (2007)*
Freshwater input from tributaries	*There are a number of small streams, of which the Boesmans, Platkloof and Brak appear to be the most important, which flow into the Berg River downstream from the measuring gauge just below the Misverstand Dam. The only major inflow within the tidal reach of the Berg River Estuary is the Sout River that joins the estuary upstream of Jantjiesfontein but downstream of Steenbokfontein.*
Mean monthly evaporation rates	*Mean monthly evaporation rates used in the study are those reported for the Great Berg estuary in CSIR (1993). Monthly mean average evaporation rates obtained from Ninham Shand Inc and reported in CSIR (1993) are the data used in the study. The values compare well with those reported in the South African Atlas of Climatology and Agrohydrology (Schultze et al., 2008)*
Temperature and salinity for the sea and river (at the head of the estuary)	*As temperature was not modeled only salinity needed to be specified at the upstream and downstream boundaries of the Berg River Estuary. The salinity at the open-ocean was assumed to be 35 ppt and a 0 ppt inflow was assumed at the head of the estuary. The initial salinity distributions for the various scenarios are based on measured data. These salinity distributions are described in more detail in the model set-ups.*
Longitudinal salinity profiles	*The initial salinity distributions for the various scenarios are based on measured data as measured by the CSIR (Taljaard et al. 1992; Slinger & Taljaard 1996; Slinger et al. 1996) and as part of the Berg River Baseline Programme (Schumann 2007).*
Longitudinal temperature profiles	*Temperature was not modeled, however, should information on temperature distributions have been required, initial temperature distributions for the various scenarios could have been based on data as measured by the CSIR (Taljaard et al. 1992; Slinger & Taljaard, 1996; Slinger et al. 1996) and as part of the Berg River Baseline Programme (Schumann, 2007).*
Model calibration and verification:	
Water levels	*Water levels suitable for calibrating tidal water level variations along the length of the Berg estuary have been at the following locations (CSIR, 1992, 1993):* • *The Mouth (chainage 0 km)* • *Kliphoek (chainage 16.3 km)*

DATA TYPE	*COMMENT*
	• *Kersefontein (chainage 45,1 km)* • *Rasgat (chainage 55,5 km)* • *Southrivier (62,9 km)* • *Steenboksfontein (68,4 km)* *These data were obtained for the period of 5 – 19 March 1990.* *Longer time series of water level measurements (albeit a fewer locations) are available as follows:* *i) Water levels measured by the South African Hydrographic office (1996, 1997 and for the period 2000 to 2008. Measured data are not available for the period 1997-1998);* *ii) Water levels measured by DWAF (Department of Water Affairs) at a location just inside the mouth of the estuary (Laaiplek - G1H074);* *iii) Water levels measured by DWAF (Department of Water Affairs) at a location just downstream of the Railway Bridge (Kliphoek – G1H024);* *iv) Water levels measured by DWAF (Department of Water Affairs) at Jantjiesfontein (G1H023).* *Scumann (2007) reports that water level data are also available at a location near the Misverstand Dam (G1h031), however these data were not required for this study.* *Beck & Basson (2007) report that the water levels at G1H024 are surveyed relative to MSL, however communication with DWAF (and data available on the DWAF web-site) could not confirm this. The analyses by Schumann & Brink (2009) provide clear evidence that the Laaiplek measurements and possibly those further upstream were not surveyed relative to MSL.*
Longitudinal temperature profiles	*Selected longitudinal profile data from a CSIR measurement programme between 1989 and 1995 (22 Sections) and from the Berg River Baseline Monitoring Programme (13 sampling exercises) undertaken between November 2002 and November 2005 (Schumann, 2007). Each sampling exercise during the Berg River Baseline Monitoring Programme comprised longitudinal sections measured during both Spring and Neap high and low tides.*
Longitudinal temperature profiles	*Selected longitudinal profile data from a CSIR measurement programme between 1989 and 1995 (22 Sections) and from the Berg River Baseline Monitoring Programme (13 sampling exercises) undertaken between November 2002 and November 2005 (Schumann 2007). Each sampling exercise during the Berg River Baseline Monitoring Programme comprised longitudinal sections measured during both Spring and Neap high and low tides.*

An important parameter is the freshwater inflow into the estuary. Monthly mean freshwater inflows to the estuary under natural conditions, pre-Berg River dam and post-Berg River dam conditions were provided by Aurecon. In addition, monthly mean data were provided for a range of future scenarios under consideration. However the most useful data were those provided by Beck & Basson (2007) who routed and estimated the daily freshwater inflows

into the estuary for the period 1996-2003. These data were used in all of the model studies reported here (*e.g*. the estimation of shorter tem variations in freshwater inflow and the characterisation of "typical" flood events).

In principle the most representative stream flow data for the estuary are those measured at the Misverstand weir, however, there are concerns (due to its irregular nature) that their may be "under-gauging" of the flows at this weir. A potential compensating factor is that in reality that there may be significant abstraction of water below the Misverstand weir, suggesting that the actual flow into the estuary may be less than would be measured by an accurate gauging station at Misverstand. In the Berg River baseline monitoring study the Misverstand weir stream flow estimates were considered to represent the freshwater inflows into the estuary.

3.3. **Model** Set-up

There were two model set-ups, the first for the water quality modelling and the second for the flood modelling. The major effort in both the model set-ups went into the accurate specification of bathymetry and water level variability in the estuary. The model bathymetry used in the water quality (salinity) modelling study was used to correct the channel bathymetry in the digital elevation model.

Of greatest importance is the accurate resolution of the major bathymetric features of the estuary that includes the upstream channel depths, low-lying areas adjacent to the main channel (*e.g*. "De Plaat" and the low lying areas in the middle reaches of the estuary) and the topography and connectivity of low-lying areas in the adjacent flood plain.

3.3.1. Computational grid and bathymetry

The digital elevation model from the previous modelling study was found to be somewhat deficient in that the channel depths were not always accurately represented, particularly at the estuary bends. The reasons for these inaccuracies are described in Section A2.4. In order to get a better representation it was necessary to "survey in" some 63 cross-sections measured by the CSIR in the period 1990 to 1994 as these were not fully geo-referenced. Not all of the cross-sections were used as some were both inconsistent with those measured for the Berg River baseline survey and were not consistent with the general topography/bathymetry of the estuary. During the calibration exercise for the water quality study, some of the sections needed to be deepened to enable accurate simulation of the changes in water level and lags along between the mouth and the head of the estuary. Also added was a more realistic bathymetry in the partially occluded "oxbow" meander in the vicinity of Kliphoek. These adjusted data were not incorporated into the DTM but rather were used to modify the gridded model bathymetry, the reason being that these were model-derived rather than measured data.

The lagoon area at the mouth was surveyed by the CSIR in 1986, 1987, 1988, twice in 1990, in 1997 and in 1999. These data were fully geo-referenced (Clarke 1880) and referenced to MSL. The co-ordinates were converted to WG19. Two surveys of the lagoon area or blind

arm (3 March 1990 and 8 September 1990) were combined and used to set up the model bathymetries (Figure 3.1).

Also added to the data used to develop the model bathymetries were survey data for the estuary mouth as measured by Triton Surveys in January 2003 and offshore bathymetry data digitised from SAN Charts 1009 and 118. The resultant new DTM and the supplemental bathymetry data as described above all contain depths that are all referenced to MSL (or LLD). This means that the mean water level in St Helena Bay and the estuary Z_0 = ~0.2m needs to be included in the tidal constituents used to predict tidal water levels. The bathymetry data were then used to set up two model bathymetries, one for the water quality (salinity) modelling and another for the flood modelling.

The computational grid designed for the water quality modelling was optimised for the anticipated longer simulation runs by including only those areas that were likely to be inundated by extreme spring tides (~ 1.2 m MSL) plus a 0.2 m allowance for a possible elevation of water levels in the estuary due to sub-tidal influences on water levels (Figure 3.2a and b). This approach ensured that the correct wetting and drying of the tidal flats and marshes occurred. This was important as these storage areas potentially have a significant influence on tidal water levels in the estuary. In the middle to upper reaches were tidal effects are somewhat reduced, this inclusion of areas up to 1.4 m MSL may seem unnecessary. However, the inclusion of these regions in the middle and upper reaches means that some allowance is made for the higher water levels in these regions occurring during freshettes and small floods. To ensure that the full extent of the estuary undergoing variation in tidal variations in water level was included in the model (and to avoid reflection of the tide from the upper model boundary), the computational grid was extended upstream as far as the first clear structure considered likely to restrict the propagation of tidal effects further upstream. The computational grid extends some 10 km upstream of the recognised upper extent of water level variability in the estuary based on observations.

The resultant computational grid and associated bathymetry allows reasonably accurate simulation of flows up to 100 to 200 m^3/s. In the upper reaches of the estuary where water level rise above 1.4 m, the flows is in any case mostly constricted to the major channel (the very reason for the rise in water level with increased freshwater flow in these upper reaches). Consequently, the use of a computational grid that mostly resolves only the main channel is unlikely to introduce significant error in these upper reaches.

For the flood modelling a regular grid with a 15-m resolution throughout the computational domain was used. Such a high-resolution grid was required to adequately resolve the channel depth in the upper reaches of the estuary where the main channel is not very wide.

As noted earlier, substantial effort was required to remove artificial constrictions in the estuary channel due to the under-sampling inherent when surveying cross-sections at only a limited number of locations along the length of the estuary. During the calibration exercise,

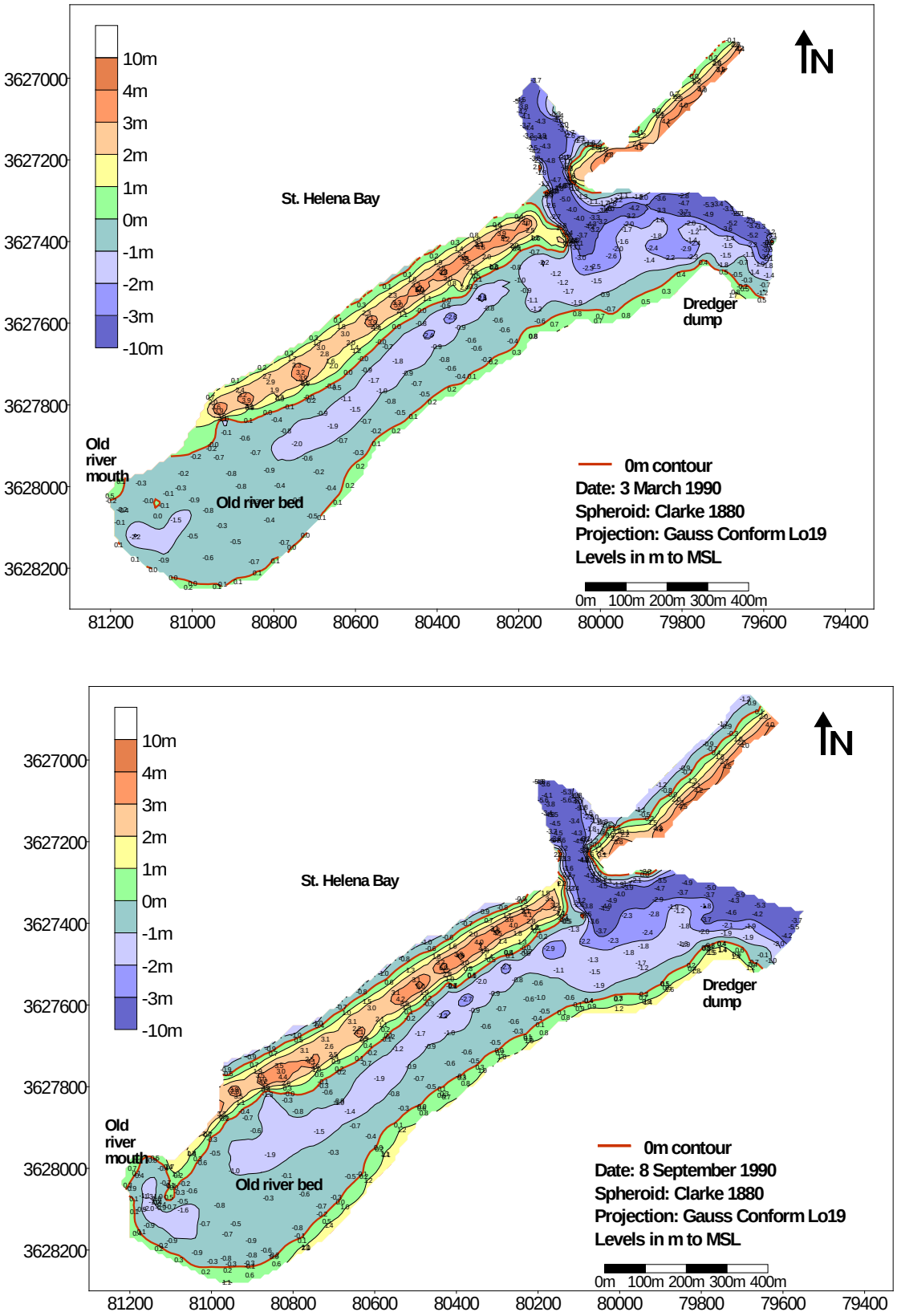

Figure 3.1 **The two bathymetric surveys of the lagoon or "blind-arm" area used in the modelling studies**

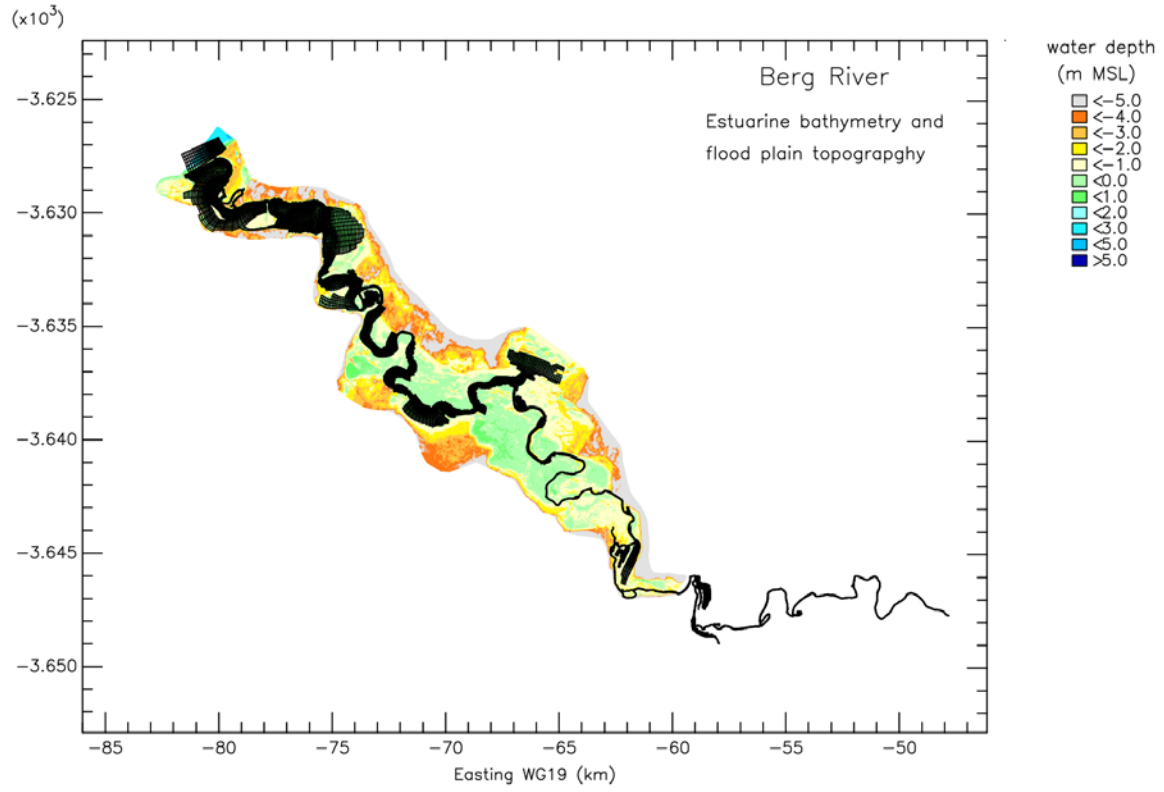

Figure 3.2a The full extent of the computational grid used in the water quality modelling.

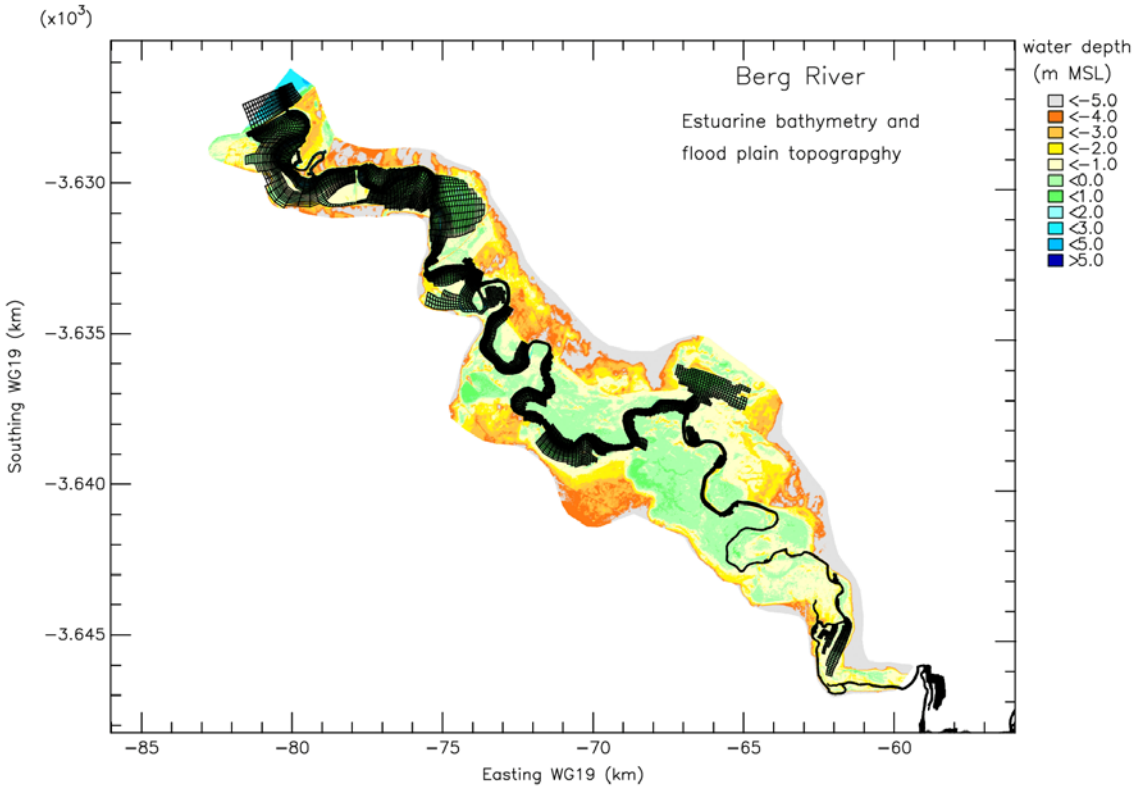

Figure 3.2b A zoomed in view of the computational grid showing the low-lying areas included in the water quality model.

the simulated water level variability along the length indicated locations where there was likely to be unrealistic constrictions in the channel. These restrictions in the channel were removed during the calibration exercise. The resultant model bathymetry used in the water quality modelling is given in Figures 3.3a to f.

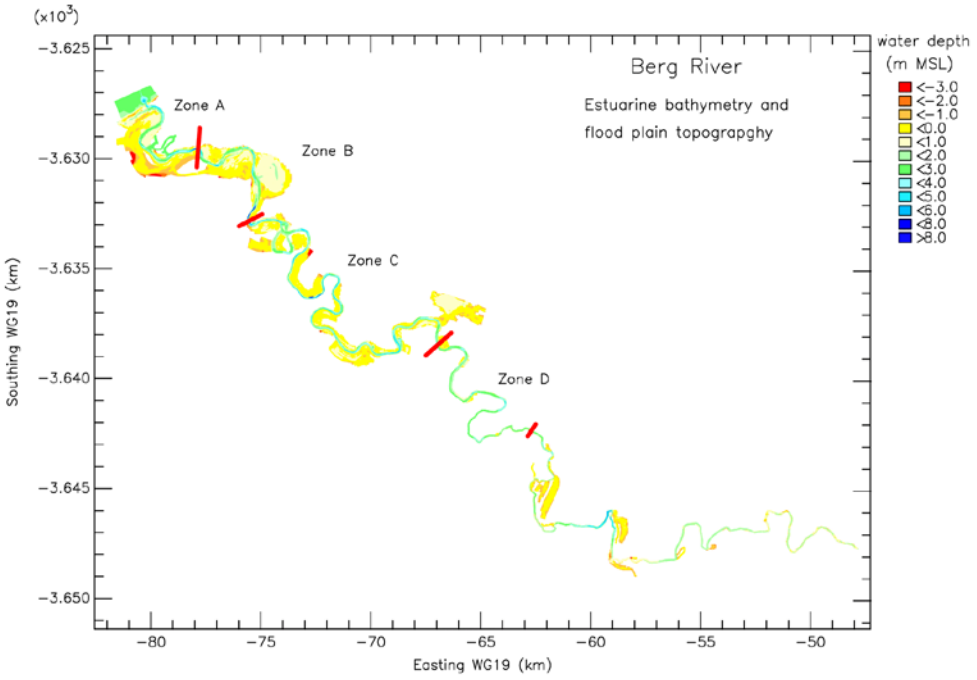

Figure 3.3a The model bathymetry used in the water quality modelling (Full domain).

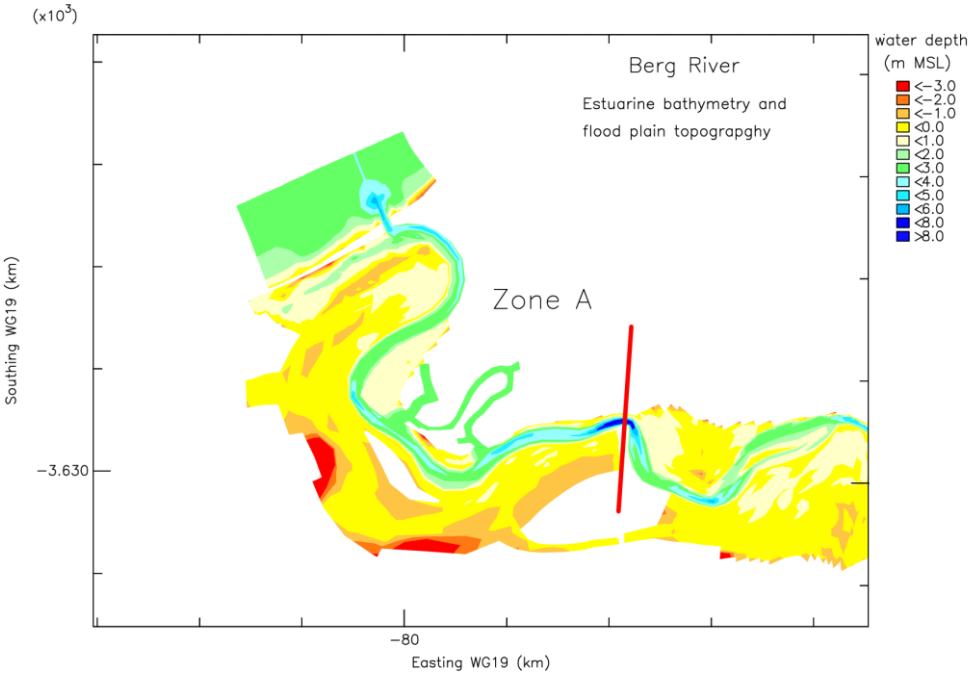

Figure 3.3b The model bathymetry used in the water quality modelling (Zone A).

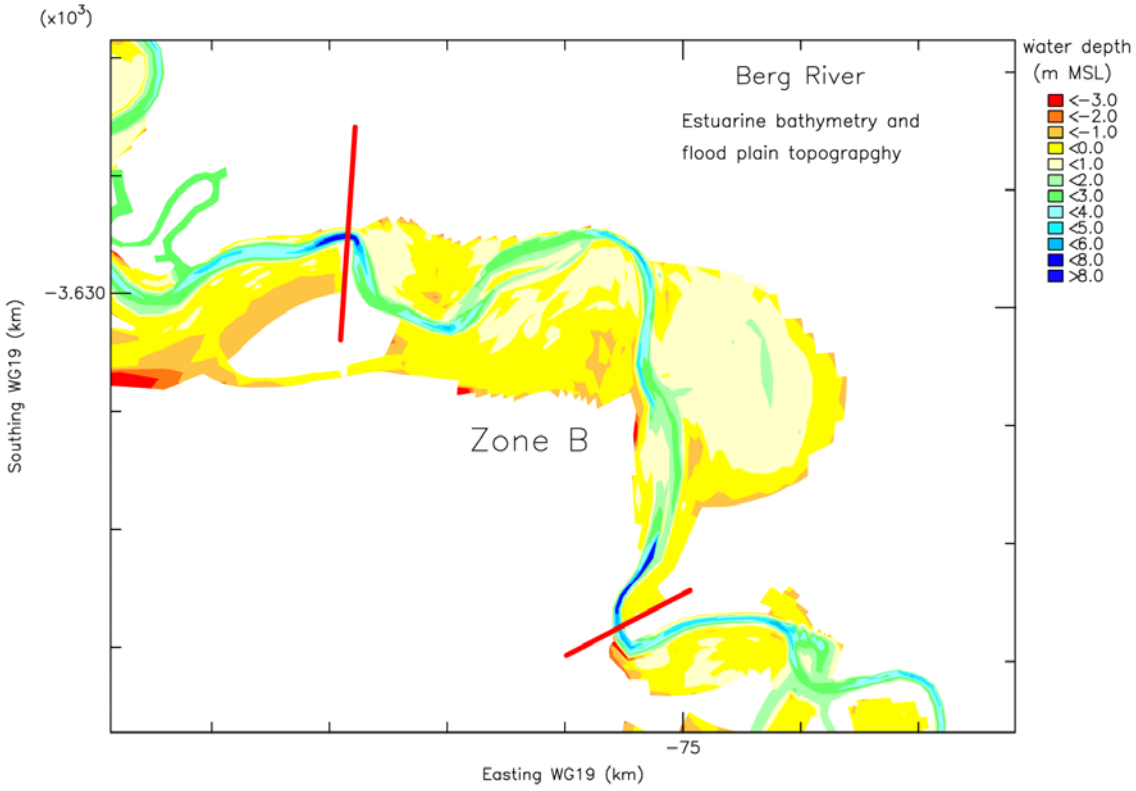

Figure 3.3c The model bathymetry used in the water quality modelling (Zone B).

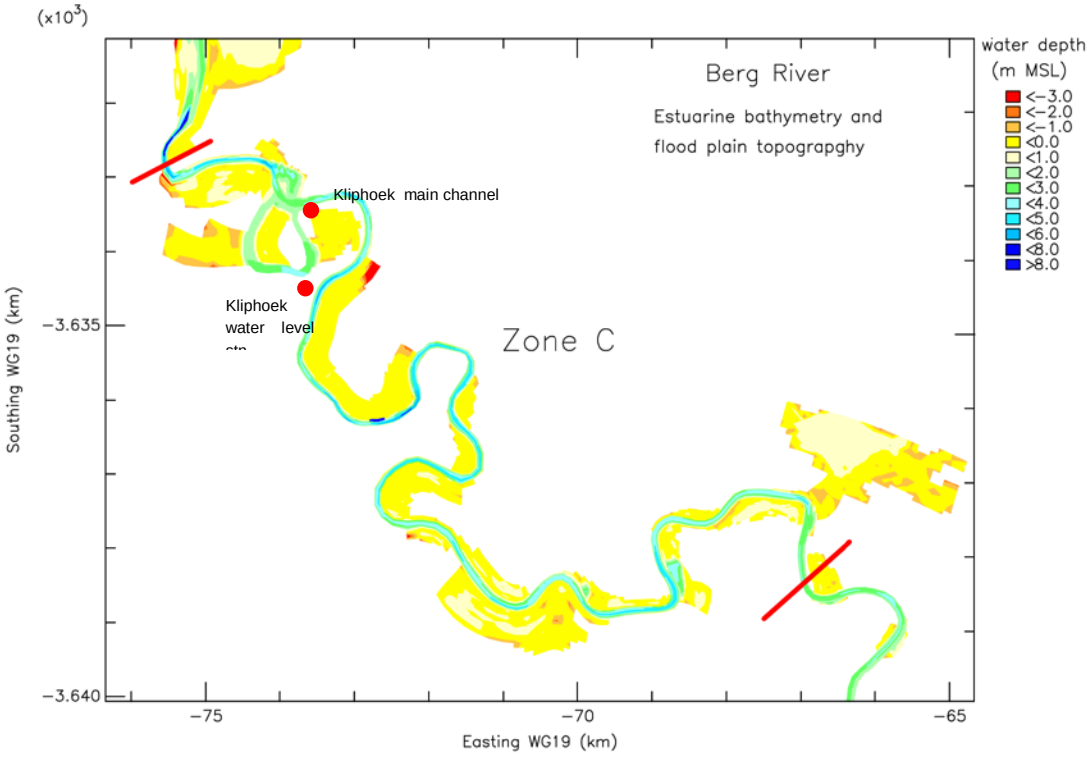

Figure 3.3d The model bathymetry used in the water quality modelling (Zone C).

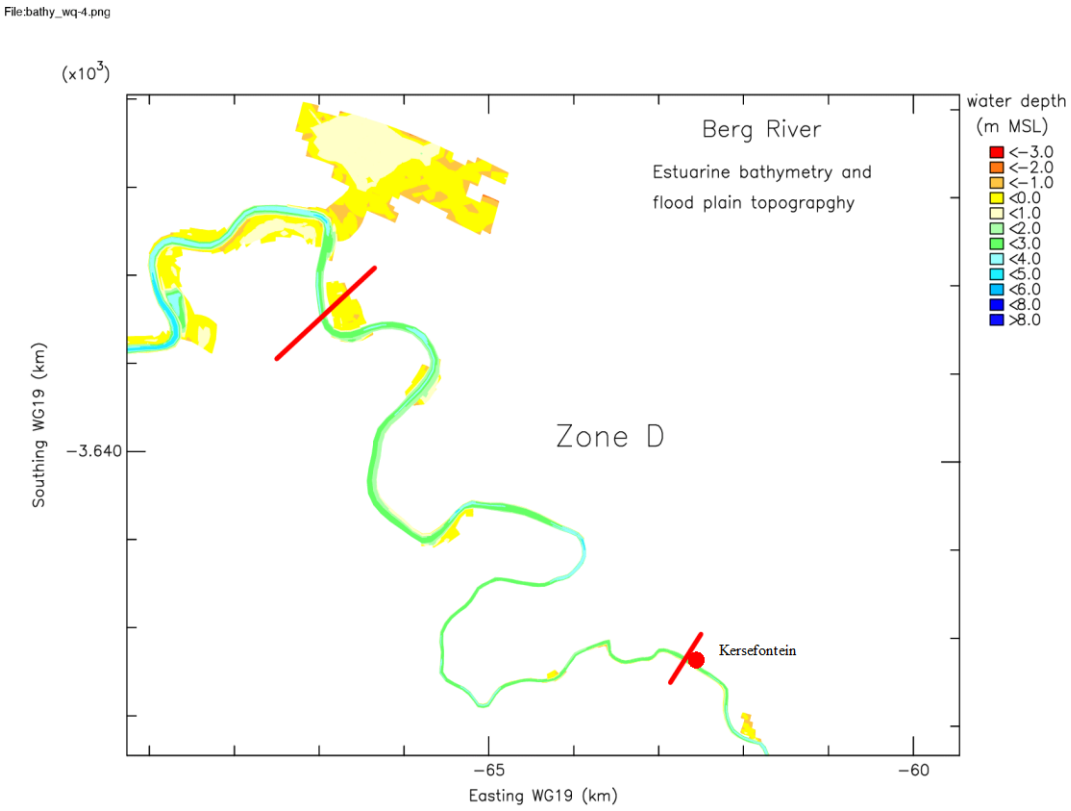

Figure 3.3e The model bathymetry used in the water quality modelling (Zone D).

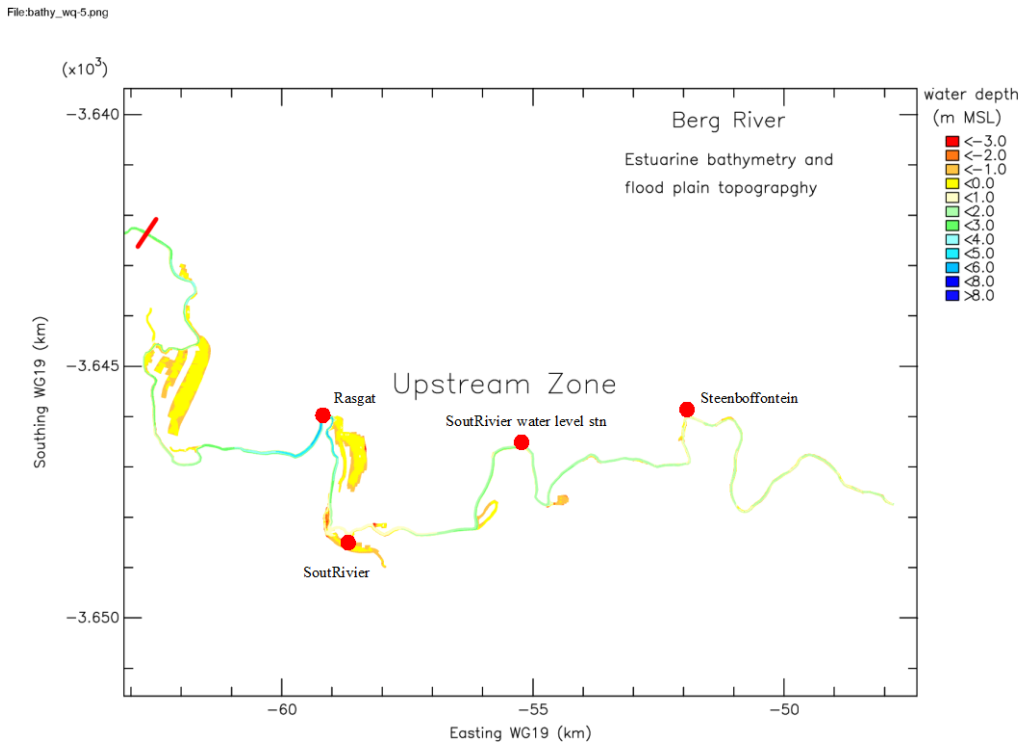

Figure 3.3f The model bathymetry used in the water quality modelling (upstream of Zone D).

These modifications to the channel bathymetry were then incorporated into the flood model bathymetries as they would be likely to affect the flood modelling results significantly for the smaller floods. These data are not plotted, however, the extent of the computational grid and the associated bathymetry used in the flood modelling study is evident in Figure 3.1 above (i.e. the region for which the a detailed bathymetry has been plotted). Note that the computational grid for the flood modelling has been extended upstream compared to that used by Beck & Basson (2007) as this was deemed necessary to reduce the errors introduced by truncating the upstream extent of the computational grid used in the flood modelling. The further extension upstream of the computational grid used in the flood modelling was not possible due to the limited extent of the DTM.

The bathymetry data show that the channel narrows and becomes more shallow upstream of the boundary between Zone C and D and then becomes even narrower and shallower upstream of about 40 km upstream. The narrower and shallower the channel is, the more readily it is flushed by freshwater inflows. This results in the upper regions of the estuary responding quite readily and rapidly to even small freshwater inflows.

A vertically integrated model has been used for both the water quality and flooding study. The rather ephemeral nature of stratification in the system means that mixing associated with periods of stratification can readily be incorporated into the model by increasing the assumed dispersion coefficients in the models.

3.3.2. Open Ocean Boundary Conditions

As no times series data were available for salinities at or near the mouth, a salinity of 35 PSU was assumed for the open ocean and a Thatcher-Harleman boundary condition was used with a “return period” or “time lag” of 1 hour. If the coastal ocean included in the model was large enough and were ocean dynamics adequately resolved in the coastal region offshore of the Berg River mouth, such a Thatcher-Harlemann condition would not be required. However, despite the fact that almost no coastal ocean area is included in the model, the water quality modelling is relative insensitive to this parameter as most of the scenarios modelled were for occasions when the lower reaches of the estuary remain highly saline.

At the open ocean boundaries the water level specified was that of the predicted tides, except for the calibration studies where actual measured data were used. The tidal predictions were made using the tidal constituents for Saldanha Bay (Rosenthal & Grant 1989). The long term mean of Saldanha Bay is approximately 0.16 m, however assuming a value of 0.21 m better matches the measured water levels in the estuary. Consequently the tidal predictions have been made using a mean level $A_0 = 0.21$ m and the 8 largest tidal constituents for Saldanha Bay (Table 3.2). Errors introduced by uncertainties in the vertical datums are likely to be < 0.1 m and consequently should not be a limitation in the modelling studies.

Table 3.2 Tidal constituents used to predict the tides in the open ocean.

TIDAL CONSTITUENT	AMPLITUDE (m)	PHASE (degrees)
Ao (Z_0)	0.260	0.000
M_2	0.489 3	90.61
S_2	0.212 9	111.98
N_2	0.131 5	78.76
K_2	0.070 3	112.23
K_1	0.055 5	134.79
P_1	0.014 4	131.00
μ2	0.020 9	64.44
O_1	0.015 4	260.06

3.3.3. Upstream Boundary Condition

The boundary conditions imposed at the upstream model boundary in the water quality modelling comprised a range of freshwater inflows as provided by Aurecon. In the flood modelling idealised flood inflows (obtained from the 1996 to 2003 data on Beck and Basson (2007) were used.

3.3.4. Surface fluxes

Atmospheric fluxes, specifically evaporative fluxes and rainfall need to be included in the model as, on longer times scales (seasonal), these fluxes influence significantly the salinity distributions within the estuary. These effects are greatest in the middle reaches where there is limited flushing of the estuarine waters both from the mouth and the upstream extremities of the estuary.

The influence of evaporation on the salinity distributions within the estuary has been simulated by the CSIR (1993) both to test the sensitivity of the salinity distributions to low flow conditions and future development scenarios. In this study, the same mean monthly potential evaporation rates for the region (source: Ninham Shand as reported in CSIR 1993) have been used. These values are tabulated below (see Table 3.3) and are in close agreement with A-Pan equivalent reference potential evaporation as reported in the South African Atlas of Climatology and Agrohydrology (Schultze *et al*. 2008) and those reported in DWAF (2007a).

Also required in order to model the net evaporative effects, are the rainfall over the estuary as well as the rainfall temperature. In the modelling undertaken here the rainfall temperature is not required as temperature is not modelled. For the purpose of setting up the requisite input files to the model, the rainfall temperature has been assumed to be the same as the

estimated monthly mean air temperatures based on data obtained from Langebaanweg (du Toit 1988).

The monthly rainfall over the estuary has been estimated using the South African Atlas of Climatology and Agrohydrology (Schultze *et al*. 2008). The annual sum of these monthly mean rainfall estimates is approximately 5% less than the annual mean rainfall reported for the quarternary catchment G10M (DWAF, 2007a) considered to be representative of the rainfall occurring over the Berg River estuary.

Table 3.3 Mean monthly potential evaporation, estimated mean monthly rainfall and air temperature for the Berg River estuary.

Month	Mean monthly potential evaporation rates (mm/month)	Estimated mean monthly rainfall (mm/month)	Estimated mean monthly air temperature (ºC)
October	197	3	20.5
November	264	5	20.0
December	316	10	19.0
January	319	20	17.5
February	253	40	16.0
March	246	50	14.5
April	152	55	13.5
May	95	50	13.0
June	65	30	14.5
July	65	15	16.0
August	84	5	18.5
September	125	5	20.0
Annual Total	**2181**	**288**	**-**

3.3.5. Initial conditions

As is typically done in such modelling studies (to avoid problems with wetting and drying in the model during its initiation), the model simulations initially were started at peak high tide. This is particularly recommended where there is significant wetting and drying of tidal flats in the model (as is the case here).

The initial sea level in the water quality model simulations was set equal to the water level imposed at the open boundary (i.e. predicted offshore water level at high tide). This proved problematic as this initiated a large volume exiting the estuary. This outflow, occasioned by the fact that true high tidal levels do not propagate upstream over the full length of the

estuary, resulted in the initial salinity distributions being distorted (i.e. the waters in the estuary became too fresh shortly after the initiation of the simulations).

The initial water levels for the flooding scenarios modelled were obtained by setting the initial water levels to near low tide levels and then slowly increasing the freshwater inflows at the upstream boundary over a period of 24 hours to representative winter base flows (12 m^3/s, 18 m^3/s and 35 m^3/s) and maintaining these flows for a total of three days. The initial water level distributions obtained these three days were the water levels applied in the flooding studies.

In the water quality model simulations investigating i) the ease with which saline waters are flushed from the estuary during high freshwater inflow or flood period; and ii) the flows required to totally flush the estuary, late summer salinity distributions (March 1990) were used to initialise the model simulations. In simulations designed to determine the salinity distribution in the Berg River in summer to late summer under various present and future flow scenarios (in particular the maximum upstream extent of the penetration of saline waters), the model was initialised with salinity distributions typical of late spring (November 2004). No salinity data were required to initialise the flood model as salinity was not simulated.

3.3.6. Model Parameters

The model parameters were selected from experience, similar studies, and literature, and subsequently optimised in the calibration exercise. The optimal model parameters used in the water quality modelling and flood modelling studies are listed in Tables 3.4 and 3.5, respectively.

Table3.4: Numerical parameters used in DELFT3D-FLOW for the water quality modelling study

PARAMETER	PARAMETER VALUE
Time step	60 seconds
No of vertical layers	1
Horizontal viscosity	1.0 $m^2.s^{-1}$
Background vertical viscosity (1)	0.000 05 $m^2.s^{-1}$
Horizontal diffusivity	5.0 $m^2.s^{-1}$
Background vertical diffusivity (1)	0.000001 $m^2.s^{-1}$
Chézy coefficient	(see Figure 3.4)
Wind stress coefficient (2)	Not used
Advection scheme	Cyclic method
Flooding depth (Threshold depth)	0.10 m
Drying depth (Marginal depth)	0.05 m
Sigma-coordinates correction (3)	Off
Evaporation	On
Forester filter horizontal	On
Atmospheric heat flux model	Not used

Notes:
(1) These background values are added to the viscosity/diffusivity calculated by the *k-ε* turbulence closure scheme.
(2) Wind forcing was not used in the model simulations.

The bottom friction in the water quality modelling was increased at the upstream extremity of the model. This was to damp any reflection of the tidal wave moving up the estuary from the upper boundary of the model. The bottom friction coefficient was also increased in the low-lying areas adjacent to the main channel of the estuary. (Figure 3.4). This was to make allowance for increases in friction resulting from vegetation and any grasses in these areas.

The bottom friction was defined using a Manning coefficient. Initially, to be consistent with the Beck & Basson (2007) study, values of more or less the same magnitude were used in the flood modelling (see Table 2.5). However, a literature search, coupled with an assessment of the nature of the likely flood plain "roughness" led to higher friction coefficients being used in the flood modelling study, particularly over the adjacent flood plain. In the absence of detailed knowledge of the "roughness" of the various surfaces, a Manning friction coefficient was defined that was a function of depth. In the main channel of the estuary the Manning coefficient could be as low as 0.024 $m^{-1/3}$.s (which is slightly higher than the general Manning coefficient used in the Beck and Basson study) while in the adjacent flood plain areas the Manning coefficient increased with decreasing depth and could reach maximum value of 0.04 $m^{-1/3}$.s.

The selection of appropriate friction coefficients for the flooding study is crucial as, in principle, these assumptions could affect the inundation areas significantly. If the friction in the main channel is overestimated and that in the adjacent flood plain underestimated, this could lead to greater inundation in the upstream reaches and less flooding in the lower reaches. Conversely, should the friction in the channel be underestimated and that in the flood plains overestimated, then inundation in the upstream reaches could be underestimated and that in the lower reaches overestimated. Should the friction coefficient be overestimated throughout the model, this could lead to sharper and higher flood water level peaks. Conversely should the friction parameters be underestimated throughout the model, flood peaks could be flatter and more diffuse than in reality.

Simulations were undertaken determine the sensitivity of the model runs to realistic changes in bottom friction parameterisations. In general, the percentage change in the inundation area between the various simulations did not exceed one percent for each flood size considered, however for the smaller flood sizes the percentage change in inundation area ranged between 1.5% and 2%. This is the same order of magnitude in the changes observed between inundation areas for the same flood size but different winter base flow conditions or between successive flood size classes for the same winter base flow conditions.

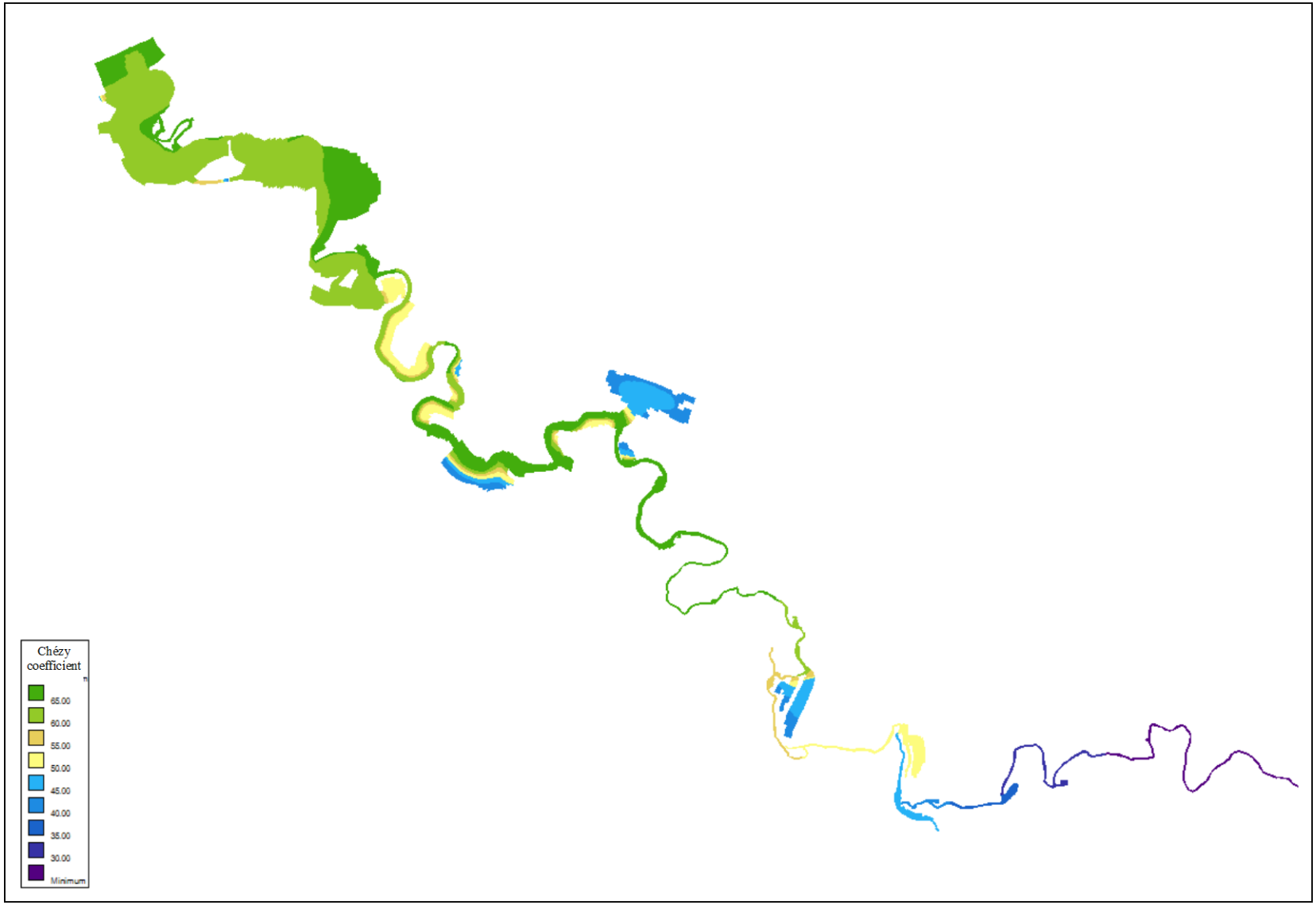

Figure 3.4 Bottom friction parameter (Chézy - $m^{½}.s^{-1}$) used in the water quality modelling

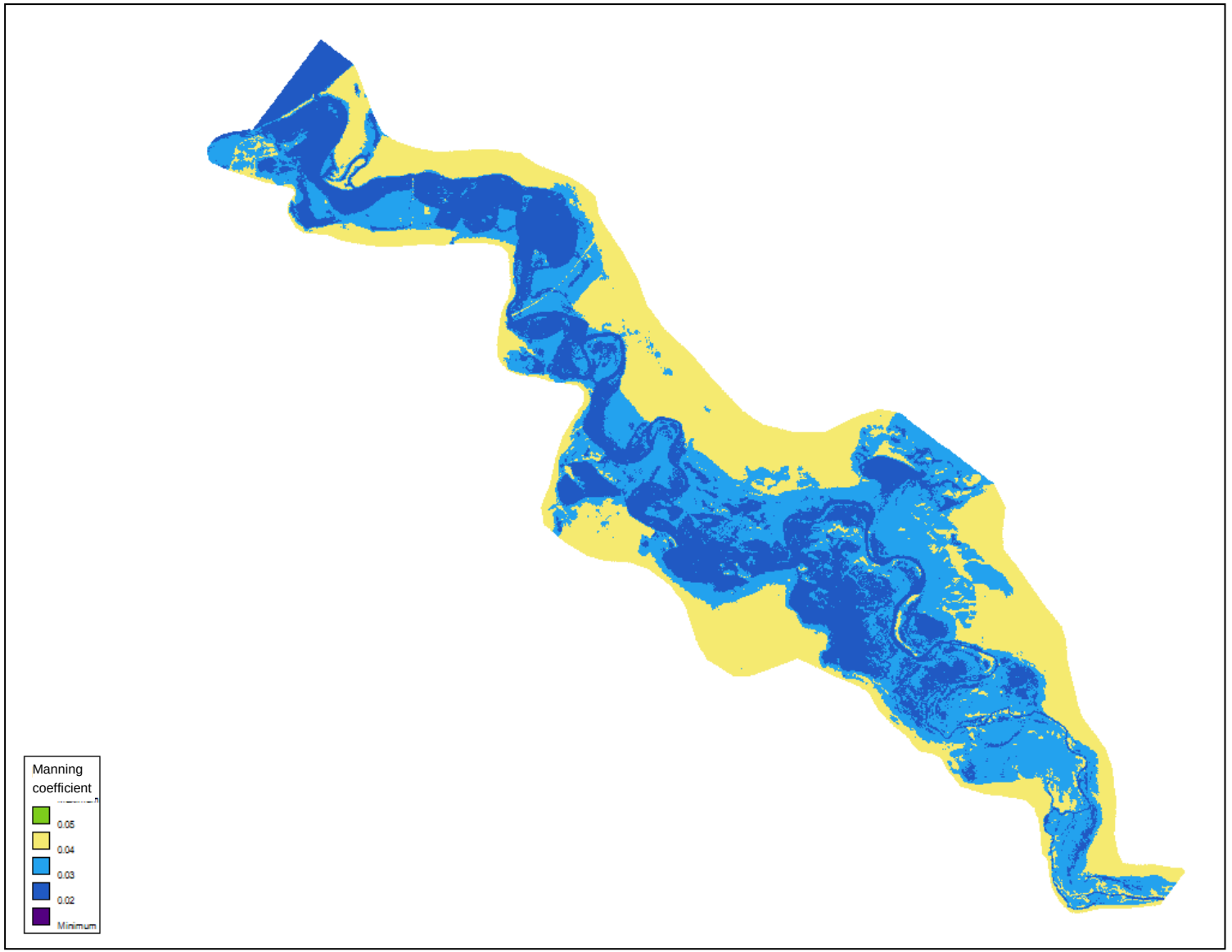

Figure 3.5: Bottom friction parameter (Manning – $m^{-1/3}.s$) used in the water quality modelling.

Table 3.5 Numerical parameters used in DELFT3D-FLOW for the flood modelling study

PARAMETER	PARAMETER VALUE
Time step	15 seconds
No of vertical layers	1
Horizontal viscosity	1.0 $m^2.s^{-1}$
Background vertical viscosity (1)	0.000 05 $m^2.s^{-1}$
Background vertical diffusivity (1)	0.000001 $m^2.s^{-1}$
Manning coefficient	(see Figure 3.5)
Wind stress coefficient (2)	No wind forcing in model
Advection scheme	Cyclic method
Flooding depth (Threshold depth)	0.10 m
Drying depth (Marginal depth)	0.05 m
Evaporation	On
Forester filter horizontal	On
Atmospheric heat flux model	Not used

Notes: (1) These background values are added to the viscosity/diffusivity calculated by the *k-ε* turbulence closure scheme.

(2) Wind forcing was not used in the model simulations.

3.3.7. Monitoring Stations and defined zone in the Berg River Estuary.

The various zones defined for the Berg River Estuary are described in Figure 2.17 for the water quality modelling study and in Figure 2.12 for the flood modelling study.

Water quality stations have been defined and used in the water quality sampling programmes over the years. These have been used in the present water quality modelling to help interpret the model outputs (see Table 3.6 and Figure 3.6). The distance from estuary mouth reported in Table 3.6 show small differences when compared to previous studies. These distances were calculated by defining a high resolution path up the centre channel of the estuary in Google Earth ©. These differences are small and are not significant within the context of this study.

Table 3.6 Water Quality Stations and chainages from the estuary mouth

Site	Latitude	Longitude	Chainage (m)
B00	32° 46.223' S	18° 08.671' E	0
Laaiplek_WL	32° 46.262' S	18° 08.994' E	545
B01*	32° 46.359' S	18° 09.053' E	690.
B02	32° 46.502' S	18° 09.092' E	970
B03*	32° 46.873' S	18° 08.593' E	2 040
B04*	32° 47.311' S	18° 08.687' E	3 075

Site	Latitude	Longitude	Chainage (m)
B05*	32° 47.264' S	18° 09.347' E	4 230
B06	32° 47.476' S	18° 09.874' E	5 240
B07	32° 47.483' S	18° 10.258' E	5 855
B08	32° 47.593' S	18° 11.224' E	7 915
B09*	32° 48.083' S	18° 11.869' E	10 302
B10	32° 48.687' S	18° 11.891' E	11 395
B11	32° 49.331' S	18° 11.756' E	12 580
B12	32° 49.264' S	18° 12.566' E	13 945
Kliphoek-main	32° 49.367' S	18° 12.721' E	14 535
Kliphoed-WL	32° 49.861' S	18° 12.673' E	14 660
B13	32° 49.834' S	18° 13.373' E	16 130
B14	32° 50.622' S	18° 13.819' E	20 695
B15	32° 51.487' S	18° 13.560' E	24 520
B16	32° 52.325' S	18° 15.112' E	28 475
B17	32° 51.655' S	18° 16.814' E	32 800
B18	32° 52.646' S	18° 17.943' E	36 200
B19	32° 53.516' S	18° 18.537' E	39 860
B20	32° 54.550' S	18° 18.016' E	43 560
Kersefontein	32° 54.250' S	18° 19.765' E	46 930
B21	32° 54.430' S	18° 19.812' E	46 960
Jantjiesfontein	32° 55.533' S	18° 19.811' E	51 000
B22*	32° 55.777' S	18° 19.811' E	51 530
B23*	32° 56.736' S	18° 20.421' E	53 945
B24*	32° 56.670' S	18° 21.689' E	56 320
Rasgat	32° 56.276' S	18° 22.173' E	57 528
B25*	32° 56.857' S	18° 22.160' E	58 700
SoutRivier	32° 57.532' S	18° 22.822' E	61 110
SoutRivier_wl	32° 56.585' S	18° 24.536' E	65 070
Steenbokfontein	32° 56.288' S	18° 26.659' E	70 987

In the flood modelling study, the same areas of interest as defined by Beck & Basson (2007) has been used. The labelling of these sites remains the same as in Beck & Basson (2007). In their study, time series were plotted at each of these locations. These time series were used in the flood modelling to identify pans or low-lying areas that had a similar behaviour to pans, i.e. filled and then did not drain but rather dried out over time.

Beck & Basson (2007) associated a representative area with each of these time series locations and also reported a rough classification for each of these areas. The representative area for each pan was obtained from the Berg River Baseline Monitoring Programme as rough areas contained in an Excel spreadsheet. These are the data that were used in this study.

The location of each of these time series is given in Figures 3.7a to e. The original classifications of each are listed appendices to the report of Beck & Basson (2007).

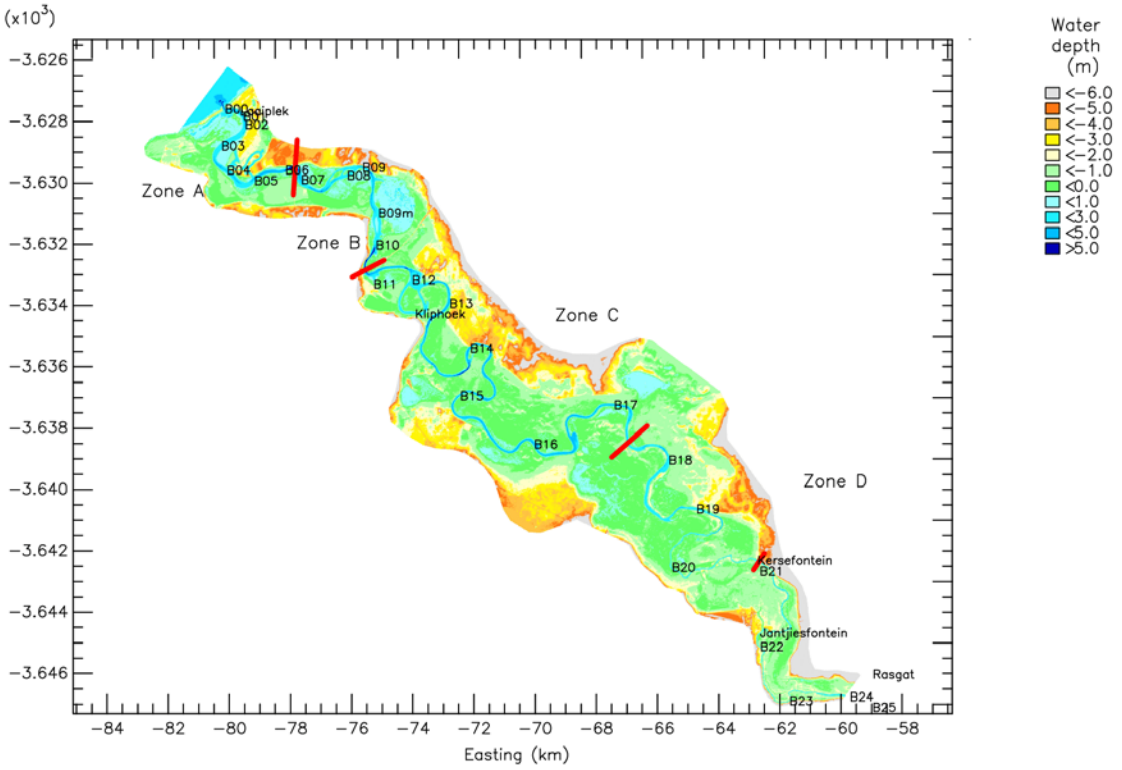

Figure 3.6a Water quality station locations in the Berg River estuary and associated zonation.

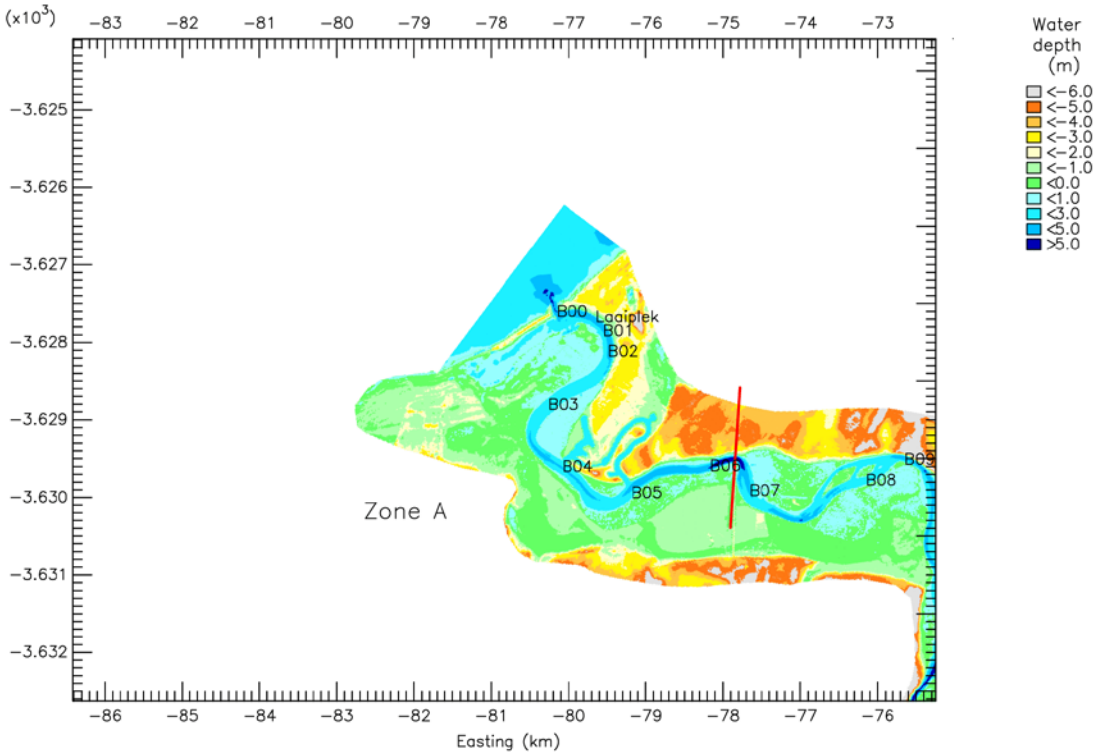

Figure 3.6b Water quality station locations in Zone A of the Berg River estuary

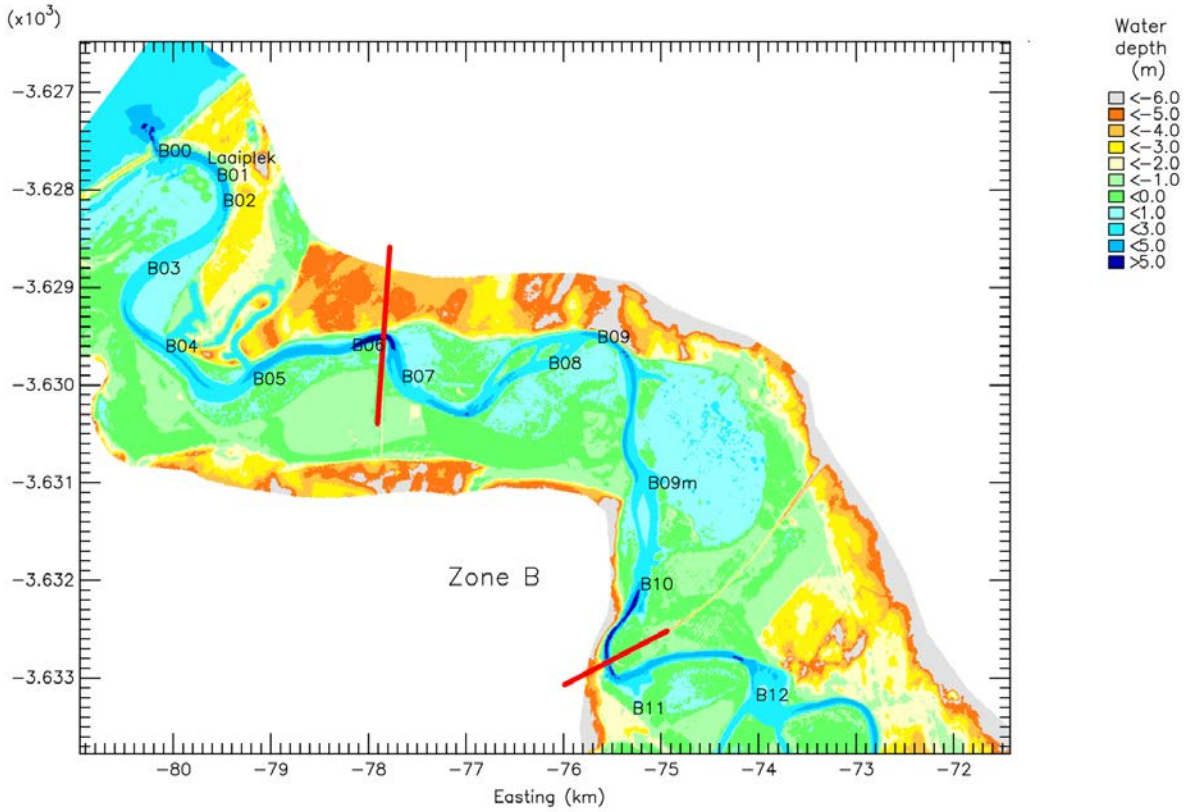

Figure 3.6c Water quality station locations in Zone B of the Berg River estuary.

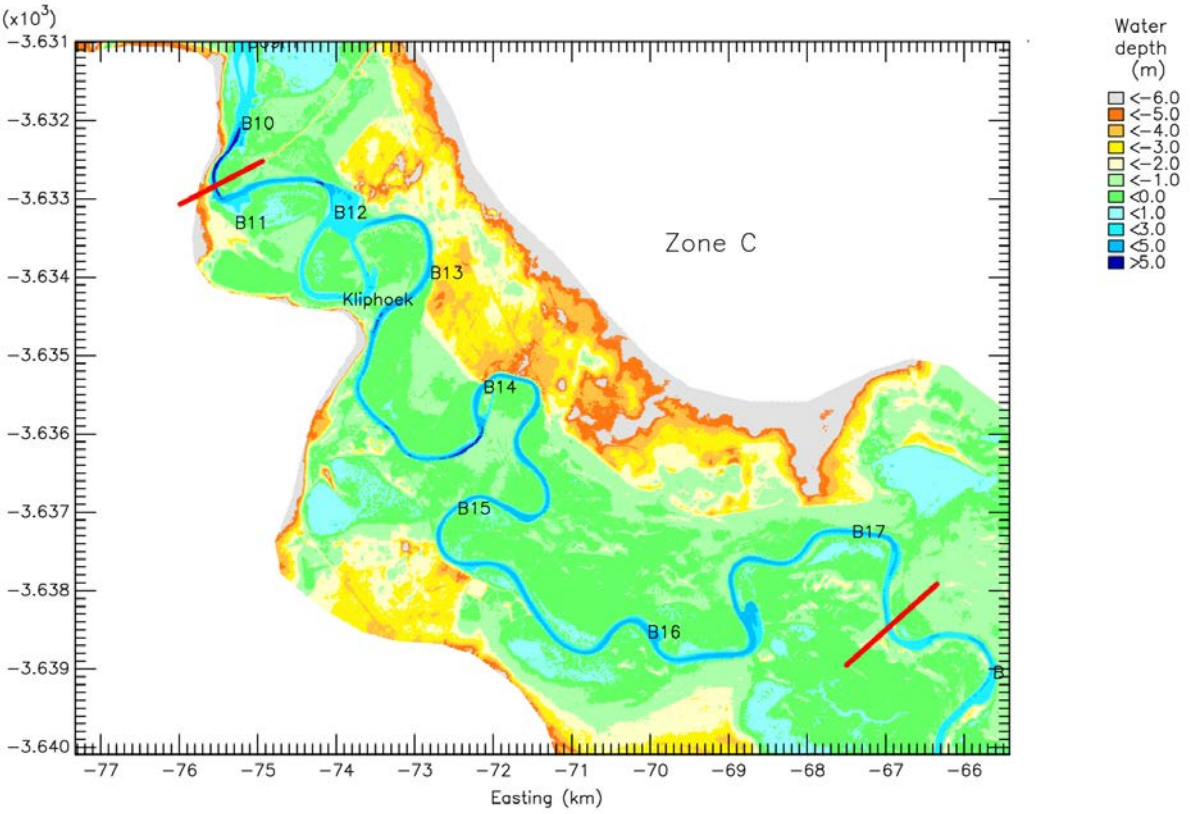

Figure 3.6d Water quality station locations in Zone C of the Berg River estuary

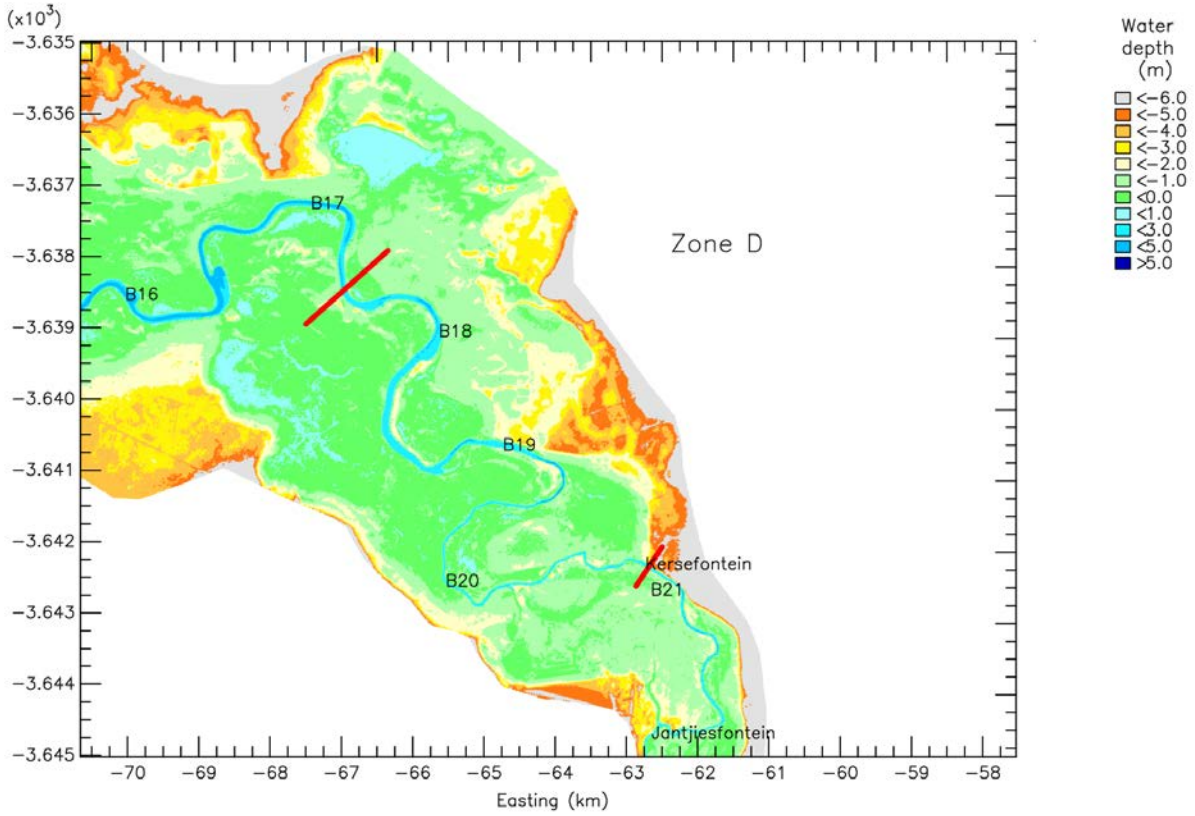

Figure 3.6e Water quality station locations in Zone D of the Berg River estuary

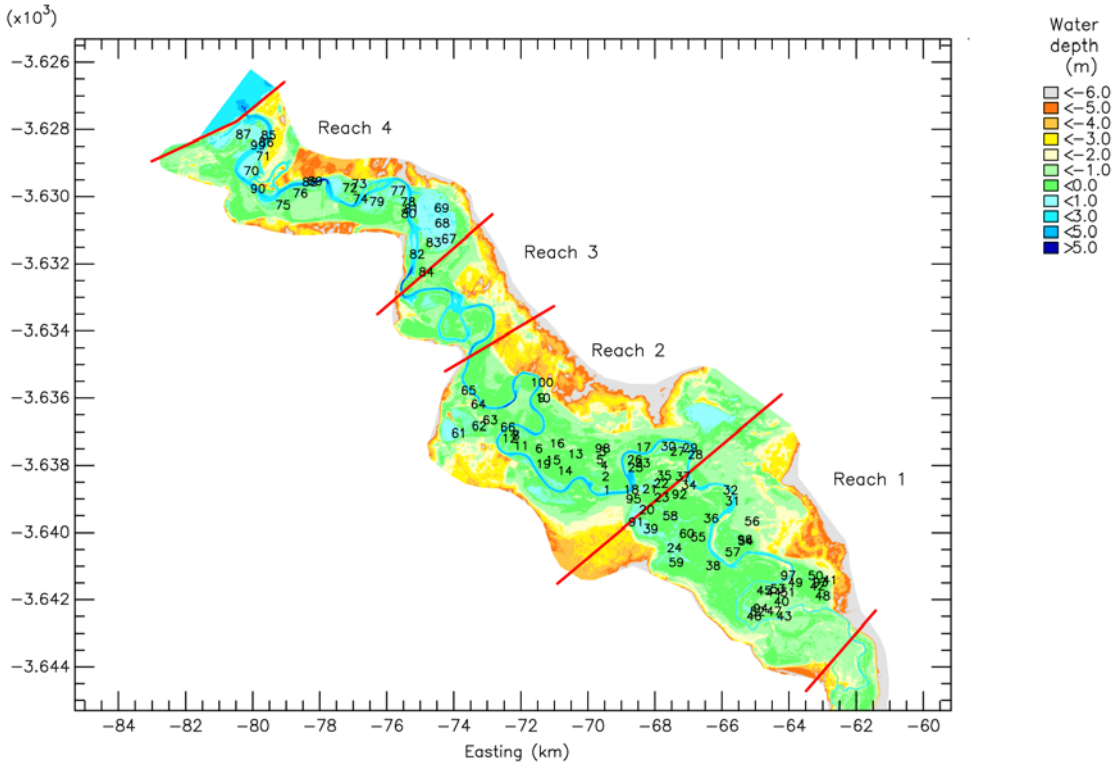

Figure 3.7a Time series locations used in the Berg River estuary flood modelling study.

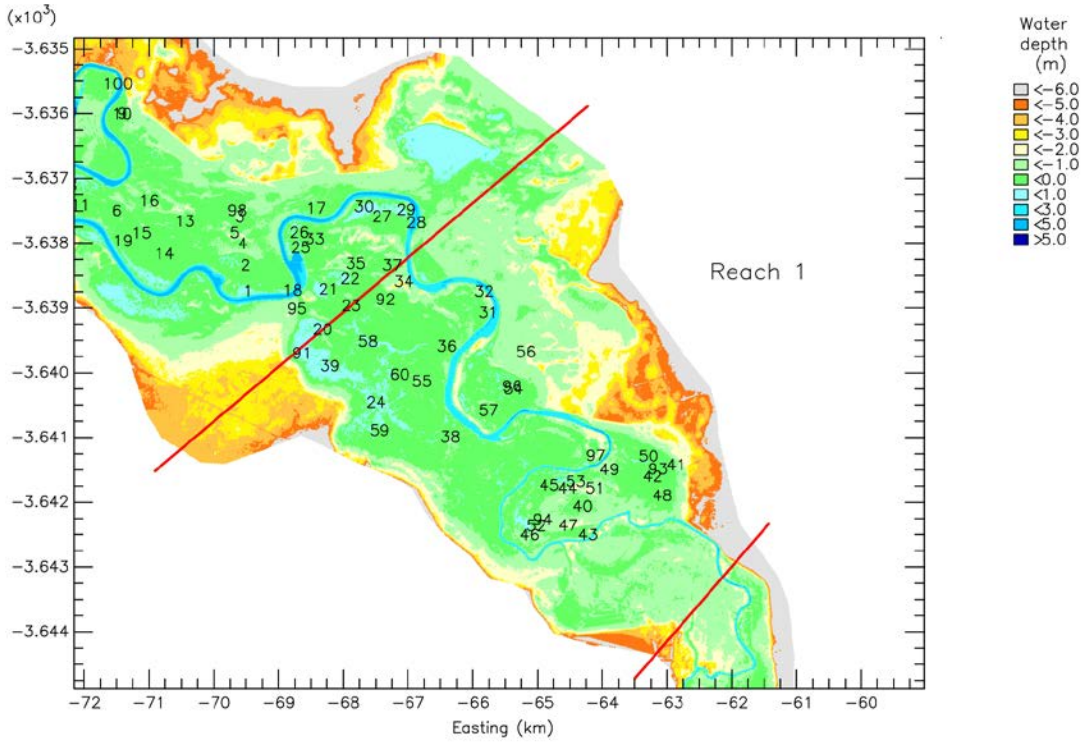

Figure 3.7b Time series locations in Reach 1 as used in the Berg River estuary flood modelling study.

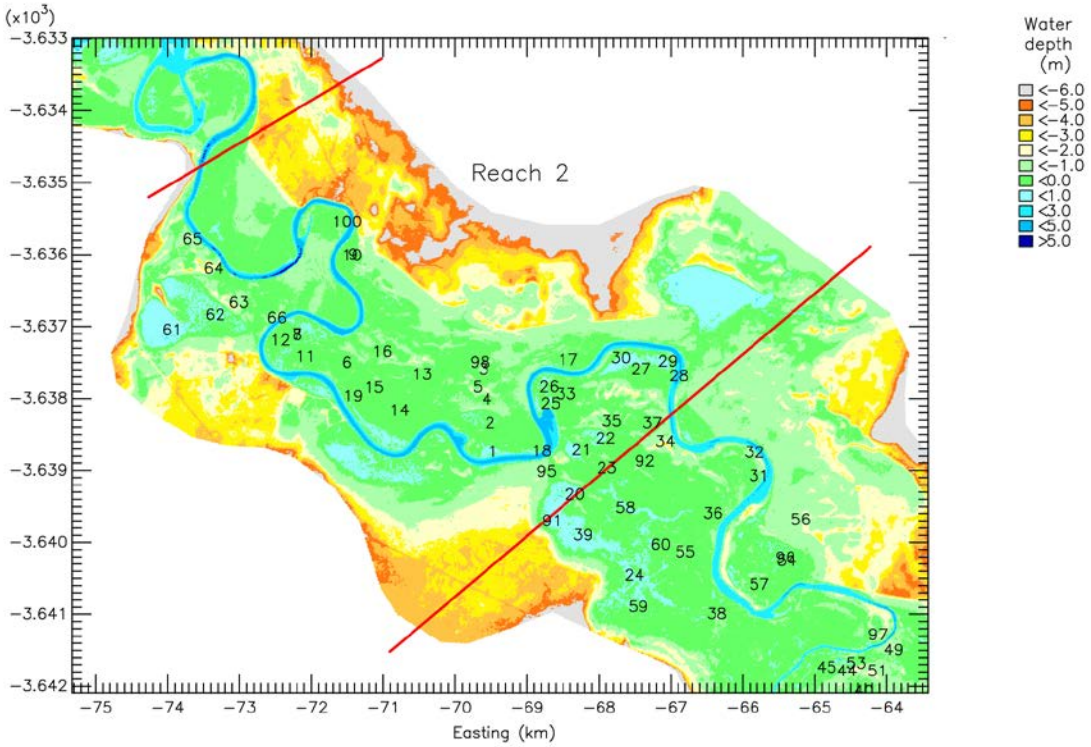

Figure 3.7c Time series locations in Reach 2 as used in the Berg River estuary flood modelling study

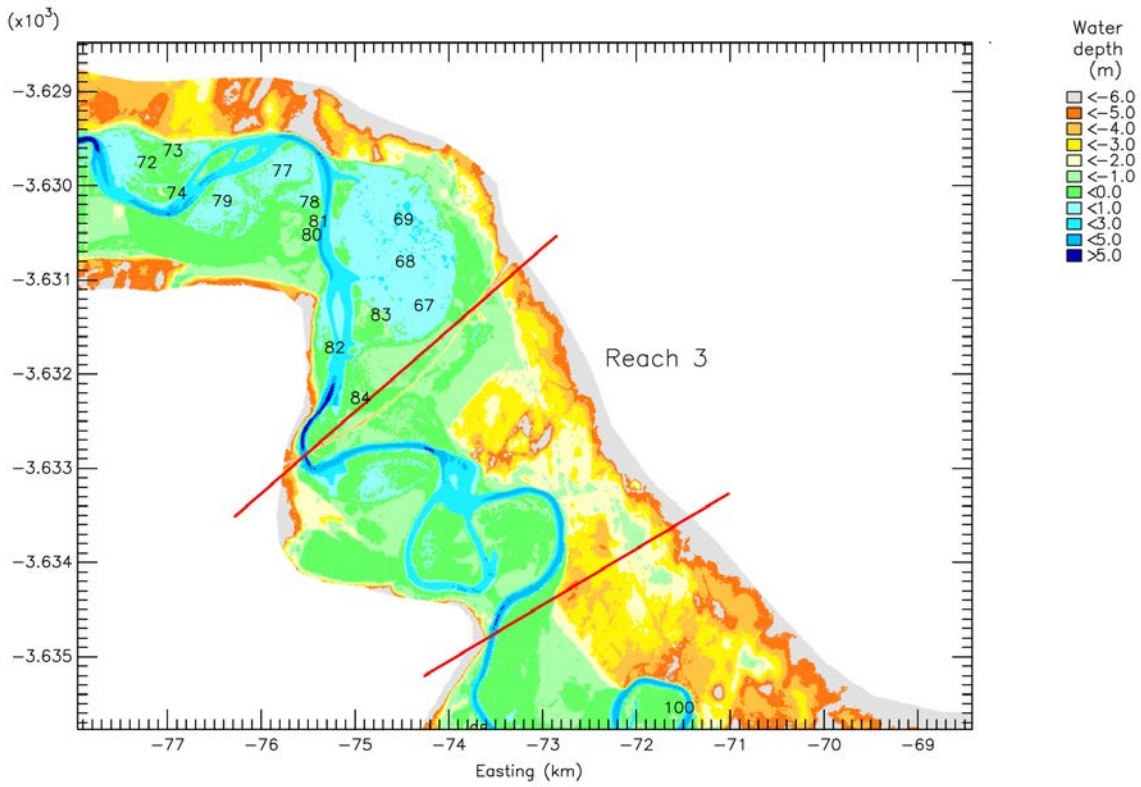

Figure 3.7d Time series locations in Reach 3 as used in the Berg River estuary flood modelling study

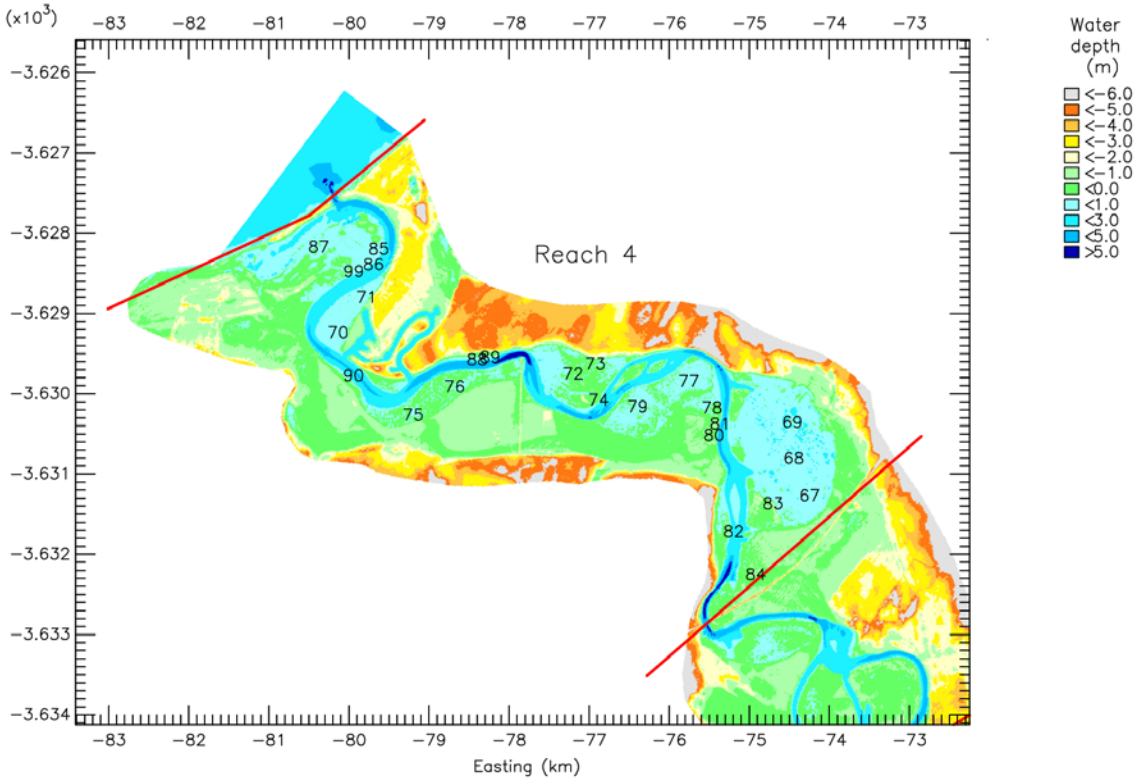

Figure 3.7e Time series locations in Reach 4 as used in the Berg River estuary flood modelling study

3.4. Model calibration and verification

In calibrating the model the most important factor is to ensure an accurate representation of bathymetry in the model. Significant effort was taken to ensure that the model bathymetry was correct.

For the water quality (salinity) modelling, the calibration exercise comprised:

- a calibration of water levels along the full length of the estuary;
- a calibration of salinity distributions on longer time-scales using measured salinity profiles (see Annex A).

As the model was not relied upon to provide results at shorter time scales, no event-scale calibration of salinities was undertaken. In any case, the data for such a short term model verification is extremely limited. The "calibration and verification" of salinity in the model therefore is one where the focus has been on the broad seasonal characteristics of the extent of upstream penetration of saline water during seasonal low flow conditions.

3.4.1. Water level calibration

The first step in the calibration of the water quality model was undertaken using water level data at a number of sites along the length of the estuary. In the calibration procedure, the discrepancies between the observed and modelled results were minimised by "tuning" model parameters such as boundary conditions (tidal amplitudes), water depths, storage volumes and bed roughness.

In the initial calibration simulations of the water quality model, inconsistencies in the bathymetry were corrected based on the water level behaviour in the estuary, as changes in bathymetry typically affect tidal amplitudes the most. In most South African estuaries the bathymetry of the mouth of the estuary is a major factor in the calibration of tidal water levels; however, here the deep mouth conditions meant that this was not the case.

Once the bathymetric effects had been corrected, the bottom friction co-efficients in the model were used to calibrate both the tidal amplitudes and tidal phase lags at a number of upstream locations in the estuary. The locations chosen were Laaiplek, Kliphoek, Kersefontein, Rasgat, Soutkloof and Steenboksfontein.

The modelled water level data at these locations compare reasonably well with the measured data both in amplitude and phase lag. The only exception to this is the modelled and measured water levels at Kersefontein. The model does not seem to fully simulate the amplification of tidal water levels that has been measured at Kersefontein. This amplification of the tide is based on one set of observations undertaken by the CSIR in 1990 and seems to be localised as tidal levels at Jantjiesfontein some 4.5 km upstream of Kersefontein are very similar to those at Rasgat ~10 km upstream of Kersefontein. The only explanation for the amplified tide at Kersefontein is that the river channel narrows and restricts tidal variability

upstream of Kersefontein but downstream of Jantjiesfontein. There is evidence of such narrowing, however, the amplification effect seems to be unexpectedly large. Future measurement campaigns should verify these observations and also seek to provide greater clarity of the flows and water level variability in these upper reaches of the estuary.

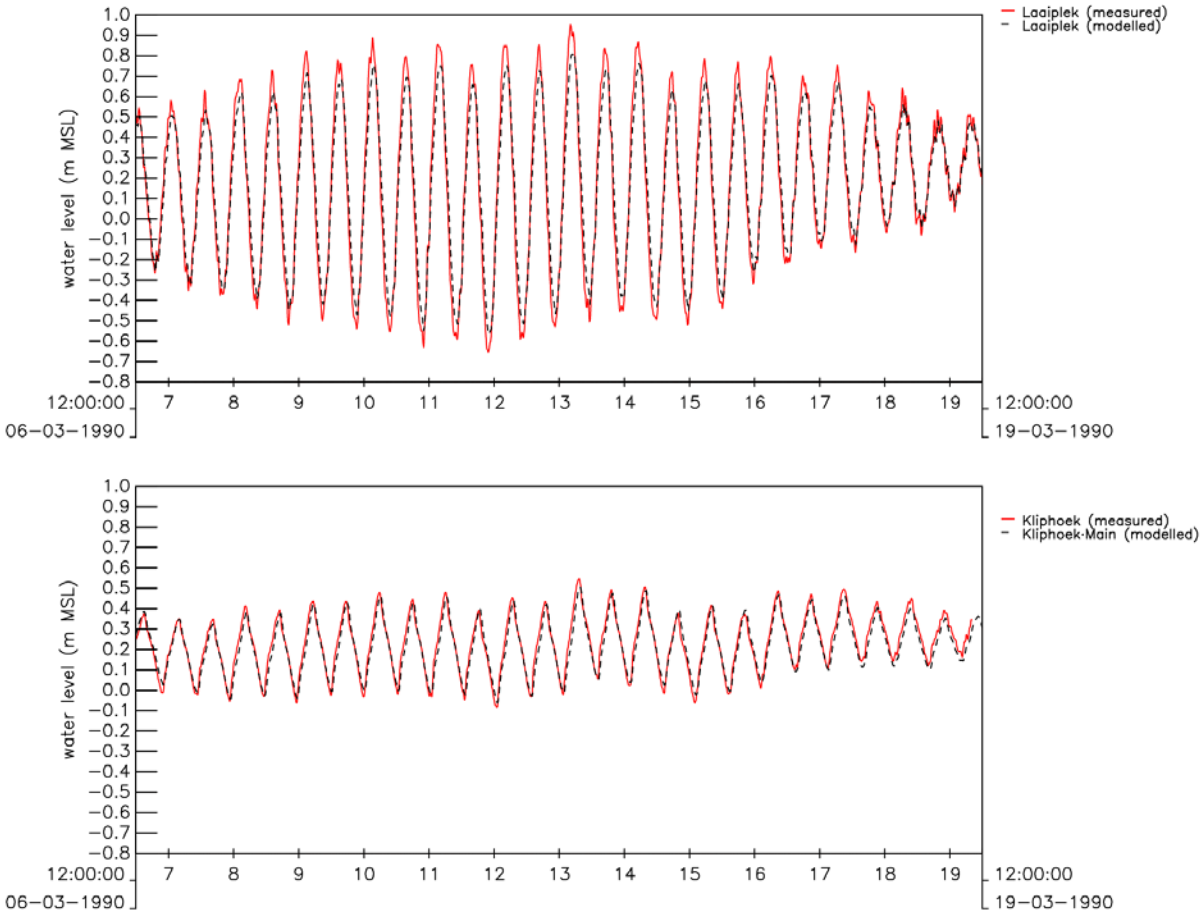

Figure 3.8a Comparison of modelled and measured water levels at Laaiplek (near the estuary mouth) and Kliphoek.

3.4.2. Salinity calibration

Further calibration of the DELFT3D-FLOW model was undertaken using the most conservative tracer, salinity, as on the time scales being simulated it is a reflection of the model transport (advection) and turbulent mixing (diffusion) only.

As noted in Annex A, the salinity distribution can change quite significantly on shorter time scales, in particular the upstream penetration of saline waters in the estuary between Stn 14 (21 km upstream) and Stn 18 (35 km upstream) is quite sensitive to both the preceding spates as well as the magnitude of the base flows occurring around the time of the observations. Given the scarcity of longitudinal profile measurements taken on the events scale (i.e. as a sequence of longitudinal profiles measures every couple of days or at most weeks apart) and the sensitivity of the salinity distributions of the middle to upper reaches to

freshwater spates, the opportunity to calibrate the water quality model on the event scale is limited.

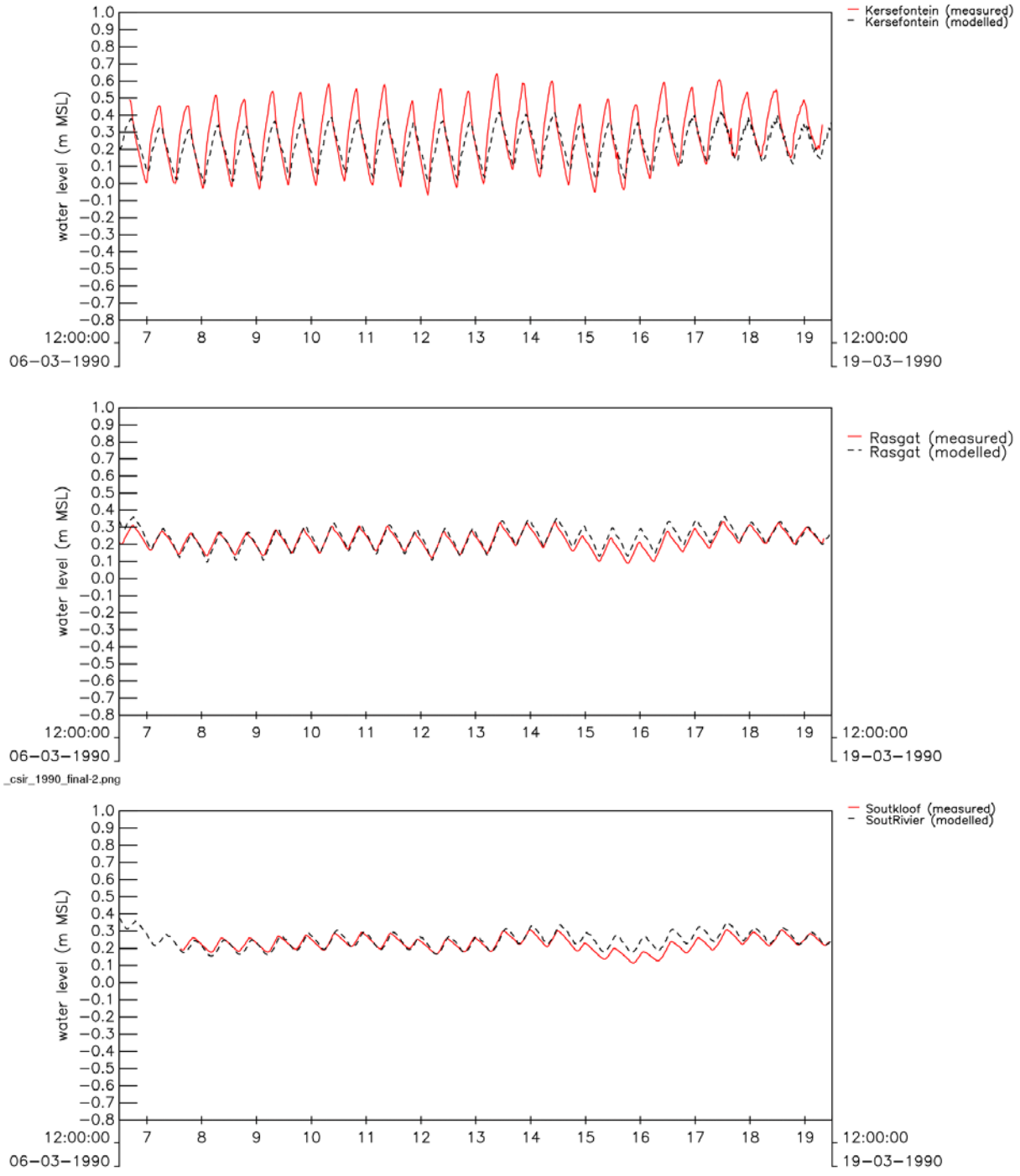

Figure 3.8b Comparison of modelled and measured water levels at Kersefontein, Rasgat and Soutkllof

As the focus of the study was on longer term salinity distribution, a comparison was made between the modelled and observed salinity distributions during the various seasons of the

year for typical (median) monthly flow conditions. The model calibrations indicated that the upstream distributions of salinity obtained from the model during the transition period from winter to summer freshwater inflows and during late summer/early autumn, correlated quite well with measured salinity distributions for these periods. This provided confidence in the predictions of the maximum upstream penetration of saline waters in late summer.

However, in the lower to middle and middle reaches of the estuary where the flushing is limited, the model predicted salinity distribution higher than those observed in these reaches. Salinities greater than 35 PSU were predicted for this region.

Analysis of the evaporation in the model and the nature of the model grid suggested that net evaporation (i.e. evaporation – rainfall) may have been overestimated by a factor of up to two. This is due to the fact that the model grid covers shallow areas that at times are wet and other times are dry. The nature of the wetting and drying algorithm is such that there remains a retention volume in the dry cells. The evaporation algorithm works on the area of the model so evaporative effects will be overestimated whenever the water levels are below the maximum water levels accommodated within the model grid. The area of the grid below ~ 1.2m is roughly 1,8 times that of the grid below 0.2 m MSL. It is for this reason that it is believed that the evaporative effects are overestimated in the model by a factor of up to two times.

However this error is not sufficient to account for all of the excess salinity observed in the lower reaches of the estuary and another reason needs to be sought for some of the higher salinities observed. Any groundwater inputs into the model have been ignored as no robust estimate exists of such groundwater inputs into the estuary. Ignoring potential groundwater inputs could be part of the cause of the higher salinities simulated in the lower to middle reaches of the estuary. Figures 2.18 and 2.19 in Section B2.3.2 suggest that there may be substantial groundwater inflows into the estuary between 20 km and 40 km upstream, *i.e*. into the low-lying areas in the middle reaches of the estuary.

Using the evaporation data in Table 3.3, theoretically the net evaporation throughout the estuary (assuming 0.2 m MSL water levels) can be as high as 1.5 m^3/s in summer and as low as in winter. Combined freshwater inflows (river and groundwater) would need to be of this order to prevent salinities rising about that of seawater. As salinity higher than 35 PSU is not observed in the main channel of the estuary, the implication is that groundwater inflows must be as high as 0.9 m^3/s in summer (evaporation of 1.5 m3/s – river inflows of 0.3 m^3/s) or that the potential evaporation figures in Table 3.3 are too high.

One-dimensional model simulations undertaken by the CSIR in 1993 simulated salinities exceeding 35 PSU in the lower to middle reaches of the estuary (5 to 25 km upstream) from January onwards for summer base flows of between 0.0 and 0.6 m^3/s. As this one-dimensional model should not suffer the inaccuracies in evaporative effects due to wetted and drying tidal flats and marshes, the higher salinities (~ 38 PSU) modelled can be considered to be due to the fact that groundwater inflows were also ignored in this model.

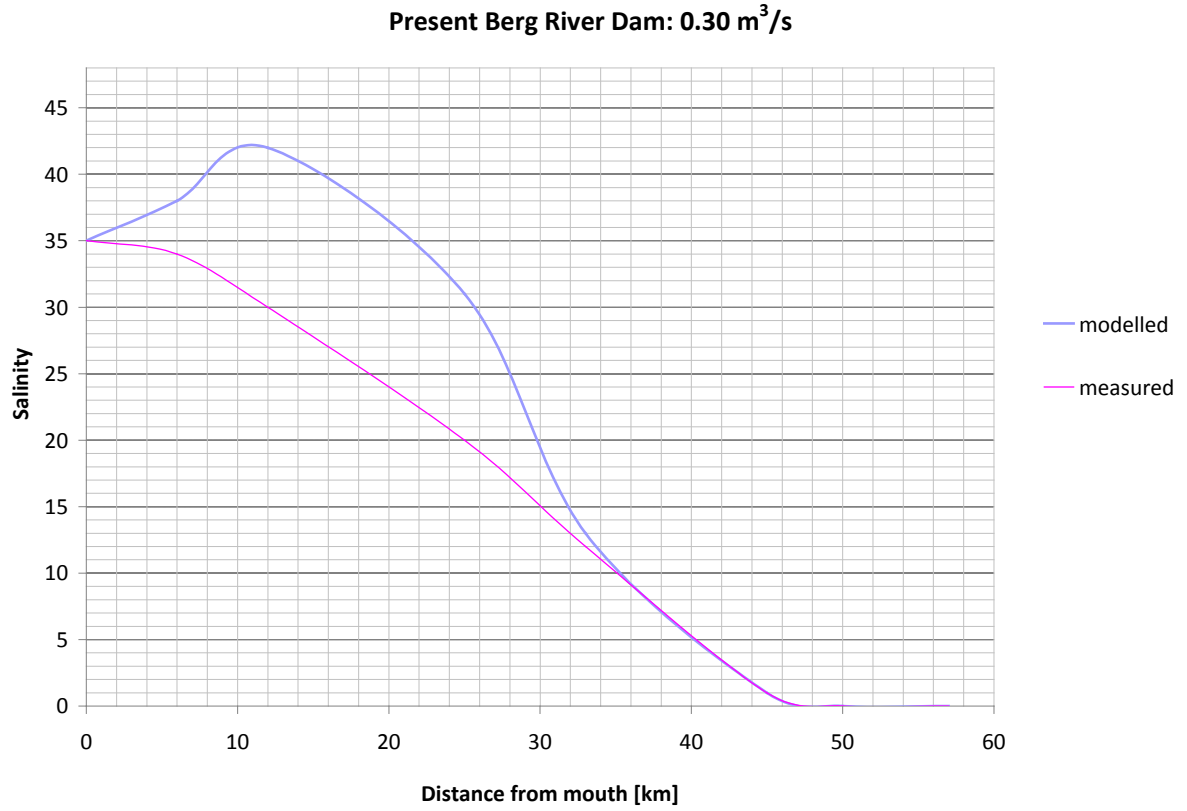

Figure 3.9 Comparison of modelled versus measured salinity in the middle and upper reaches if the Berg River estuary.

Long-term simulations of salinity distributions under present day conditions correspond well with the observed salinity distribution upstream of 25 km from the mouth of the estuary (Figure 3.9).

In summary, the water quality model simulates unrealistically high salinities in the lower or middle reaches of the estuary due both to the fact that evaporative effects have been overestimated in the Delft3D-Flow model and that groundwater inflows have been ignored. Consequently, the model results for the water quality model are only considered to be substantively correct upstream of 25 km from the mouth of the estuary.

3.4.3. Flood level calibration

Due to the dearth of water level data between Kliphoek and Jantjiesfontein, a robust calibration exercise could not be undertaken for the flood model. However comparison of:

- the flood model water levels and the observed water levels at Jantjiesfontein (G1H023) and the railway bridge (G1H024); and,
- the fact that the flood model seemed to be relatively insensitive to bottom friction parameterisations;

suggest that the flood model was adequately calibrated or verified for the purposes of this study were the focus is on relative changes in flooding behaviours.

Beck & Basson (2007) adjusted their flood model parameters until the simulated water levels at Jantjiesfontein (G1H023) were within 0.5m of the measured water levels at this site. In general the simulated water levels in their model were between 0.1 and 0.3 m lower than the observed water levels at G1H024 (Railway Bridge).

The analysis of water levels from the present flood modelling study suggests that the simulated water levels at Jantjiesfontein (G1H023) were within 0.2 m of the measured water levels at this site. In general the simulated water levels in the present flood model were usually between 0.1 and 0.2 m lower than the observed water levels at G1H024 (Railway Bridge). The reason for this small discrepancy is unknown.

4. Water Quality Model Results

4.1. Scenarios Modelled

The flow scenarios modelled are required to resolve the ***salinity distributions*** in the Berg River Estuary under the various scenarios. This requires very accurate resolution of the along channel bathymetry, and consequently requires a computational grid that follows the channel, but that also includes low lying areas adjacent to the channel that may be inundated under the various "non-flood" scenarios and consequently act as storage areas. For this purpose, a tidal model has been used. It should be noted that this model will not perform well for very high inflow or flood scenarios as it makes only limited allowance for flooded areas (see Section B3.3.1).

In terms of salinity distributions, flow scenarios have been designed to answer the following questions:

i) What happens to salinities in the Berg River in summer under various present and future flow scenarios (marine-dominated state);
ii) What flows flush the Berg River estuary 1/3 and 2/3 of its longitudinal; extent at the end of summer (transition state);
iii) Under what flows does the Berg River become freshwater dominated (freshwater dominated state).

Scenarios to investigate flushing dynamics in the estuary

To investigate the flows leading to flushing of the system to approximately 1/3 and 2/3 of the along channel extent of the estuary downstream of the head of the estuary, requires that a series of "freshettes" to be simulated in the flow ranges of 5, 7, 10, 15, 20, 30, 60, 100 m^3/s. Each of these simulations is one month in duration and takes approximately 12 to 16 hours of computational time.

Finally "flood conditions" flow ranges of 100, 160 and 300 m^3/s have also been simulated for a duration of one month (each also requiring approximately 12 to 16 hours of computational time). Due to the limited coverage of the water quality model grid, limited representation of "storage areas" in the model may lead to inaccuracies in the predicted salinity distributions for these scenarios. The greater the simulated inflow, the greater the likelihood and magnitude of inaccuracies in the predicted salinity distributions.

Scenarios to investigate seasonal salinity distribution in the estuary

To investigate the seasonal salinity distributions under various base flow conditions requires that simulations be undertaken for an approximate 6 to 8 month period of base flows following the freshwater dominated state. Ideally, flow ranges required to be simulated include median and representative "drought" base flow scenarios of under reference, pre-Berg River dam, present and five future scenario conditions (8 x 2 x (6 to 8) months), *i.e.* a total of 16 scenarios each taking approximately 2.5 days of computational time. The median scenarios and drought scenarios are defined by representative flows (*i.e*. median and

10%tile flow scenarios) running from December to April, using late spring (end of November 2004) salinity distributions as starting conditions for the simulations[12].

Due to computational resource constraints and project timelines, only the median scenarios have been simulated. The estimated mean monthly freshwater inflows indicate very little difference between the median and 10 percentile mean monthly summer base flows (representing "drought" conditions). Despite the small differences between the median and "drought" mean monthly summer base flows, extreme scenario conditions (representative of "drought" conditions) were investigated by running low summer base flow runs for two months using representative late summer (end of March 1990) salinity distributions as starting conditions for the simulations. The purpose of these simulations was to investigate possible extreme conditions in terms of salinity penetration upstream in periods of "drought".

The initial flow scenarios provided for the modelling study proved to be inaccurate. Both sets of measured data (historic data and those reported in Schumann 2007), suggested that both winter flows and particularly summer base flows were being overestimated. The initial model simulations also seemed to indicate that particularly the summer base flows were being over-estimated as calibration of the model results using plausible ranges of model parameters proved to be impossible. The salinity distributions simulated for all of the scenarios indicated very little penetration of saline waters upstream to the extent anticipated, based on previous measurements (Schumann 2007).

The inflow data under the various scenarios proposed were subsequently revised (based on other non-modelling considerations) and the model simulations repeated. Much more realistic results were obtained for these model simulations. While unfortunate, this incident had value in that it demonstrated the sensitivity of particularly the upstream salinity distributions to relatively small changes in the freshwater inflows upstream. It also highlighted the difficulty in accurately estimating freshwater inflows into the estuary under summer base flow conditions. This makes it difficult to distinguish between the various proposed new scenarios based solely on the model simulations of salinity distributions.

This led to a much more extensive set of model simulations being undertaken than was originally anticipated. The most likely summer base flow entering the estuary is expected to be in the order of 0.3 m^3/s (possibly due to reducing abstractions over weekends). However, given the uncertainty in the estimated summer base flows, additional simulations were undertaken assuming summer base flows of 0.9 m^3/s (base flow due to spillage over Misverstand), 0.15 m^3/s (assumed low base flow condition) and an extreme situation of 0.0 m^3/s. However, this additional computational requirement was offset by fact that only the most extreme of the proposed new scenarios were simulated. The reason for this is that i) the uncertainty in the summer base flows, and ii) the sensitivity of the model to relatively small changes in summer base flow, means that it is unlikely that one can robustly

[12] Initiallly the model simulations were run from September to the end of March, however the results proved to be inaccurate as the September and October monthly freshwater inflows are still quite variable (floods interspersed with periods of base flow. Such flows are not well represented by the monthly mean flows provided for the modelling study. Applying these freshwater inflows as monthly mean flows rather than daily flows comprising floods interspersed with period of relatively low base flows, overestimates the flushing of the estuary and consequently underestimates the salinities in the estuary. Model simulations were thus only started in November when the flows are more regular and consequently are better represented by the monthly mean flows used in the modelling studies. To get a better idea of the salinity distributions at the end of the dry summer season the models simulations were run to the end of April.

distinguish between the various proposed new scenarios based solely on the model simulations of salinity distributions.

The original "erroneous" estimates on monthly mean freshwater inflows to the estuary (representing the most likely flow conditions) and the 10 percentile freshwater inflows (representing drought conditions) are listed in Tables 4.1a and A4.1b, respectively. The revised median and 10 percentile mean monthly freshwater inflow data are listed in Tables 4.2a and A4.2b.

The scenarios finally simulated are listed in Table 4.3 above. Each run was started at the transition to the dry season (December) and run for five months (i.e. until the end of the dry season in April). Median monthly flows were used in the simulations so shorter term variability such as individual floods, were not resolved. This was not considered problematic as the issue being investigated was the seasonal changes and the extremes of upstream salinity penetration in the upper reaches of the estuary.

4.2. Model Results

Due to the nature of the model set-ups the effects of evaporation were overestimated especially in the lower reaches of the estuary (see Section A3.4.2). Consequently only the salinity distributions upstream of approximately 25 km were considered robust enough upon which to base conclusions.

Time series of salinity were output for locations 0km, 6 km, 25 km, 33km, 45 km, 50 km and 57 km upstream of the mouth of the estuary. The outcomes of the model simulations are as follows:

- Reference conditions
    - Saline waters rarely penetrated further than 25 km upstream at the end of the low flow season
- Pre-Berg River Dam
    - *Summer base flow = 0.15 m³/s*: At the end of the low flow season saline water (< 2 psu) penetrates as far as 50 km upstream, 21 psu is observed at 33 km upstream, 4 psu is observed at 45 km upstream
    - *Summer base flow* = 0.30 m³/s: At the end of the low flow season saline water (< 1 psu) penetrates as far as 45 km upstream and 14 psu is observed at 33 km upstream
    - *Summer base flow* = 0.90 m³/s: At the end of the low flow season saline water (< 2psu) penetrates beyond 33 km upstream but not as far as 45 km upstream
- Present Day (post Berg River Dam)
    - *Summer base flow* = 0.15 m³/s: At the end of the low flow season saline water (< 2 psu) penetrates as far as 50 km upstream, 24 psu is observed at 33 km upstream and 5 psu is observed at 45 km upstream

Table 4.1a Median Flow Scenarios (original erroneous estimates)

Median Flows	Scenario code	Oct	Nov	Dec	Jan	Feb	March	Apr	May	Jun	Jul	Aug	Sept
Natural	**BergNat**	22.2	12.5	7.3	4.8	4.6	5.0	7.9	25.9	46.9	65.0	60.2	38.1
PreDam	**NoBRD**	11.1	7.0	2.7	0.9	0.9	0.7	3.9	11.4	23.0	35.7	36.8	23.5
Present	**PresentBRD**	8.3	6.0	2.6	0.9	0.8	0.7	3.4	6.9	16.1	27.7	28.7	20.2
VV1	**VV1**	6.2	6.0	2.6	0.9	0.8	0.7	3.4	4.8	13.3	24.9	28.5	17.6
VV2a	**VV2a**	5.3	6.0	2.6	0.9	0.8	0.7	3.4	4.0	9.1	18.5	29.6	17.2
VV2b	**Vv2b**	5.3	6.0	2.6	0.9	0.8	0.7	3.4	4.0	9.1	17.6	18.8	13.9
Misverstand C	**Misv C**	8.4	6.2	2.8	1.2	1.1	0.9	2.7	6.9	16.3	23.9	17.1	15.7
Misversand D	**Misv D**	8.0	5.3	2.6	1.2	1.1	0.9	2.2	6.9	16.0	21.1	14.3	14.5

Table 4.1b Drought Flow Scenarios: 10 percentile flows (original erroneous estimates)

Median Flows	Scenario code	Oct	Nov	Dec	Jan	Feb	March	Apr	May	Jun	Jul	Aug	Sept
Natural	**BergNat**	15.3	8.9	4.7	3.6	3.2	2.5	3.9	8.3	15.8	21.9	32.8	23.6
PreDam	**NoBRD**	6.2	4.6	1.7	0.7	0.6	0.5	1.9	3.9	7.3	11.2	17.2	12.5
Present	**PresentBRD**	5.2	4.3	1.7	0.7	0.6	0.5	1.8	2.7	6.2	8.8	11.3	8.4
VV1	**VV1**	4.0	4.3	1.7	0.7	0.6	0.5	1.8	2.3	4.0	6.3	8.8	6.3
VV2a	**VV2a**	3.3	4.3	1.7	0.7	0.6	0.5	1.8	1.5	3.0	4.9	7.4	5.3
VV2b	**Vv2b**	3.3	4.3	1.7	0.7	0.6	0.5	1.8	1.5	3.0	4.9	6.5	4.6
MisverstandC	**MisvC**	4.9	3.5	1.9	1.0	0.9	0.6	1.5	2.8	6.5	7.9	8.6	8.2
MisverstandD	**MisvD**	4.5	3.3	1.9	1.0	0.9	0.7	1.5	2.8	6.5	7.9	7.9	7.3

Table 4.2a Median Flow Scenarios (assuming a summer base flow of approximately 0.3 m^3/s)

Median Flows	Scenario code	Oct	Nov	Dec	Jan	Feb	March	Apr	May	Jun	Jul	Aug	Sept
Natural	**BergNat**	21.5	10.5	4.5	2.4	1.5	1.8	5.9	21.0	44.3	65.0	62.6	39.3
Present	**PresentBRD**	11.1	5.1	0.3	0.3	0.3	0.3	2.0	11.4	23.0	35.7	36.8	23.5
PreDam	**NoBRD**	8.3	4.0	0.3	0.3	0.3	0.3	1.4	6.9	16.1	27.7	28.7	20.2
VV1	**VV1**	6.2	4.0	0.3	0.3	0.3	0.3	1.4	4.8	13.3	24.9	28.6	17.6
VV2a	**VV2a**	5.3	4.0	0.3	0.3	0.3	0.3	1.4	4.0	9.2	18.5	29.6	17.2
VV2b	**Vv2b**	5.3	4.0	0.3	0.3	0.3	0.3	1.4	4.0	9.2	17.6	18.8	13.9
Misverstand	**MisvC**	8.4	4.2	0.3	0.3	0.3	0.3	0.8	6.9	16.3	23.9	17.1	15.7
MisterstandD	**MisvD**	8.00	3.4	0.2	0.3	0.2	0.2	0.3	6.9	16.0	21.1	14.3	14.5

Table 4.2b Drought Flow Scenarios: 10 percentile flows (assuming a summer base flow of approximately 0.3 m^3/s)

10%tile Flows	Scenario code	Oct	Nov	Dec	Jan	Feb	March	Apr	May	Jun	Jul	Aug	Sept
Natural	**BergNat**	13.8	7.00	2.6	1.5	0.9	0.6	2.1	5.5	14.6	21.5	33.5	25.1
Present	**PresentBRD**	5.2	2.3	0.3	0.3	0.3	0.3	0.3	2.7	6.2	8.8	11.3	8.4
PreDam	**NoBRD**	6.2	2.7	0.3	0.3	0.3	0.3	0.3	3.9	7.3	11.3	17.2	12.5
VV1	**VV1**	4.0	2.3	0.3	0.3	0.3	0.3	0.3	2.3	4.0	6.3	8.8	6.3
VV2a	**VV2a**	3.3	2.3	0.3	0.3	0.3	0.3	0.3	1.5	3.0	4.9	7.4	5.3
VV2b	**Vv2b**	3.3	2.3	0.3	0.3	0.3	0.3	0.3	1.5	3.0	4.9	6.5	4.6
MisverstandC	**MisvC**	4.9	1.6	0.3	0.3	0.3	0.3	0.3	2.8	6.5	7.9	8.6	8.2
MisverstandD	**MisvD**	4.5	1.3	0.3	0.3	0.3	0.3	0.3	2.8	6.5	7.9	7.9	7.3

Table 4.3: Seasonal scenarios simulated to assess changes in salinity in the Berg River Estuary under reference, pre- and post-Berg River Dam and potential future flow conditions associated with proposed development options in the catchment.

Scenario code	Summer base flow	Oct	Nov	Dec	Jan	Feb	Mar	Apr	May	Jun	Jul	Aug	Sept
Natural conditions (pre-development)													
BergNat	(as estimated)	21.48	10.53	4.54	2.35	1.54	1.78	5.94	20.97	44.27	65.02	62.56	39.31
No Berg River Dam (conditions prior to the construction of the Berg River Dam)													
NoBRD	0.30 m3/s	11.12	5.07	0.30	0.30	0.30	0.30	1.99	11.40	22.96	35.69	36.79	23.48
	0.90 m3/s	11.12	5.07	0.90	0.90	0.90	0.90	1.99	11.40	22.96	35.69	36.79	23.48
	0.15 m3/s	11.12	5.07	0.15	0.15	0.15	0.15	1.99	11.40	22.96	35.69	36.79	23.48
Present conditions (conditions after the construction of the Berg River Dam)													
PresentBRD	0.30 m3/s	8.28	4.02	0.30	0.30	0.30	0.30	1.42	6.90	16.13	27.74	28.66	20.15
	0.90 m3/s	8.28	4.02	0.90	0.90	0.90	0.90	1.42	6.90	16.13	27.74	28.66	20.15
	0.15 m3/s	8.28	4.02	0.15	0.15	0.15	0.15	1.42	6.90	16.13	27.74	28.66	20.15
Raised Misverstand, Imposed resdss ifrD. Ifr = 15% of natural flow													
MisvD	0.30 m3/s	7.99	3.36	0.15	0.30	0.21	0.15	0.30	6.91	16.00	21.10	14.34	14.51
	0.90 m3/s	7.99	3.36	0.90	0.90	0.90	0.90	0.90	6.91	16.00	21.10	14.34	14.51
	0.15 m3/s	7.99	3.36	0.15	0.30	0.21	0.15	0.30	6.91	16.00	21.10	14.34	14.51
	0.00 m3/s	7.99	3.36	0.00	0.00	0.00	0.00	0.30	6.91	16.00	21.10	14.34	14.51

- *Summer base flow* = 0.30 m³/s: At the end of the low flow season saline water (< 1 psu) penetrates as far as 45 km upstream and 16 psu is observed at 33 km upstream
- *Summer base flow* = 0.90 m³/s: At the end of the low flow season saline water (< 3psu) penetrates beyond 33 km upstream but not as far as 45 km upstream
- *Summer base flow* = 0.30 m³/s with sea level rise of 0.5m: At the end of the low flow season saline water (< 2 psu) penetrates as far as 50 km upstream, 26 psu is observed at 33 km upstream (This is similar to the salinity distribution for present day 0.15 m³/s flows, *i.e.* the assumed sea level rise 0.5 m is equivalent to a halving of the 0.3 m³/s summer base flow)

- Misverstand D (worst case)
  - *Summer base flow* = 0 m³/s: At the end of the low flow season saline water (< 2 psu) penetrates as far as 57 km upstream, 30 psu[13] (?) observed at 33 km upstream, 9 psu observed at 45 km upstream, 5 psu observed at 50 km upstream
  - *Summer base flow* = 0.15 m³/s: saline water (< 2 psu) penetrate as far as 50 km upstream, 25 psu observed at 33 km upstream, 6 psu observed at 45 km upstream
  - *Summer base flow* = 0.30 m³/s: start to see evidence of saline water (> 0 psu) at 50 km, saline water (< 2 psu) penetrates as far as 45 km upstream, 20 psu observed at 33 km upstream
  - *Summer base flow* = 0.90 m³/s: saline water (< 4psu) penetrates beyond 33 km upstream but not as far as 45 km upstream
  - *Summer base flow* = 0.30 m³/s with sea level rise of 0.5m: not simulated

For ease of interpretation the above results are summarised in Table 4.4. Annex B contains modelled salinity distributions for the period December to April for each of the scenarios in Table 4.3.

[13] Given the errors introduced by the effective "overestimation" of evaporative effects (associated with exact nature of the model set-ups), there is considerable uncertainty around this figure.

Table 4.4 Summary of salinity simulated for the upstream reaches of the Berg River Estuary under various scenarios[14]

Scenario code	Summer base flow	Salinity (psu)				
		25 km	33 km	45 km	50 km	57 km
Natural conditions (pre-development)						
BergNat	(as estimated)	**1** (0-2)	**~0** -	**~0** -	**~0** -	**~0** -
No Berg River Dam (conditions prior to the construction of the Berg River Dam)						
NoBRD	0.30 m3/s	*	**16** (13-18)	**1** (0-1)	**~0** -	**~0** -
	0.90 m3/s	**14** (10-18)	**3** (2-4)	**~0** -	**~0** -	**~0** -
	0.15 m3/s	*	**22** (20-24)	**4** (4-5)	**2** (2-3)	**~0** -
Present conditions (conditions after the construction of the Berg River Dam)						
PresentBRD	0.30 m3/s	*	**16** (14-18)	**1** (0-1)	**~0** -	**~0** -
	0.90 m3/s	**15** (10-18)	**3** (2-4)	**~0** -	**~0** -	**~0** -
	0.15 m3/s	*	**24** (22-26)	**5** (4-6)	**3** (2-3)	**~0** -
Raised Misverstand, Imposed resdss ifrD. Ifr = 15% of natural flow						
MisvD	0.30 m3/s	*	**20** (18-22)	**1** (1-2)	**~0** -	**~0** -
	0.90 m3/s	**16** (12-20)	**4** (3-4)	**~0** -	**~0** -	**~0** -
	0.15 m3/s	*	**24** (22-26)	**6** (5-7)	**3** (2-3)	**~0** -
	0.00 m3/s	*	**~30**** (28-32)	**11** (10-12)	**6** (6-7)	**2** (2-3)-

[14] * Not reported due to modelling limitations and associated uncertainties

** Uncertain value due to limitations of modelling

5. Flood Model Results

5.1. Scenarios Modelled

The flood scenarios that need to be considered are those that will help to characterise the inundation characteristics of the flood plain under the various scenarios considered[15].

5.1.1. Background

The flooding characteristics of the Berg Estuary are complex (Beck & Basson 2007, Schumann, 2007). Factors that influence the extent of flooding are:

- the general extent of inundation of the flood plain at the start of a flood, influenced by characteristic winter base flow water levels and the magnitude and timing of prior flood events. Beck & Basson (2007) have characterised these effects using the upstream water levels (G1H023: Jantjiesfontein) as an index[16];
- the tidal state (that influences mostly the inundation in the mid to lower reaches of the estuary); and
- non-tidal sea level fluctuations entering the estuary.

Ideally the approach should be to simulate representative wet and dry year scenarios for the winter season for all 7 of the development scenarios proposed. However, this approach would require that detailed inflow scenarios would need to be developed for each of the 7 scenarios. Given the two wet and dry year scenarios, this would imply that 14 winter seasons of approximately 6 months would need to be simulated. The computational resources and time required for such a modelling study are untenable.

Such an approach would provide the ideal outputs of time series of the flooding extent (water depth) at points in the estuary that are considered important. However these model outputs would then need to be carefully analysed to assess and describe the changes between the various scenarios which in itself is a significant effort. Furthermore, it is not clear how successful such an approach would be in discerning the relative differences between the various scenarios considered.

In summary:
Such an approach is not feasible due to the fact that the computational resources, time and funds were not available to undertake such a study. Further, this approach would require that at least 14 inflow scenarios be developed for the study and that the resultant output would still require significant analysis before the changes between the various scenarios could be "scored" (both abiotic and biotic).

15 It should be noted here that the initial flow scenarios provided to the CSIR were erroneous in that they overestimated the low flow conditions. There was some modification of the higher flow on either side of the low flow period in the Berg River. While these modifications required a re-run of the water quality simulations, their influence on the flood modelling study was negligible as the modifications did not change the approach and categories of base flow conditions developed for the flooding scenarios.

16 The use of this upstream water level index does not fully characterise the effects of the magnitude, timing and duration of prior flood events. This can only be accounted for by long duration seasonal simulations that include flood sequences as they occurred in reality.

Here an alternative approach has been developed that takes a focuses on assessing the relative differences between the scenarios proposed for a range of idealised flood scenarios. Initially, the flood modelling study was based on the insights provided and relationships developed in the previous Beck & Basson (2007) study. However, concerns around the initial water levels assumed in these studies and the manner in which Beck & Basson (2007) did the flood modelling required that the flood modelling exercise be repeated.

In the Beck and Basson study the following simulations were undertaken:

- ***Pre and post-dam flood scenarios*** comprising simulations of 5 flood scenarios for present (no Berg River Dam) and post-dam (Berg River Dam) scenarios, respectively.;
- **Seasonal flood scenarios** comprising simulations of higher flow months of the year (April to September) for a "wet" (1999) and "dry" (2003) year;
- **Investigative flood scenarios** comprising simulation of a range of floods over a six year period that occurred under a range of both upstream and downstream water levels.

These simulations represent an enormous computational effort providing a number of important insights into the flooding behaviour of the Berg estuary. The results of these simulations allowed a more focussed flooding assessment to be undertaken for the present RDM process. In particular, the above range of simulations helped to define the role of pre-flood water levels associated with winter "base" flows in determining the extent of flooding in the various reaches of the Berg estuary. Also of relevance, but of lesser importance are the water level variations occurring at the mouth of the estuary.

Results of the winter (high flow) season flooding studies of Beck & Basson (2007).

The results of the winter (high flow) season flooding studies of Beck & Basson (2007) were used to define the effect of the flooding behaviour of the Berg River Estuary on the pans in the adjacent flood plain. Simulated flood water levels were recorded for a total of important 100 locations in the estuary, many of these being pans. These results were used to identify pans of relevance to this study. A limitation of the model simulation however was that evaporative effects were not taken into account. These effects have been included in the present study and help to provide an indication of how rapidly the pans dry out.

Results of the investigative flooding studies of Beck and Basson (2007).

The results of the investigative flooding studies of Beck & Basson (2007) were used to develop relationships[17] between flood extents and variables such as flood peak volume, flood peak discharge, initial upstream water levels in the main channel (associated with the prevailing magnitude of the winter base flows) and initial sea water levels. A separate relationship was developed for each of the four defined flood reaches (see Figure 12).

These main finding was that initial water level prior to the flooding plays an important role in the extent of inundation in the adjacent flood plain. Further observations were that:

[17] There is a concern that flood peak and flood volume are highly correlated parameters and it is not clear whether allowance was made for this fact when developing the regression relationships.

- only in the upper reaches (flood Reach 1 and 2) is there a strong correlation between flood peaks and the area of inundation;
- the flood volume is positively correlated with the flood volumes, especially in Reaches 1 and 2; and
- there exists an inverse correlation between initial water level at the estuary mouth and the inundation area.

Given the results of detailed analysis of water level variations along the estuary (Section 2.3.2), it is not surprising that the correlation between flood peaks and volumes is only significant in the upper two flood reaches as it is here that the inflows have the greatest effect on water level. Careful consideration of the modelling results indicates that the magnitude of the flood peak and the rapidity with which it develops, has the greatest influence on water levels in the main channels and the flooding of areas immediately adjacent to the main channel. Flood volume is determined both by the magnitude of the flood peak and the duration of the flood. The greater the duration of the flood (and consequently elevated water levels), the more the water that is able to flow into low - lying areas more distant from the main channel, *i.e*. the greater the inundation area associated with the flood. The correlation of flood inundation area with flood volume therefore is due both to the elevated water levels and the duration for which these water levels remain elevated.

Beck & Basson's (2007) reported strong and clear correlation between upstream initial water level and the inundation area is somewhat surprising. More careful analysis of the modelling approach suggests that the effect of initial upstream water levels has been overemphasised. The reason for this assertion is that the initial water levels assumed in the modelling study either comprise a linear interpolation along the estuary of the initial upstream water level and the initial water level at the mouth of the estuary, or worse, the assumption that the initial upstream water level prevails over the whole model domain (as suggested by the earlier pre- and post-dam flooding results reported by Beck & Basson (2007). The assumption of the same initial upstream water level over the whole domain would seriously bias model results in that there would be extensive "pre-flooding" of the flood plain. Figures 5.1 a to c indicates the extent to which spurious "pre-flooding" of the estuary and its flood plain would be assumed for various starting assumptions for the flood plain modelling.

The net effect of such assumptions would be to overemphasise the effect of initial upstream water levels (i.e. base flow volumes) on the flood inundation areas and consequently to underestimate the effect of flood peaks and volumes on flood inundation areas.

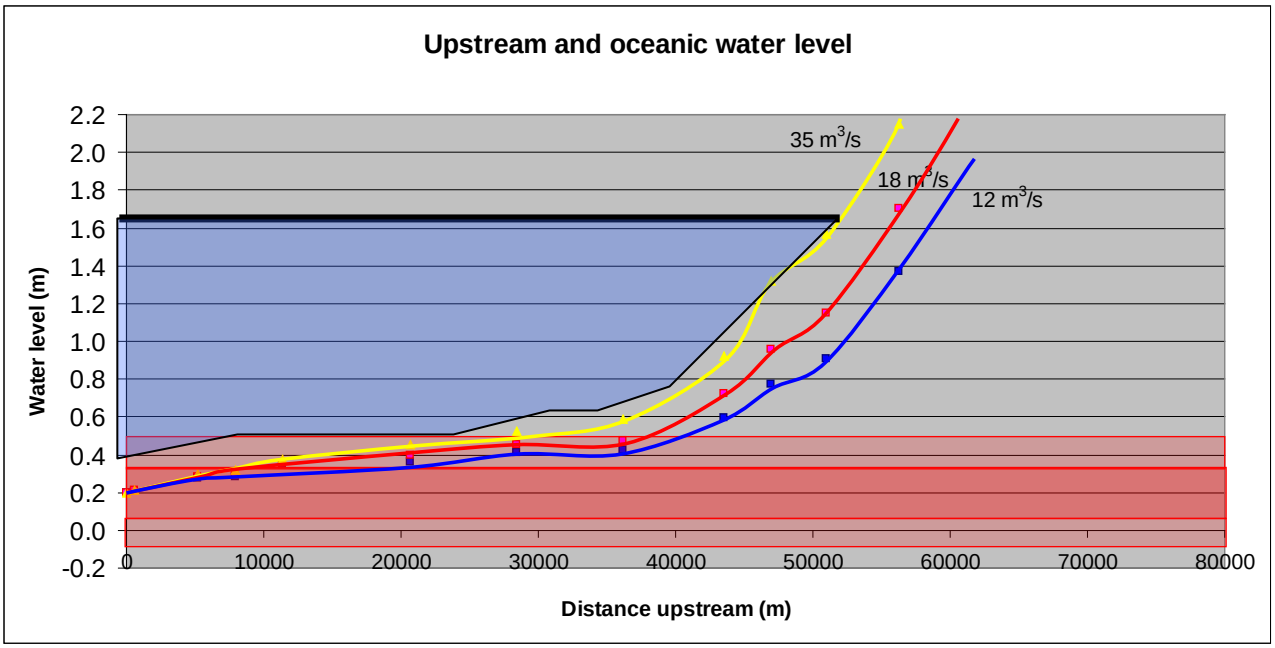

Figure 5.1a **Schematic of the along estuary water level profile associated with various winter base flows. Superimposed (blue fill area) is the spurious "volume" of water that would be assumed to be on the flood plain if one was to assume that the upstream water level measured at Jantjiesfontein was to prevail over the whole estuary as an initial condition for the flooding simulations**

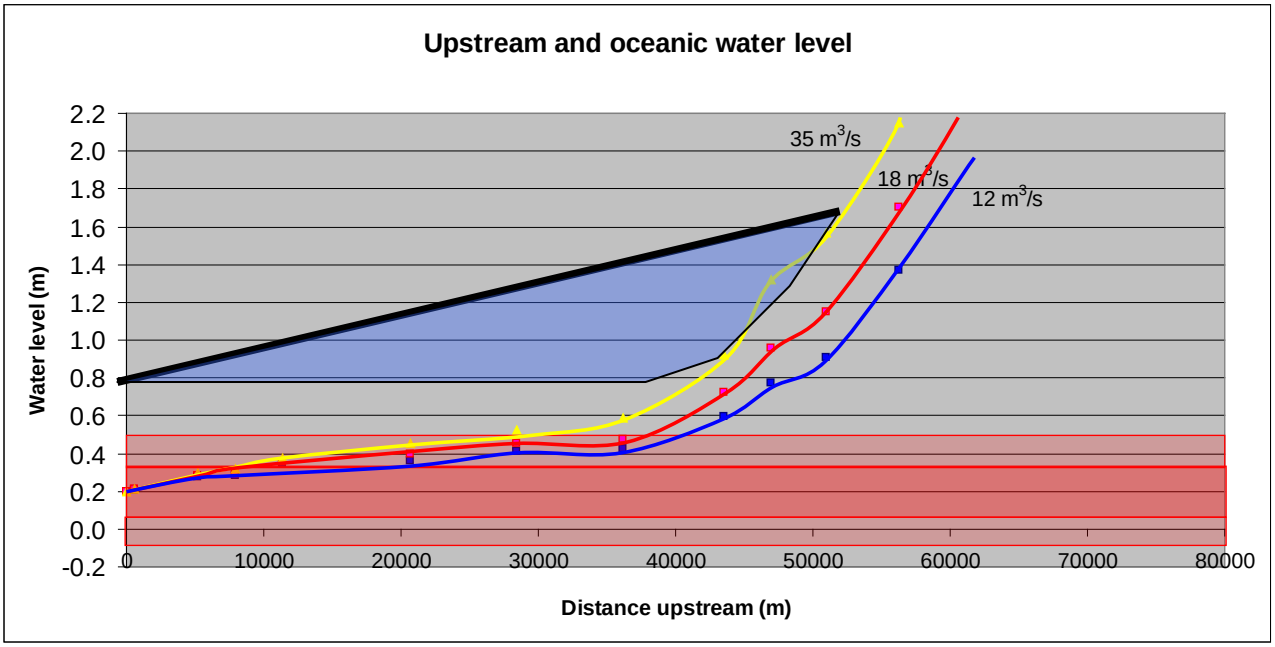

Figure 5.1b **Schematic of the along estuary water level profile associated with various winter base flows. Superimposed (blue fill area) is the spurious "volume" of water that would be assumed to be on the flood plain if one was to assume that the upstream water level measured at Jantjiesfontein and initial high tide water levels at the mouth were to be linearly interpolated to provide an initial conditions for the model simulations**

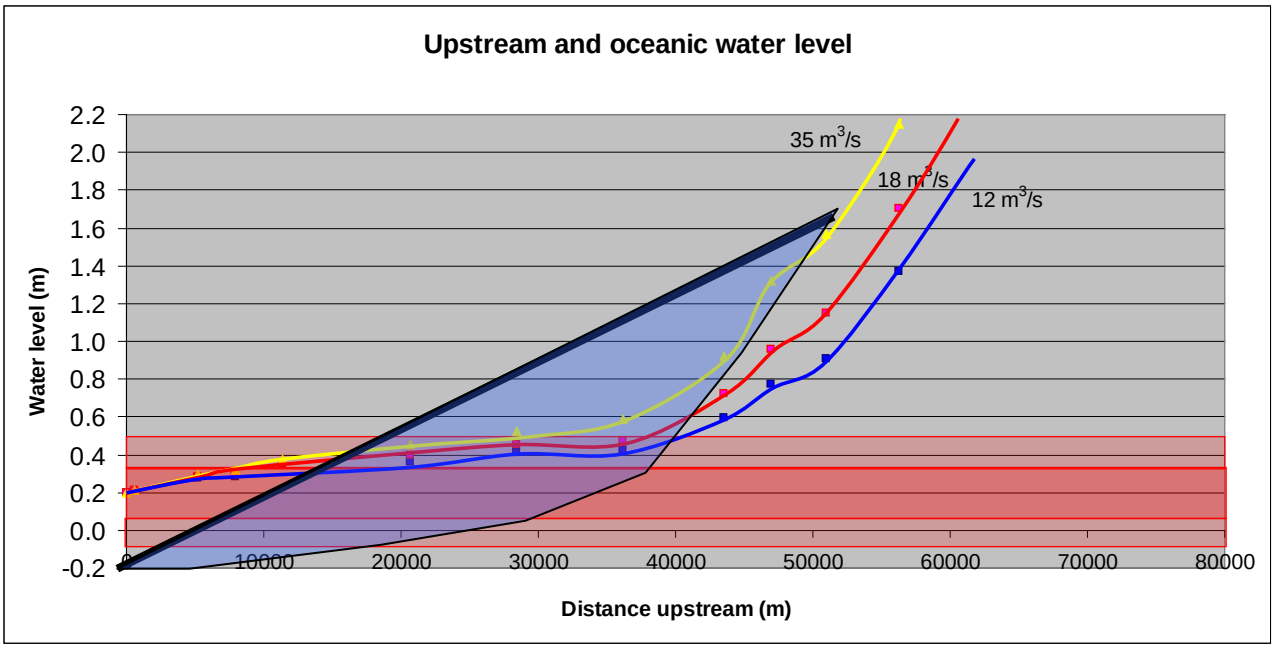

Figure 5.1c Schematic of the along estuary water level profile associated with various winter base flows. Superimposed (blue fill area) is the spurious "volume" of water that would be assumed to be on the flood plain if one was to assume that the upstream water level measured at Jantjiesfontein and initial low tide water levels at the mouth were to be linearly interpolated to provide an initial conditions for the model simulations

While intuitively one would expect a clear relationship between the offshore water level variations that propagate upstream (in approximately 10 hours - Schumann (2007), the reported relationship between the initial offshore water level and extent of flooding of the flood plain is not convincing. Of particular concern is the inverse relationship between the offshore water levels and the extent of flooding in all reaches. An explanation could be that the generally higher water levels in the estuary allow for more rapid in-channel flows and a resultant decrease in flooding. More likely is that the initial flooding water levels are not easily defined (*i.e*. should one use an instantaneous water level measurement just prior to the flood or should one use the maximum water level experienced during the flood?). For this reason, the relationship reported between offshore water levels and the flooding extent is deemed too unreliable to use in this study. Indeed, due to the poor (and unexpected inverse) relationship between sea level at the mouth of the estuary and flood inundation level, Beck & Basson (2007) undertook a number of flood simulations where the water level at the mouth at the estuary was assumed to be zero so as to remove this potentially confounding effect. This approach reduced the somewhat arbitrary nature with which "spurious" volumes of water had been added as initial conditions in their flood model simulations but nevertheless still resulted in an overestimate the effects of winter base flows on flood inundation areas, and consequently an underestimation of the effect of higher flood peaks and volumes on the extent of flood inundation areas.

5.1.2. Scenarios used to assess RDM flooding requirements

While these initial flooding studies were necessary to provide an understanding of the flooding behaviours of the Berg River Estuary, they are not suited to investigating the flood regime differences between the 7 scenarios considered in this RDM study. However, these results have

enabled an approach to be developed which indeed is able to distinguish between the flooding regimes of the various proposed development scenarios put forward for this study (Table 5.1).

Table 5.1 Scenarios to be investigated in the RDM study.

ID	Scenario Description *	HFY (Mcm)	Estuary MAR (Mcm)	HFY: Difference from BRD	HFY: % Difference from BRD
BergNat	Natural	-	980.84		
PresentBRD	Present day with Berg River Dam in Place	547	423.34	85	100.0%
NoBRD	Present day without Berg River Dam	462	550.15	0	130.0%
VV1	Augmentation of Voelvlei dam - Phase1 - No raising. 3m³/s diversion	574	392.77	112	92.8%
VV2a	Augmentation of Voelvlei dam - Phase2a - No raising. 20m3/s diversion	591	381.13	129	90.0%
Vv2b	Augmentation of Voelvlei dam - Phase2b - 20m³/s diversion, raise voelvlei dam by 9m	613	305.07	151	72.1%
MisvC	Raised Misverstand, Imposed resdss ifrC. Ifr = 23% of natural flow	571	268.33	109	63.4%
MisvD	Raised Misverstand, Imposed resdss ifrD. Ifr = 15% of natural flow	585	238.78	123	56.4%

* **- In some cases smaller schemes may achieve similar yields**

The methods used in this study need to be able to distinguish between the flooding behaviours of the estuary between the various scenarios considered. Ideally the approach would be to simulate representative wet and dry year scenarios for the winter season for all 7 of the scenarios considered. This approach would require that detailed inflow scenarios be developed for each of the 7 scenarios. Given the two wet and dry year scenarios, this would imply that 14 winter seasons of approximately 6 months would need to be simulated. The computational resources and time required for such a modelling study was untenable. This approach would provide the ideal outputs of time series of the flooding extent (water depth) at points in the estuary that are considered important. These data would then need to be carefully analysed to assess and describe the changes between the various scenarios which in itself is a significant effort.

Initial Assessment

Initially this study accepted that the relationships developed between the initial water levels upstream (that are a proxy for the extent of flood plain inundation prior to the flood event under consideration) were valid. Based on this assumption scenarios were developed that explicitly ***focussed on the changes in winter "base flow" indicated in the various scenarios provided as it was anticipated that these winter "base flows" would result in significantly different upstream "background" water levels and consequently flood inundation areas for specified flood sizes under the various scenarios***. Initially, the intention of the flood modelling study was to investigate combinations of various upstream water levels (due to winter "base flows") and flood events to determine their effect on the extent of flooding in the various flood reaches and consequently distinguish between the likely flooding behaviour of the 7 scenarios being assessed.

Analysis of water levels at Jantjiesfontein, Kliphoek and offshore show a clear relationship between upstream water levels and winter base flow (see Figure 2.11). Based on a review of low flow hydrology by Smakhtin (2001), the winter base flows in the initial flow scenarios supplied were estimated using the 25 percentile values of the mean monthly flows for the period June to August (Table 5.2). Inclusion of the month of September in the calculation does not change the estimated base flows significantly. Visual inspection of the times series of inflows into the upper estuary (Figures 2.15 and 2.16) suggest that these estimates are robust.

While the final corrected flow scenarios supplied to the modelling team indicated slightly different magnitude base flows to those originally provided, the observed changes were not significant and consequently did not change the categories indicated in Table 5.2).

Initially a range of representative flood events were assessed under each of these "base flow" scenarios:

I. Winter base flows > 30 m^3/s representing reference conditions
II. Winter base flows ranging between 15 and > 30 m^3/s representing conditions before the building of the Berg River Dam
III. Winter base flows < 15 m^3/s representing encompassing present conditions, as well as all of the future scenarios proposed for this study.

These winter base flows represent upstream water elevations at Jantjiesfontein of 2.3m, 1.6m and 1.2 m, respectively.

Table 5.2 Winter base flow categories used in developing the model flood scenarios.

Winter Base Flow Category	Estuarine inflow range (m^3/s)	Upstream water level (m)	Scenario ID	25 percentile monthly flows (m^3/s)	
				June – August	June to September
1	**> 30**	**~2.3**	**BergNat**	35.7	34.0
2	**15 - 30**	**~1.6**	**NoBRD**	17.8	17.3
3	**<15**	**~ 1.2**	**PresentBRD**	13.4	12.9
			MisvC	12.2	11.9
			MisvD	11.4	10.9
			VV1	10.8	10.4
			VV2a	8.0	8.1
			Vv2b	7.8	7.6

Based on these combinations (*i.e.* of winter base flows and flood size), the likely maximum flood extents and durations of inundation of various locations were assessed for the 7 scenarios considered (see Table 5.3). The range of flood considered were 100 m^3/s, 200m^3/s, 300m^3/s, 400 m^3.s, 500m^3/s, 600m^3/s, 800 m^3/s and 1000 m^3/s, which are the same flooding regimes originally

defined by Beck & Basson (2007) in their modelling study for the Berg River Baseline monitoring programme.

Table 5.3 Flood scenarios considered in this study.

Flood size m^3/s	Base flow range: > 30 m^3/s Upstream water level: 2.3 m	Base flow range: 15 - 30 m^3/s Upstream water level: 1.6 m	Base flow range: < 15 m^3/s Upstream water level: 1.2 m
100	Scenario 1.1	Scenario 121	Scenario 3.1
200	Scenario 1.2	Scenario 2.2	Scenario 3.2
300	Scenario 1.3	Scenario 2.3	Scenario 3.3
400	Scenario 1.4	Scenario 2.4	Scenario 3.4
500	Scenario 1.5	Scenario 2.5	Scenario 3.5
600	Scenario 1.6	Scenario 2.6	Scenario 3.6
800	Scenario 1.7	Scenario 2.7	Scenario 3.7
1000	Scenario 1.8	Scenario 2.8	Scenario 3.8

This initial assessment was based was based on the relationships developed by Beck & Basson (2007), supplemented by relationships developed between:

I. The inundated area in a particular reach versus the mean water level in that reach;
II. The inundated volume in a particular reach versus the mean water level in that reach

In this initial assessment a mean maximum water level was estimated for each flood size, based on the predicted inundation area obtained using the relationships developed by Beck & Basson (2007) and relationships between water levels in the various reaches and the area of the flood plain below that water level (Figure 5.2a). Using this estimated maximum water level (averaged over each flood reach) representative of each flood scenario considered, the inundation area was plotted without needing to resort to flood model simulations[18]. Similarly the estimated maximum water level in each reach was used to determine whether pans in that reach would be filled or not. This information, together with the estimated pan volumes in Basson & Beck (2007), was used to estimated the extent of inundation of flood pans in each defined "flood" reaches.
Unsurprisingly, these initial results showed the flooding regime to be significantly influenced by upstream water levels at the start of a flooding sequence as well as sub-tidal water level fluctuations at the mouth of the estuary (Beck & Basson (2007). The indication of a significant relationship between the extent of flooding under the various flood sizes and the winter base flow, suggested an assessment approach whereby consideration would need to be given to the likely changes in inundation extents for a particular flood size but changing winter base flows.

This initial approach, in not requiring explicit flood modelling, was efficient. However, it was flawed in that it was based on the relationships reported by Beck & Basson (2007) that in all likelihood overestimated the effect of winter base flows and underestimated the effect of flood peak sizes and flood volumes. Furthermore, a mean maximum water level was estimated for each flood reach. Insofar as the maximum water level in a specific reach changes only linearly with distance

[18] This method, whilst computationally efficient in that it did require explicit model simulations, did not take into account the dynamic aspects of flooding such as the time taken for low lying areas to flow, *etc*.

downstream, this approach is reasonably accurate (as the water level at each pan location was estimated using linear interpolation). In the extreme upper reaches of the estuary there is considerable (non-linear) downstream variation in the maximum water level observed for each flood scenario. Consequently the estimated flood volume in these upper reaches are less accurate, but nevertheless perfectly adequate for the purposes of this study.

An analysis of both measured and modelled water levels confirm that the effect of upstream water level (*i.e*. magnitude of winter base flows) has been overemphasised in the Beck & Basson (2007) study. The flood modelling study therefore was simplified and only the "extreme" winter base flow flood scenarios were simulated, *i.e*. flood scenarios under high winter base flows of > 30 m^3/s representing natural conditions in the Berg River estuary prior to developments in the catchment and under low winter base flow conditions < 15 m^3/s that are representative of both present conditions and all of the proposed future development scenarios[19].

The tabulated results from this simplified set of scenarios indicate that there is only an approximate 2 to3 % change in flood extents between the same size floods for winter base flows for the reference conditions (35 m^3/s) and those that typically expected to occur for the proposed new development scenarios (12 m^3/s). Tabulated results clearly indicate that this difference is small (compare Table 5.4a and b).

There is, however, a greater change in the flood extents in particular reaches between the same size floods for winter base flows for the reference conditions (35 m^3/s) and those that typically expected to occur for the proposed new development scenarios (12 m^3/s). For small floods (~100 m^3/s) the flooded area in Reach 1 is approximately 3%, and in reach 2 approximately 2%, greater for the high winter base flow simulations than for the low winter base flow simulations. For floods of 200m^3/s the flooded area in Reach 1 is approximately 1%, in reach 2 approximately 3%, and in reach 3 approximately 4%, greater for the high winter base flow simulations than for the low winter base flow simulations. For floods of 300m^3/s the flooded area in Reach 1 is approximately 1%, in reach 2 approximately 3%, and in reach 3 approximately 2%, greater for the high winter base flow simulations than for the low winter base flow simulations. The differences in flood extents for flood sizes greater than this, is less than 2-3% between the high and low winter base flow scenarios.

Similarly the influence of sub-tidal water levels on the flood extents is not the same throughout estuary, although the water level changes due to sub-tidal water variability at the mouth of the estuary are observed to remain unattenuated throughout the estuary.

Additional simulations (not reported here) indicate that, of equal significance to that of subtidal sea level variability, is whether the flooding occurs during spring or neap tide conditions, particularly in the lower to middle reaches where tidal variability remains significant.

[19] The actual inflows simulated were 35 m^3/s and 12 m^3/s.

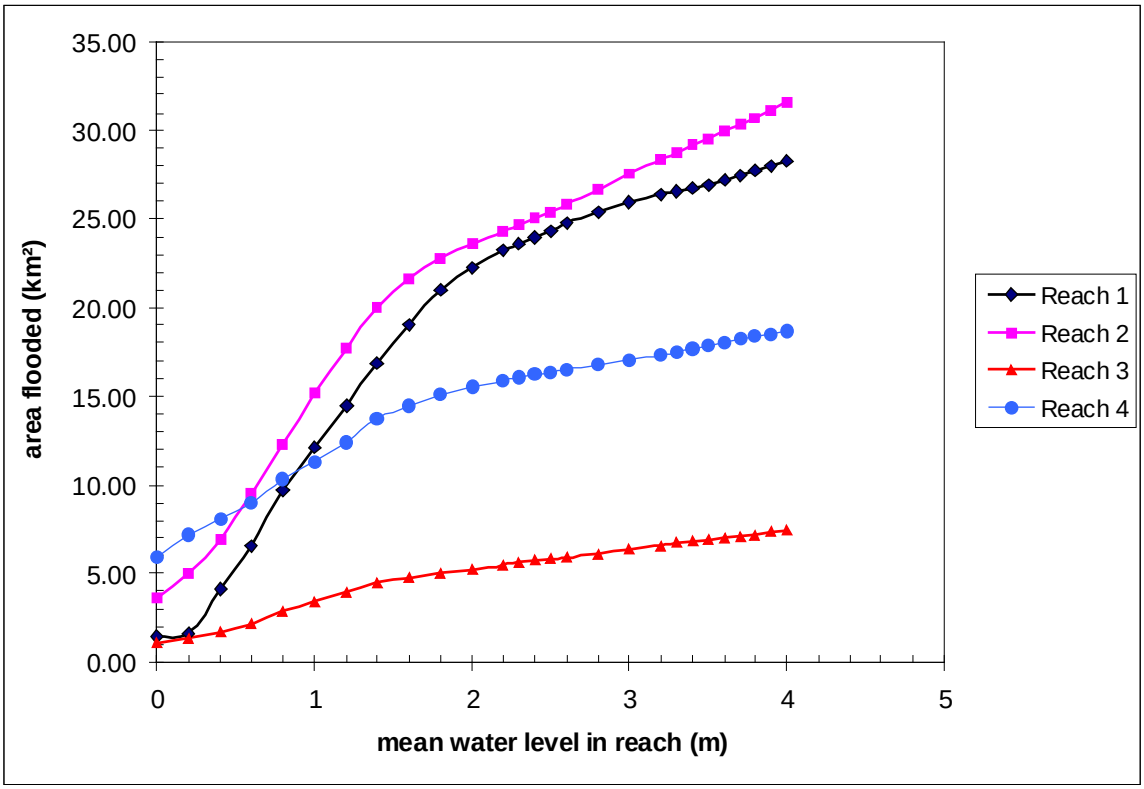

Figure 5.2a **Area of flood plain that would be inundated as a function of mean water level in the various reaches of the Berg River estuary.**

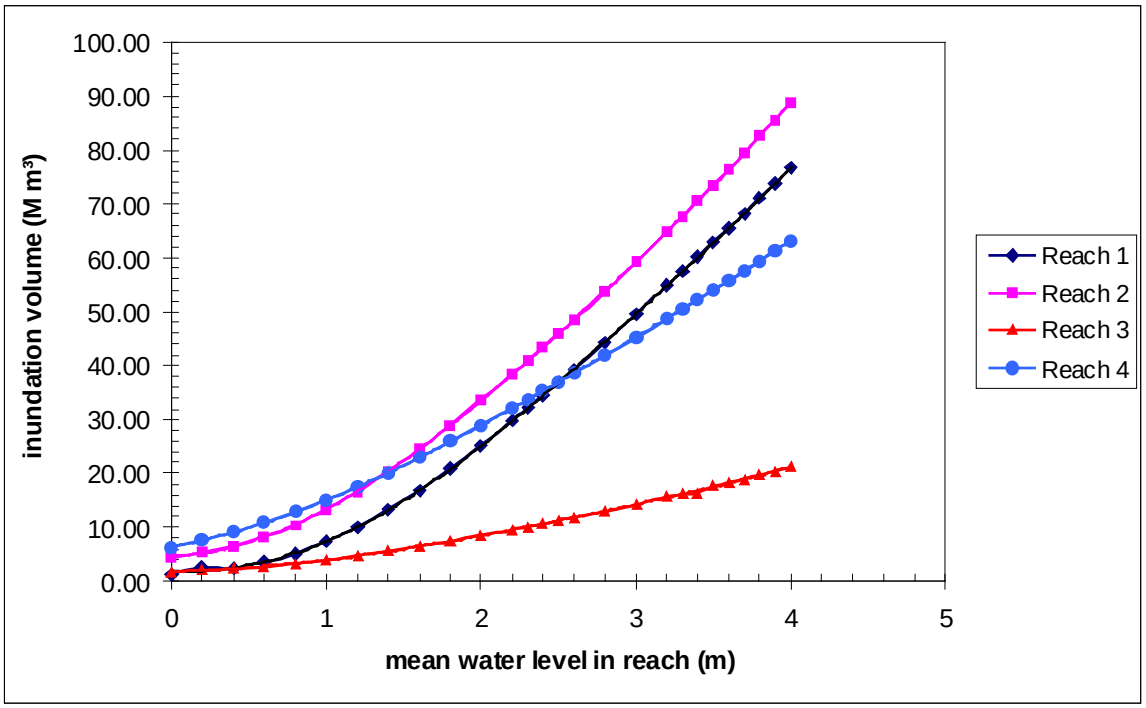

Figure 5.2a **Volume of water in the area of flood plain that would be inundated as a function of mean water level in the various reaches of the Berg River estuary.**

The extent of inundation of pans and the duration for which they remain under water is also an important ecological indicator for the health and abundance of the birds that use these pans to feed. Consequently, the maximum pan area inundated under each flood size was estimated for each of the four river reaches. The maximum flood extent would determine whether a pan was filled or not. Beck & Basson (2007) did not consider evaporative effects in their flooding simulations.

Using the times series simulations of Beck & Basson (2007), pans to be included in the "total area of pans inundated" in the analysis were selected by including only those pans that clearly were filled by floods and remained filled (as evaporative effects were not taken into account in the Beck & Basson (2007) study, *i.e*. they were not areas that could drain once the water had subsided. A visual assessment of the selected pans confirmed that the areas selected did indeed comprise pans.

Also estimated was the rate at which the pans inundation area would shrink due to evaporative effects[20]. The long-term evaporative effects were added to the results by reducing the water level in each pan under consideration by the net expected water loss (evaporation – rainfall) for the months of August to November. August 1st was the assumed start date from which evaporative effects were considered, *i.e*. the assumption being that the pans had been flooded towards the end of the high flow season. This provides a "worst case" scenario for the drying out of pans after flooding. During the wet season it is expected that the pans would be flooded on a number of occasions.

The tabulated flood modelling results list the maximum pan area inundated under each flood size was estimated for each of the four river reaches. Also estimated was the rate at which the pans area decreased due to evaporation. Estimated pan areas were estimated at 30 days after the flood event, 60 days after the flood event and 120 days after the flood event. These pan areas are only valid under the assumption that no further flood events occurred after the initial flood event. This idealised approach is an extremely conservative approach, as in reality further flood events may well have occurred and filled one, more or all of the pans.

Additional scenarios were modelled that provided further insights into the flooding dynamics of the estuary. These included simulations during neap tide conditions and simulations where a water level increase of 0.5 m was assumed at the mouth, a proxy for both sub-tidal increases in water level expected during the high flow period (due to prevailing NW winds) and potential sea level rise scenarios. These results indicated that elevations in sub-tidal water levels have a significant effect on the area inundated by a particular flood size, the effects being greatest for the smaller floods (<200 m^3/s). The effects of this rise in water levels is significant for all flood sizes but is only significant in the middle to upper reaches for flood sizes <400 m^3/s. For flood sizes larger than this

20 Whilst the magnitude of evaporation effects is irrelevant in areas that are drained after a flood event, evaporation effects are important in the pans. Each pan when filled has a characteristic depth and spatial extent that would decrease over time due to evaporation. This rate of evaporation and resultant change in water depth and extent of the pan is unique to each pan. In this study we have assumed that evaporation is the only factor reducing water depth of these pans (*i.e*. no loss of water due to seepage).

Table 5.4a Flood extents of flood plain and pans for a range of flood sizes under reference condition winter base flows (35 m^3/s)

Peak	Volume	Winter Baseflow				Flood Peak				Pans, marshes and inundated mudflats				
		Area	Area	Duration	Figure No	Area	Area	Duration	Figure No	Area	Area	% area remaining 30 days	% area remaining 60 days	% area remaining 120 days
m^3/s	M m^3	ha	%	days		ha	%	days		ha	%			
1000	257	2557.4	36.9	90	0	6927.9	100.0	10 - 20	0	1088.4	100.0	84.0	71.6	31.2
800	203	2557.4	36.9	90	0	6692.4	96.6	10 - 20	0	1088.4	100.0	84.0	71.6	31.2
600	149	2557.4	36.9	90	0	6149.6	88.8	10 - 15	0	1088.4	100.0	84.0	71.6	31.2
500	125	2557.4	36.9	90	0	5810.1	83.9	10- 14	0	1088.4	100.0	84.0	71.6	31.2
400	96	2557.4	36.9	90	0	5471.1	79.0	7 - 14	0	1088.4	100.0	84.0	71.6	31.2
300	65	2557.4	36.9	90	0	5000.8	72.2	7 - 10	0	942.9	86.6	70.9	59.2	22.4
200	42	2557.4	36.9	90	0	4457.1	62.7	5 - 10	0	923.2	84.8	69.2	57.9	22.4
100	15	2557.4	36.9	90	0	3789.4	54.7	5 - 7	0	783.0	71.9	56.9	47.3	18.1

Table 5.4b Flood extents of flood plain and pans for a range of flood sizes under future scenario winter base flows (12 m^3/s)

Peak	Volume	Winter Baseflow				Flood Peak				Pans, marshes and inundated mudflats				
		Area	Area	Duration	Figure No	Area	Area	Duration	Figure No	Area	Area	% area remaining 30 days	% area remaining 60 days	% area remaining 120 days
m^3/s	M m^3	ha	%	days		ha	%	days		ha	%			
1000	257	2407.2	34.7	90	0	6827.4	98.5	10 - 20	0	1088.4	100.0	83.9	71.5	31.2
800	203	2407.2	34.7	90	0	6684.2	96.5	10 - 20	0	1088.4	100.0	83.9	71.5	31.2
600	149	2407.2	34.7	90	0	6105.2	88.1	10 - 15	0	1088.4	100.0	83.9	71.5	31.2
500	125	2407.2	34.7	90	0	5759.3	83.1	10- 14	0	1088.4	100.0	83.9	71.5	31.2
400	96	2406.9	34.7	90	0	5393.1	77.8	7 - 14	0	1088.4	100.0	83.9	71.5	31.2
300	65	2407.2	34.7	90	0	4901.3	70.7	7 - 10	0	942.9	86.6	70.9	59.2	22.4
200	42	2406.9	34.7	90	0	4329.5	62.5	5 - 10	0	923.2	84.8	69.2	57.8	22.4
100	15	2407.2	34.7	90	0	3521.1	50.8	5 - 7	0	783.0	71.9	56.9	47.3	18.1

* The percentage area of inundated flood plain is normalised to the maximum flooded area under the maximum flood conditions simulated (*i.e.* 1 000 m^3/s)

* The percentage area of inundated flood plain is normalised to the possible flooded pan area of the pans under consideration

the effects of such a rise in water levels is limited in all but the lower reaches of the estuary where the “flooding” effect is more related to higher tidal water levels (i.e. tidal water levels plus the 0.5 m rise in water levels) than the effect of flow waters.

Plots of the flooding extents for the various flood sizes under winter base flows of 35 m^3/s and 12 m^3/s are contained in Annex C as are the results for a 0.5 m elevation in offshore water levels that could be considered to represent the effects of either potential sea level rise scenarios or the effects of subtidal or event scale elevations in water level due to changes in offshore conditions).

The conclusion of the flood modelling study is that:
“Differentiating between the various proposed future scenarios in terms of changes in flooding extents therefore cannot be done on changes in winter base flow alone. Rather it is the change in flood size, timing and number of flood events in each flood size class that determine the regularity and extent of flooding of both the flood plain and its associated pans.”

Such an analysis of the the change in flood size, timing and number of flood events in each flood size class for the various proposed scenarios is contained in the main report.

6. Conclusions and Recommendations

The water quality modelling indicated that the major changes in salinity distribution occur between natural conditions and the present. The changes between the pre-Berg River dam and present conditions are relatively small, i.e. much of the damage has already been done. Under the more extreme development scenarios, the upstream penetration of saline water is expected to extend beyond the present limit located approximately at Kersefontein (approximately 47 km upstream). The model results indicate that the upstream salinity penetration is very sensitive to the assumed summer base flows. For summer base flows of 0.3 m^3/s (our present best guess), the upstream penetration of salinity is unlikely to change very much, i.e. saline waters will penetrate a further 3 to 4 km upstream at the most assuming that the summer base flows do not drop below this level. However, should the summer base flows drop from 0.3 m3/s to 0.15 m3/s, the net results would be an upstream penetration of saline beyond Kersefontein to a location between 50 and 57 km upstream. Should the summer base flows be reduced to zero, the saline water will penetrate beyond 57 km upstream.

The flood modelling results indicated that the previously reported strong relationship between flooding extents and winter base flows has been overemphasised. The present flood modelling results indicate that this relationship is only significant for smaller floods (< 200 m^3/s) and then only in the upper reaches of the estuary. Consequently, differentiating between the various proposed future scenarios in terms of changes in flooding extents therefore cannot be done on changes in winter base flow alone. Rather, it is the change in flood size, timing and number of flood events in each flood size class that will determine the regularity and extent of flooding of both the flood plain and its associated pans. However, as flooding extent in the upper reaches of the Berg estuary is influenced to some extent by changes in winter base flow, it is the change in flood size, timing and number of the smaller flood events that is the most relevant in differentiting between the various proposed development scenarios. These analyses are contained in the main body of this report.

The two major uncertainties affecting analyses based on the modelling results are:

- The uncertainty in the magnitude of summer base flows. The salinity distriubutions in the upstream reaches (particularly the maximum extent of the upstream penetration of saline waters), is very sensitive to the assumed magnitude of these summer base flows.
- The lack of water level data in the Berg estuary between the Kliphoek water level gauge and that at Jantjiesfontein. The lack of water level data in the region lying between these two locations is problematic and without such data it is not possible to fully understand the flood dynamics in these important low lying regions. The absence of such water level data also means that it is not possible to robustly calibrate flood models.

The recommendations of this study are that:

- The summer base flow conditions be better estimated. The judicious siting of a gauging weir just upstream of the upper boundary of the estuary would go a long way to removing these uncertainties.
- A water level gauge be sited in the Berg River estuary at a location between approximately 25 km and 40 km upstream (preferably at approximately 33 km upstream).

7. References

Beck, J.S. & G.R. Basson (2004). Estuarine hydrodynamics. In Clark, B. (Ed.) Berg River Baseline Monitoring Programme Initialisation Report – Volume 2. Cape Town, Anchor Environmental Consultants. pp. 9–51.

Beck, J.S & G.R Basson (2007). Chapter 2: Hydraulics and Fluvial Morphology. Final Report - Volume 3: Estuary And Floodplain Environment. Clark, B.M & Ratcliffe G. (Eds). Report prepared for the Department of Water Affairs and Forestry, DWAF Report No. P WMA 19/G10/00/1907. Pretoria, p20-83.

Brundrit, G.B. 1984. Monthly mean sea level variability along the west coast of southern Africa. South African *Journal of Marine Science* 16: 195–203.

Cooper, J.A.G. (2001) Geomorphological variability among micro tidal estuaries from the wave-dominated South African coast. *Geomorphology*, 40, 99–122

CSIR (1992) Assessment of hydrodynamic and water quality aspects of the Berg River Estuary 1989/1990. CSIR Report EMAS-D 92006, 41pp + 33pp App..

CSIR (1993) Salinity distributions and aspects of flooding in the Berg River estuary obtained using the MIKE-11 modelling system: Model Applications and preliminary results, CSIR Report EMAS-C/SEA 93037, 38pp + 7pp App.

Day, J.H. 1981. Estuarine ecology with particular reference to southern Africa. AA Balkema, Cape Town.

De Cuevas, B.A., Brundrit, G.B. & Shipley, A.M. 1986. Low-frequency sea-level fluctuations along the coasts of Namibia and South Africa. *Geophysical Journal of the Royal Astronomical Society* 87: 33–42.

Du Toit, P.S. (1988) Climate of South Africa (Climate statistics up to 1984), WB40, South African Weather Bureau, Department of Environmental Affairs, Government Printer, Pretoria, 1at Edition.

DWAF 1993. Hydrology of the Berg River Basin. prepared by R. R. Berg of Ninham Shand Inc. in association with BKS Inc. as part of the Western Cape System Analysis. DWAF Report No. PG000/00/2491.

DWAF (2007a) *Berg River Baseline Monitoring Programme Final Report – Volume 1: Introduction to the Berg River Catchment; Groundwater and Hydrology*, Ractliffe, G. (ed.): DWAF Report No. P WMA 19/G10/00/1807.

DWAF (2007a) *Berg River Baseline Monitoring Programme Final Report – Volume 1: Introduction to the Berg River Catchment; Groundwater and Hydrology*, Ractliffe, G. (ed.): DWAF Report No. P WMA 19/G10/00/1807.

DWAF (2007b) *Berg River Baseline Monitoring Programme Final Report – Volume 2: Riverine Baseline Monitoring Programme and Statement of Baseline Conditions.* Clark Ractliffe, G. (ed.): DWAF Report No. P WMA 19/G10/00/1807.

DWAF (2007c) *Berg River Baseline Monitoring Programme Final Report – Volume 3: Estuary and Flood Plain Environment*, Clark, B. (ed.): DWAF Report No. P WMA 19/G10/00/1907.

DWAF (2007d) *Berg River Baseline Monitoring Programme Final Report – Volume 4: Social and Cultural Aspects*, Clark, B.. (ed.): DWAF Report No. P WMA 19/G10/00/2007.

DWAF (2007e) *Berg River Baseline Monitoring Programme Final Report – Volume 5: Synthesis*, Clarke, B. and G. Ractliffe (eds.):, DWAF Report No. P WMA 19/G10/00/2107.

DWAF (2007f) *Berg River Baseline Monitoring Programme Final Report – Volume 6: Berg River Groundwater Atlas. Cl*arke, B. and G. Ractliffe (eds.): DWAF Report No. P WMA 19/G10/00/ 2107.

Dyer, K.R. (1997) Estuaries: a physical introduction. John Wiley & Sons Ltd, Chichester, England.

Howard, G. & G. Ractliffe (2007) Chapter 5: Berg River Catchment, In *Berg River Baseline Monitoring Programme Final Report – Volume 1: Introduction to the Berg River Catchment;*

Groundwater and Hydrology, Ractliffe, G. (ed.): DWAF Report No. P WMA 19/G10/00/1807, pp 8 – 52.

Hughes, P., Brundrit, G.B. & Shillington, F.A. 1991. South African sea-level measurements in the global context of sea-level rise. *South African Journal of Science* 87: 447–453.

Huizinga, P, J.H. Slinger & J. Boroto (1994) The hydrodynamics of the Berg River estuary – a preliminary evaluation with respect to mouth entrainment and future impoundment. *In*: Western Cape System Analysis. Water requirements for the maintenance of the Berg River Estuary. Volume I: Report on work session. *NSI Report No*. **2095/5131**. Report prepared by Ninham Shand Consulting Engineers for the Department of Water Affairs and Forestry

Largier, J. L., C. Attwood & J. Harcourt-Baldwin (2000) The hydrographic character of the Kynsna Estuary, *Trans. Roy. Soc. S. Afr.* 55(2), 107-122.

Morant, P. D., H J Heydorn & J R Grindley (2001) Report No. 41 Groot-Berg (Cw15) Estuaries of the Cape, Part II: Synopses of available information on Individual Systems, Eds. P D Morant and A E F Heydorn, CSIR Research Report 440, CSIR Environmentek, Stellenbosch, 108pp. (Draft Report)

Nelson,G. & Hutchings, L. 1983. The Benguela upwelling area. Progress in Oceanography 12: 333–356.

Open University (1989) Waves, Tides and Shallow-water Processes. Oxford, Pergamon Press. 187 pp.

Ractliffe, G. (2007) Chapter 2: Berg River Catchment, In *Berg River Baseline Monitoring Programme Final Report – Volume 1: Introduction to the Berg River Catchment; Groundwater and Hydrology*, Ractliffe, G. (ed.): DWAF Report No. P WMA 19/G10/00/1807, pp 8 – 52.

Rosenthal, G. & S. Grant (1989) Simplified tidal prediction for the South African coastline. S. A. J. Sci., 85, 104-107.

Schultze, B.R. 1984. Climate of South Africa: Part 8 General Survey.Weather Bureau Report WB28. 329 pp.

Schultze, R.E. 1997. South African Atlas of Agrohydrology and -Climatology. Technical Report TT82/96. WRC, Pretoria.

Schultze, R.E., M. Maharaj, M.L. Warburton, C.J. Gers, M.C.J. Horan, R.P. Kunz and D.J. Clark (2008) South African Atlas of Agrohydrology and -Climatology. Technical Report WRC Report 1489/1/08 (CD-ROM), WRC, Pretoria.

Schumann, E. H. (2007) Chapter 3: Water Chemistry - Salinity, Temperature, Oxygen and Turbidity. In: Berg River Baseline Monitoring Programme Final Report - Volume 3: Estuary And Floodplain Environment. Clark, B.M & Ratcliffe G. (Eds). Report prepared for the Department of Water Affairs and Forestry, DWAF Report No. P WMA 19/G10/00/1907. Pretoria, p20-83.

Schumann, E.H. (2009) The Berg Estuary: Water structures and dynamics Transactions of the Royal Society of South Africa Vol. 64(2): 164–180, 2009.

Schumann, E.H. & K.H. Brink (2009) Tidal and subtidal water level fluctuations in the Berg Estuary Transactions of the Royal Society of South Africa Vol. 64(2): 181–188, 2009.

Shillington, F.A. (1984) Long period edge waves off southern Africa. Continental Shelf Research, 3, 343-357.

Shillington, F.A. 1998. The Benguela upwelling system off southwestern Africa. In Robinson, A.R. & Brink, K.H. (Eds) The Sea: The Global Coastal Ocean, Regional Studies and Syntheses 11: 583–604.

Slinger, J.H. & Taljaard, S. (1994) Preliminary investigation of seasonality in the Great Berg Estuary. Water SA 20: 279–288.

Slinger, J.H. & Taljaard, S. (1996) Water quality modelling of estuaries. Field data collection for calibrating the Mike 11 water quality module on the Great Berg Estuary. CSIR Data Report EMAS-D 96002. Stellenbosch.

Slinger, J.H, Taljaard, S. & Visser, E. (1996) Water quality modelling of estuaries. Field data collection for calibrating the Mike 11 water quality module on the Great Berg Estuary. CSIR Data Report EMAS-D 96004. Stellenbosch.

Slinger, J.H., S. Taljaard, M. Rossouw & P. Huizinga (1998) Water quality modelling of estuaries. WRC Report no 664/1/98 (ISBN 1 86845 438 X)

Smakhtin, V.U. (2001) Low flow hydrology: a review. Journal of Hydrology 240: 147–186.

Taljaard , S and J.H. Slinger (1992).Assessment of hydrodynamic and water quality aspects of the Berg River Estuary 1989/1990. CSIR Report EMAS-D 92006, Stellenbosch, 41pp.

Taljaard, S., Slinger, J.H., Skibbe, E., Fricke, A.H., Kloppers, W.S. & Huizinga, P. (1992) Assessment of hydrodynamic and water quality aspects of the Berg River Estuary – 1989/990. CSIR Data Report EMAS-D 92006. Stellenbosch.

Triton Surveys (2003) Bathymetry of the Berg River Mouth – January 2003, unpublished survey data, Triton Surveys, P/O/ Box 18597, Wynberg 7800, Cape Town.

Turpie, J & B. Clark (2007) Chapter 3: Estuary conceptual model. In: *Berg River Baseline Monitoring Programme Final Report – Volume 5: Synthesis*, Clarke, B. and G. Ractliffe (eds.):, DWAF Report No. P WMA 19/G10/00/2107, p51-80.

Tyson, P.D. 1986. Climatic Change and Variability in Southern Africa. Cape Town, Oxford University Press. 220 pp.

WL| delft hydraulics (2009) DELFT3D-FLOW User Manual Version 3.14 (Revision: 7864), WL | Delft Hydraulics, The Delft, Netherlands, 644pp.

ANNEX A: SALINITY DISTRIBUTIONS IN THE BERG ESTUARY

Of particular relevance to this study are the salinity distributions:

i) during and following high freshwater inflow periods when the estuary comprises mainly freshwater, except near the mouth where tidal flows result in higher salinities being measured near the mouth.

ii) at the end of low flow periods when the maximum upstream intrusion of saline waters occurs.

However also of relevance are periods of transition between:

i) the more saline conditions in late summer and autumn and the mostly freshwater conditions typical of winter (*i.e*. during autumn when the first significant rains and freshwater inflows into the estuary occur, at times resulting in vertical changes of up to 5 psu in the middle to upper reaches of the estuary - these effects are mostly observed during neap tide conditions when the tidal flows are weakest), and;

ii) the often highly saline conditions of mid to late autumn and the largely freshwater conditions following winter freshettes and floods),

Here we have focussed mainly on the late autumn period when reductions in summer base flows and/or the delays in the first freshwater inflows of winter may result in higher salinity waters penetrating far upstream. This upstream penetration more saline waters in autumn, together with the potential reductions in occurrence and extent of flooding, pose the greatest risks to the estuary under future development scenarios.

Longitudinal section of salinity have been measured on a number of occasion since 1989 (*e.g*. Slinger & Taljaard, 1994; Slinger & Taljaard, 1996, Slinger *et al*., 1996, Schumann, 2007). During the period 1989 to 1996, the CSIR measured 22 longitudinal sections on 18 different days Temperature and salinity profiles were measured at each station while dissolved oxygen and pH were measured only at the surface and near the bottom (in many cases these parameters were measured only at the surface). These data are summarised in (Schumann 2007) who subjected only a sub-set of these data to further analysis.

A total of 52 longitudinal sections of salinity were measured during the Berg River Baseline monitoring programme (Schumann, 2007). These were more or less equally distributed in time between:

i) the peak freshwater inflow period (approximately August),

ii) the transition period between the winter high freshwater inflow period and the summer base flow period,

iii) the late summer period (February) following the extended low summer base flow conditions;

iv) the transition period between the low summer base flow and high freshwater inflows typical of the winter months.

As noted above of greatest relevance in this study are the salinity distributions during the autumn months when the upstream penetration of saline waters in the greatest.

Schumann (2007) has summarised these salinity distributions for February, May, August and November (Figure A1). Unfortunately these distributions were plotted against station number consequently the relevant information the longitudinal distance upstream is lost. However reference to the longitudinal sections reported in Figure A4 to A6 allow such information to be inferred.

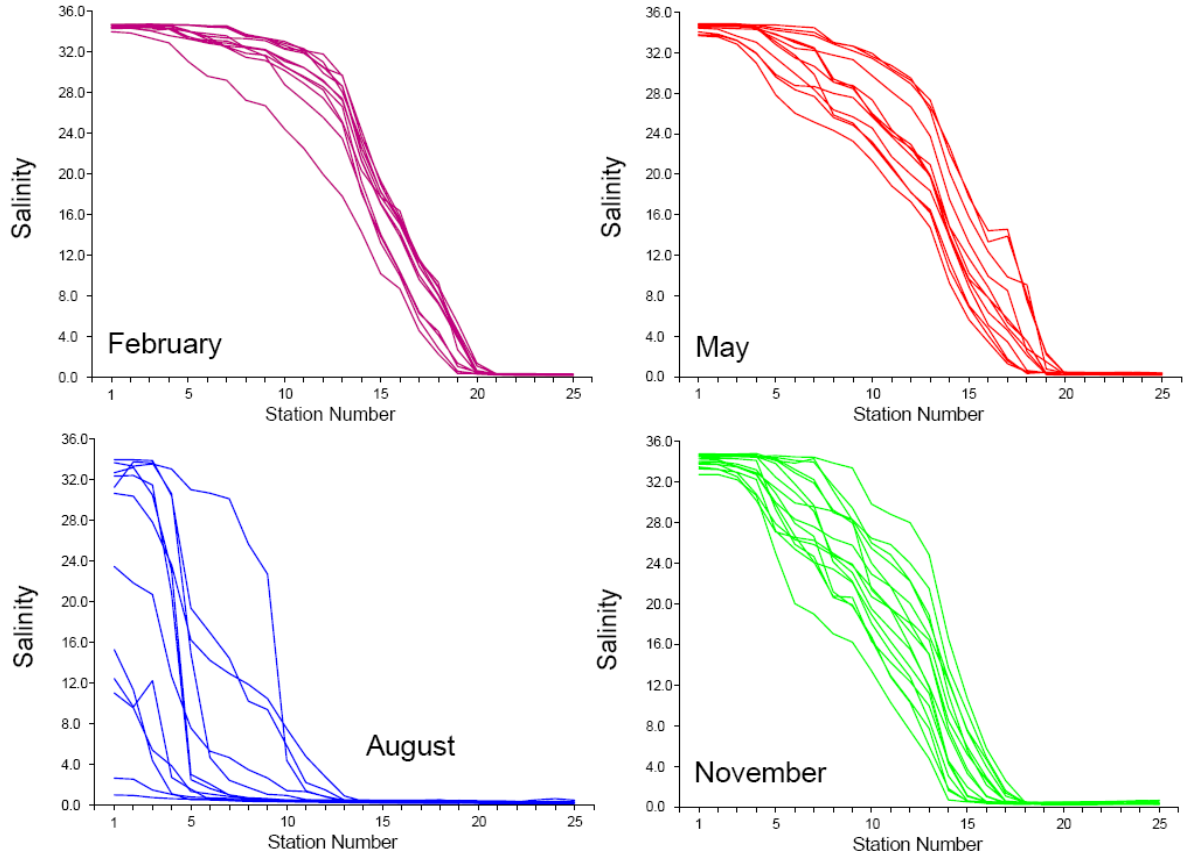

Figure A1 Vertically-integrated values of salinity at each of the stations for all the experimental sections measured on the Berg Estuary during the specified months (after Schumann, 2007).

The most extreme upstream penetration of saline water, to Stn 21 (Kersefontein) or approximately 47 km upstream, occurs in February or in the months immediately thereafter. The maximum upstream penetration of saline waters decreases thereafter as the first rains and associated freshwater inflows of the wet winter season start to flush the upper reaches of the estuary. In this early transition period (May) the 1 {SU isoline typically lies between Stn 18 and 20 (*i.e.* approximately 37 to 44 km upstream).

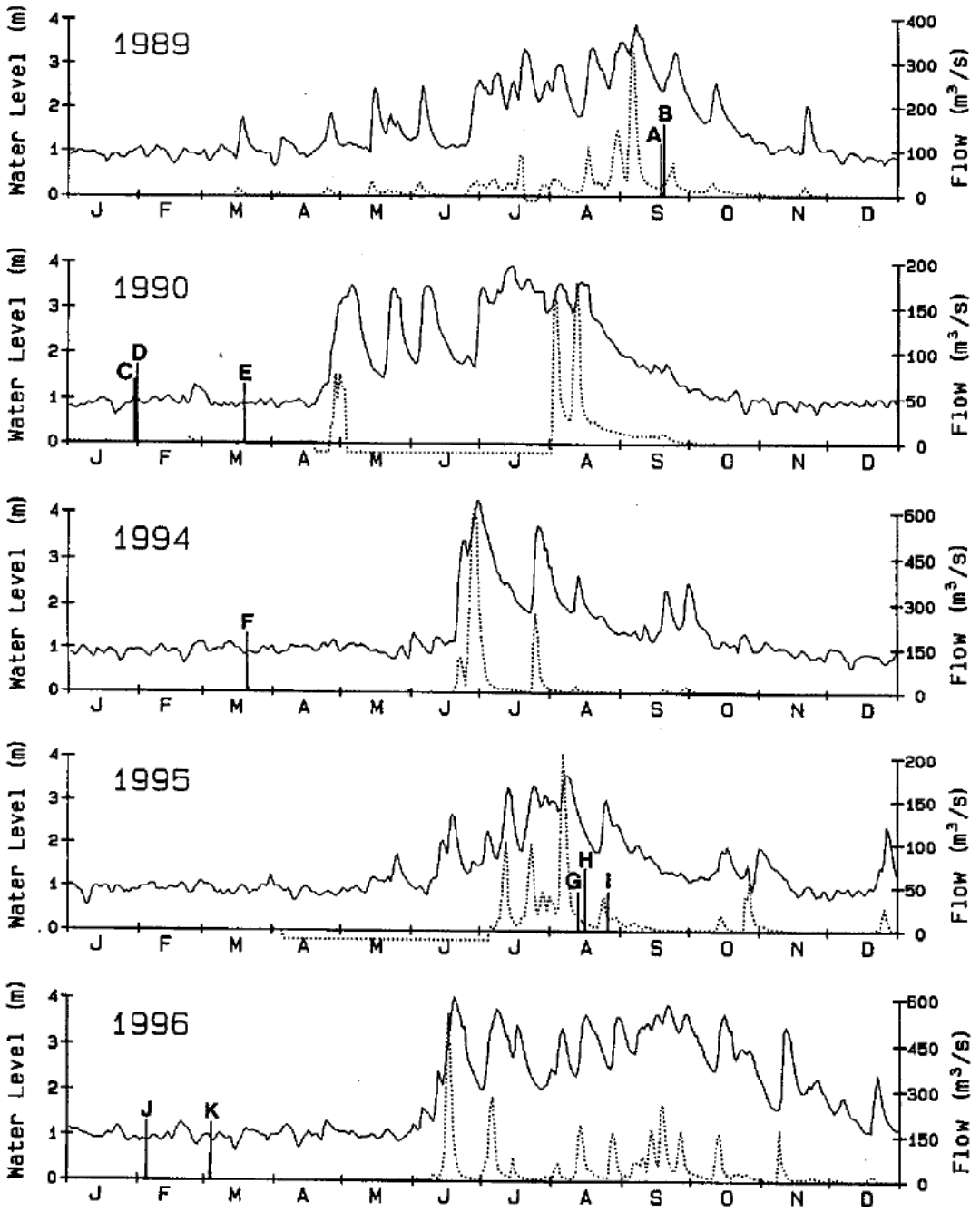

Figure A2 **Measurements of water level made at Jantjiesfontein (solid line), and the stream flow measured at Misverstand (dotted line) over the years 1989, 1990, 1994, 1995 and 1996 (after Schumann, 2007). The stream flow measured at Misverstand is here considered to adequately represent the relative differences (magnitude and timing) of the freshwater inflows into the estuary during this period. The times at which the various salinity sections (reported in Schumann, 2007) were measured by the CSIR during this period are indicated (A to K). Note the different scales for the stream flow for the different years. Where the dotted line is negative no measurements are available.**

During the peak freshwater inflow period (August), flood waters flush the estuary, sometimes resulting in almost freshwater flowing out through the estuary mouth into the adjacent ocean. As the freshwater inflows reduce after approximately September, tidal flushing of the lower estuary

allows salinities to increase rapidly. By November, saline waters of up to 24 PSU penetrate as far upstream as Stn 13 (or approximately 16 km upstream). Depending on the rate of freshwater inflow during the wet season, salinities at Stn 13 range between 4 and 24 PSU. Similarly the salinities at Stn 15 (approximately 24 km upstream) range between 1 and 12 PSU. Salinities of >1 PSU are rarely, if ever, observed upstream of Stn 18 (36 to 37 km upstream) during this period. The 1 PSU isohaline is observed typically to be located between Stn 15 and 17 (*i.e.* between 24 and 33 km upstream) during this period.

The freshwater inflows into the estuary can be quite variable both in their magnitude and period in which they occur. Significant variability can be introduced by inter-annual variability in the magnitude and timing of the freshwater inflows. Examples are the low freshwater inflows and the early end to freshwater inflows of 1994 compared to the much higher freshwater inflows of 1996 that extended late into the season (Figure A2) and the late but reduced freshwater inflows that occurred in 2003 compared to the earlier and significantly larger freshwater inflows that occurred in 2002 (Figure A3).

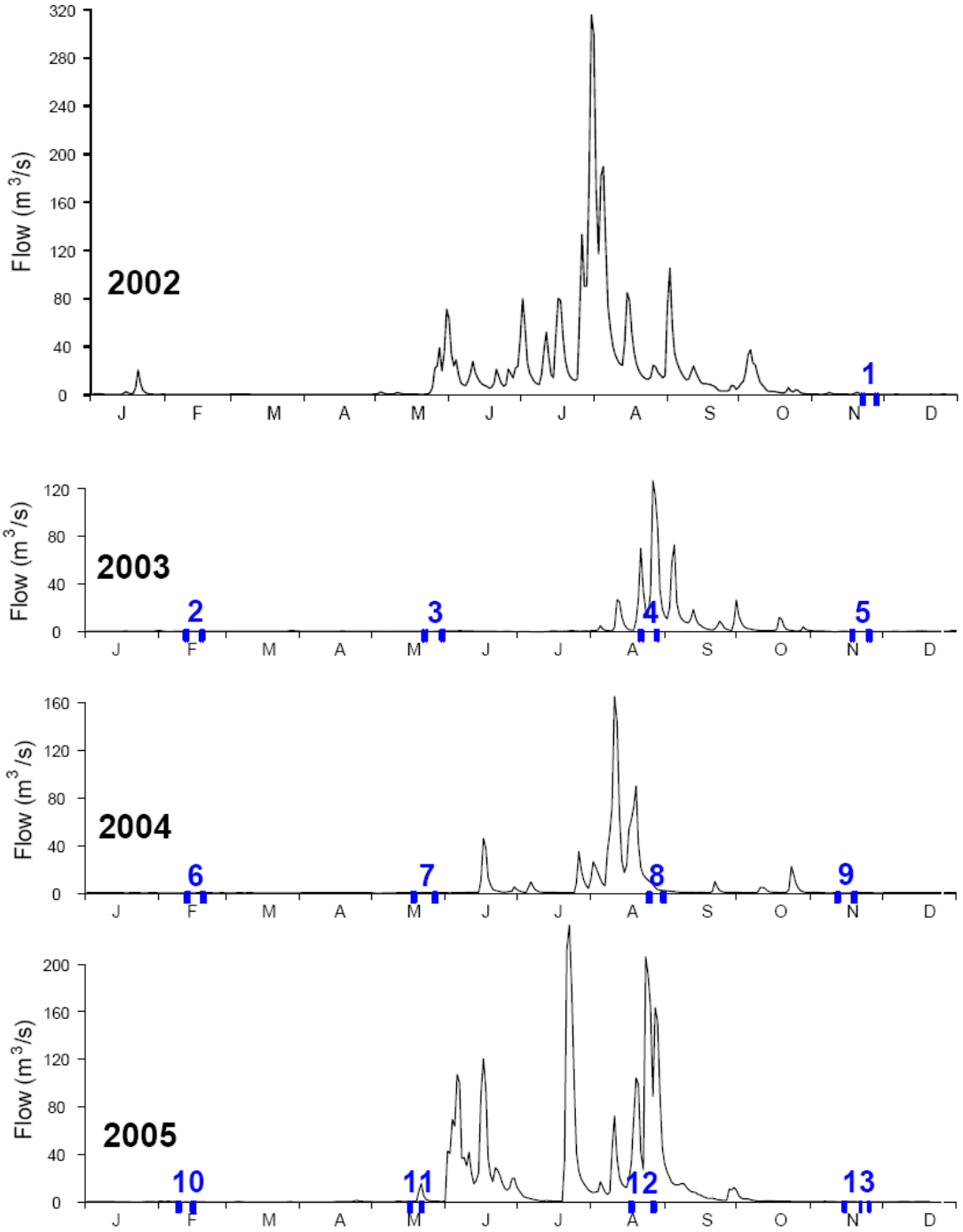

Figure A3 **Freshwater inflow at the Misverstand Dam that is considered to be reasonably representative of the freshwater inflows into the estuary (after Schumann, 2007). The blue number in the figures represent the 13 occasions that field measurements were made during the Berg River baseline monitoring study.**

If potential future changes in freshwater inflow scenarios are to be assessed in terms of their effect on longitudinal salinity distributions in the estuary, three initial salinity distributions are of relevance to the modelling study:

I. The longitudinal salinity distributions towards the end or immediately after the high inflow period (September). These constituted the starting conditions for model simulations

investigating the effects of the various proposed development scenarios on conditions in the estuary starting at periods of peak winter inflows (July/August) and ending in late summer/ early autumn after an extended period of low summer base flow conditions. The range of measured longitudinal salinity distributions for this are reported in Figures A4a to d (CSIR data) and A5a to d (Schumann, 2007).

II. The longitudinal salinity distributions towards the end of the transition period between high winter inflows and the low summer base flow conditions (November). These constitute the starting conditions for model simulations of the effects of various scenarios for periods of low summer base flows. The range of possible longitudinal salinity distributions are reported in Figures A4a to d (Schumann, 2007). The CSIR did not obtain measurements during this transition period (the longitudinal section measured by the CSIR in November 1996 did not extend sufficiently upstream to be useful.)

III. .The longitudinal salinity distribution at the end of the low summer base flow period (March). These could constitute the starting conditions for analyses considering extreme low or extended low summer base flow conditions. The range of possible longitudinal salinity distributions for late summer to mid-autumn are reported in Figures A5a to d (Schumann, 2007).

The data in Figures A4a to d suggest that freshwater inflows of between 170 m^3/s and 350 m^3/s persisting for a couple of days or more are generally sufficient to almost completely flush the estuary, resulting in almost fresh waters exiting the estuary mouth. The data in Figures A5a to A5d confirm that freshwater inflows exceeding 150 m^3/s are sufficient to almost completely flush the estuary.

The longitudinal salinity distributions towards the end of the transition period (November), *i.e*. just before the freshwater inflows settle towards the low base flows typical of the summer period, are quite variable (Figure A6 a to d). Seemingly, the longitudinal salinity distributions are extremely sensitive to whether there has been a freshwater spate prior to the observations and also the level of base flow. The observations in November 2002 were obtained some 10 days (spring tide observations) to two weeks (neap tide observations) after freshwater inflows of 10 to 11 m^3/s had occurred over a couple of days, followed by steady base flows of 4 to 5 m^3/s. This resulted in saline waters not being able to penetrate upstream of Stn 15 (approximately 25 km upstream). The observations in November 2003 were obtained some two (neap tides observations) to 4 weeks (spring tide observations) after freshwater inflows of approximately 11 m^3/s occurred for a couple of days, followed by steady base flows of 1 to 2 m^3/s. These low base flows resulted in the saline waters penetrating upstream almost to Stn 18 (*i.e*. approximately 35 km upstream). The observations obtained in November 2004 were obtained some 3 weeks (spring tide observations) to 4 weeks (neap tide observations) after flows of 25 to 30 m^3/s had occurred for a couple of days, followed by steady decline in freshwater flows to approximately 2 m^3/s as measured at the time that the observations were made. The observations in November 2005 were obtained following flows of 7 m^3/s for a couple of weeks in October, followed by a spate of 5 to 6 m^3/s between one (spring tide observations) to two weeks (neap tide observations) prior to the observations being made. The steady base flows around the time of the observations ranged between 2 to 4 m^3/s during the spring tide observations, reducing to approximately 1 m^3/s during the neap tide observations.

The above results suggest that the upstream penetration in the estuary between Stn 14 (21 km upstream) and Stn 18 (35 km upstream) is quite sensitive to both the preceding spates as well as the magnitude of the base flows occurring around the time of the observations.

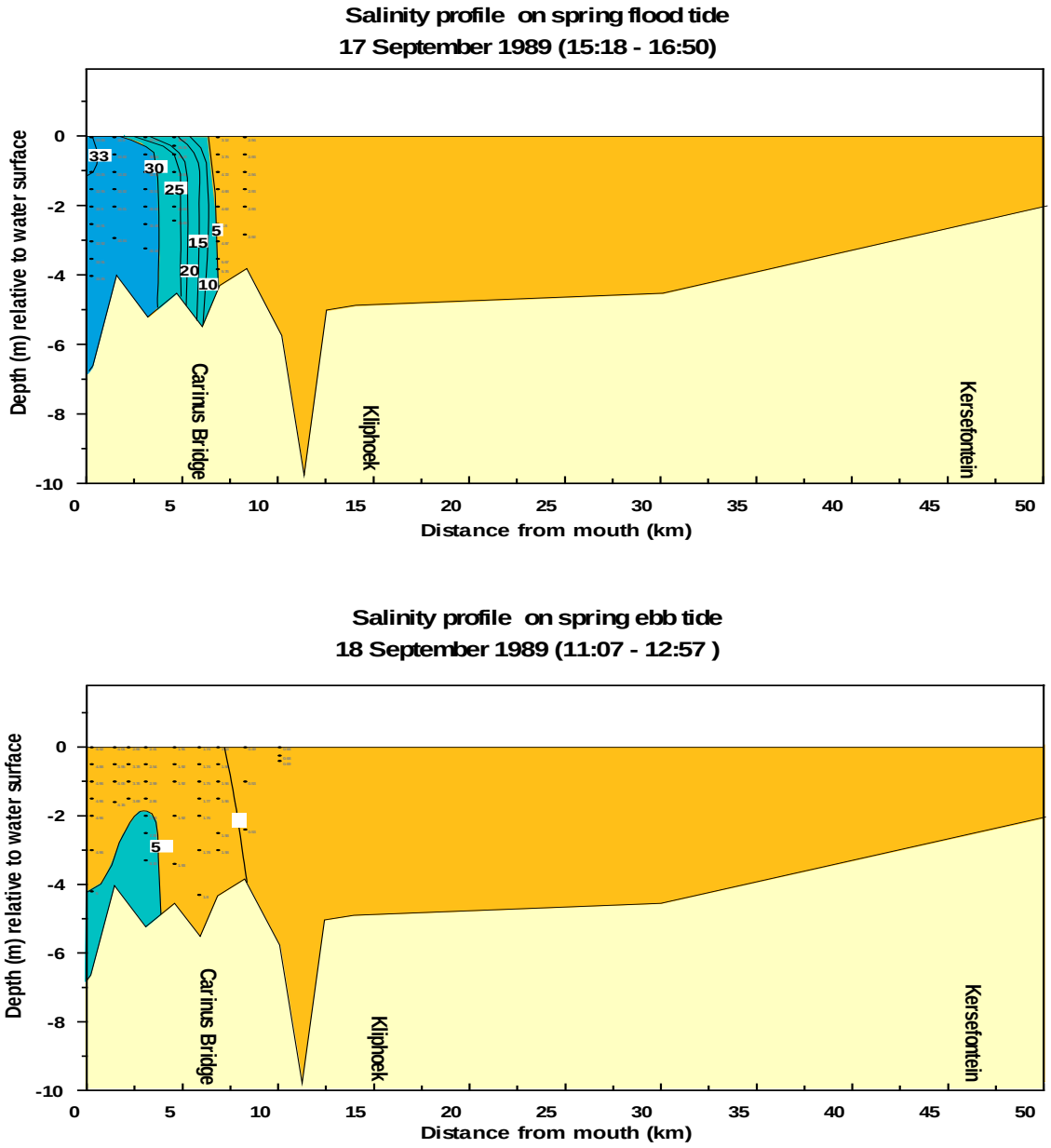

Figure A4a Longitudinal salinity distribution in the Berg River Estuary as measured by the CSIR shortly after the winter high freshwater inflow period[21] - Spring flood and ebb tide. (see annotations A and B in Figure A3).

[21] The above sections (A and B) were measured about 10 days after a spate which reached a peak flow of 354 m^3/s on 5 September, 1989 with 334 m^3/s recorded on 6 September (Schumann, 2007).

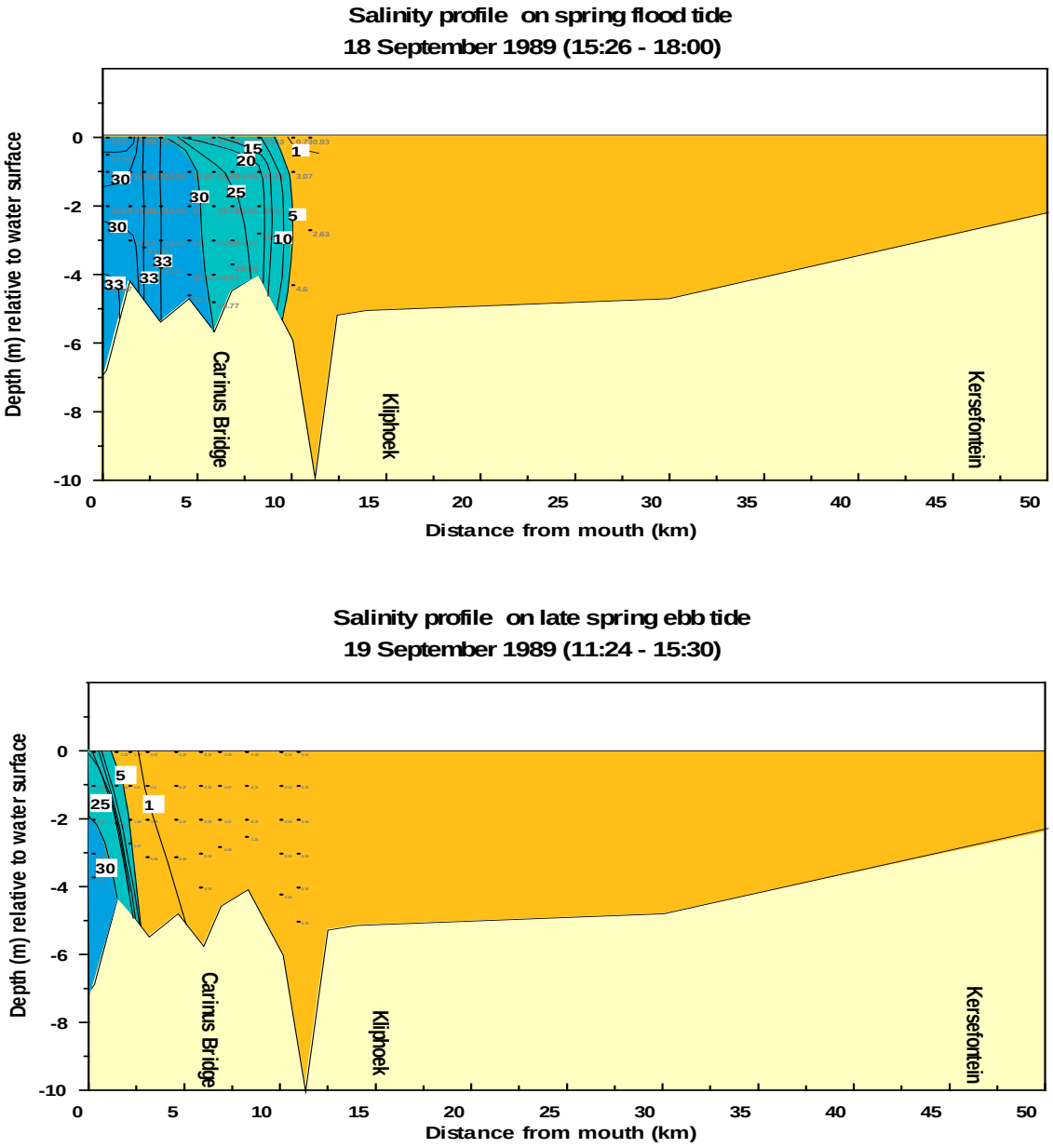

Figure A4b **Longitudinal salinity distribution in the Berg River Estuary as measured by the CSIR shortly after the winter high freshwater inflow period[22] - Spring flood and ebb tide. (see annotations A and B in Figure A3)**

22 The above sections (A and B) were measured about 10 days after a spate which reached a peak flow of 354 m^3/s on 5 eptember, with 334 m^3/s recorded on 6 September (Schumann, 2007).

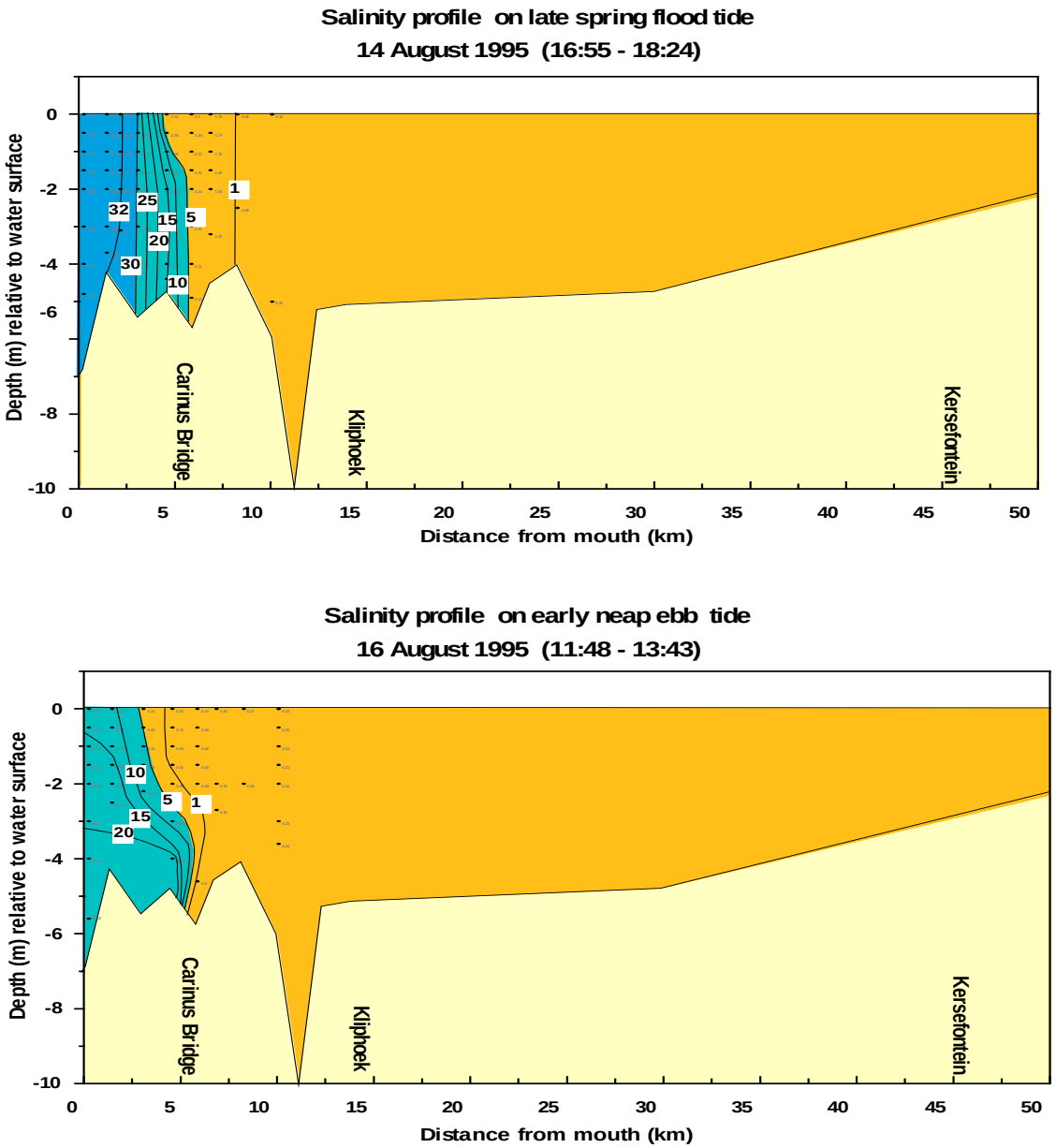

Figure A4c **Longitudinal salinity distribution in the Berg River Estuary as measured by the CSIR during the winter high freshwater inflow period[23] – Late spring flood tide and Neap ebb tide (See annotations G and H in FigureA3).**

[23] The measurements in 1995 (G and H) were taken after a spate on 6 August 1995, which reached a maximum daily flow of 205 m^3/s, tailing off on 7 August 1995 to 170 m^3/s (Schumann, 2007).

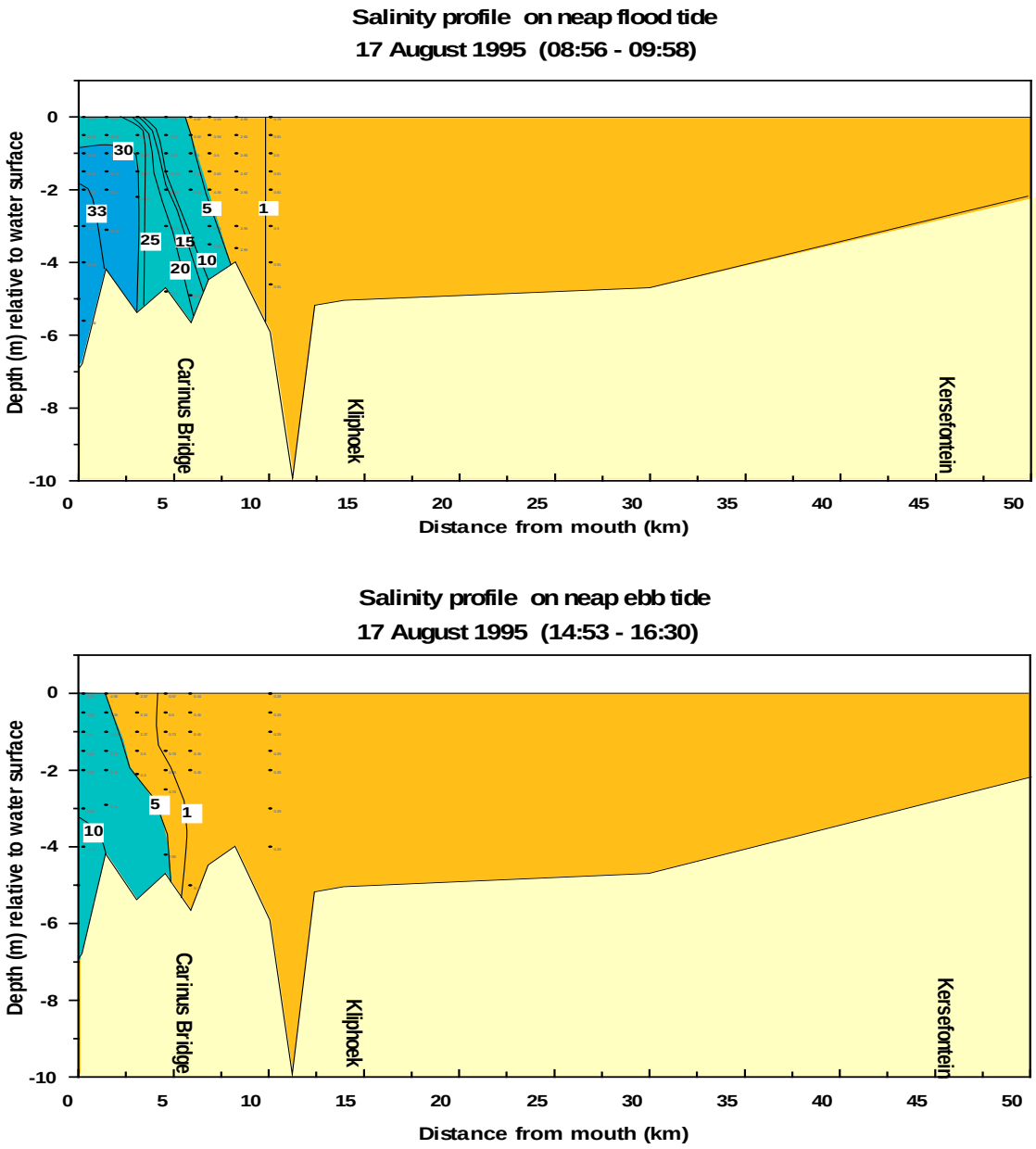

Figure A4d **Longitudinal salinity distribution in the Berg River Estuary as measured by the CSIR during the winter high freshwater inflow period[24] – Late spring flood tide and Neap ebb tide (See annotations G and H in FigureA3).**

[24] The measurements in 1995 (G and H) were taken after a spate on 6 August, 1995 which reached a maximum daily flow of 205 m3/s, tailing off on 7 August 1995 to 170 m^3/s.

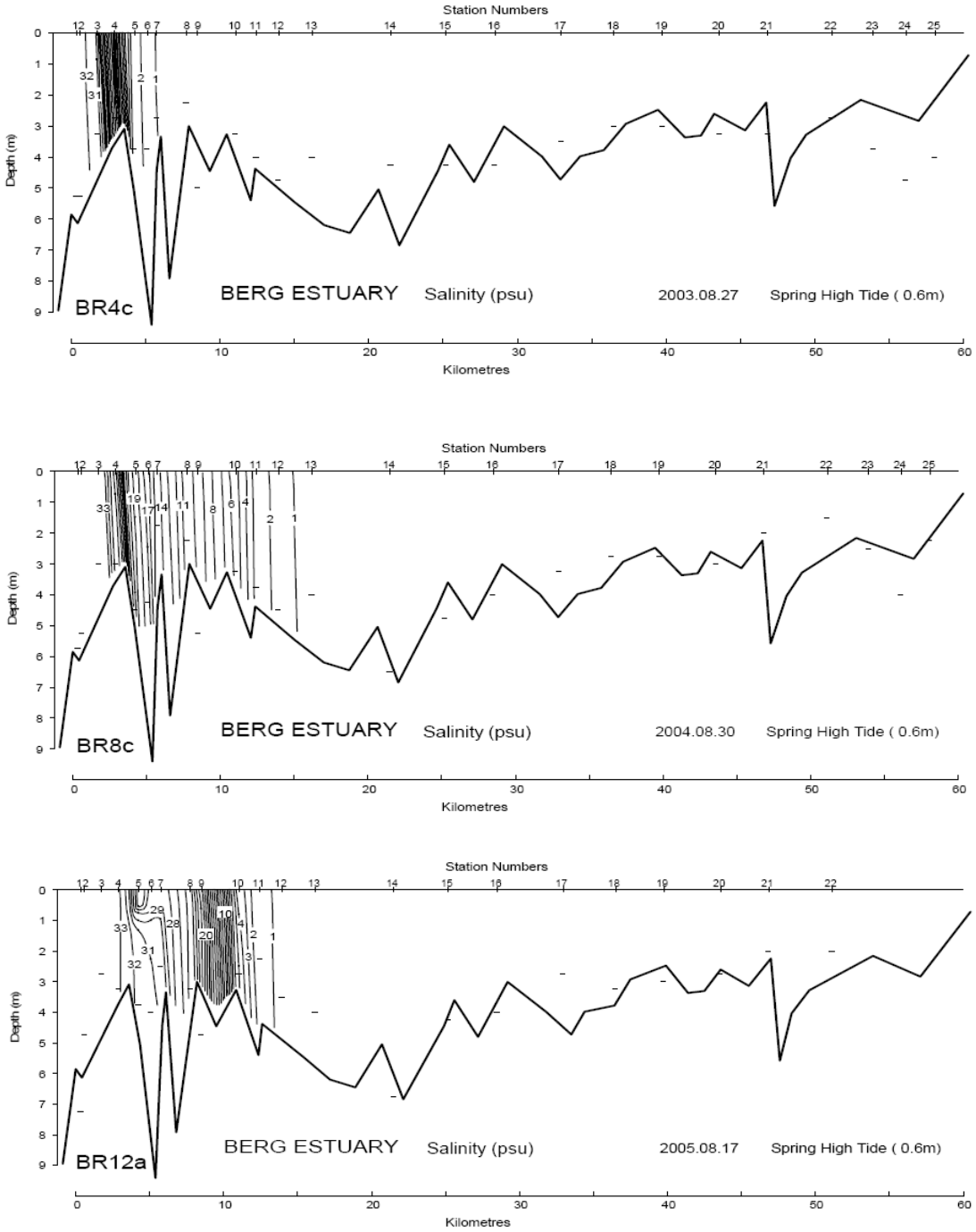

Figure A5a Longitudinal salinity distribution in the Berg River estuary as measured in the month of August (after Schumann, 2007) – Spring high tide[25].

25 The measurements were taken during freshwater inflows of approximately 150 m^3/s, the August 2004 measurements were taken approximately three weeks after a spate of 100 to 140 m^3/s over a couple of days, while the August 2005 measurements were obtained approximately one moth after freshwater flows peaking at 170 m^3/s and a few days after elevated freshwater inflows over a couple of days of approximately 50 to 60 m^3/s.

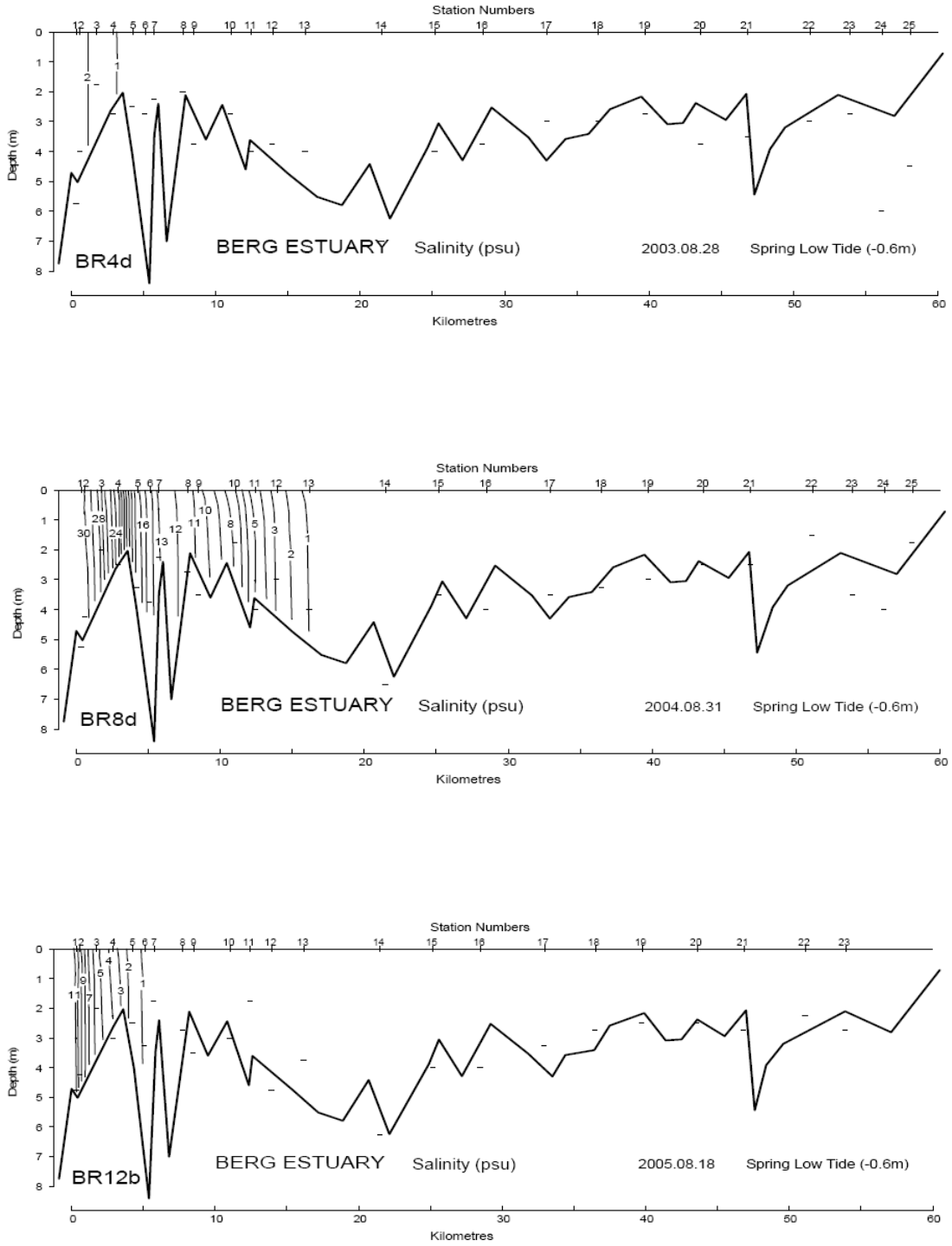

Figure A5b Longitudinal salinity distribution in the Berg River estuary as measured in the month of August (after Schumann, 2007) – Spring low tide[26].

[26] The August 2003 measurements were taken during freshwater inflows of approximately 150 m^3/s, the August 2004 measurements were taken approximately three weeks after a spate of 100 to 140 m^3/s over a couple of days, while the August 2005 measurement were obtained approximately one moth after freshwater flows peaking at 170 m^3/s and a few days after elevated freshwater inflows over a couple of days of approximately 50 to 60 m^3/s.

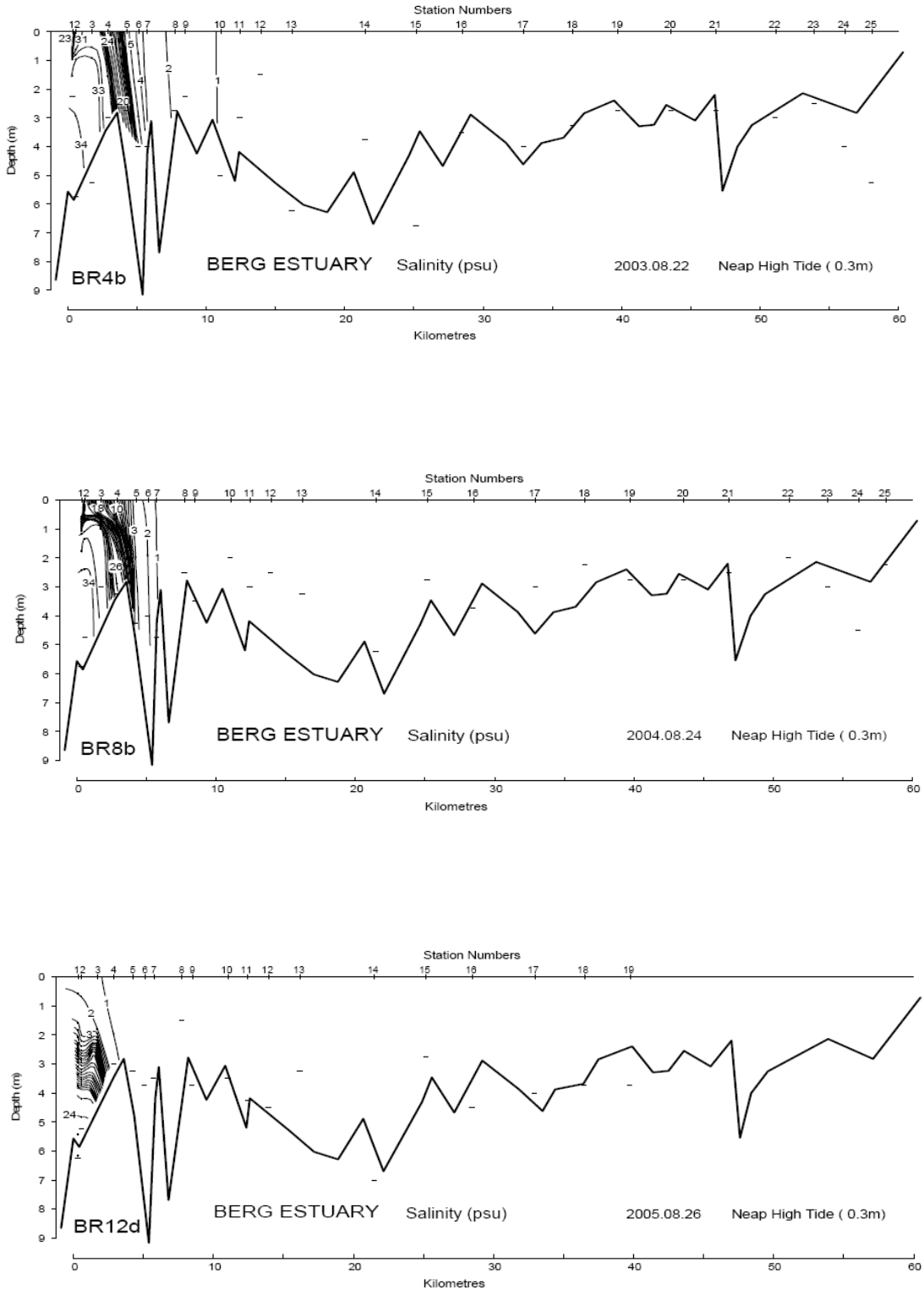

Figure A5c Longitudinal salinity distribution in the Berg River estuary as measured in the month of August (after Schumann, 2007) – Neap high tide[27].

[27] The measurements were taken during freshwater inflows of approximately 80 m^3/s, , the August 2004 measurements were taken approximately three weeks after a spate of 100 to 140 m^3/s over a couple of days, while the August 2005 measurements were obtained a couple of days after a peak fresh water inflow of 170 m^3/s that exceeded 100 m^3/s for approximately a one week period.

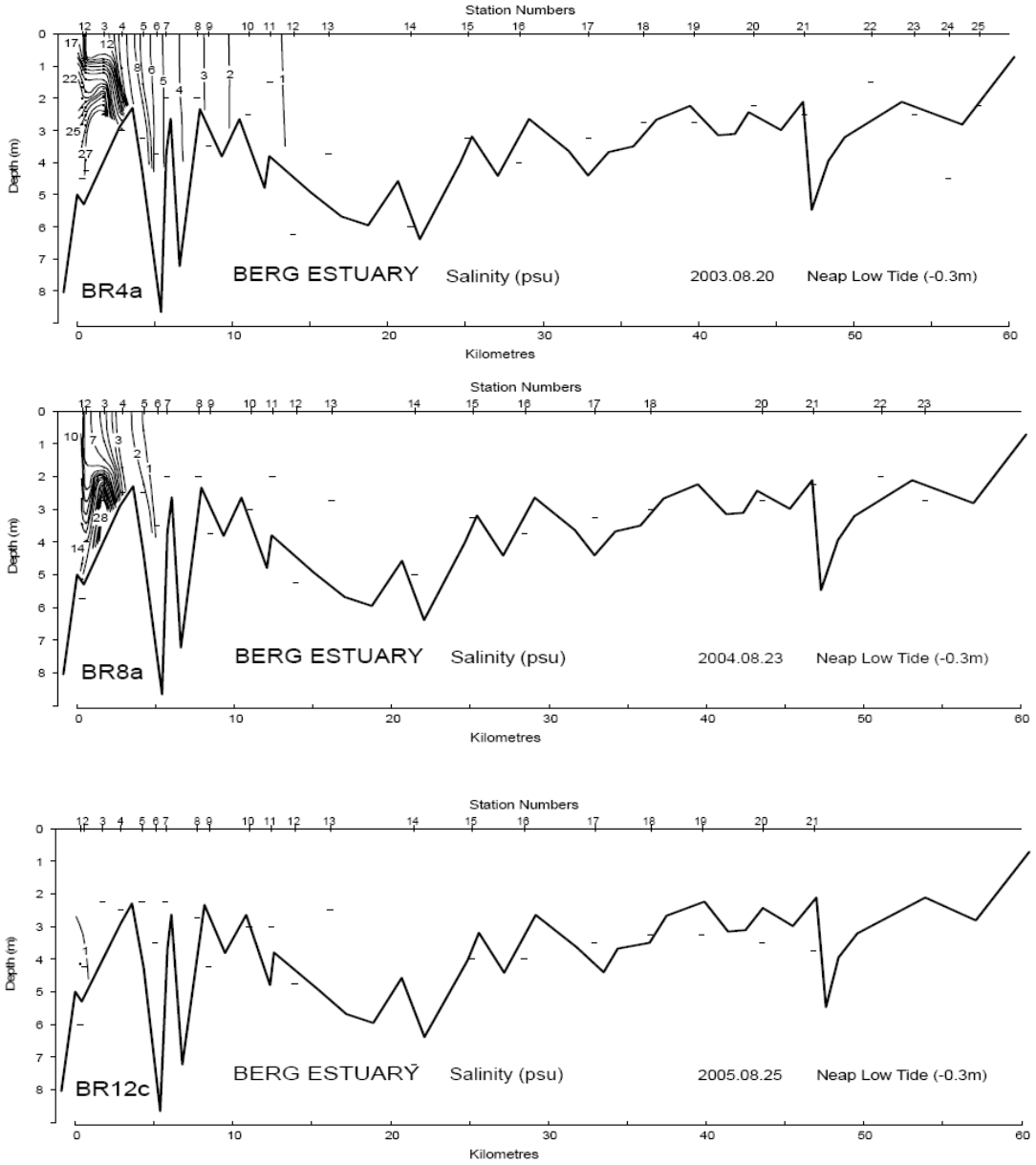

Figure A5d Longitudinal salinity distribution in the Berg River estuary as measured in the month of August (after Schumann, 2007) – Neap low tide[28].

[28] The measurements were taken approximately one week after fresh water inflows of 40 m^3/s, the August 2004 measurements were taken approximately three weeks after a spate of 100 to 140 m^3/s over a couple of days, while the August 2005 measurements were obtained were obtained a couple of days after a peak fresh water inflow of 170 m^3/s that exceeded 100 m^3/s for approximately a one week period.

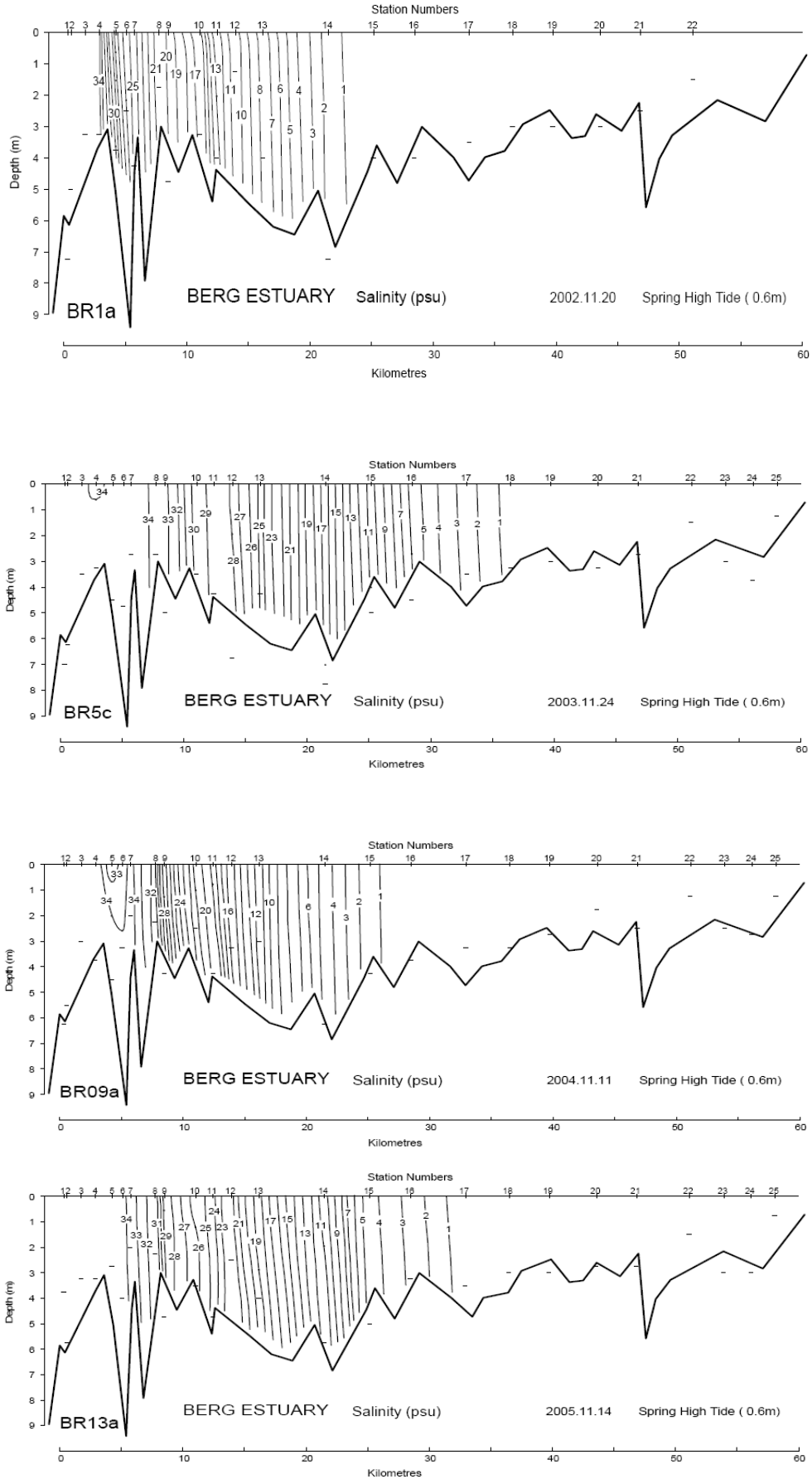

Figure A6a Longitudinal salinity distribution in the Berg River estuary as measured in the month of November (after Schumann, 2007) - Spring high tide.

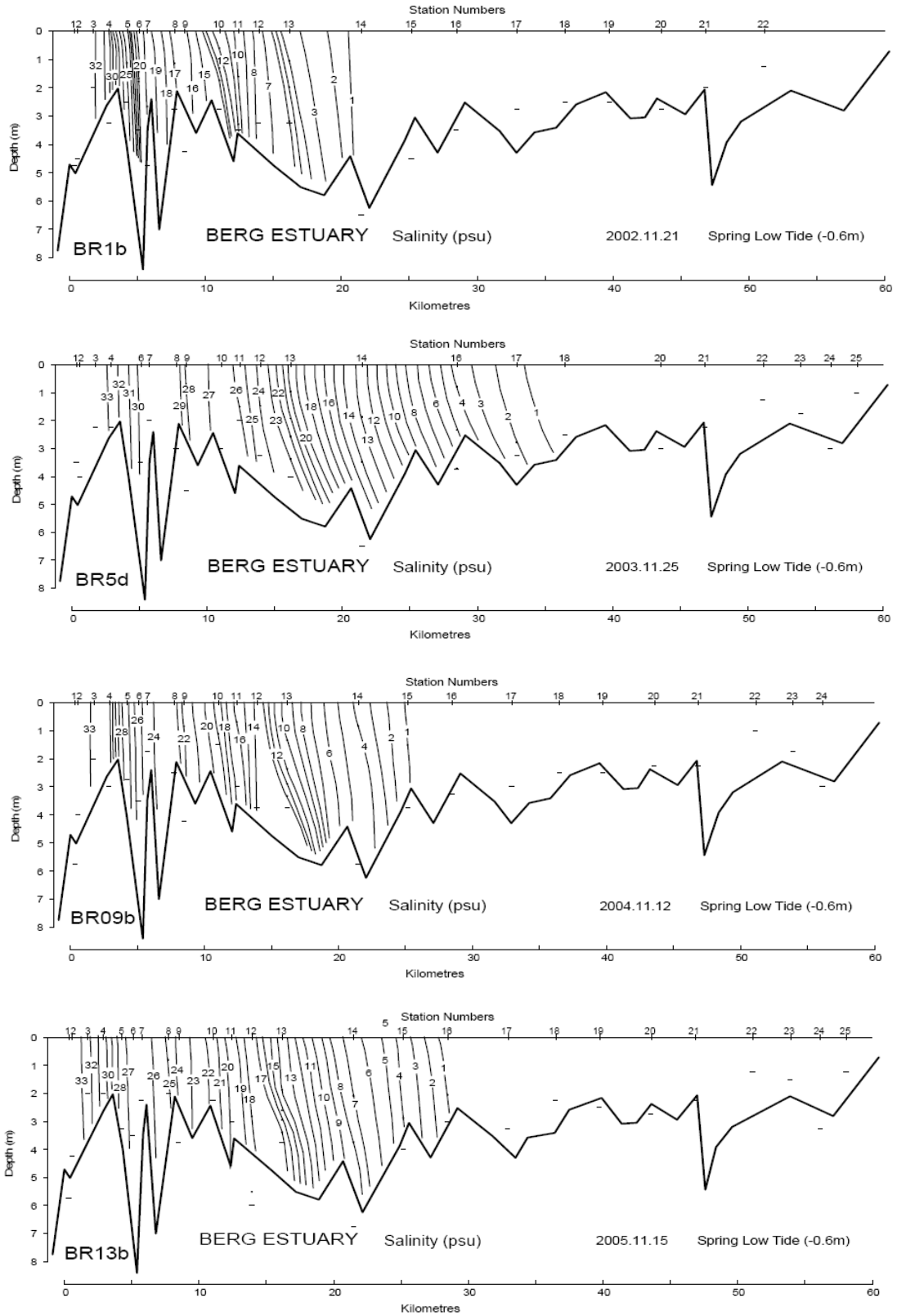

Figure A6b Longitudinal salinity distribution in the Berg River estuary as measured in the month of November (after Schumann, 2007) - Spring low tide

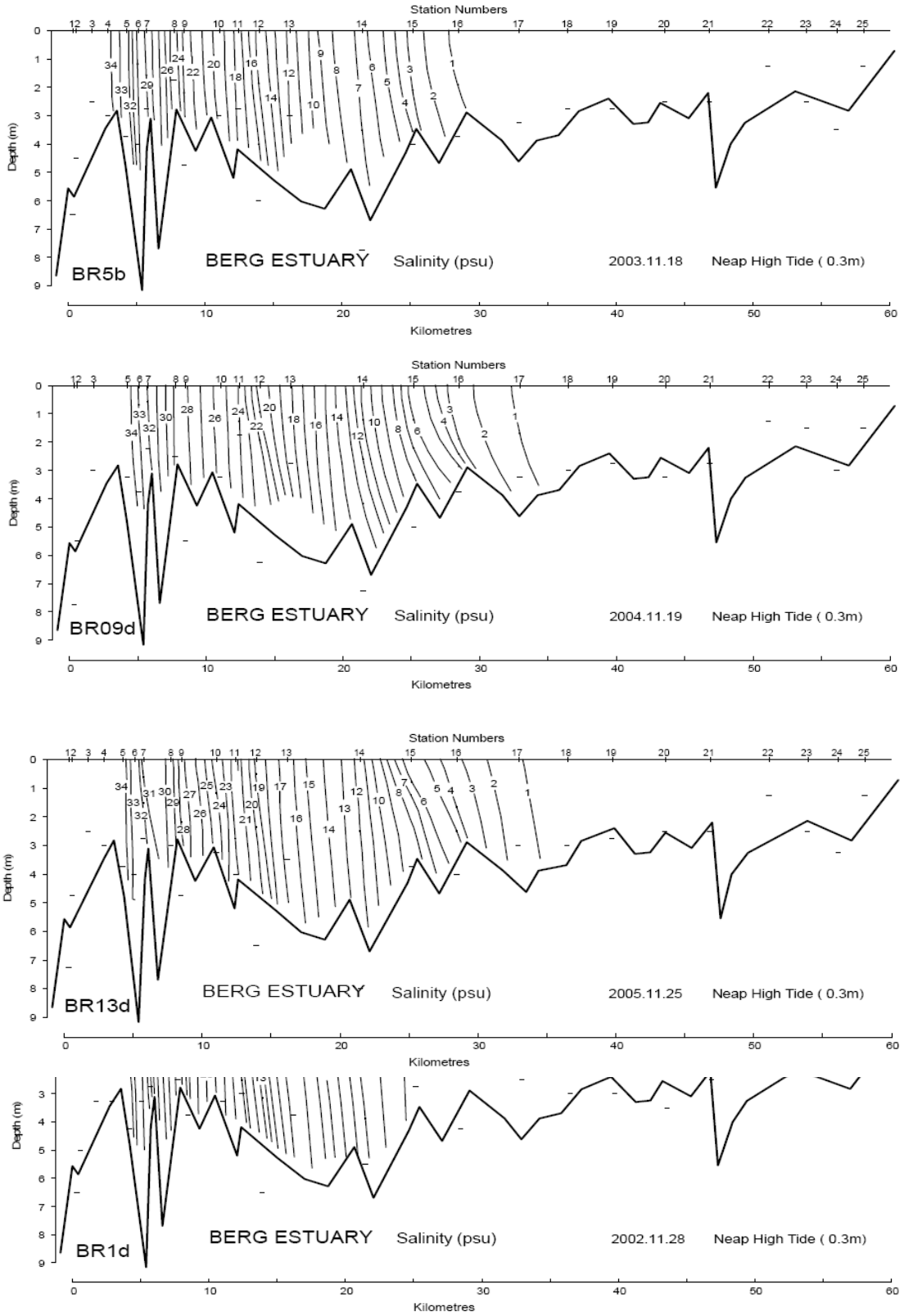

Figure A6c Longitudinal salinity distribution in the Berg River estuary as measured in the month of November (after Schumann, 2007) – Neap high tide

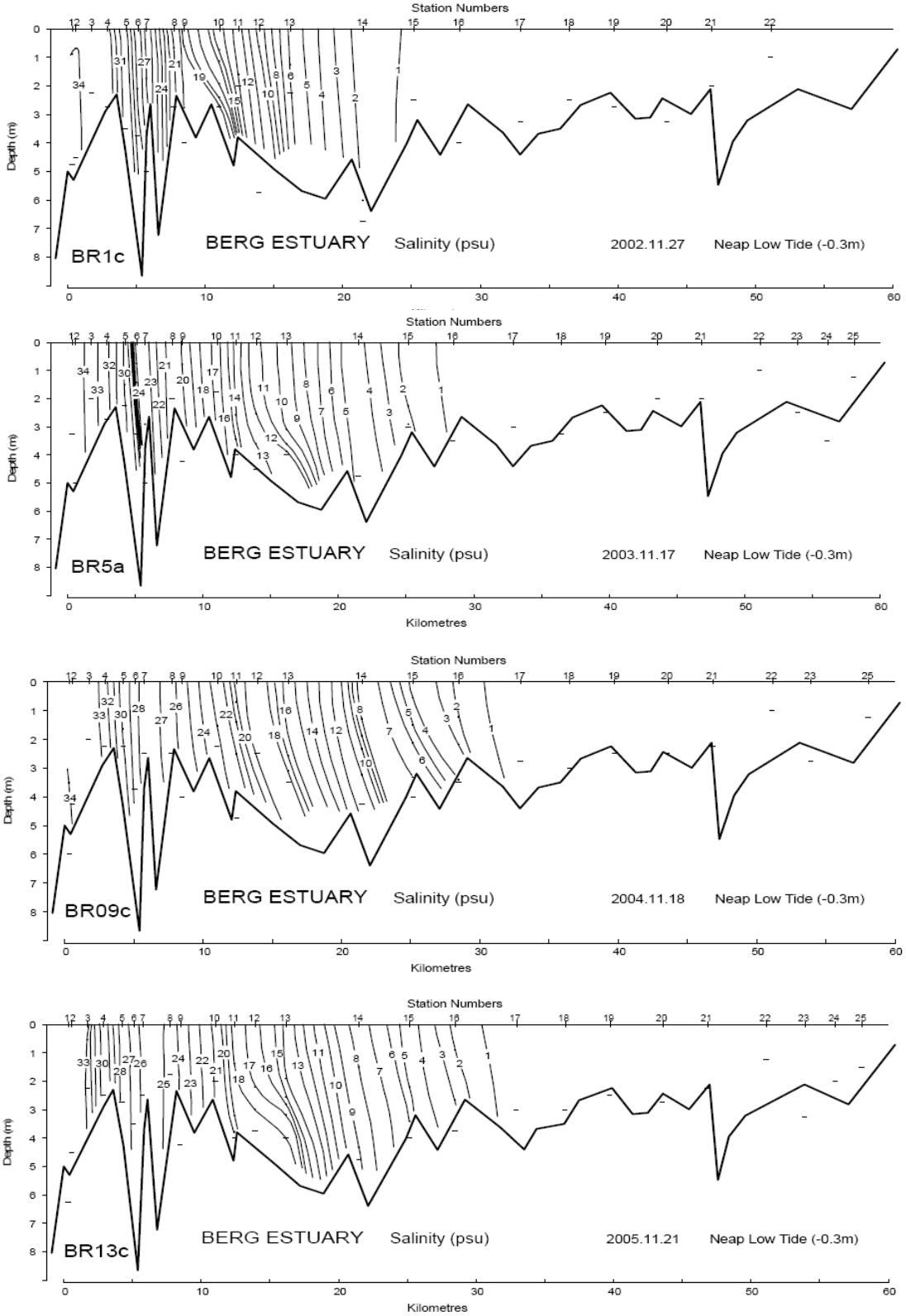

Figure A6d Longitudinal salinity distribution in the Berg River estuary as measured in the month of November (after Schumann, 2007) - Neap low tide

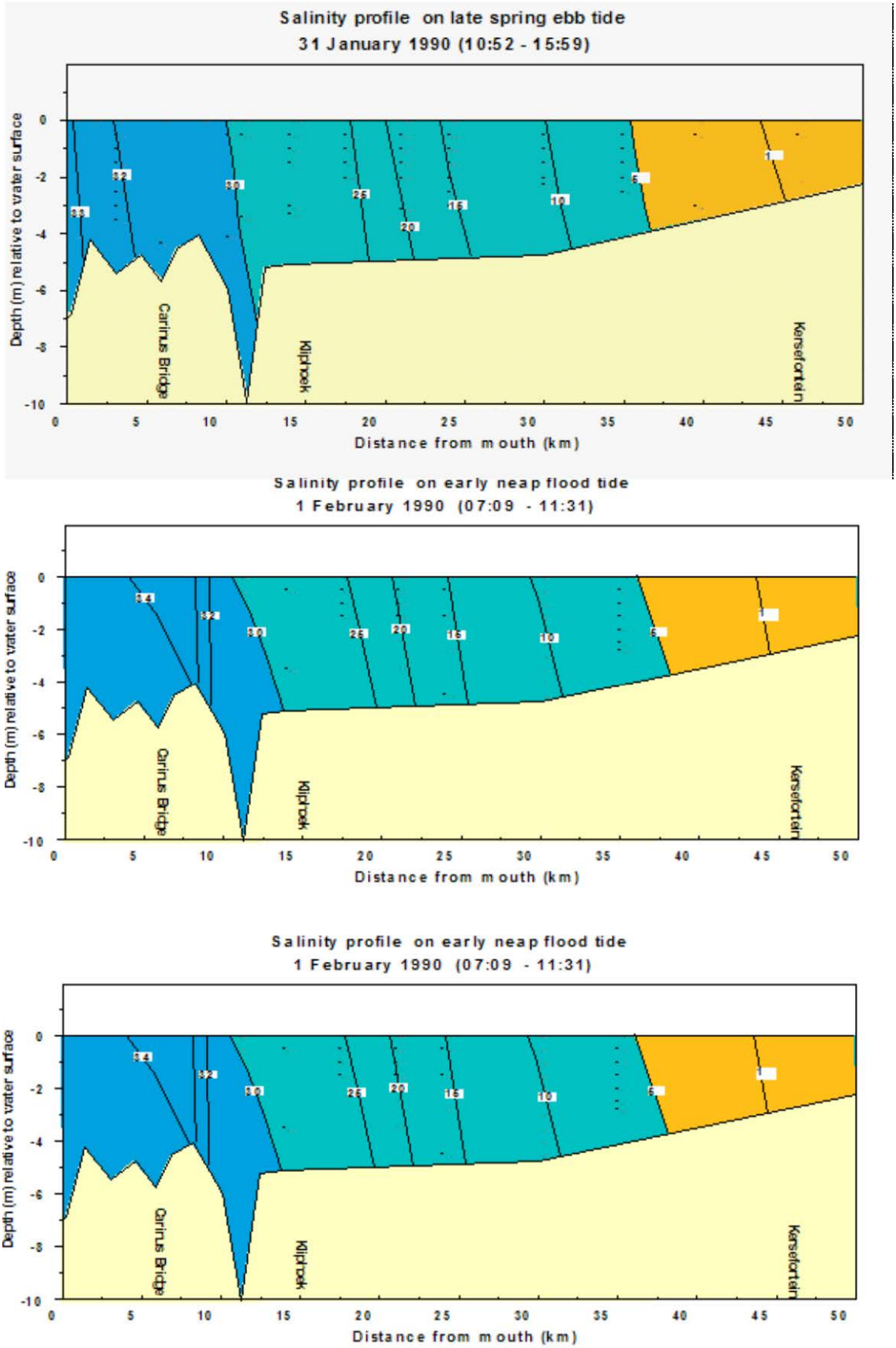

Figure A7a **Longitudinal salinity distribution in the Berg River estuary as measured in summer/late summer, *i.e.* after an extended period of summer low base flows (see annotations C and D in Figure A3)**

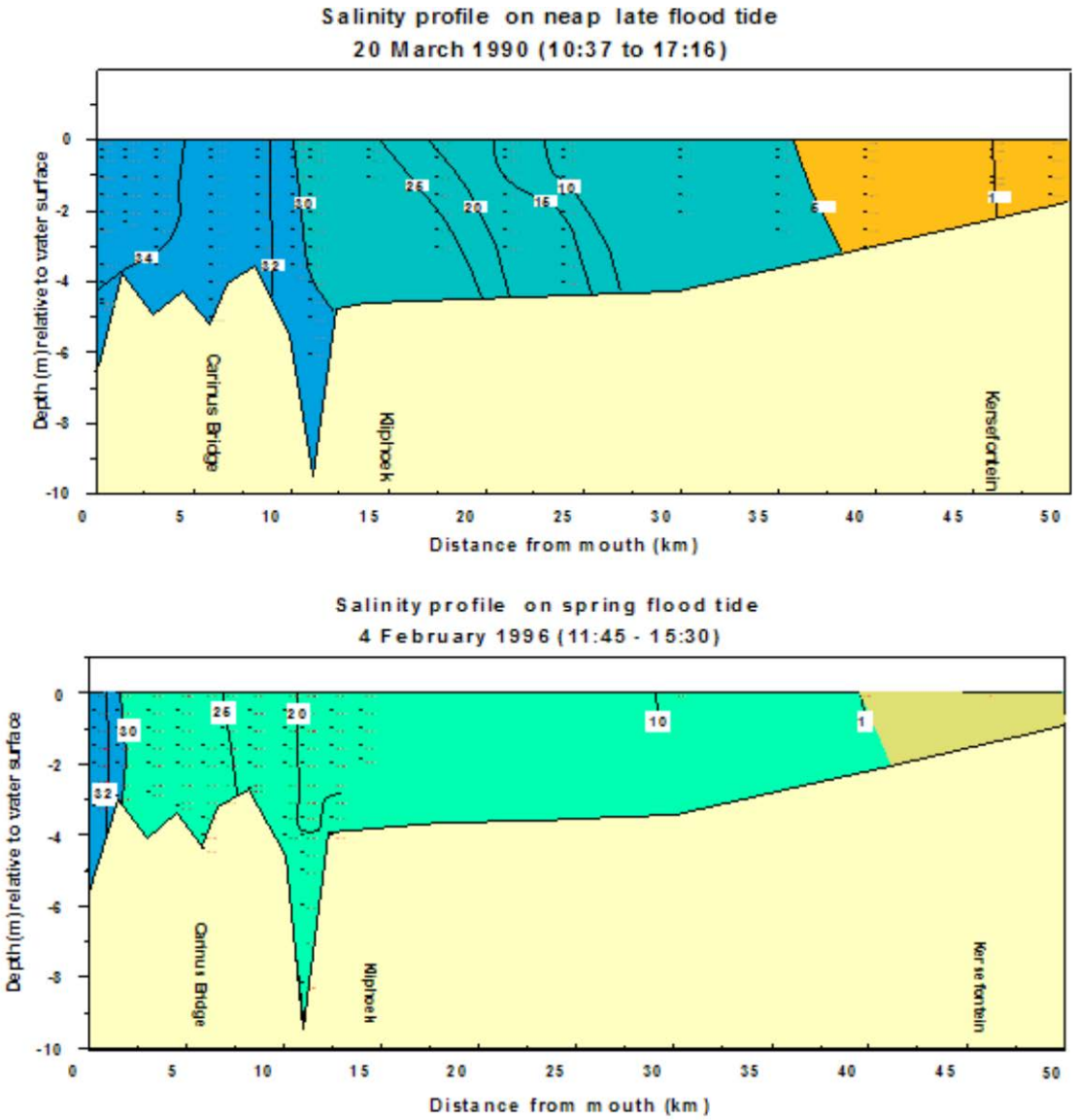

Figure A7b **Longitudinal salinity distribution in the Berg River estuary as measured in late summer *i.e.* after an extended period of summer low base flows (see annotations E and J in Figure A3).**

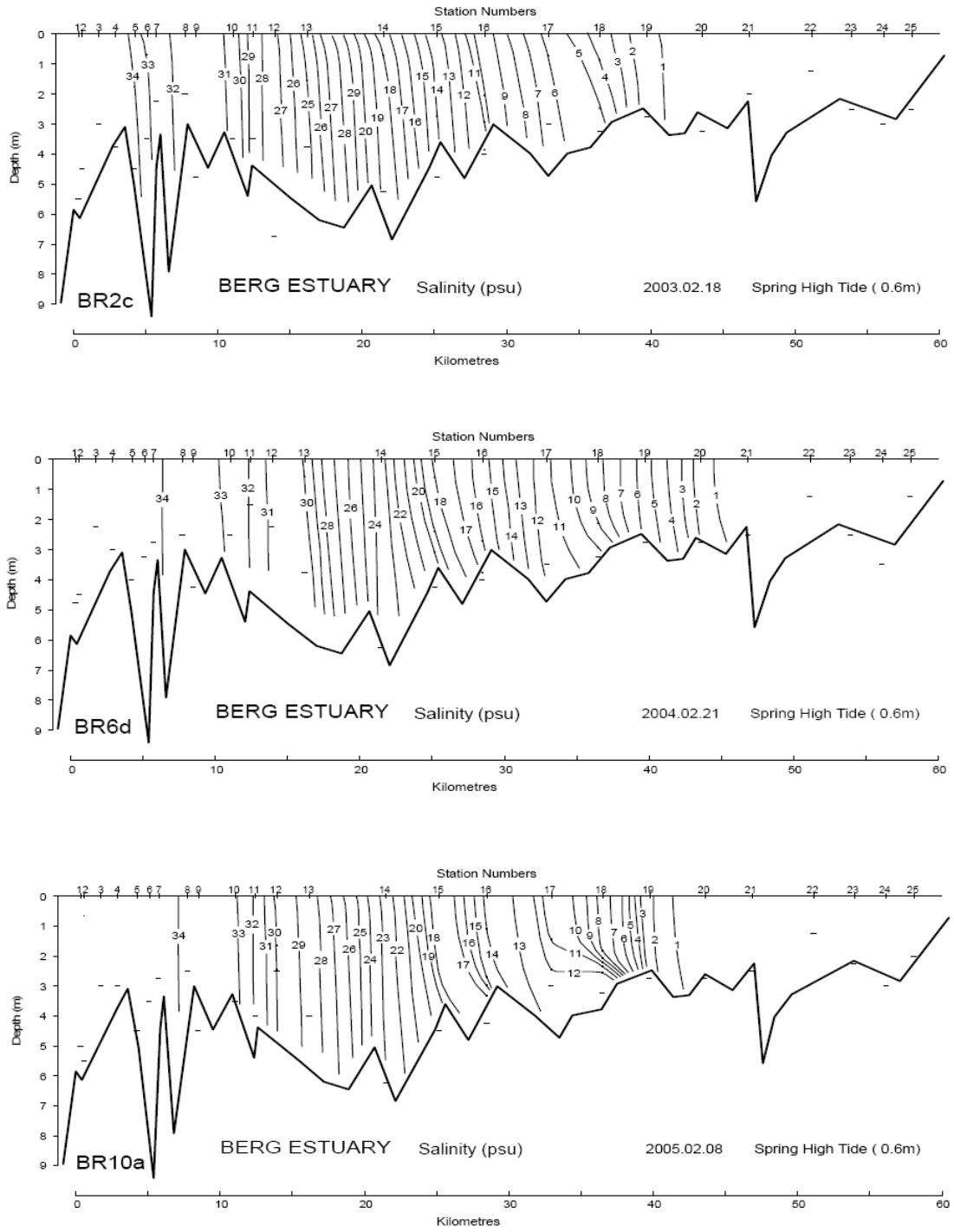

Figure A8a Longitudinal salinity distribution in the Berg River estuary as measured in the month of February, i.e. after an extended period of summer low base flows (after Schumann, 2007) - Spring high tide

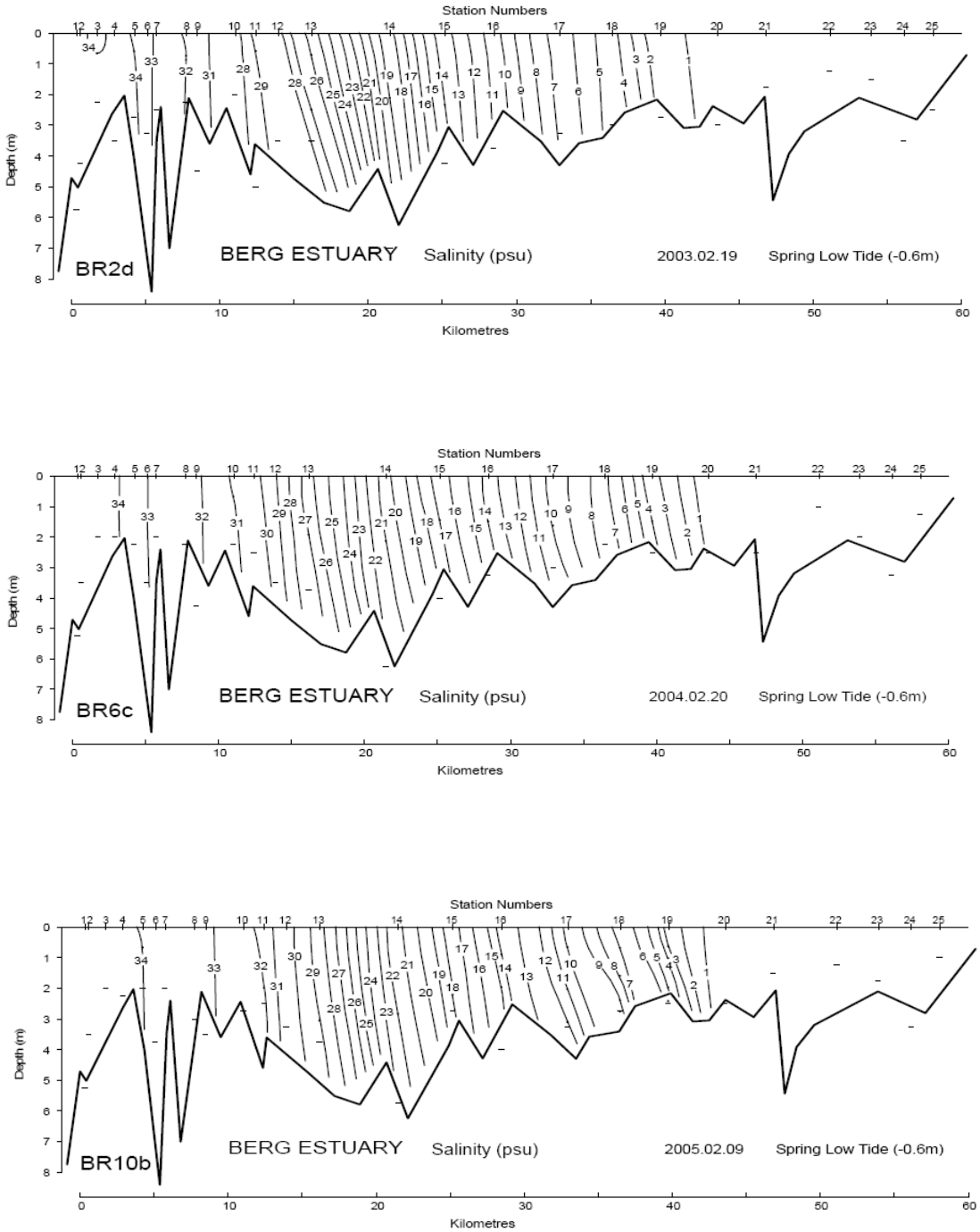

Figure A8b Longitudinal salinity distribution in the Berg River estuary as measured in the month of February, i.e. after an extended period of summer low base flows (after Schumann, 2007) - Spring low tide

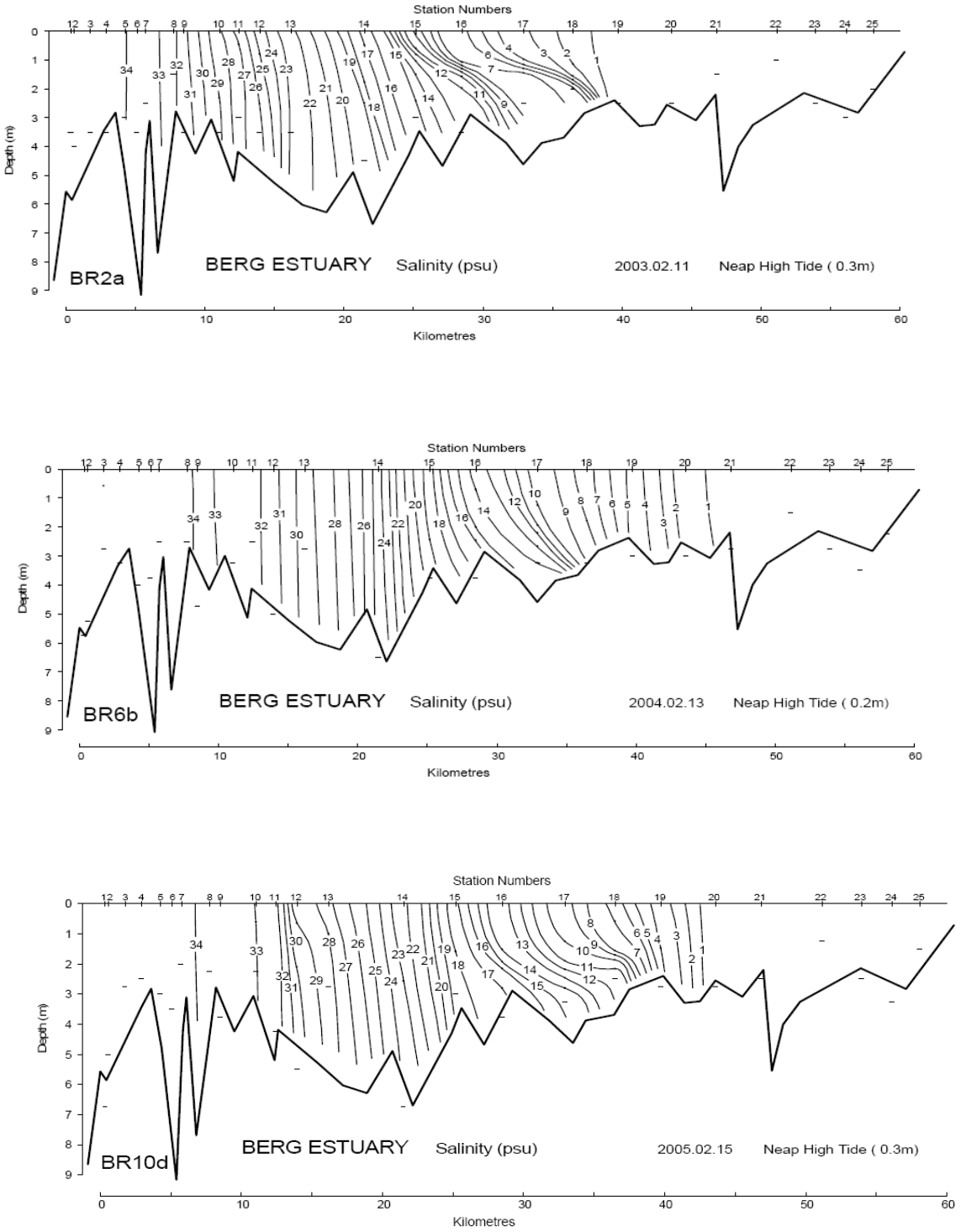

Figure A8c Longitudinal salinity distribution in the Berg River estuary as measured in the month of February, *i.e.* after an extended period of summer low base flows (after Schumann, 2007) - Neap high tide

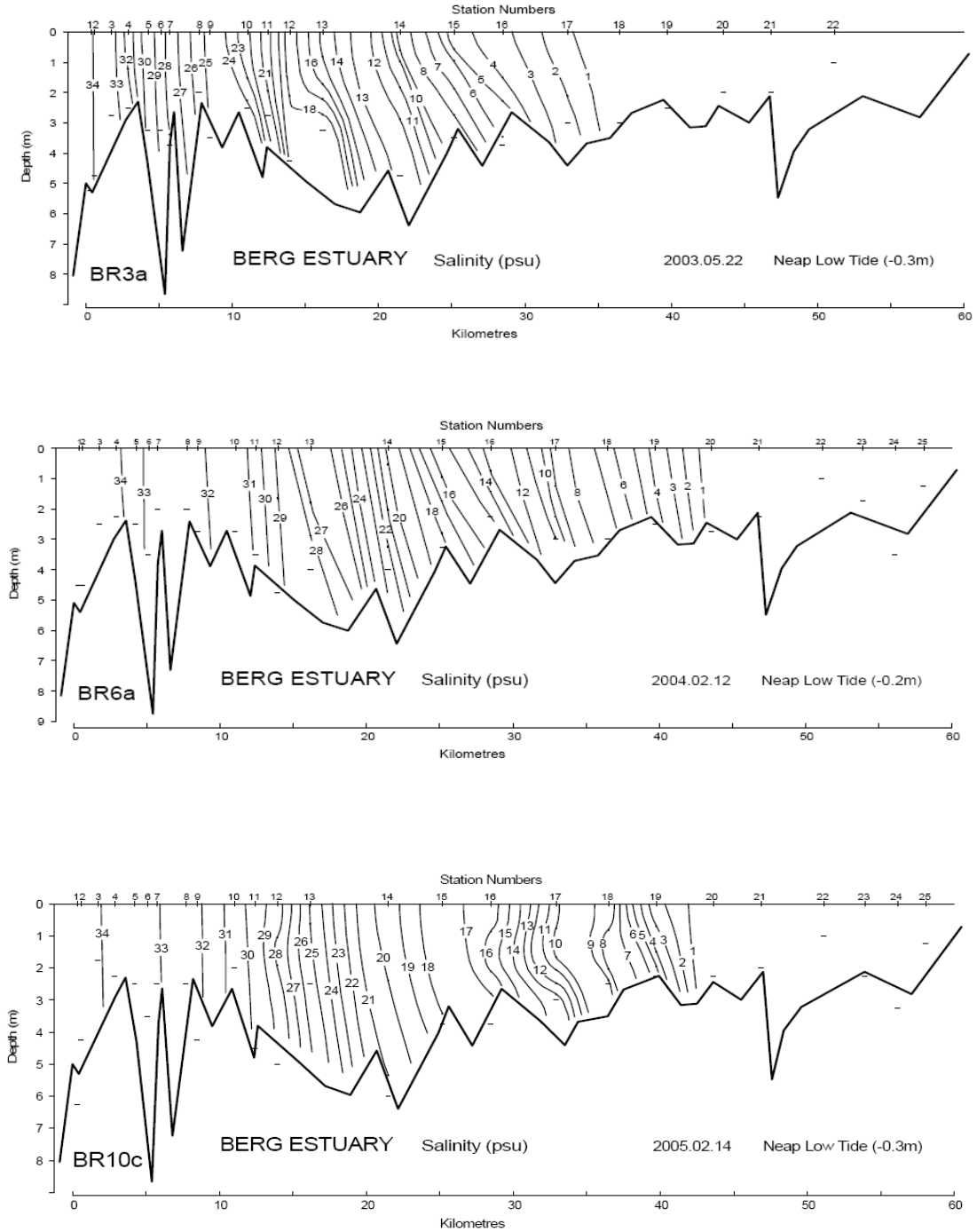

Figure A8d Longitudinal salinity distribution in the Berg River estuary as measured in the month of February, i.e. after an extended period of summer low base flows (after Schumann, 2007) - Neap low tide

ANNEX B: RESULTS OF THE WATER QUALITY MODELLING STUDY

This Annex contains plots of the simulated salinity distributions in the Berg River estuary under:

- Natural conditions (BergNat)
- PreBerg River dam (NoBRD)
- Present day conditions (PresentBRD)
- A representative worst case condition for the proposed future developments (MisvD)

These scenarios are summarized in the table below.

Scenario code	Summer base flow
Natural conditions (pre-development)	
BergNat	**(as estimated)**
No Berg River Dam (conditions prior to the construction of the Berg River Dam)	
NoBRD	**0.30 m3/s**
	0.90 m3/s
	0.15 m3/s
Present conditions (conditions after the construction of the Berg River Dam)	
PresentBRD	**0.30 m3/s**
	0.90 m3/s
	0.15 m3/s
Raised Misverstand, Imposed resdss ifrD. Ifr = 15% of natural flow	
MisvD	**0.30 m3/s**
	0.90 m3/s
	0.15 m3/s
	0.00 m3/s

All simulated salinities downstream of 25 km have been “greyed out”. There is a lack of confidence in these simulated salinities due to both deficiencies in the modeling of evaporation and the fact that groundwater effects were not included in the model.

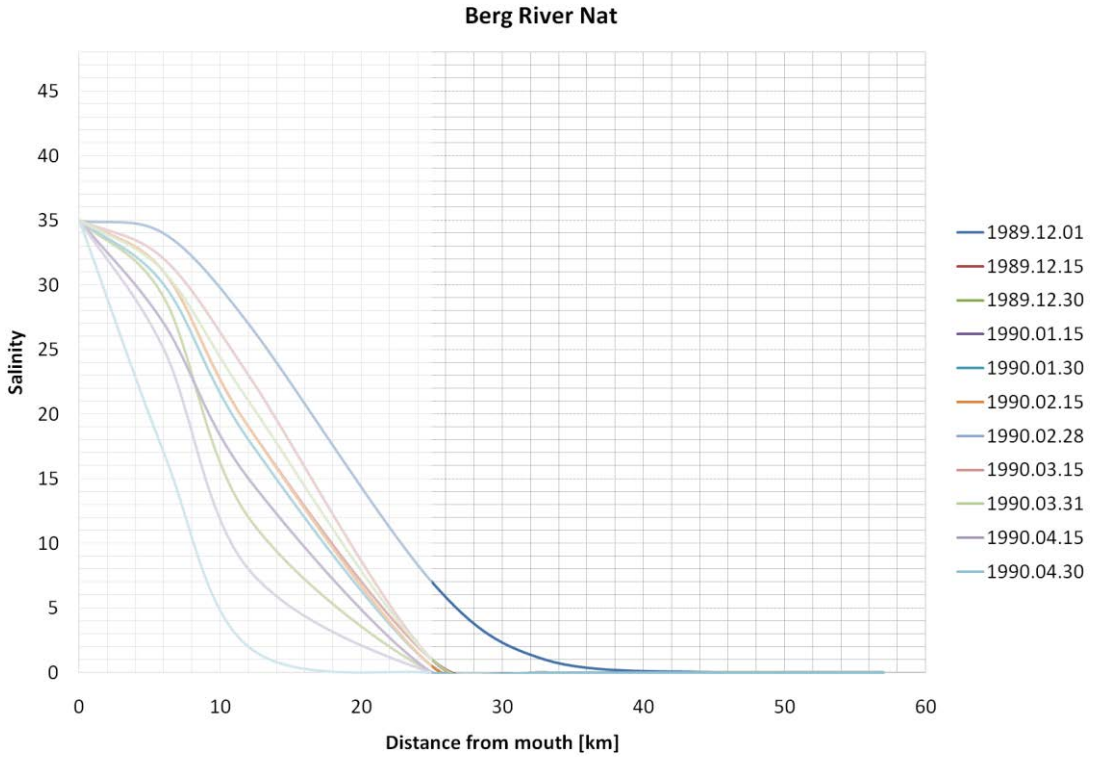

Figure B1 **Longitudinal salinity distribution in the Berg River estuary for the low flow period (December to April) under natural or reference conditions, plotted against distance upstream of the estuary mouth.**

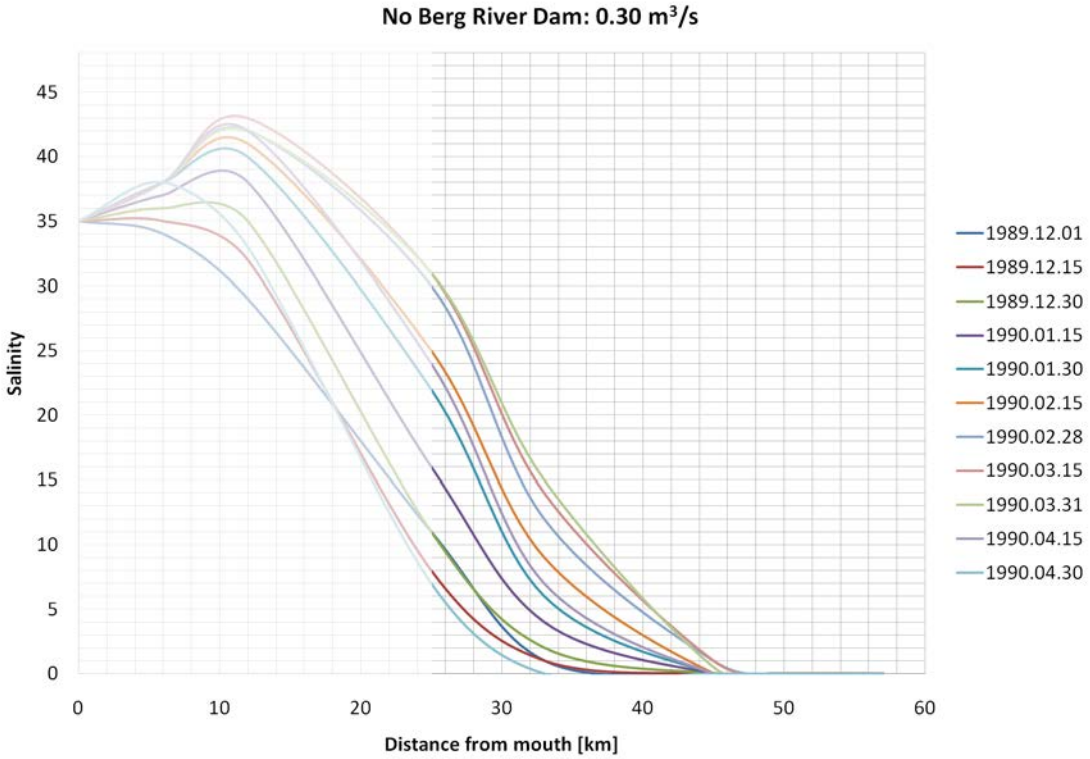

Figure B2 **Longitudinal salinity distribution in the Berg River estuary for the low flow period (December to April) under pre-Berg River dam conditions (at a best estimate summer base flow of 0.3 m^3/s), plotted against distance upstream of the estuary mouth.**

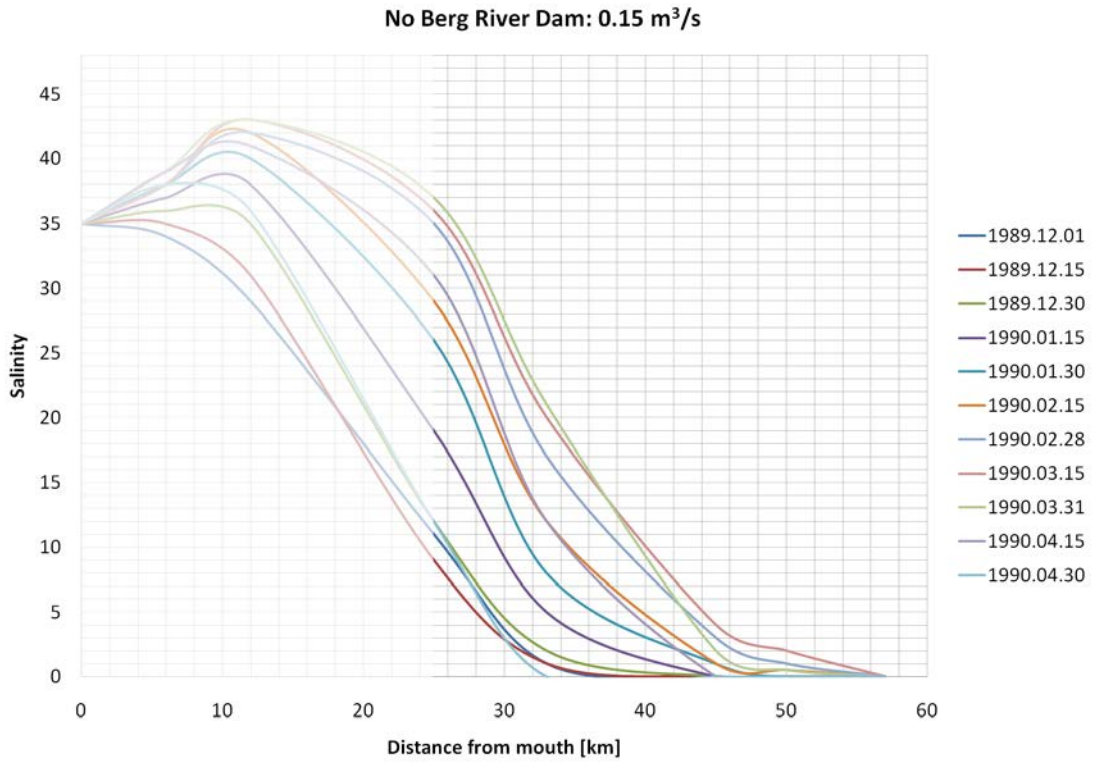

Figure B3 **Longitudinal salinity distribution in the Berg River estuary for the low flow period (December to April) under pre-Berg River dam conditions (at a lower estimated summer base flow = 0.15 m^3/s), plotted against distance upstream of the estuary mouth.**

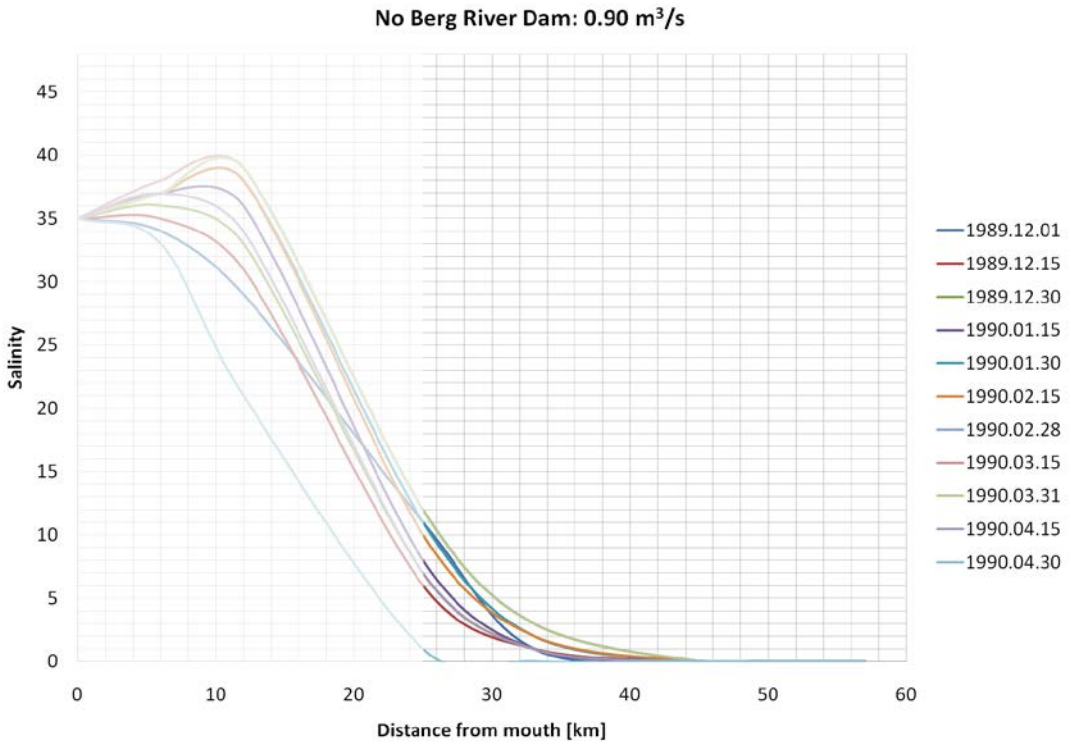

Figure B4 **Longitudinal salinity distribution in the Berg River estuary for the low flow period (December to April) under pre-Berg River dam conditions (at an upper estimated summer base flow = 0.90 m^3/s), plotted against distance upstream of the estuary mouth.**

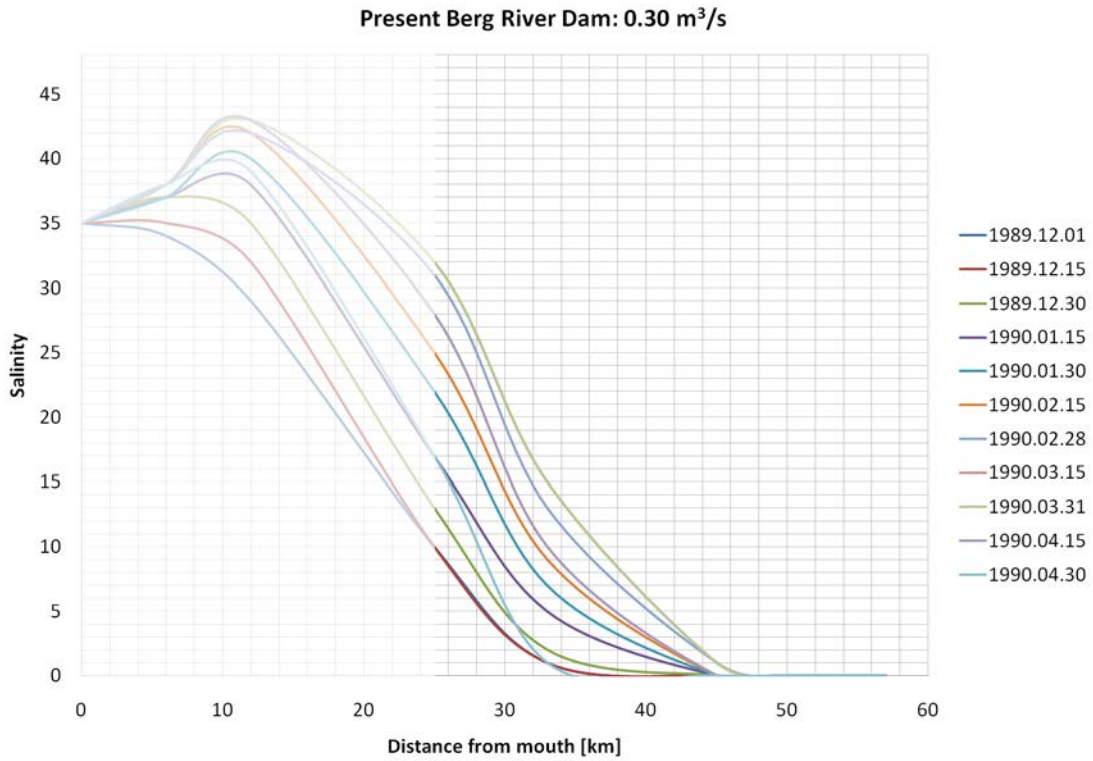

Figure B5 **Longitudinal salinity distribution in the Berg River estuary for the low flow period (December to April) under present day conditions (at a best estimate summer base flow of 0.3 m^3/s), plotted as a function of distance upstream of the estuary mouth.**

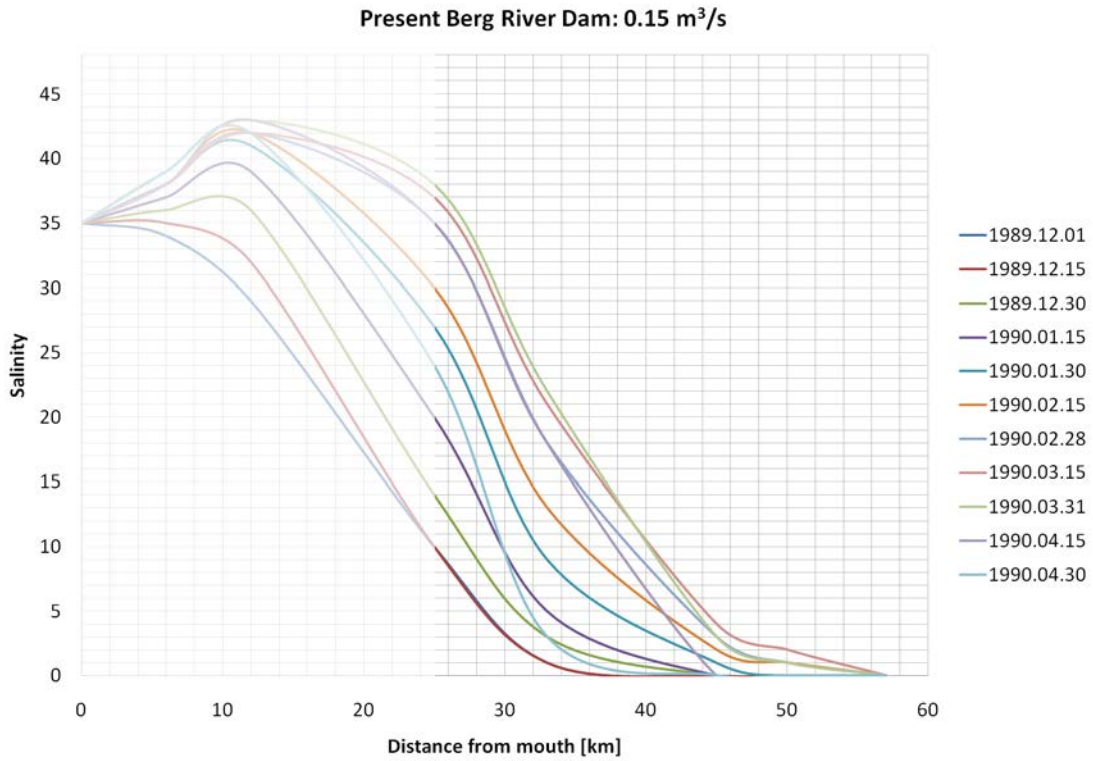

Figure B6 **Longitudinal salinity distribution in the Berg River estuary for the low flow period (December to April) under present day conditions (at a lower estimated summer base flow = 0.15 m^3/s), plotted against distance upstream of the estuary mouth.**

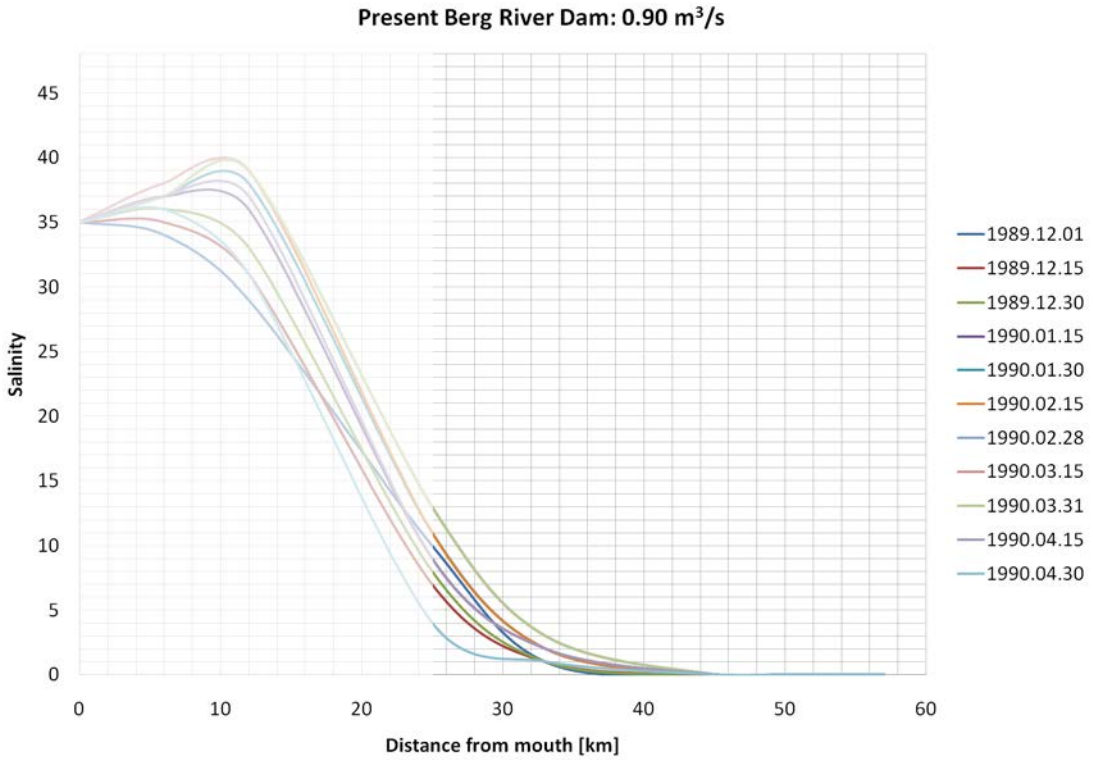

Figure B7 **Longitudinal salinity distribution in the Berg River estuary for the low flow period (December to April) under present day conditions (at an upper estimated summer base flow = 0.9 m^3/s), plotted against distance upstream of the estuary mouth.**

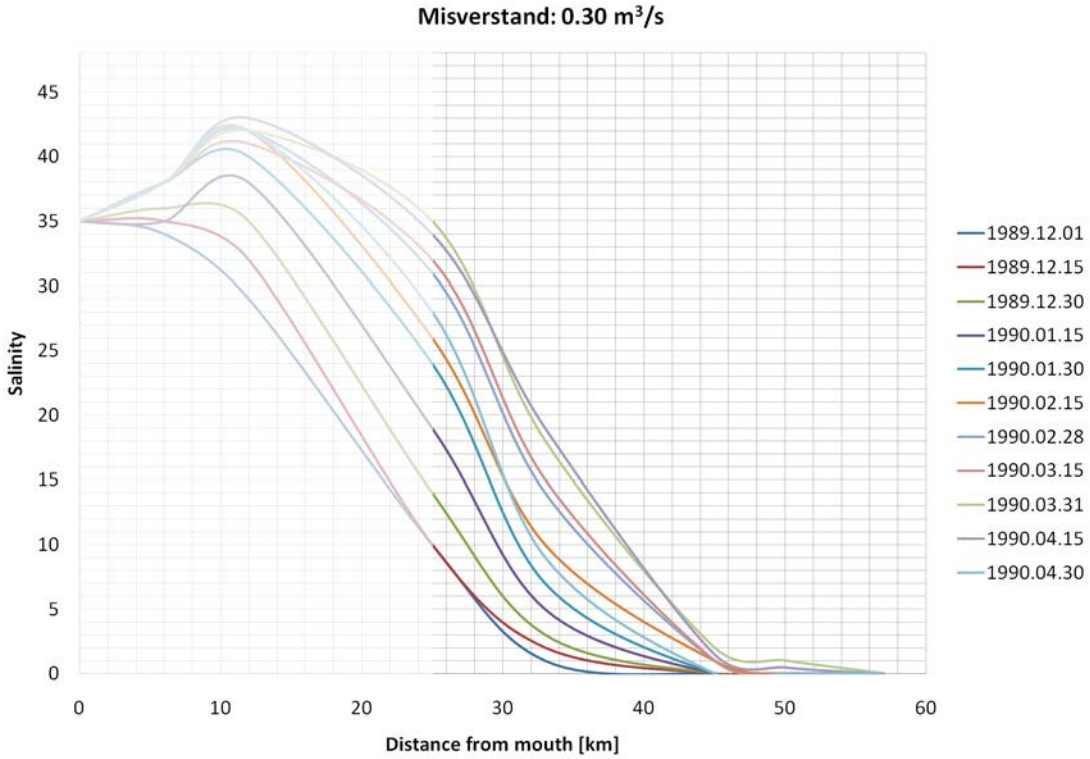

Figure B8 **Longitudinal salinity distribution in the Berg River estuary for the low flow period (December to April) under worst case future development conditions (at a best estimate summer base flow of 0.3 m^3/s), plotted as a function of distance upstream of the estuary mouth.**

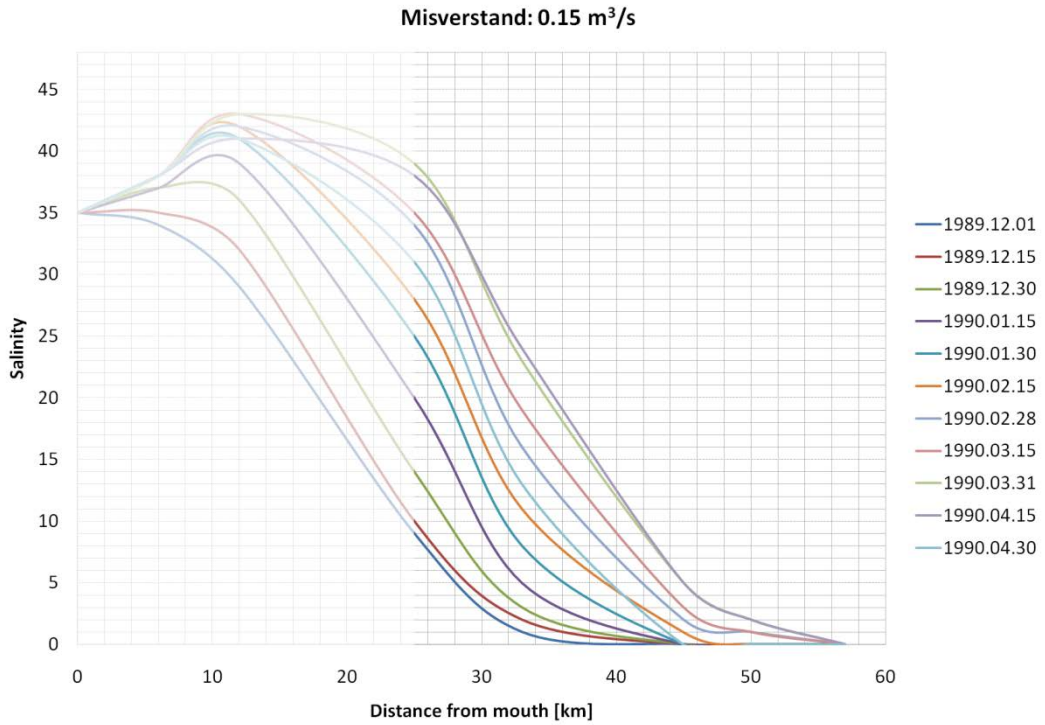

Figure B9 **Longitudinal salinity distribution in the Berg River estuary for the low flow period (December to April) under worst case future development conditions (at a lower estimated summer base flow = 0.15 m³/s), plotted against distance upstream of the estuary mouth.**

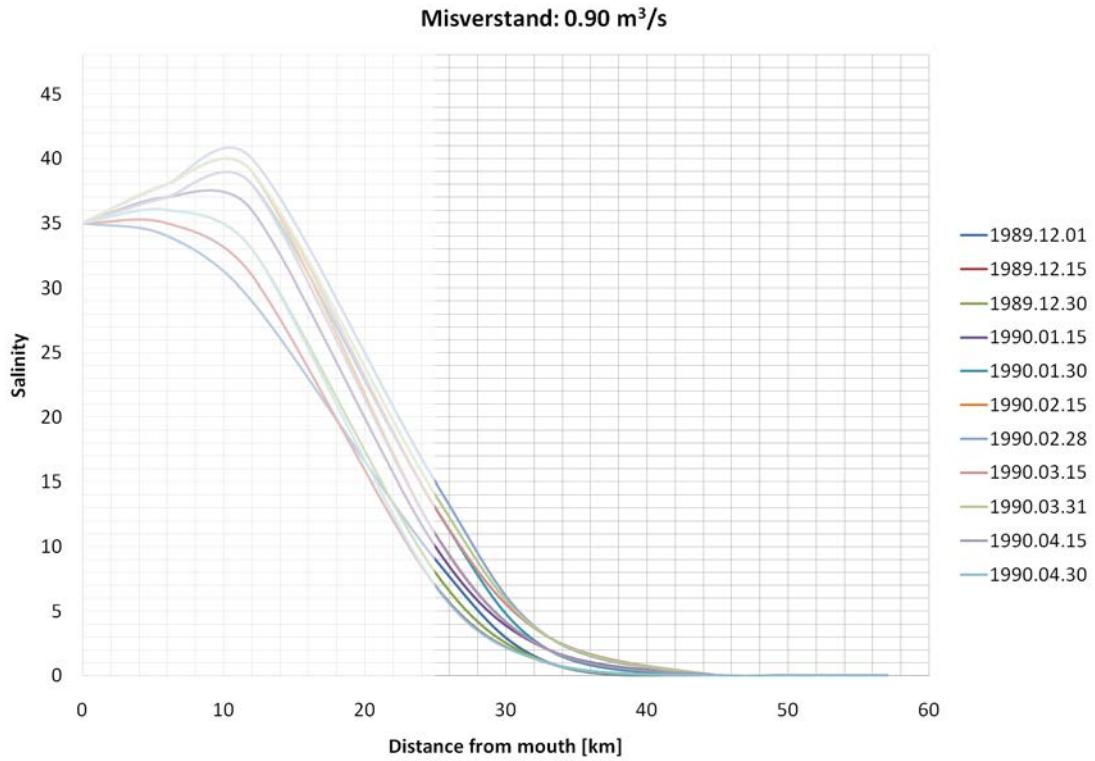

Figure B10 **Longitudinal salinity distribution in the Berg River estuary for the low flow period (December to April) under worst case future development conditions (at a lower estimated summer base flow = 0.15 m³/s), plotted against distance upstream of the estuary mouth.**

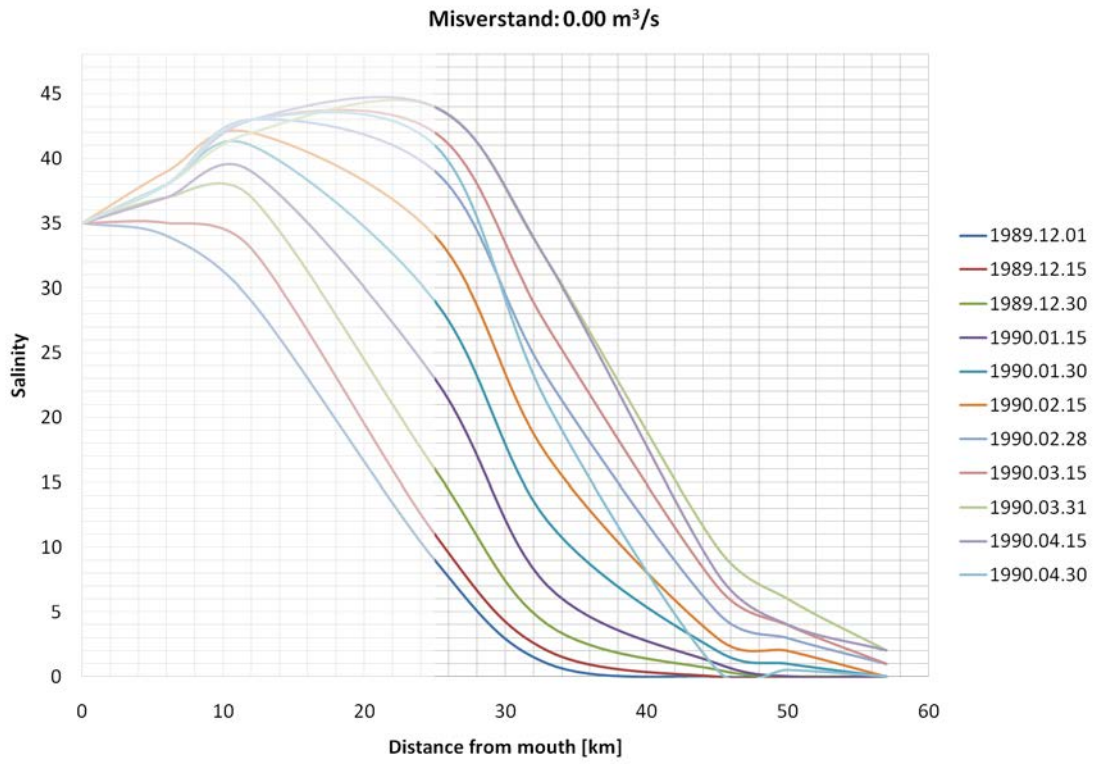

Figure B11 Longitudinal salinity distribution in the Berg River estuary for the low flow period (December to April) under worst case future development conditions (at a worst case summer base flow = 0.0 m^3/s), plotted against distance upstream of the estuary mouth.

ANNEX C: RESULTS OF THE FLOOD MODELLING STUDY

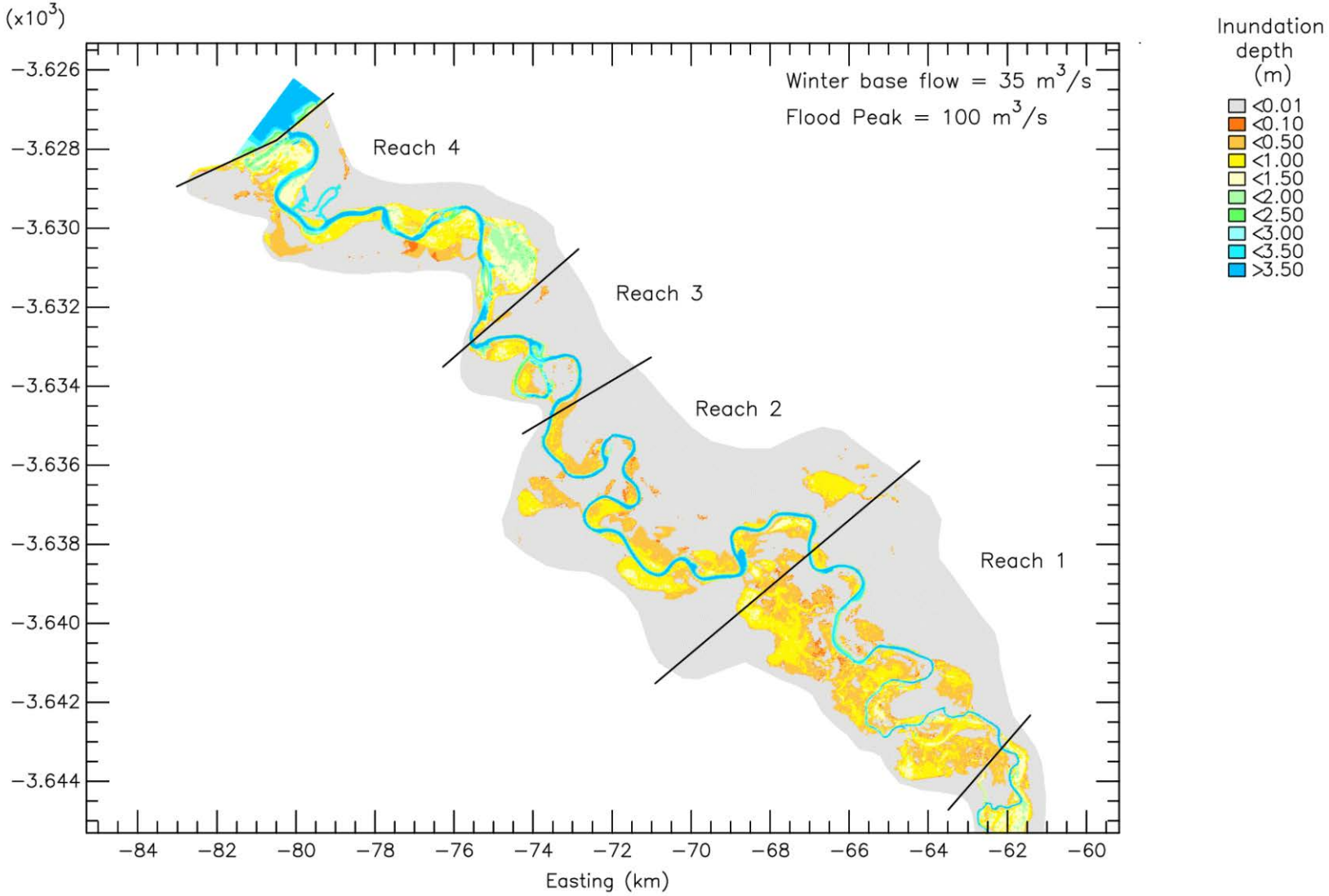

Figure C1a Depth of inundation of the Berg River floodplain for a 100 m^3/s flood under winter base flow conditions of 35 m^3/s

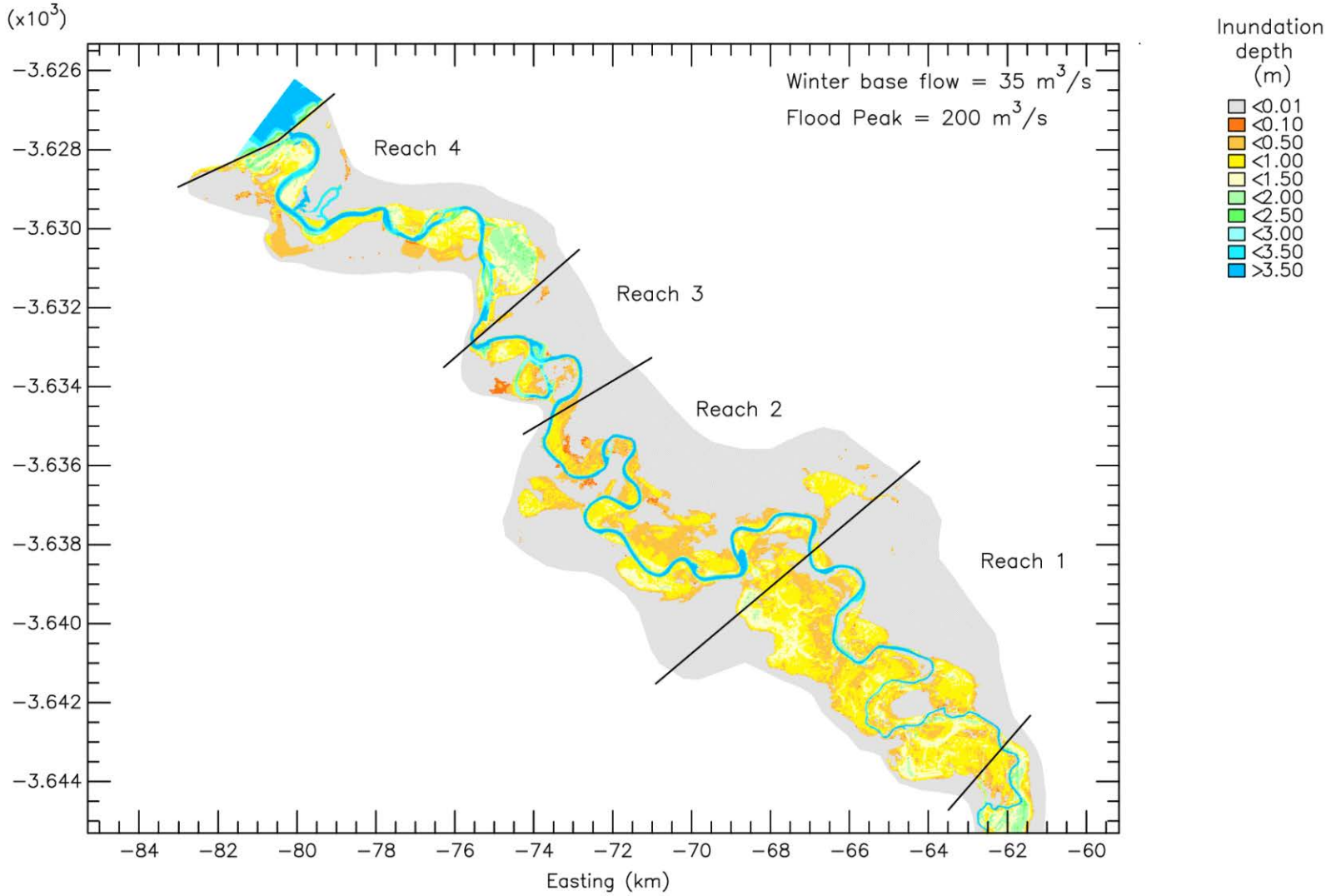

Figure C1b Depth of inundation of the Berg River floodplain for a 200 m^3/s flood under winter base flow conditions of 35 m^3/s

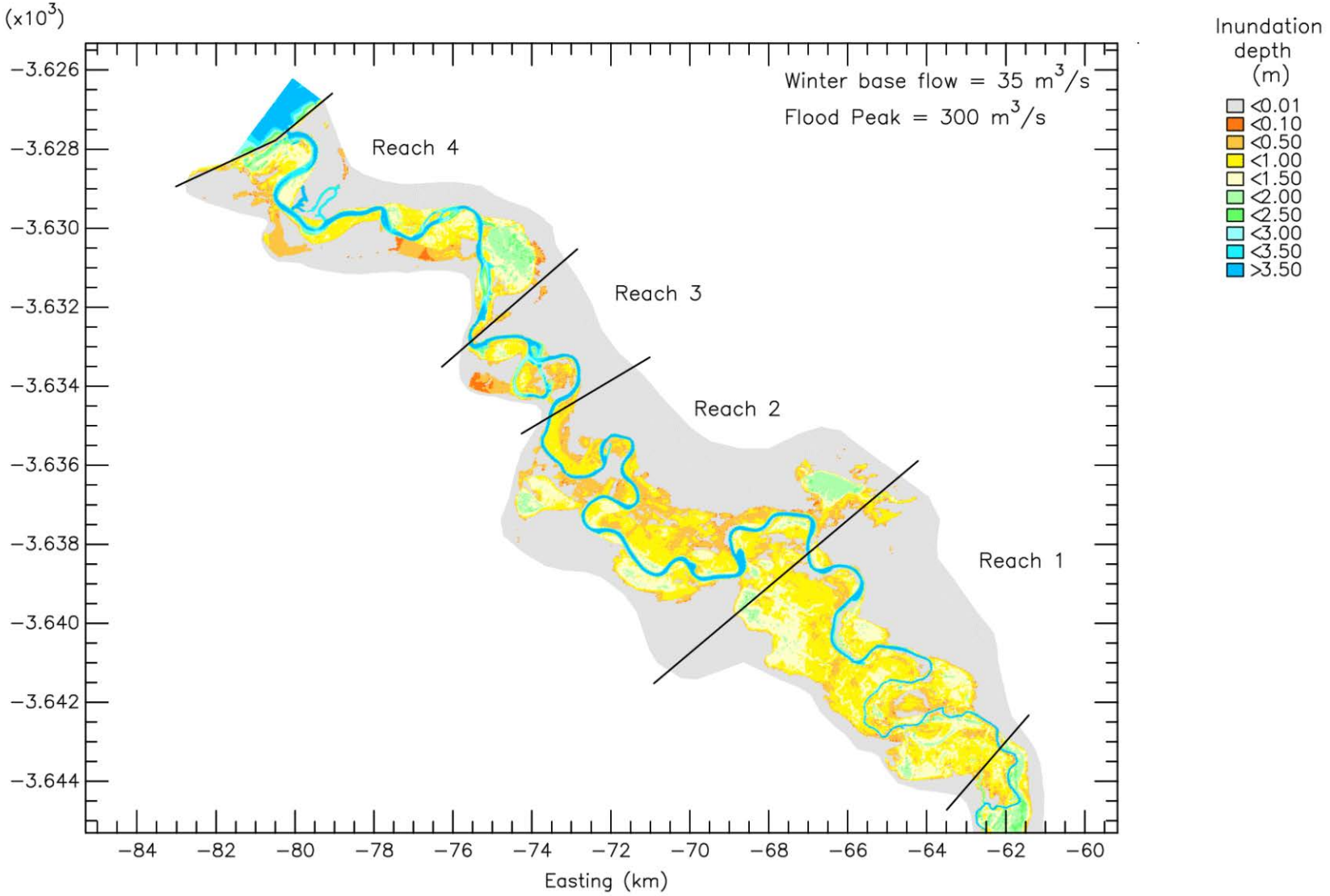

Figure C1c Depth of inundation of the Berg River floodplain for a 300 m^3/s flood under winter base flow conditions of 35 m^3/s

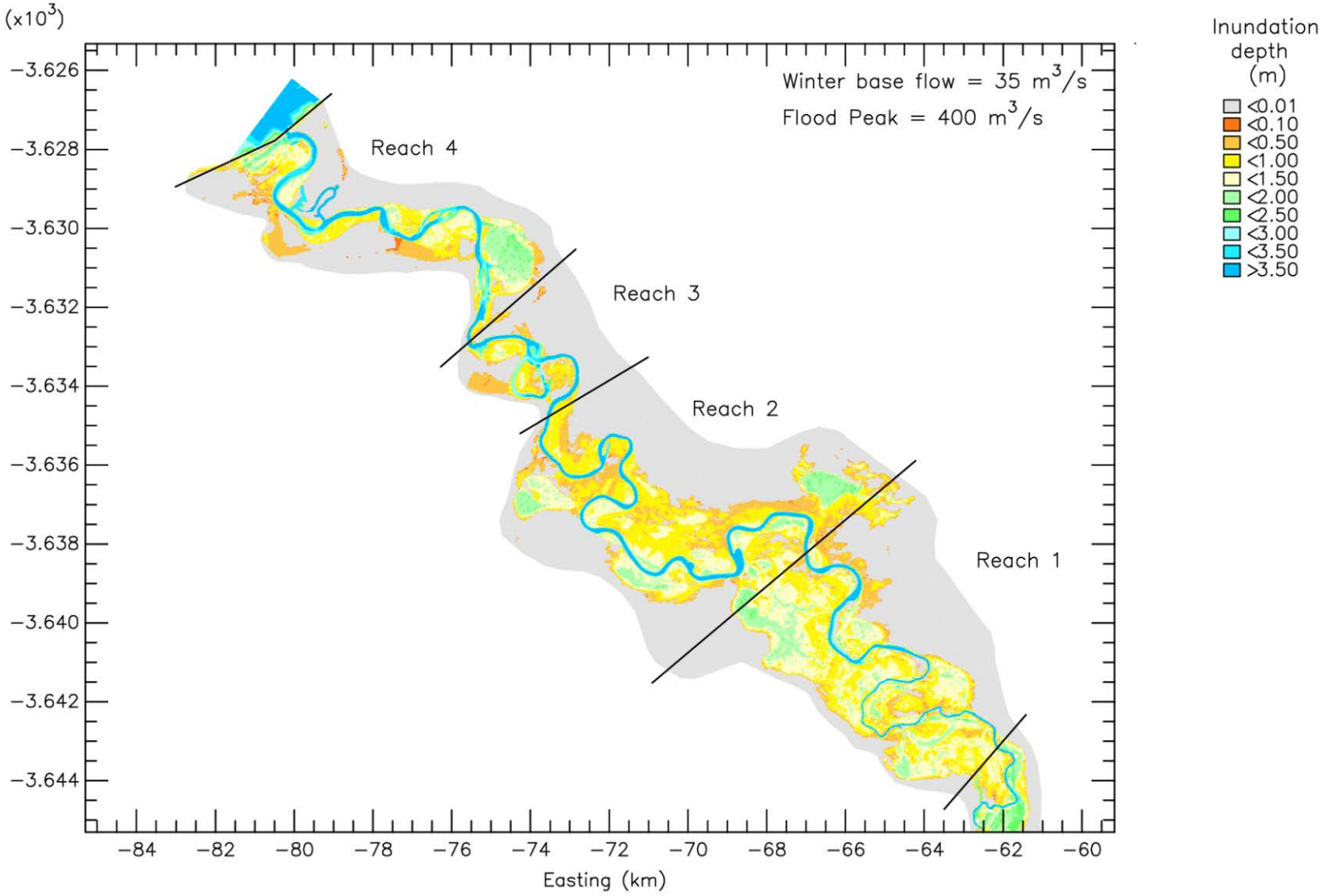

Figure C1d Depth of inundation of the Berg River floodplain for a 400 m^3/s flood under winter base flow conditions of 35 m^3/s

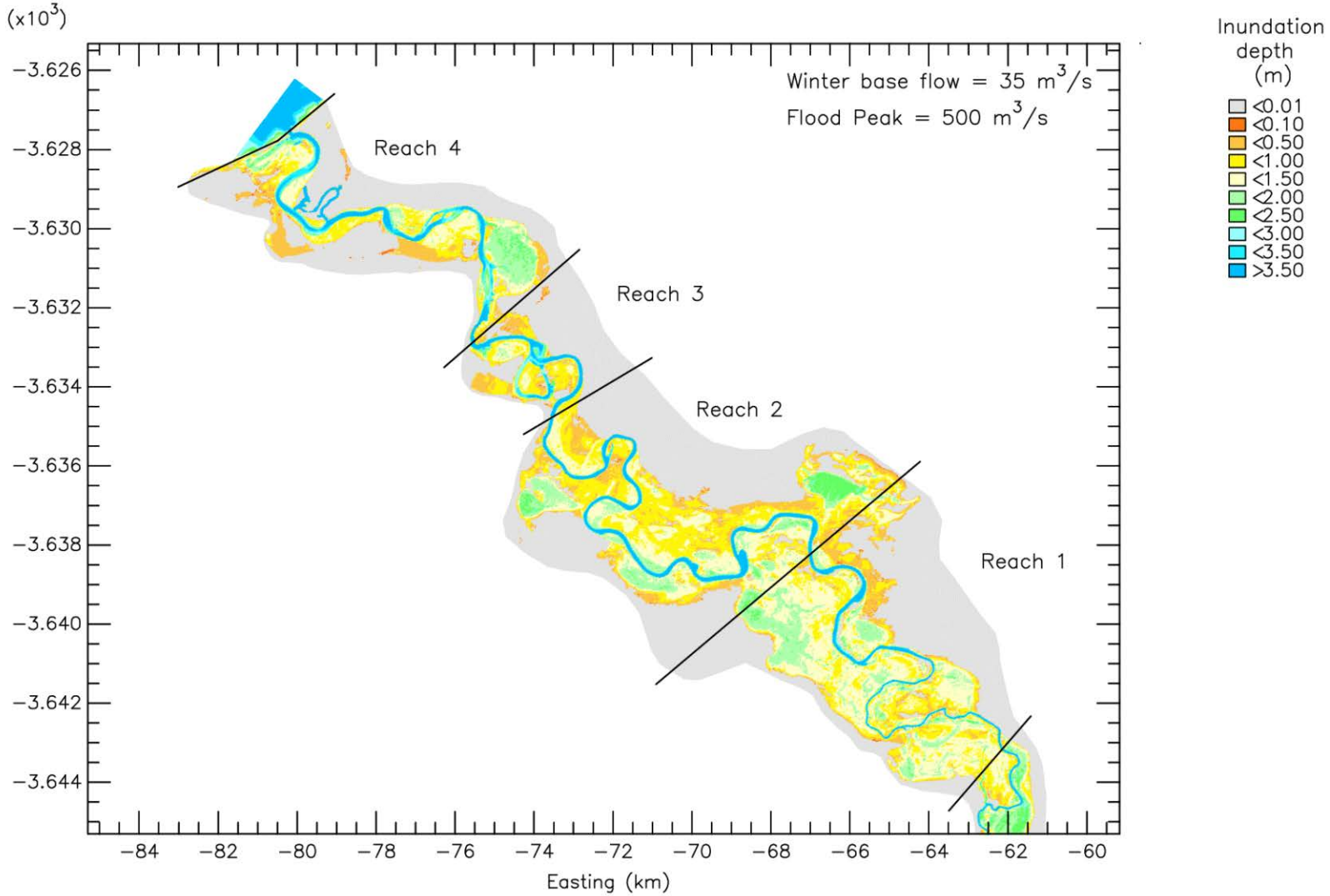

Figure C1e Depth of inundation of the Berg River floodplain for a 500 m^3/s flood under winter base flow conditions of 35 m^3/s

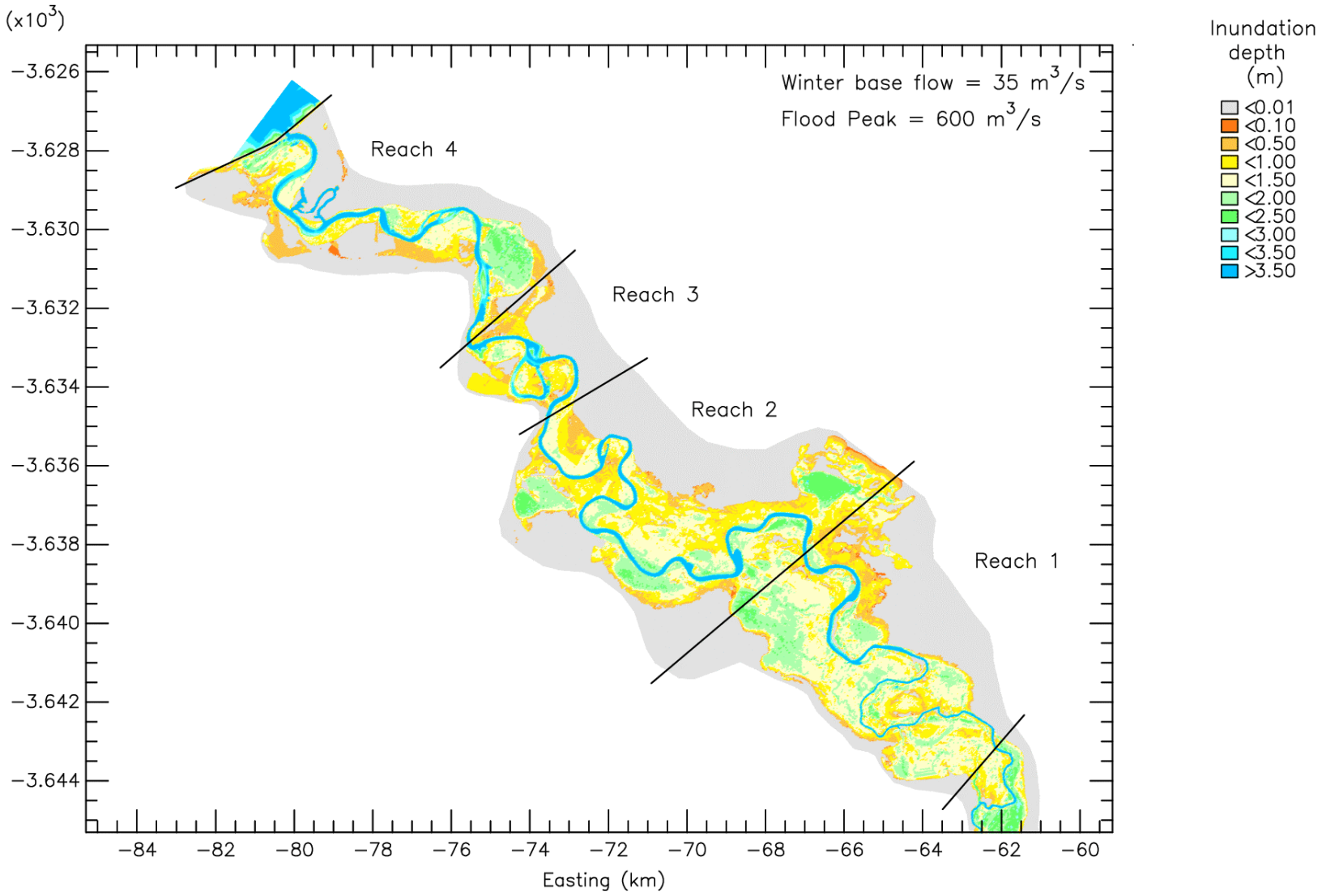

Figure C1f Depth of inundation of the Berg River floodplain for a 600 m^3/s flood under winter base flow conditions of 35 m^3/s

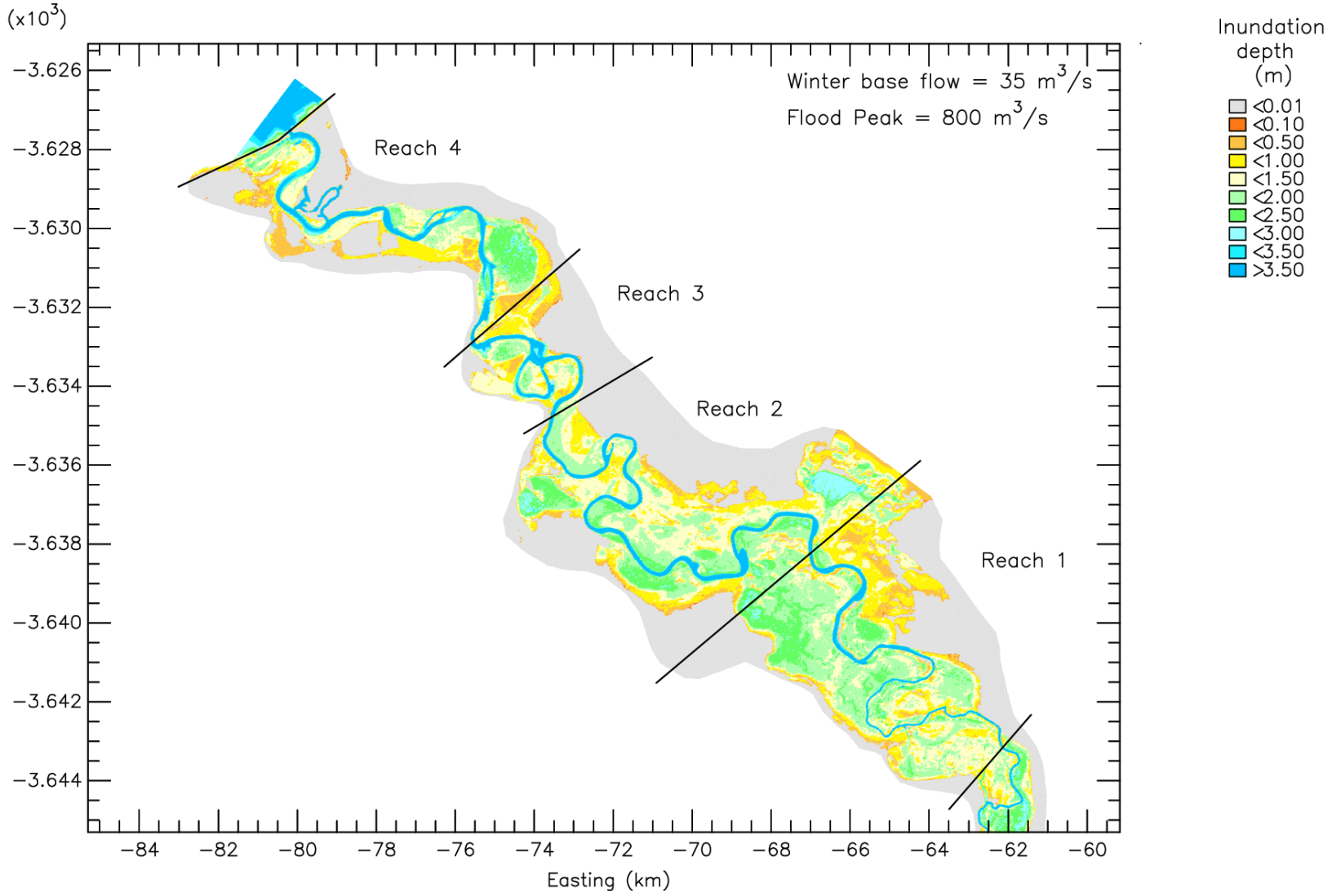

Figure C1g Depth of inundation of the Berg River floodplain for a 800 m^3/s flood under winter base flow conditions of 35 m^3/s

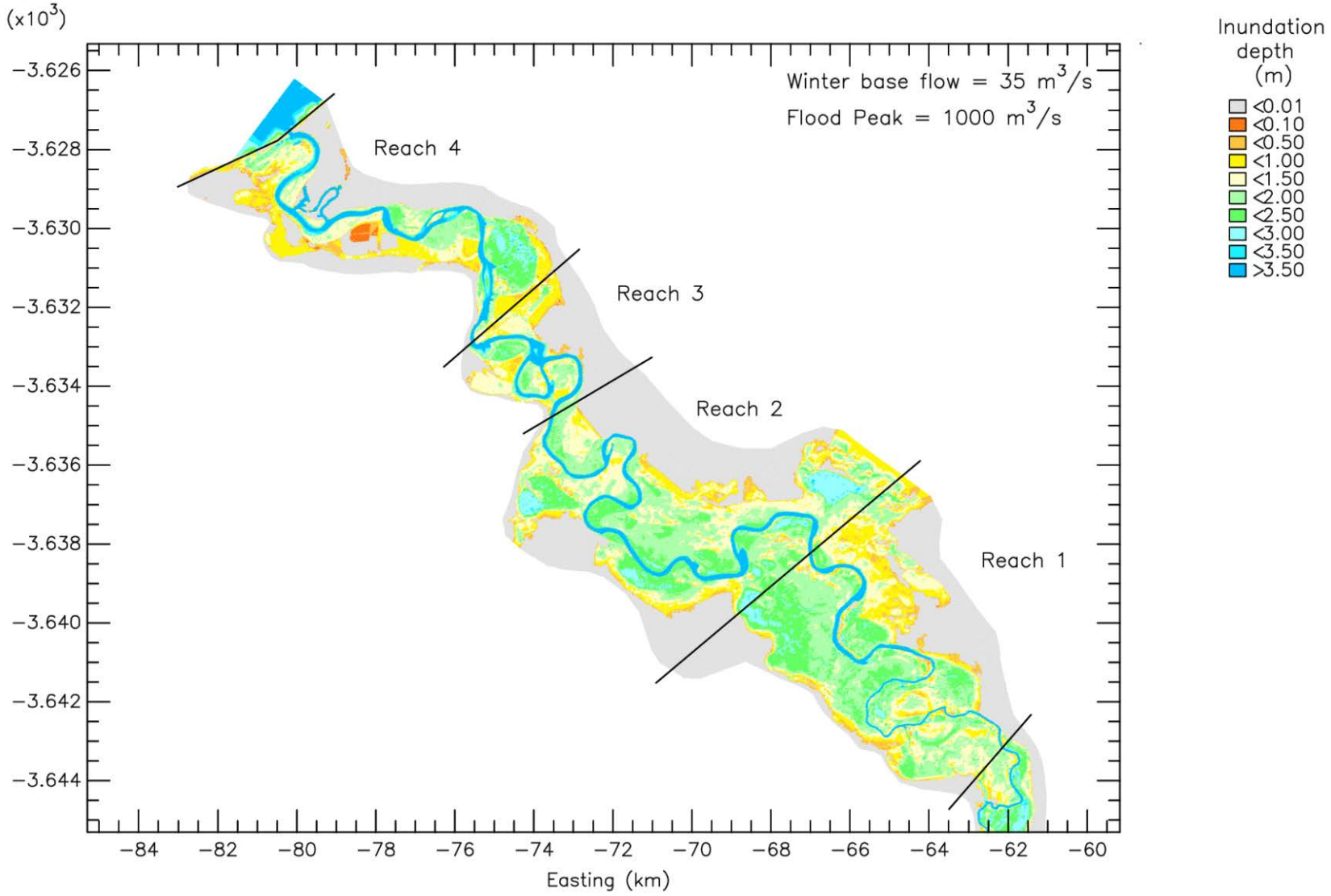

Figure C1h Depth of inundation of the Berg River floodplain for a 1000 m^3/s flood under winter base flow conditions of 35 m^3/s

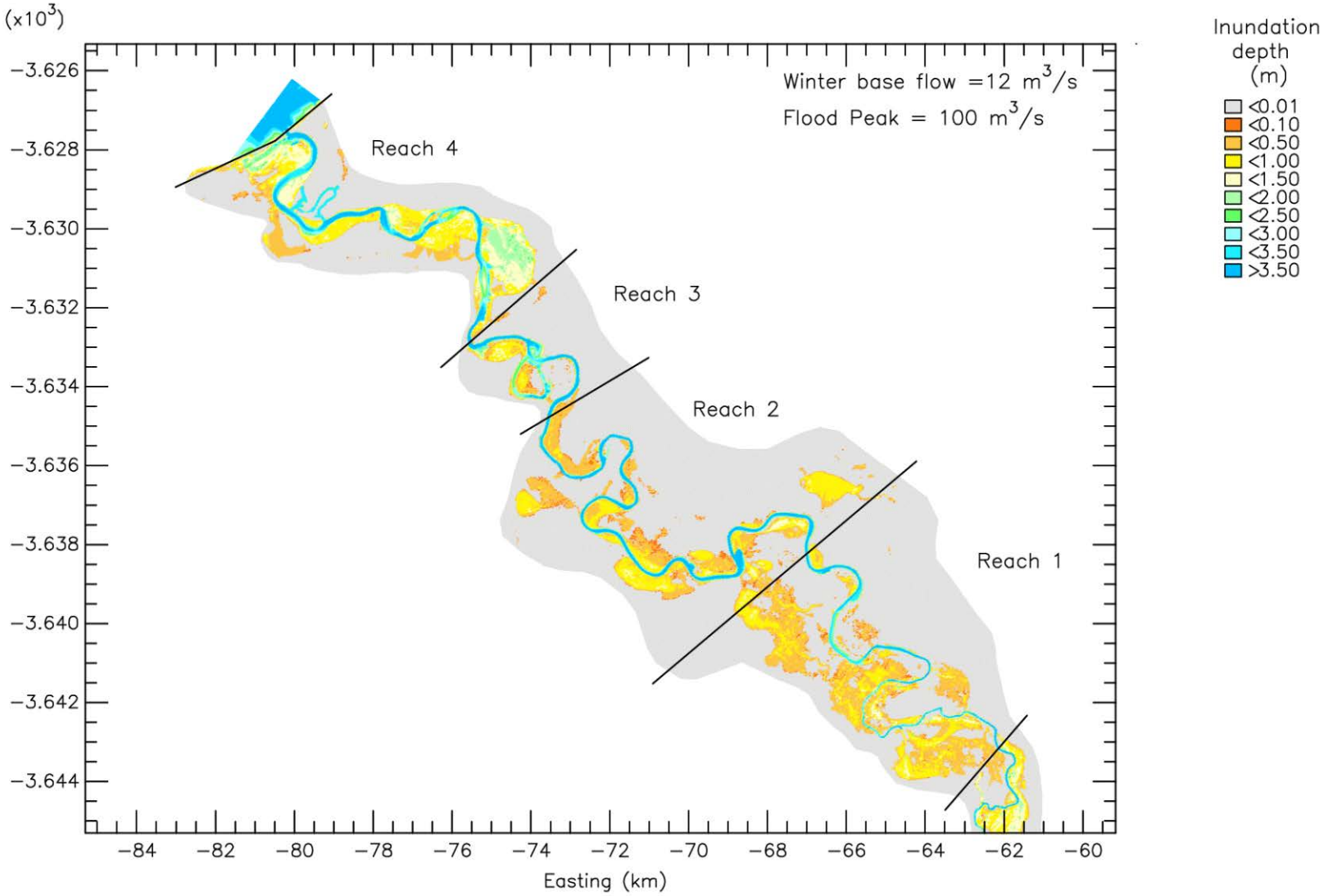

Figure C2a Depth of inundation of the Berg River floodplain for a 100 m^3/s flood under winter base flow conditions of 12 m^3/s

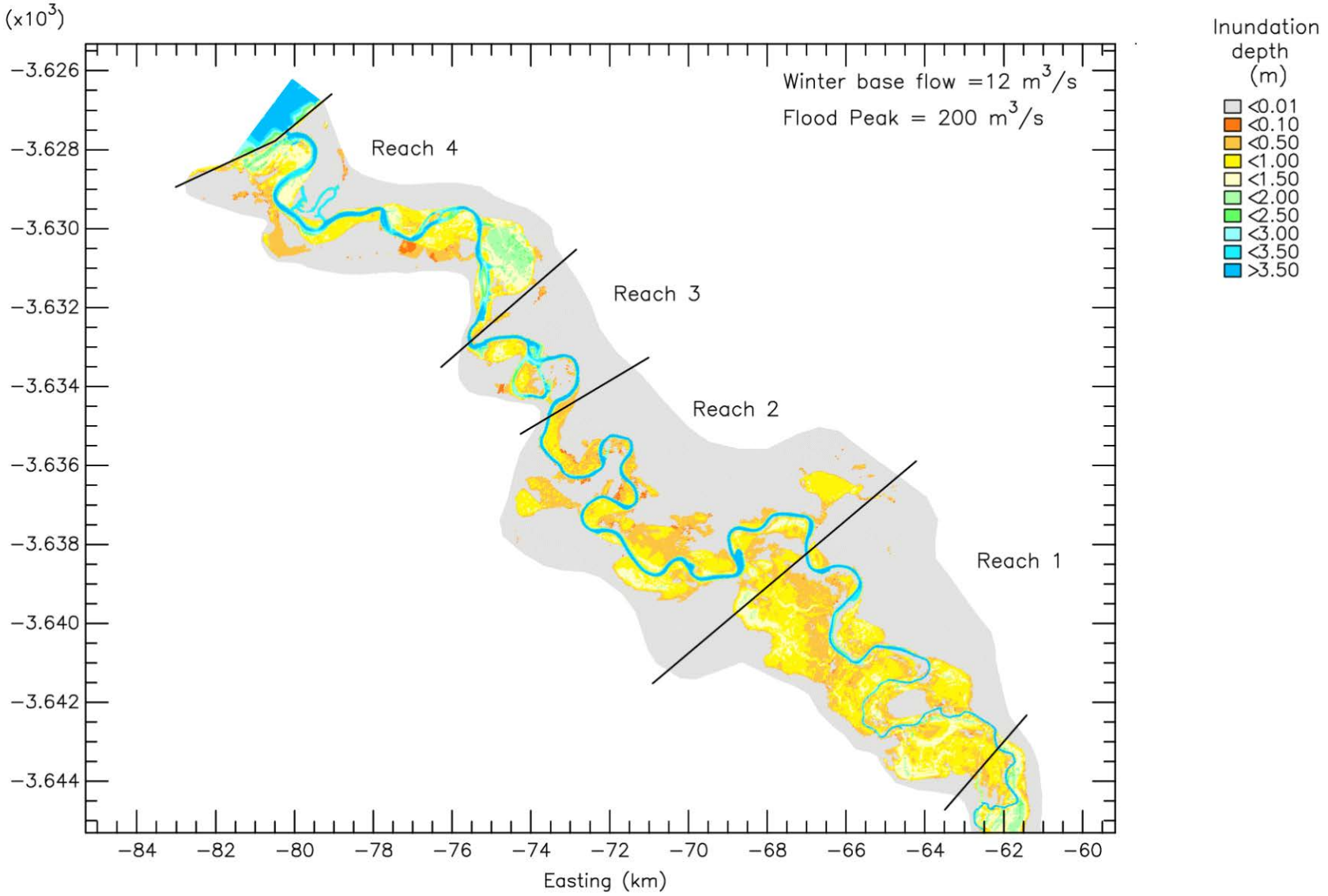

Figure C2b Depth of inundation of the Berg River floodplain for a 200 m^3/s flood under winter base flow conditions of 12 m^3/s

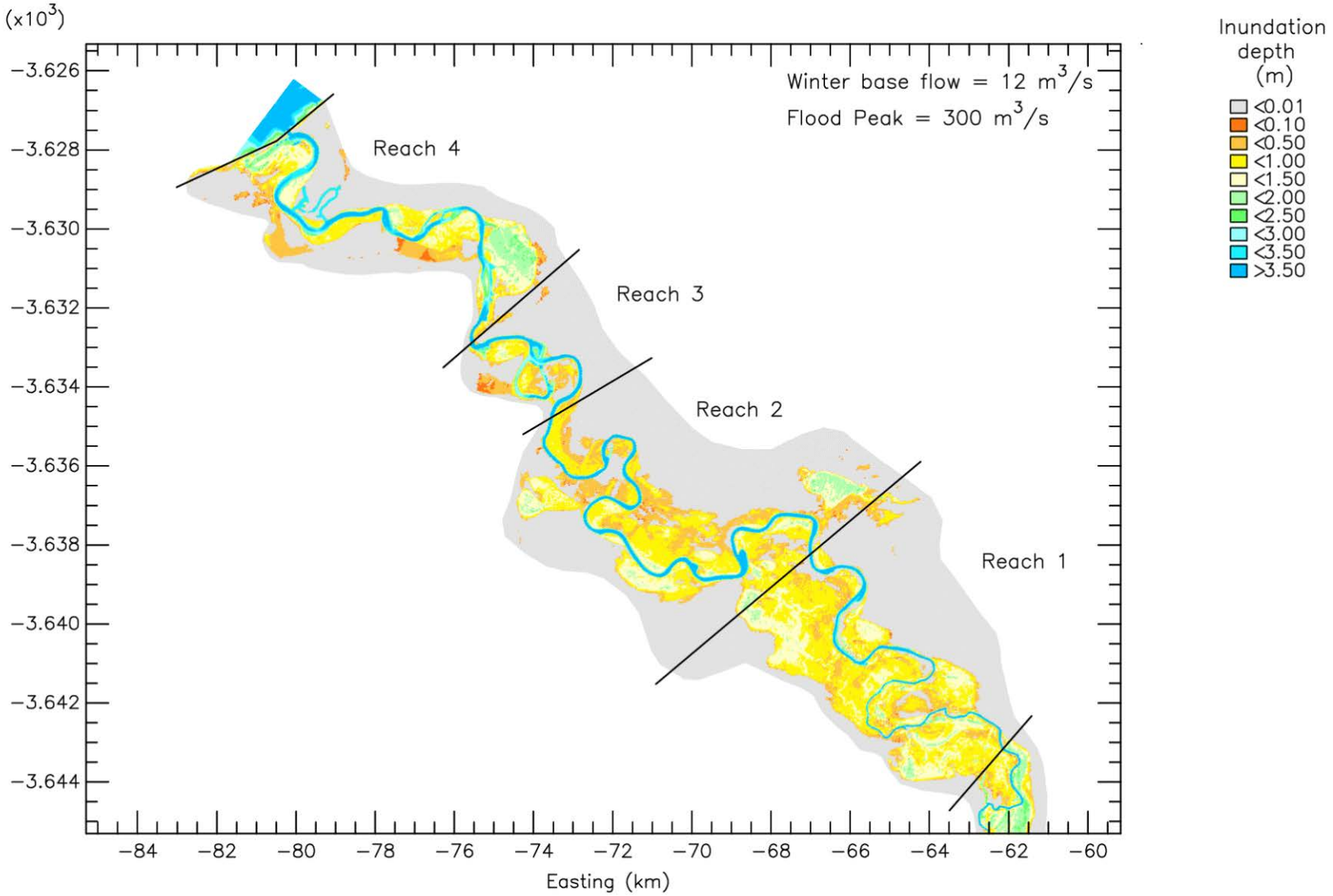

Figure C2c Depth of inundation of the Berg River floodplain for a 300 m^3/s flood under winter base flow conditions of 12 m^3/s

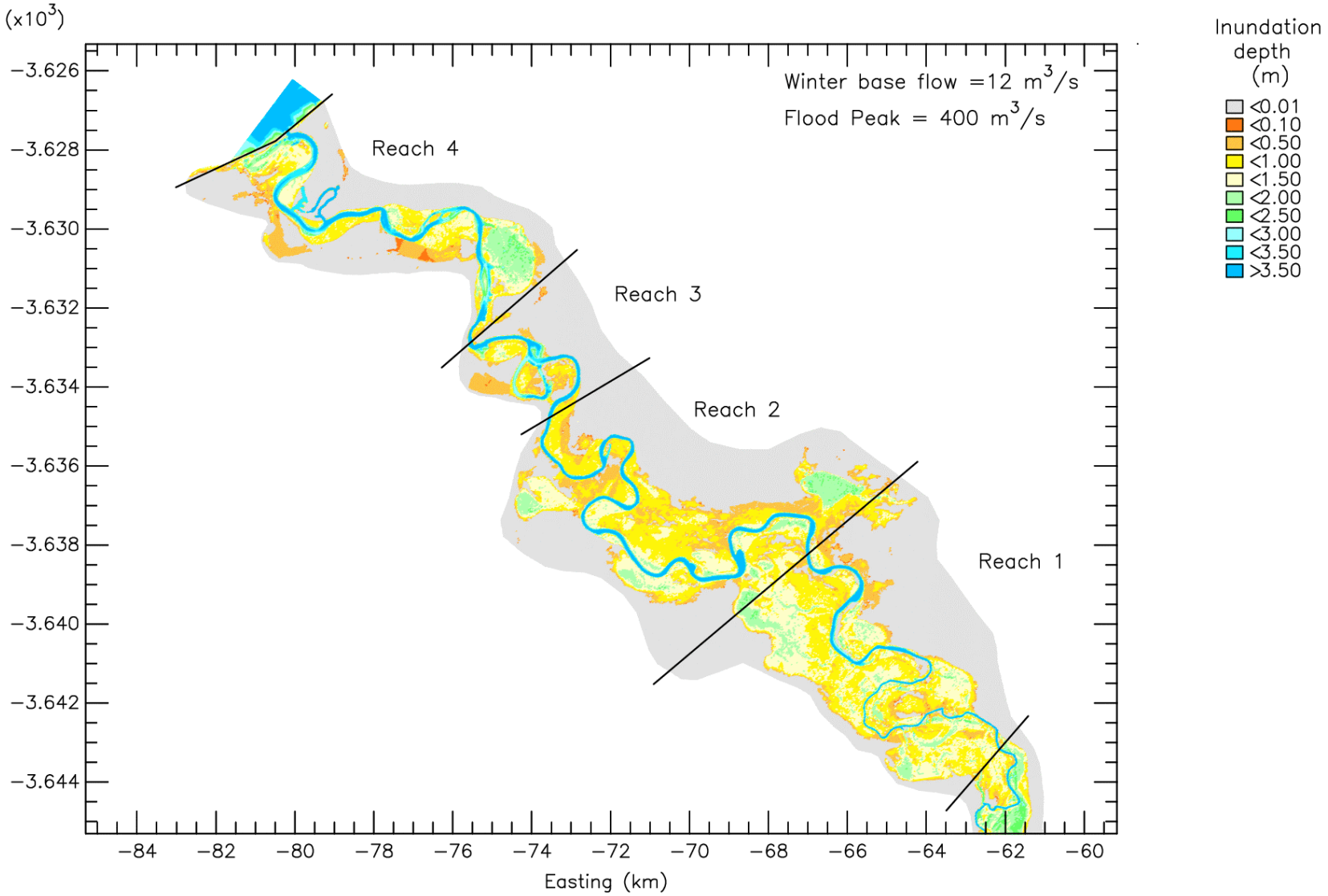

Figure C2d Depth of inundation of the Berg River floodplain for a 400 m^3/s flood under winter base flow conditions of 12 m^3/s

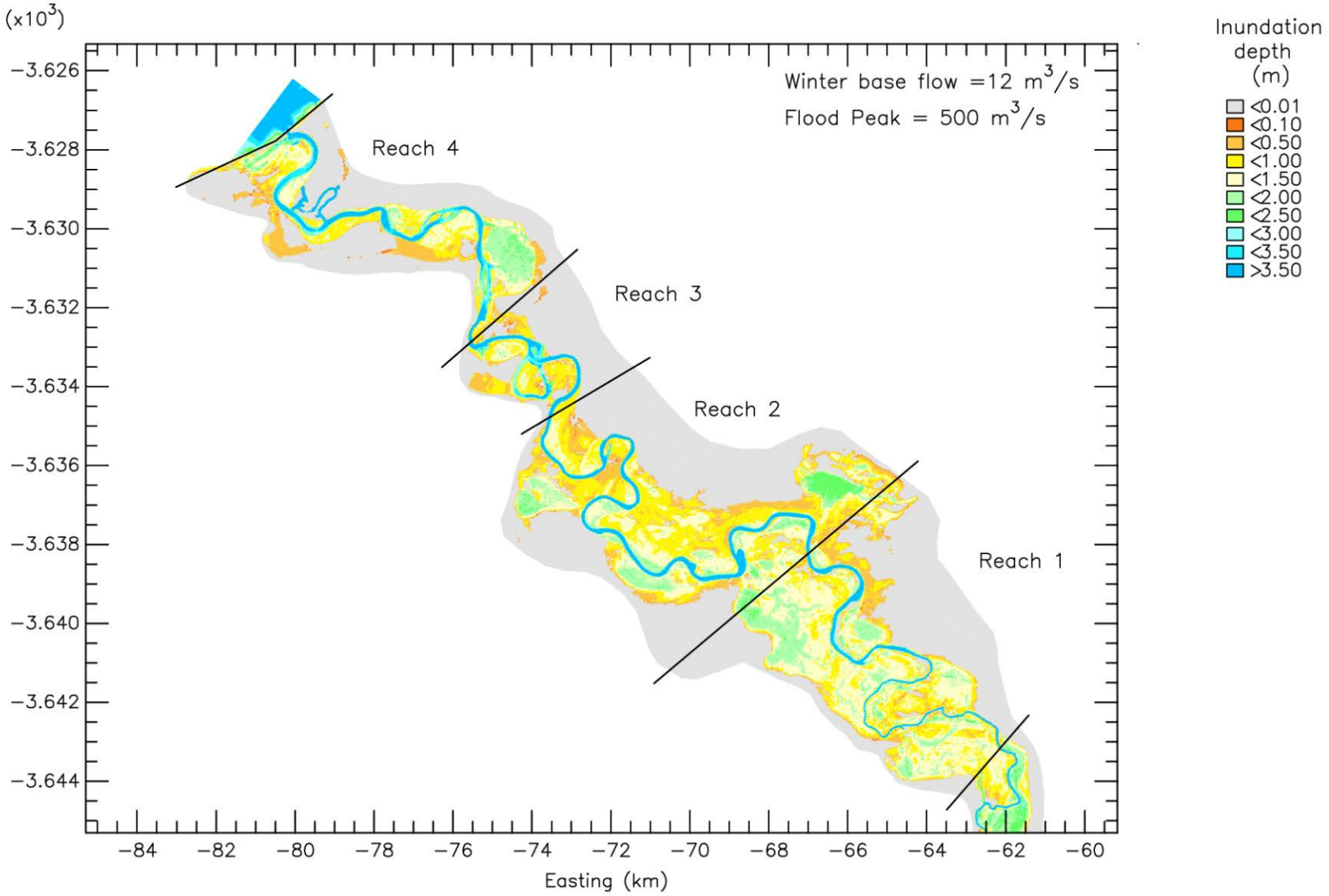

Figure C2e Depth of inundation of the Berg River floodplain for a 500 m^3/s flood under winter base flow conditions of 12 m^3/s

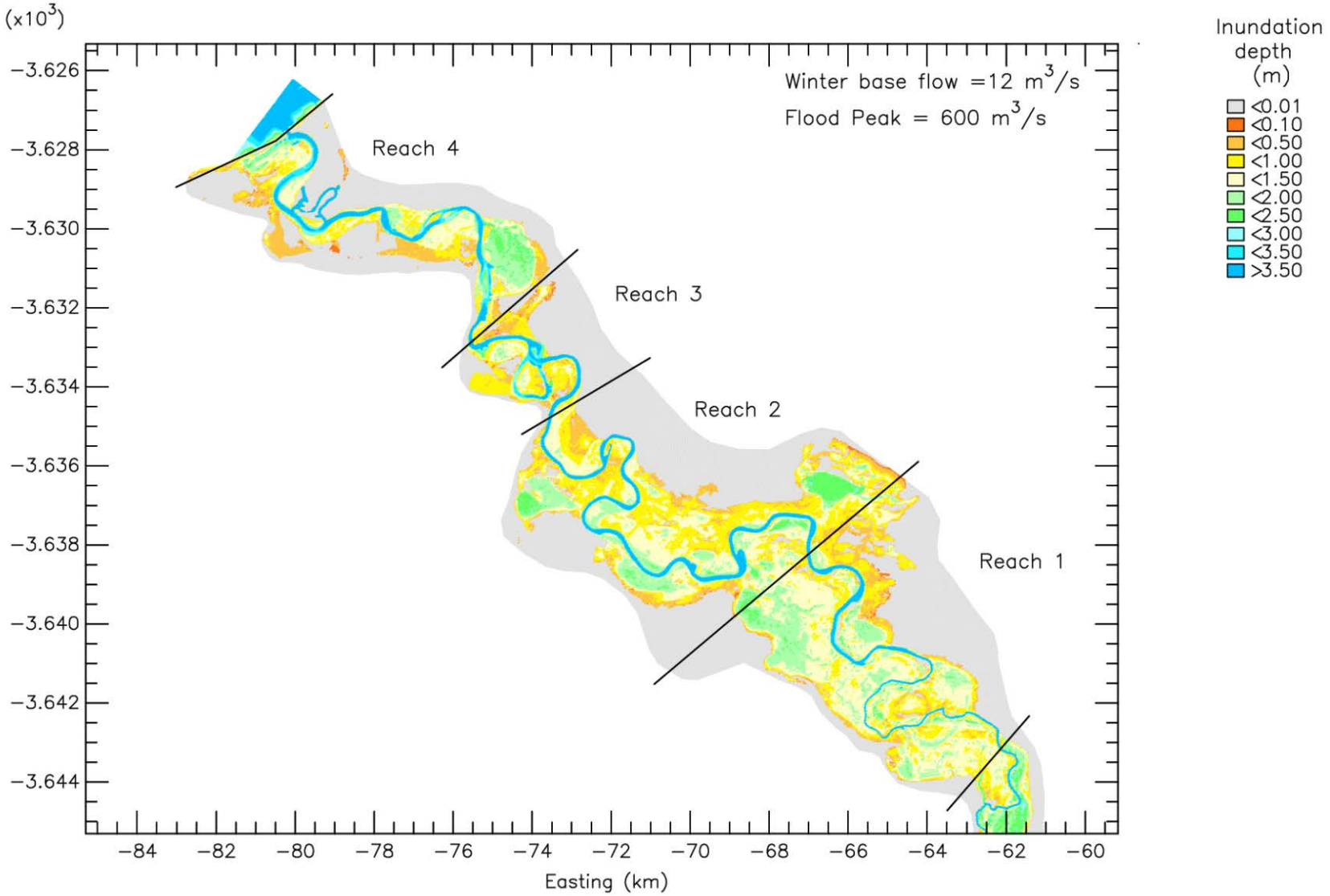

Figure C2f Depth of inundation of the Berg River floodplain for a 600 m^3/s flood under winter base flow conditions of 12 m^3/s

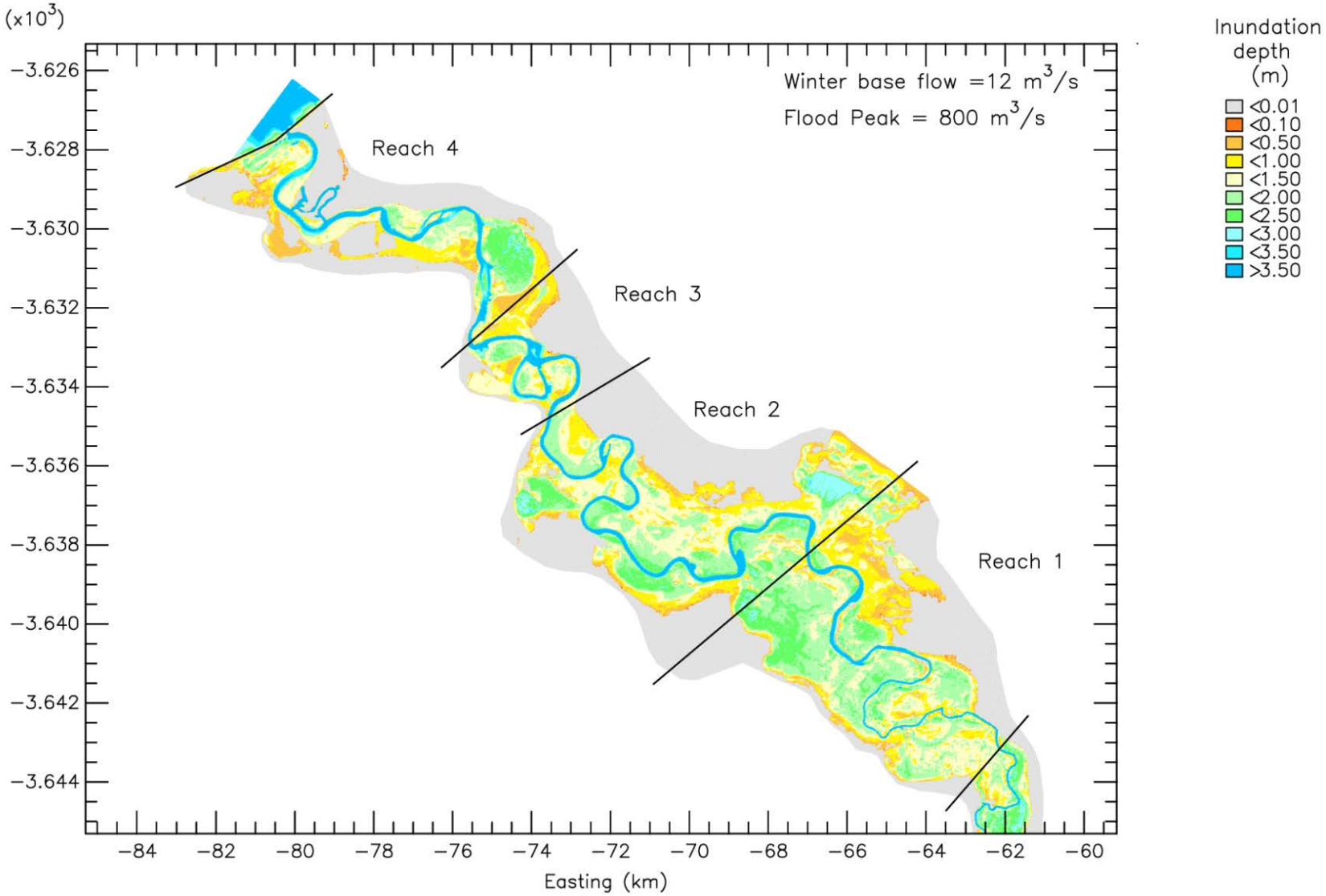

Figure C2g Depth of inundation of the Berg River floodplain for a 800 m^3/s flood under winter base flow conditions of 12 m^3/s

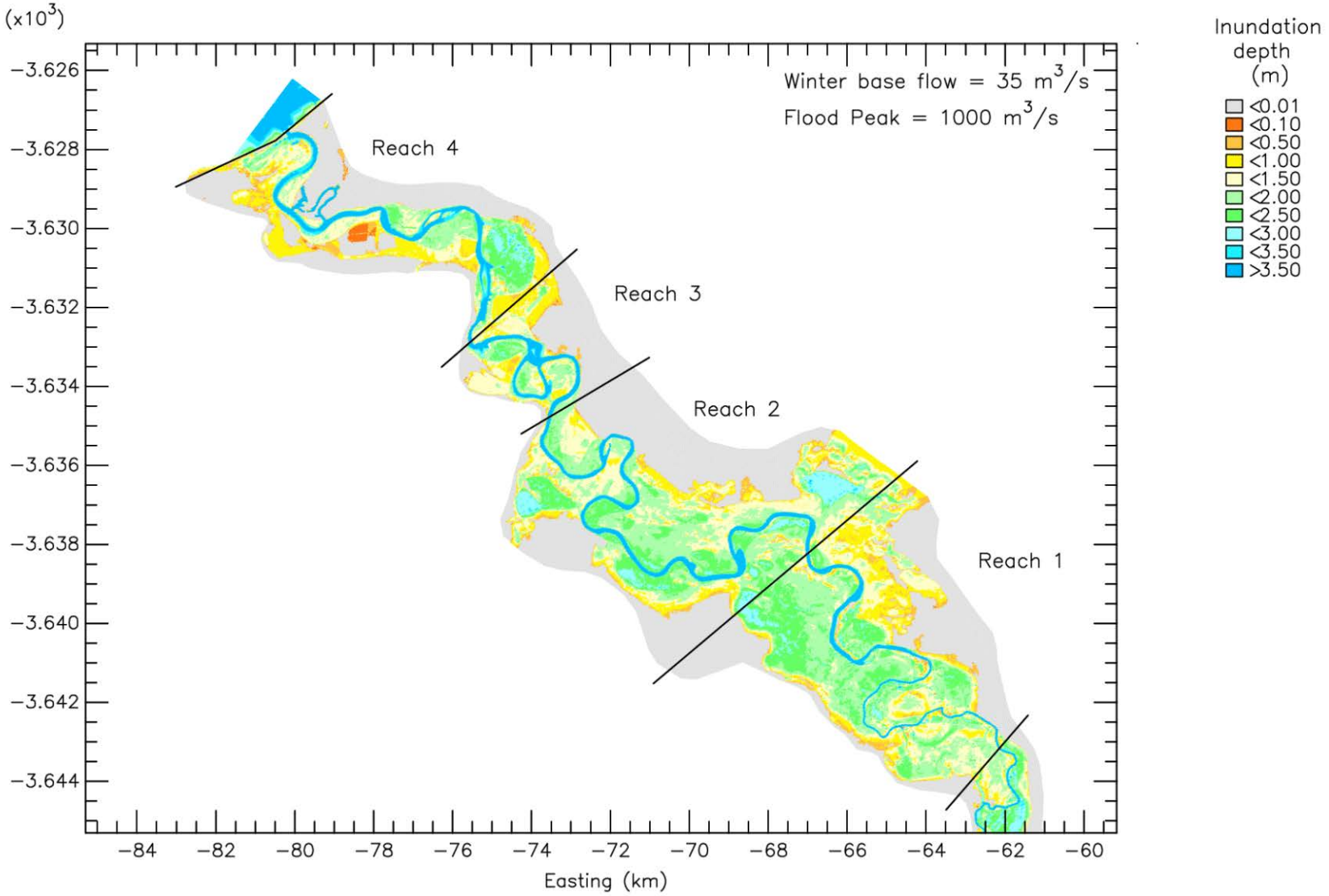

Figure C2h Depth of inundation of the Berg River floodplain for a 1000 m^3/s flood under winter base flow conditions of 12 m^3/s

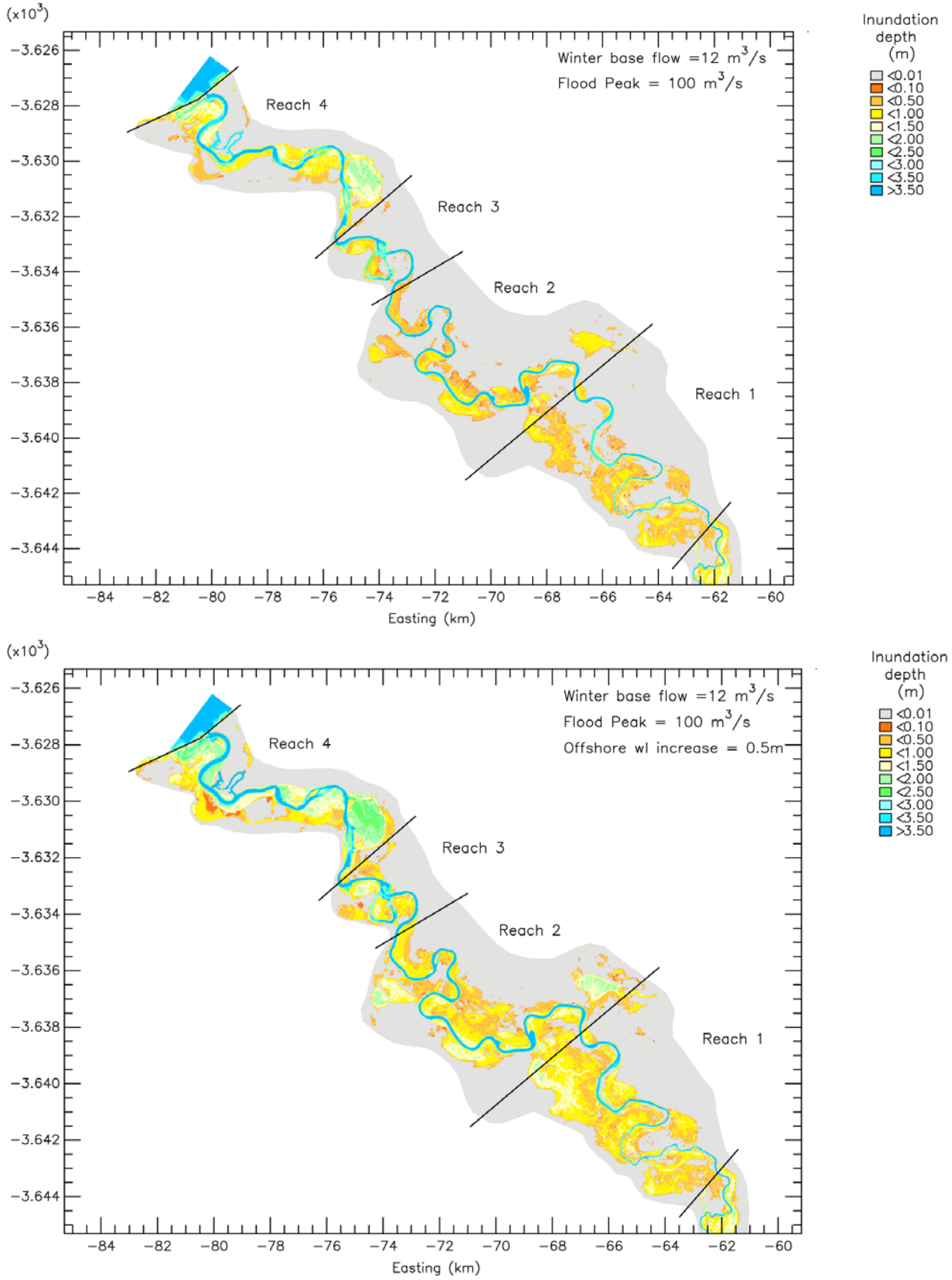

Figure C3a **Depth of inundation of the Berg River floodplain for a 100 m^3/s flood a) under winter base flow conditions of 12 m^3/s and b) under winter base flow conditions of 12 m^3/s and a 0.5m elevation in water level at the estuary mouth.**

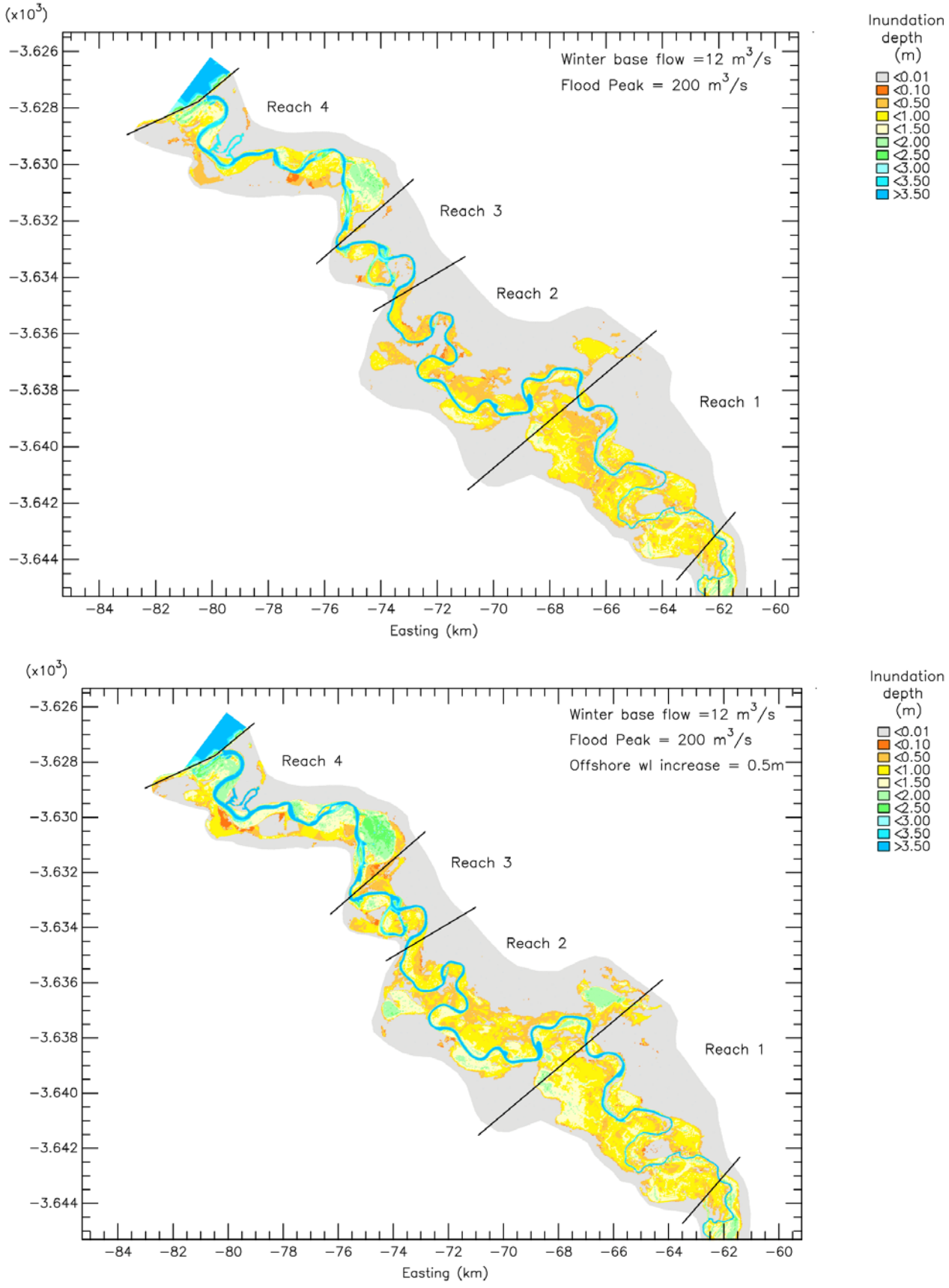

Figure C3b **Depth of inundation of the Berg River floodplain for a 200 m^3/s flood a) under winter base flow conditions of 12 m^3/s and b) under winter base flow conditions of 12 m^3/s and a 0.5m elevation in water level at the estuary mouth.**

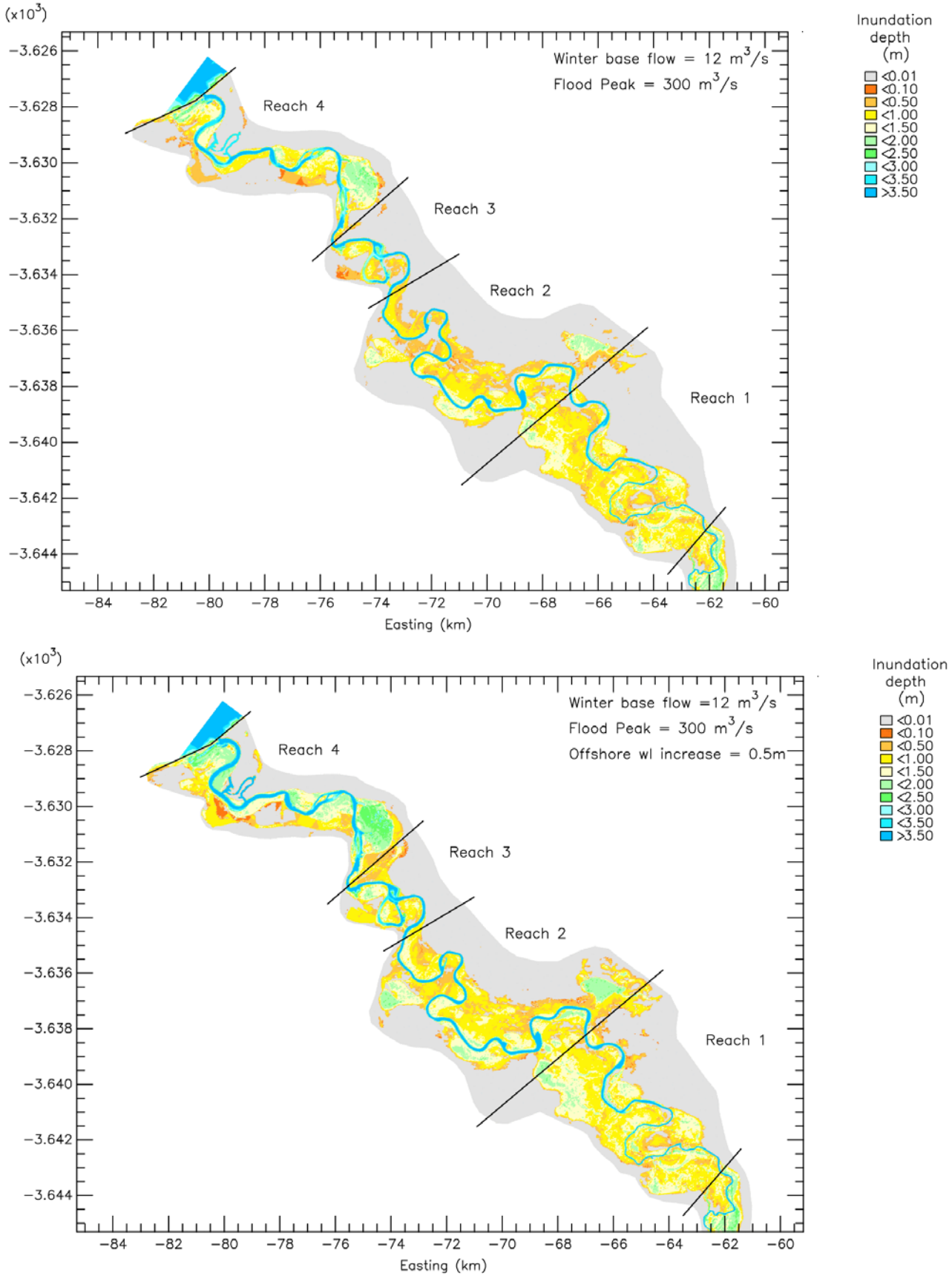

Figure C3c **Depth of inundation of the Berg River floodplain for a 300 m^3/s flood a) under winter base flow conditions of 12 m^3/s and b) under winter base flow conditions of 12 m^3/s and a 0.5m elevation in water level at the estuary mouth.**

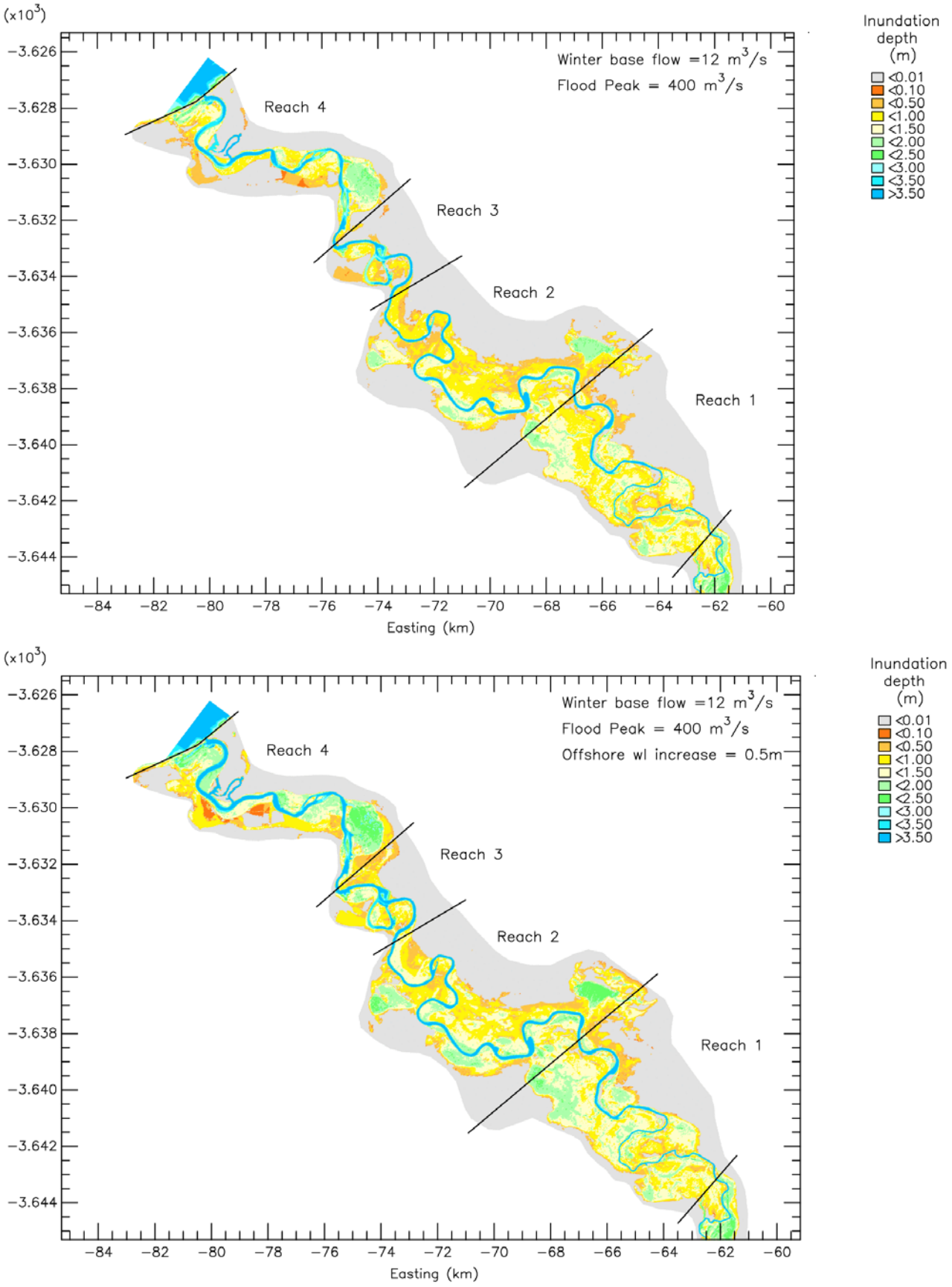

Figure C3d **Depth of inundation of the Berg River floodplain for a 400 m^3/s flood a) under winter base flow conditions of 12 m^3/s and b) under winter base flow conditions of 12 m^3/s and a 0.5m elevation in water level at the estuary mouth.**

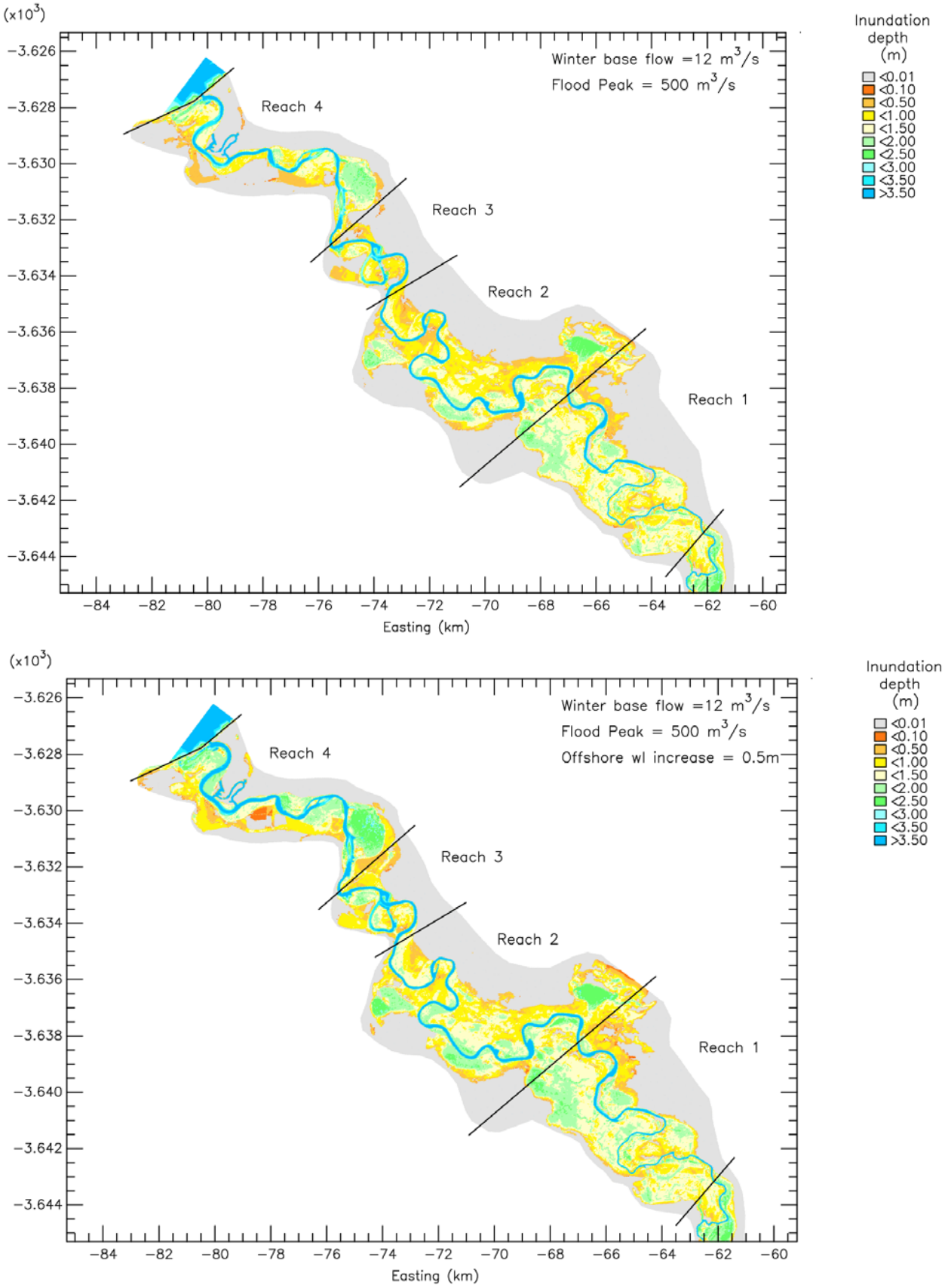

Figure C3e **Depth of inundation of the Berg River floodplain for a 500 m^3/s flood a) under winter base flow conditions of 12 m^3/s and b) under winter base flow conditions of 12 m^3/s and a 0.5m elevation in water level at the estuary mouth.**